

EST 1892

**London
South Bank
University**

**Heterogeneous Catalytic Conversion of Carbon
Dioxide into 1,2-Butylene Carbonate and Styrene
Carbonate**

By

Victor Nnamdi Onyenkeadi

**A Doctoral Thesis submitted in partial fulfillment of
the requirements for the award of the degree of
Doctor of Philosophy in Chemical Engineering**

Centre for Energy and Environment Research,

School of Engineering

January 2019

© Victor Nnamdi Onyenkeadi

*This thesis is dedicated to the lovely memory of my first offspring
Eleanor Onyenkeadi who passed away a week after her birth, you
are always remembered.*

ACKNOWLEDGEMENTS

I would firstly, thank God Almighty for the strength, good health, and the wealth of knowledge given to me to complete my PhD thesis. I owe my sincere gratitude to my parents for not only their financial support but for continuous encouragement. I am most grateful to Professor Basu Saha (my supervisor) for his continuous guidance and support right from the beginning of my PhD research work to the end. I would not forget the professional advice, encouragement and positive criticism that has made a tremendous impact in my chosen career and also have made me a better person in term of keeping attention to details.

I would like to acknowledge Professor David Mba for awarding me a year scholarship to complete my PhD. His generosity has helped me to achieve a step closer to my dreams. I would also extend my way thanks to Dr Suela Kellici for her support and outstanding help with catalyst preparation and characterisation. I express my thanks to Dr Adegboyega Adeleye for his amazing support, encouragement and the foundation he laid in the area of research. I would want to thank Mr Charles and Mr William (Technicians) for their wonderful support.

My deepest thanks go to my second supervisor Dr Donglin Zhao for his support toward the completion of my PhD research programme. I would also acknowledge my friends and colleagues at London South Bank University for being a friend in need during the toughest time.

The completion of my PhD research programme wouldn't have been possible without my lovely family support. I would want to thank my mother Mrs Bridget Onyenkeadi for providing me with the platform in term of financial resource to see that I complete my PhD programme. I owe my deepest gratitude to my father Mr Patrick Onyenkeadi for his prayers and continue believing in me. I express my warm thanks to my sisters (Nkem Onyenkeadi and Ifeoma Okeke), my brother (Ifeanychukwu Onyenkeadi) and my inlaws for their continuous prayers and encouragements.

Lastly, I would like to be thankful to my lovely wife Mrs Nwanneka Onyenkeadi for her continuous support and putting extra shifts to support the family and looking after our lovely children (Joshua and David) during the course of my PhD programme. I have no doubt in my heart if she has not gone extra miles in putting those extra shifts, it would not have been possible to complete my PhD research programme.

ABSTRACT

The significant increase of carbon dioxide (CO₂) into the atmosphere is alarming since the industrial revolution and this has resulted to prevailing environmental challenges such as global warming experienced in recent times. There is an urgency to reduce CO₂ emissions to a sustainable level in order to prevent global warming and climate change. Several methods of reducing CO₂ emissions have been identified. However, greener synthesis of organic carbonates such as 1,2-butylene carbonate (BC) and styrene carbonate (SC) through the utilisation of CO₂ have been identified to be valuable chemicals in chemical industry. The utilisation of CO₂ to produce value-added chemicals is considered as one of the promising technological advancements targeted at reducing CO₂ emissions to a sustainable level.

1,2-Butylene carbonate and styrene carbonate are promising green chemicals, which find their applications in chemical and pharmaceutical industries. These organic carbonates exhibit excellent chemical properties and can be used widely as intermediates to synthesise other chemicals, electrolyte to power lithium batteries and fuel additives.

The syntheses of 1,2-butylene carbonate and styrene carbonate using conventional approaches involve the use of phosgene, a toxic feedstock and produce acid waste, which is highly toxic and environmentally unfriendly. The application of solvent-free heterogeneous catalytic processes promote green processes and offer more sustainable process for the syntheses of organic carbonates.

In this work, batch experimental studies have been conducted using several commercially available heterogeneous catalysts such as ceria and lanthana doped zirconia (Ce-La-Zr-O), ceria doped zirconia (Ce-Zr-O), lanthana doped zirconia (La-Zr-O), lanthanum oxide (La-O), zirconium oxide (Zr-O) and graphene oxide supported inorganic nanocomposites where graphene oxide (GO) has been used as a suitable support and metal oxide catalyst (Ce-La-Zr/GO) has been extensively assessed for the synthesis of 1,2-butylene carbonate and styrene carbonate. Ceria, lanthana, zirconia doped graphene

nanocomposites (Ce-La-Zr/GO) have been synthesised using a new innovative approach known as a continuous hydrothermal flow synthesis (CHFS) reactor. Copper, zirconia doped graphene oxide (Cu-Zr/GO) and copper, zirconia oxide/graphene composite (HTR450) have been synthesised using conventional wet impregnation methods and assessed as suitable heterogeneous catalysts for the synthesis of 1,2-butylene carbonate *via* a facile direct route. These catalysts have been characterised using various analytical techniques such as scanning electron microscopy (SEM), transmission electron microscopy (TEM), Fourier transform infrared spectroscopy (FT-IR), X-ray diffraction (XRD), X-ray photoelectron spectroscopy (XPS), Raman spectroscopy and Brunauer-Emmett-Teller (BET) surface area measurement.

The use of a solvent-free heterogeneous catalytic process for the direct syntheses of BC and SC have been conducted in a high-pressure reactor. Various reaction parameters such as the effect of reaction temperature, CO₂ pressure, reaction time, catalyst loading, and stirring speed have been investigated to achieve the optimum reaction conditions on the conversion of epoxides and yield of cyclic carbonates. The long-term stability of the heterogeneous catalysts has been evaluated by conducting reusability studies. Copper, zirconia doped graphene nanocomposite catalyst (HTR450) and ceria, lanthana, zirconia doped graphene oxide catalyst (Ce-La-Zr/GO) have been found to be the most active and selective for the synthesis of BC as compared to other commercial catalysts evaluated in this research work. For the direct synthesis SC, ceria, lanthana doped zirconia (Ce-La-Zr-O) has been found to be the best-performed catalyst as compared to other used catalysts. The reusability studies of these HTR450, Ce-La-Zr/GO and Ce-La-Zr-O catalysts have evidently shown the long-term stability without any significant reduction in their performances.

Response Surface Methodology (RSM) in the design of experiment is used for modelling and optimisation of experiments in the process industry, catalysis and chemical reaction engineering. The application of RSM minimise the number of experiments thereby saving time and materials. Hence, RSM using box-Behnken design (BBD) has been explored to evaluate and optimise multiple responses (output variables), which are influenced by several independent variables such as

catalyst loading, temperature, CO₂ pressure, and reaction time. BBD model has been developed for the direct synthesis of SC *via* cycloaddition reaction of CO₂ to styrene oxide (SO) and direct synthesis of BC through reaction of butylene oxide (BO) and CO₂. The developed models have been used to compare the experimental results and the predicted results. Regression analyses have been carried out to establish the optimum reaction parameters for a maximum yield of SC and BC. The predicted values of BBD model are in good agreement with the experimental results with <1.5% error.

Keywords: Carbon dioxide (CO₂), heterogeneous catalysts, copper, zirconia doped graphene oxide (Cu-ZrO/GO), copper, zirconia doped graphene (HTR450), ceria, lanthana and zirconia graphene oxide (Ce-La-Zr-GO) nanocomposite, ceria and lanthana doped zirconia (Ce-La-Zr-O), continuous hydrothermal flow synthesis (CHFS) reactor, supercritical CO₂ (scCO₂), 1,2-butylene carbonate (BC), butylene oxide (BO), styrene carbonate (SC), styrene oxide (SO), butylene oxide (BO), Response Surface Methodology (RSM), Box-Behnken Design (BBD).

TABLE OF CONTENTS

ACKNOWLEDGEMENTS	ii
ABSTRACT	iv
TABLE OF CONTENTS	vii
LIST OF FIGURES	xiii
LIST OF TABLES	i
LIST OF ABBREVIATIONS	ii
LIST OF NOMENCLATURE	viii
CHAPTER 1: INTRODUCTION	1
1.1 Motivation	1
1.2 Carbon dioxide	3
1.3 Sources of carbon dioxide (CO ₂)	4
1.3.1. Natural sources of carbon dioxide	5
1.3.2 Anthropogenic sources	6
1.4 Emissions of CO ₂	7
1.5 Policies of CO ₂ emissions reduction.....	8
1.6 Solutions for CO ₂ emissions reduction	10
1.7 Developing attitude toward sustainability	11
1.8 Research aims and objectives	11
1.9 Novelty of the present study	13
1.10 Thesis structure.....	15
CHAPTER 2: LITERATURE REVIEW	18
2.1 Introduction.....	18
2.2 Carbon dioxide	18
2.2.1 Carbon cycle	19
2.2.2 Physicochemical properties of carbon dioxide	19
2.2.3 Carbon dioxide as a green solvent	22

2.3 Applications of CO ₂	23
2.3.1 Commercial applications of CO ₂	23
2.3.2 Enhanced fossil fuel recovery	24
2.3.3 Biological uses of CO ₂	25
2.3.4 Pharmaceuticals uses of CO ₂	25
2.3.5 Utilisation of CO ₂ as a chemical feedstock.....	26
2.4 Organic carbonate.....	28
2.4.1 Classification of organic carbonates	29
2.4.2 Properties and application of 1,2-butylene carbonate and styrene carbonate	31
2.4.3 Methods of organic carbonate synthesis	33
2.5 Catalysis	42
2.5.1 Classification of catalysis	42
2.5.2 Bio-catalysis	42
2.5.3 Homogeneous catalysis.....	43
2.5.4 Heterogeneous catalysis.....	50
2.6 Critical features of a high performing catalyst for cyclic carbonate synthesis	65
2.7 Conclusions.....	70
CHAPTER 3: MATERIALS AND METHODS USED FOR CATALYSTS SYNTHESIS AND CHARACTERISATION.....	71
3.1 Introduction.....	71
3.2 Metal oxides and mixed metal oxides synthesis	72
3.2.1 Graphene oxide synthesis	73
3.2.2 Lanthanum oxide synthesis	75
3.2.3 Lanthana doped zirconia oxide synthesis	76
3.2.4 Copper doped zirconia oxide synthesis.....	77
3.2.5 Copper–zirconia/graphene inorganic composite synthesis.....	78
3.2.6 Ceria-lanthana doped zirconia oxide synthesis.....	79

3.2.7 Ceria-lanthana-zirconia oxide/graphene nanocomposite synthesis	80
3.3 Physicochemical properties of heterogeneous catalysis	81
3.4 Micrometrics Analysis	83
3.5 Electron microscopy (EM)	86
3.5.1 Scanning electron microscopy (SEM)	86
3.6 X-ray photoelectron spectroscopy (XPS) analysis	87
3.7 X-ray powder diffraction (XRD) analysis	89
3.8 Fourier transform infrared spectroscopy (FT-IR) analysis	91
3.9 Conclusions	92
CHAPTER 4: GREENER SYNTHESIS OF 1,2-BUTYLENE CARBONATE FROM CO₂ USING GRAPHENE-INORGANIC NANOCOMPOSITE CATALYST	93
4.1 Introduction	93
4.2 Materials	94
4.3 Preparation and characterisation of ceria-lanthana-zirconia oxide/graphene nanocomposite synthesis <i>via</i> CHFS	95
4.3.1 Graphene oxide (GO) preparation	95
4.3.2 Preparation of ceria-lanthana-zirconia/graphene nanocomposite synthesis <i>via</i> CHFS	95
4.4 Experimental procedure for the synthesis of 1,2-butylene carbonate (BC)	96
4.5 Method of analysis	98
4.5.1 Internal standardisation	99
4.5.2 Calibration method	100
4.5.3 Chromatogram and calibration curves	102
4.5.4 Determination of BO conversion, BC yield, and selectivity	104
4.6 Results and discussion	105
4.6.1 Reaction pathway	105

4.6.2 Proposed reaction mechanism	106
4.6.3 Catalyst characterisation.....	107
4.6.4 Effect of mass transfer in heterogeneous catalytic reactions	111
4.6.5 Effect of different heterogeneous catalysts	112
4.6.6 Effect of catalyst loading	113
4.6.7 Effect of reaction time	115
4.6.8 Effect of reaction temperature	116
4.6.9 Effect of CO ₂ pressure.....	118
4.6.10 Catalyst reusability studies	119
4.7 Conclusions.....	120
CHAPTER 5: SYSTEMATIC MULTIVARIATE OPTIMISATION OF 1,2-BUTYLENE CARBONATE SYNTHESIS VIA CO₂ UTILISATION USING GRAPHENE-INORGANIC NANOCOMPOSITE CATALYSTS.....	121
5.1 Introduction.....	121
5.2 Experimental design.....	122
5.3 Statistical analysis	122
5.4 Development of regression model.....	122
5.5 Models adequacy checking.....	123
5.6 Effect of process variables and their interactions.....	128
5.6.1 Effect of individual variables on responses	128
5.6.2 Effect of variables interaction on responses.....	130
5.7 Process optimisation.....	138
5.9 Conclusions.....	139
CHAPTER 6: GREENER SYNTHESIS OF STYRENE CARBONATE USING COMMERCIAL HETEROGENEOUS CATALYSTS (METAL OXIDE AND MIXED METAL OXIDE CATALYSTS).....	140
6.1 Introduction.....	140

6.2 Materials	142
6.3 Catalyst characterisation.....	142
6.4 The synthesis of SC <i>via</i> cycloaddition reaction of CO ₂ to SO.....	148
6.5 Method of analysis	148
6.6 Results and discussion	149
6.6.1 Reaction pathway.....	149
6.6.2 Effect of mass transfer	151
6.6.3 Effect of reaction time	153
6.6.4 Effect of catalyst loading	154
6.6.5 Effect of reaction temperature	156
6.6.6 Effect of CO ₂ pressure.....	157
6.6.7 Catalyst reusability studies	158
6.7 RSM modelling and optimisation	160
6.7.1 Experimental design	160
6.7.2 Statistical analysis.....	161
6.7.3 Model development and adequacy checking	161
6.7.4 Multiple responses optimisation.....	171
6.7.5 Optimum conditions validation	171
6.8 Conclusions.....	171
CHAPTER 7: A FACILE AND GREENER SYNTHESIS OF 1,2-BUTYLENE CARBONATE <i>VIA</i> CO₂ UTILISATION USING A NOVEL COPPER–ZIRCONIA OXIDE/GRAPHENE CATALYST	173
7.1 Introduction.....	173
7.2 Materials	174
7.3. Catalyst preparation and characterisation techniques	175
7.4 Experimental design.....	176

7.5 Statistical analysis	177
7.6 Results and discussion	178
7.6.1 Catalyst characterisation.....	178
7.6.2 Model development.....	181
7.6.3 Models adequacy checking	182
7.6.4 Model validation	185
7.6.5 Batch experimental results	186
7.7 Optimisation of BO conversion, BC yield and Validation.	195
7.8 Conclusions.....	199
CHAPTER 8: CONCLUSIONS AND RECOMMENDATIONS FOR FUTURE WORK.....	200
8.1 Conclusions.....	200
8.2 Recommendations for future work.....	202
8.2.1 Developing a novel heterogeneous catalyst with higher catalytic performance	202
8.2.2 Catalyst characterisation.....	203
8.2.3 Continuous flow syntheses of cyclic carbonates.....	203
8.2.4 Synthesis of other valuable organic carbonates	203
8.2.5 Valourisation of waste CO ₂ for cyclic carbonate synthesis	203
8.2.6 Economic feasibility study of the current process	204
CHAPTER 9: REFERENCES.....	205
CHAPTER 10: APPENDICES.....	230
10.1 Appendix 1: Chromatograms	230
10.2 Appendix A: Raw data for catalysts reusability	232
10.3 Appendix B: Experimental raw data (samples)	233
10.4 Research publications.....	238
10.4.1 Journal papers	238

10.4.2 Conference papers and work presentations	239
--	------------

LIST OF FIGURES

Figure 1- 1. Yashentech's process uses carbon dioxide and methanol to produce DMC (Yashentech Corporation, 2014)	2
Figure 1- 2. Natural source of the carbon cycle.	6
Figure 1- 3. Global emission of CO ₂ from 1980 predicted to 2019. Source: U.S. Energy Information Administration, International Energy Statistics, International Energy Outlook, and Short-Term Energy Outlook.....	8
Figure 1- 4. Greenhouse gas emission trends (1990–2012), projections to 2030 and targets to 2050 (EEA, 2016).	10
Figure 2- 1. CO ₂ phase diagram	20
<i>Figure 2- 2. The application of atmospheric CO₂ (McConnell, 2012).....</i>	<i>23</i>
Figure 2- 3. Conversion of CO ₂ into value-added chemicals and synthetic fuels hierarchy.....	27
Figure 2- 4. Classification of organic carbonates (Shaikh and Sivaram, 1996) ..	30
Figure 3- 1. Schematic of a CHFS reactor set up used for catalyst production ..	72
Figure 3- 2. The schematic of experimental set-up for graphene oxide preparation	74
<i>Figure 3- 3. An image of the experimental set-up for graphene oxide preparation</i>	<i>74</i>
<i>Figure 3- 4. A schematic representation of graphite powder transformation to graphene oxide (GO)</i>	<i>75</i>
<i>Figure 3- 5. Image of (a) lanthana oxide (La-O) and (b) zirconia oxide (Zr-O)....</i>	<i>76</i>
<i>Figure 3- 6. Image of (a) lanthana doped zirconium oxide (La-Zr-O) and (b) ceria doped zirconium oxide (Ce-Zr-O).....</i>	<i>77</i>
<i>Figure 3- 7. Photographic image of (a) copper, zirconia doped graphene (Cu-Zr/GO) and (b) Heat treatment of copper, zirconia doped graphene at 723 K(HR450).....</i>	<i>79</i>
Figure 3- 8. Image of (a) ceria,lanthana, doped zirconia doped (Ce-La-Zr-O) and (b) ceria,lanthana, zirconia doped graphene (Ce-La-Zr/GO).....	81
Figure 3- 9. BET surface area and particle size trends of AP and the corresponding heat-treated Cu-Zr/graphene nanocomposite catalysts.....	85

Figure 3- 10. An X-ray photoelectron spectroscopy. Adapted from (Chorkendorff and Niemantsverdriet, 2003).....	88
Figure 3- 11. Basic set up of an X-ray Diffractometer. Adapted from (Alsaiani, 2017)	90
<i>Figure 3- 12. The interaction of X-rays within a crystal surface. Adapted from (Cassetta, 2014).</i>	90
Figure 3- 13. Schematic sketch of the essential features of a Fourier transform infrared (FTIR) spectrometer.	92
Figure 4- 1. Schematic of a CHFS reactor set up used for the production of Ce-La-Zr/GO inorganic nanocomposite catalyst.	96
Figure 4- 2. Batch experimental set-up for the synthesis of styrene carbonate.	97
Figure 4- 3. Schematic representation of the experimental set-up for the synthesis of styrene carbonate using a high-pressure reactor (Autoclave reactor). Key: AR, Autoclave reactor; RC, reactor controller; IV, inlet valve; TC, thermocouple; PG, pressure gauge; SM, stirring motor; GOV, gas outlet valve; GIV, gas inlet valve; SV, sampling valve; SCFP, supercritical fluid pump; CIV, CO ₂ inlet valve; CC, CO ₂ cylinder.	98
Figure 4- 4. Shimadzu gas chromatography (GC-2014) used for samples analysis.....	99
<i>Figure 4- 5. Typical chromatogram of a reaction mixture analysed by a Shimadzu GC-2014 gas chromatograph.</i>	102
Figure 4- 6. Calibration curve for response factor of BC using OC as an internal standard.....	103
<i>Figure 4- 7. Calibration curve for response factor determination of BO using OC as an internal standard.</i>	103
Figure 4- 8. Synthesis of 1,2-butylene carbonate (BC) using a heterogeneous catalyst. (a) Reaction scheme and (b) Plausible reaction mechanism.	106
Figure 4- 9. Initiation by adsorption of BO and CO ₂ on Ce-La-Zr/GO.	107
<i>Figure 4- 10. Ring opening of BO to form oxy-anion specie.</i>	107
Figure 4- 11. Ring closure and desorption of 1,2-butylene carbonate	107
Figure 4- 12. A schematic representation of the synthesized Ce-La-Zr/GO nanocomposite.....	108
Figure 4- 13. Transmission electron microscopy (TEM) images of (a) graphene oxide and (b) ceria, lanthana and zirconia graphene oxide (Ce-La-Zr/GO).	109

Figure 4- 14. X-ray diffraction (XRD) patterns of ceria-lanthana - zirconia/graphene oxide (Ce-La-Zr/GO), and graphene oxide (GO) catalysts..	110
Figure 4- 15. X-ray photoelectron spectroscopy (XPS) spectra showing (a) deconvoluted C 1s (b) Ce 3d and La 3d region (c) O 1s region and (d) Zr 3d region for CHFS synthesized Ce-La-Zr/GO catalysts.	110
Figure 4- 16. Effect of mass transfer resistance on conversion of 1, 2 butylene oxide (BO) against yield and selectivity of 1,2-butylene carbonate (BC). Experimental conditions: Catalyst - Ce-La-Zr/GO; Catalyst loading - 10% (w/w); CO ₂ pressure - 75 bar; Reaction temperature - 408 K; Reaction time - 20 h. ...	112
Figure 4- 17. Effect of different metal oxide, and mixed metal oxide heterogeneous catalysts as well as prepared GO via Hummer's method and Ce-La-Zr/GO inorganic nanocomposite via CHFS on conversion of BO against yield and selectivity of BC. Experimental conditions: Catalyst - Ce-La-Zr/GO; Catalyst loading - 10% (w/w); CO ₂ pressure - 75 bar; Reaction temperature - 408 K; Reaction time; 20 h; Stirring speed - 300 rpm.	113
<i>Figure 4- 18. Effect of catalyst loading on conversion of BO against yield and selectivity of BC. Experimental conditions: Catalyst - Ce-La-Zr/GO; Catalyst loading - 10% (w/w); CO₂ pressure - 75 bar; Reaction temperature; 408 K; Reaction time; 20 h, Stirring speed - 300 rpm.</i>	<i>115</i>
Figure 4- 19. Effect of reaction time on conversion of BO against yield and selectivity of BC. Experimental conditions: Catalyst - Ce-La-Zr/GO; Catalyst loading - 10% (w/w); CO ₂ pressure - 75 bar; Reaction temperature; 408 K; Stirring speed - 300 rpm.	116
Figure 4- 20. Effect of reaction temperature on conversion of BO against yield and selectivity of BC. Experimental conditions: Catalyst - Ce-La-Zr/GO; Catalyst loading - 10% (w/w); CO ₂ pressure - 75 bar; Reaction time; 20 h; Stirring speed - 300 rpm.	117
Figure 4- 22. Effect of reaction CO ₂ pressure on conversion of BO against yield and selectivity of BC. Experimental conditions: Catalyst - Ce-La-Zr/GO; Catalyst loading - 10% (w/w); Reaction temperature - 408 K; Reaction time; 20 h; Stirring speed - 300 rpm.	119
Figure 4- 23. Catalyst reusability studies on conversion of BO against yield and selectivity of BC. Experimental conditions: Catalyst - Ce-La-Zr/GO; Catalyst loading - 10% (w/w); Reaction temperature - 408 K; CO ₂ pressure - 75 bar; Reaction time; 20 h; Stirring speed - 300 rpm.	120

Figure 5- 1. Predicted versus actual values for (a) BO conversion model (b) and BC yield model	126
Figure 5- 2. The normal plot of residuals for (a) BO conversion model and (b) BC yield model	127
Figure 5- 3. The plot of residuals versus predicted response for (a) BO conversion model and (b) BC yield model.	127
Figure 5- 4. The plot of residuals versus predicted values of temperature variable for (a) BO conversion model and (b) BC yield model.....	128
Figure 5- 5. The plot showing the effect reaction temperature and pressure on BO conversion	129
Figure 5- 6. The plot showing the effect of catalyst loading and reaction time on BO conversion.....	129
Figure 5- 7. The plot showing the effect of reaction temperature and pressure on BC yield	130
Figure 5- 8. The plot showing the effect of catalyst loading and reaction time on BC yield	130
Figure 5- 9. 3D response surface and contour plot of reaction temperature and pressure versus BO conversion.....	133
Figure 5- 10. 3D response surface and contour plot of reaction temperature and pressure versus BC yield.	134
Figure 5- 11. 3D response surface and contour plot of catalyst loading and reaction time versus BO conversion.....	136
Figure 5- 12. 3D response surface and contour plot of catalyst loading and reaction time versus BC yield.	137
Figure 6- 1. <i>Scanning electron microscopy (SEM) image of zirconium oxide (Zr-O) catalysts</i>	144
Figure 6- 2. <i>Scanning electron microscopy (SEM) image of lanthanum oxide (La-O)</i>	145
Figure 6- 3. Scanning electron microscopy (SEM) image of lanthana doped zirconia (La-Zr-O).....	145
Figure 6- 4. Scanning electron microscopy (SEM) image of ceria doped zirconia (Ce-Zr-O).....	146
Figure 6- 5. Scanning electron microscopy (SEM) image of ceria and lanthana doped zirconia (Ce-La-Zr-O).....	146

Figure 6- 6. Raman spectra of ceria and lanthana doped zirconia (Ce-La-Zr-O), ceria doped zirconia (Ce-Zr-O), lanthanum oxide (La-O), lanthana doped zirconia (La-Zr-O) and zirconium oxide (Zr-O) catalysts.....	147
Figure 6- 7. X-ray diffraction (XRD) patterns of ceria and lanthana doped zirconia (Ce-La-Zr-O), ceria doped zirconia (Ce-Zr-O), lanthanum oxide (La-O), lanthana doped zirconia (La-Zr-O) and zirconium oxide (Zr-O) catalysts.....	147
Figure 6- 8. The pathway 2 is the isomerisation of SO into phenylacetaldehyde, which is an industrially important intermediate for fine chemical synthesis. The reaction could occur under mild conditions at 25 – 70°C. The pathway 1 is for SC synthesis via cycloaddition reaction of CO ₂ to SO in the presence of Ce-La -Zr-O catalyst.	149
Figure 6- 9. Effect of different catalysts on conversion of styrene oxide (SO), selectivity and yield of styrene carbonate (SC). Experimental conditions: Catalyst loading – 10% (w/w); reaction temperature 408 K; CO ₂ pressure 75 bar; reaction time 20 h; stirring speed 300 rpm.	151
Figure 6- 10. Effect of mass transfer resistance on conversion of styrene oxide (SO) against yield of (SC). Experimental conditions: Catalyst – ceria and lanthana doped zirconia (Ce-La-Zr-O); catalyst loading 10% (w/w); reaction temperature 408 K; CO ₂ pressure 75 bar; reaction time 20 h.....	153
Figure 6- 11. Time dependence and prediction by design expert (DX) model on conversion of styrene oxide (SO) against yield of styrene carbonate (SC). Experimental conditions: Catalyst – ceria and lanthana doped zirconia (Ce-La-Zr-O); catalyst loading 10% (w/w); reaction temperature 408 K; CO ₂ pressure 75 bar; stirring speed 300 rpm.	154
Figure 6- 12. Catalyst loading dependence and prediction by design expert (DX) model on the conversion of styrene oxide (SO) against the yield of styrene carbonate (SC). Experimental conditions: Catalyst – ceria and lanthana doped zirconia (Ce-La-Zr-O); reaction temperature 408 K; CO ₂ pressure 75 bar; reaction time 20 h; stirring speed 300 rpm.	155
Figure 6- 13. Temperature dependence and prediction by design expert (DX) model on conversion of styrene oxide (SO) against yield of styrene carbonate (SC). Experimental conditions: Catalyst – ceria and lanthana doped zirconia (Ce-La-Zr-O); catalyst loading 10% (w/w); CO ₂ pressure 75 bar; reaction time 20 h; stirring speed 300 rpm.	157

Figure 6- 14. Pressure dependence and prediction by design expert (DX) model on conversion of styrene oxide (SO) against yield of styrene carbonate (SC). Experimental conditions: Catalyst – ceria and lanthana doped zirconia (Ce-La-Zr-O); catalyst loading 10% (w/w); reaction temperature 408 K; reaction time 20 h; stirring speed 300 rpm	158
Figure 6- 15. Catalyst reusability studies on conversion of styrene oxide (SO), selectivity and yield of styrene carbonate (SC). Experimental conditions: Catalyst – ceria and lanthana doped zirconia (Ce-La-Zr-O); catalyst loading 10% (w/w); reaction temperature 408 K; CO ₂ pressure 75 bar; reaction time 20 h; stirring speed 300 rpm.	159
Figure 6- 16. Actual experimental data versus predicted values for SO conversion.....	166
Figure 6- 17. Actual experimental data versus predicted values for SC yield. ..	167
Figure 6- 18. Response surface plot for the effect reaction temperature and pressure on SO conversion.	169
Figure 6- 19. Response surface plot for the effect reaction temperature and pressure on SC yield.....	169
Figure 6- 20. Response surface plot for the effect reaction catalyst loading and reaction time on SO conversion.....	170
Figure 6- 21. Response surface plot for the effect reaction catalyst loading and reaction time on SC yield.	170
<i>Figure 7- 1. Schematic representation of synthesised copper zirconia doped graphene catalyst (HTR450).....</i>	<i>175</i>
Figure 7- 2. Transmission Electron Microscopy (TEM) image of Cu–Zr/graphene nanocomposite catalyst as-prepared labelled as AP	179
Figure 7- 3. Transmission Electron Microscopy (TEM) image of Cu–Zr/graphene nanocomposite catalyst heat-treated (723 K) sample labelled as HTR450.....	179
Figure 7- 4. Transmission Electron Microscopy (TEM) image of Cu–Zr/graphene nanocomposite catalyst heat-treated (873 K) sample labelled as HTR600.....	179
<i>Figure 7- 5. X-ray diffraction (XRD) patterns of copper- zirconia/graphene nanocomposite catalysts (AP, HTR450 and HTR600).....</i>	<i>180</i>
<i>Figure 7- 6. Actual experimental data versus predicted values for BC yield.</i>	<i>185</i>
<i>Figure 7- 7. Actual experimental data versus predicted values for BO conversion.</i>	<i>186</i>

Figure 7- 8. Effect of different heterogeneous catalysts for BC synthesis. Experimental conditions: catalyst loading, 7.5% (w/w); reaction temperature, 423 K; CO ₂ pressure, 80 bar; reaction time, 12 h and stirring speed, 200 rpm.	188
Figure 7- 9. Effect of external mass transfer on BO conversion and BC yield. Experimental conditions: catalyst loading, 7.5% (w/w); reaction temperature, 423 K; CO ₂ pressure, 80 bar; and reaction time, 12 h	189
Figure 7- 10. Effect of reaction time on BO conversion and BC yield. Experimental conditions: catalyst loading, 7.5% (w/w); reaction temperature, 423 K; CO ₂ pressure, 80 bar; and stirring speed, 200 rpm.	190
Figure 7- 11. Effect of catalyst loading on BO conversion and BC yield. Experimental conditions: reaction time, 12 h; reaction temperature, 423 K; CO ₂ pressure, 80 bar; and stirring speed, 200 rpm.	191
Figure 7- 12. Effect of reaction temperature on BO conversion and BC yield. Experimental conditions: reaction time, 12 h; catalyst loading, 7.5% (w/w); CO ₂ pressure, 80 bar; and stirring speed, 200 rpm.	192
Figure 7- 13. Effect of CO ₂ pressure on BO conversion and BC yield. Experimental conditions: reaction time, 12 h; reaction temperature, 423 K; catalyst loading, 7.5% (w/w); and stirring speed, 200 rpm.	194
Figure 7- 14. Effect of catalyst reusability studies on BO conversion and BC yield. Experimental conditions: reaction time, 12 h; reaction temperature, 423 K; CO ₂ pressure, 80 bar; catalyst loading 7.5% (w/w) and stirring speed, 200 rpm.	195
<i>Figure 7- 15. Response surface plot for the effect of CO₂ pressure and reaction temperature on BO conversion after optimisation.</i>	<i>196</i>
<i>Figure 7- 16. Response surface plot for the effect CO₂ pressure and reaction temperature on BC yield after optimisation.</i>	<i>197</i>
Figure 7- 17. Response surface plot for the effect reaction time and reaction catalyst loading on BO conversion after optimisation.	198
<i>Figure 7- 18. Response surface plot for the effect reaction time and reaction catalyst loading on BC yield after optimisation.</i>	<i>198</i>

LIST OF TABLES

Table 1. Percentage sources of CO ₂ for both natural and anthropogenic sources (<i>Intergovernmental Panel on Climate Change, 2007</i>)	5
Table 2- 1. Physical and chemical properties of carbon dioxide (Styring et al., 2014a)	21
Table 2- 2. Utilisation of CO ₂ (Aresta et al., 2013)	27
Table 2- 3. Physical properties of 1,2-butylene carbonate (BC) and styrene carbonate (SC)	32
Table 2- 4. Application of other cyclic carbonates	33
Table 2- 5. Heterogeneous and homogeneous catalysts comparison	51
Table 2- 6. <i>Catalytic performance of several metal oxide catalysts for the synthesis of cyclic carbonates.</i>	60
Table 2- 7. The synthesis of cyclic carbonates via mixed metal oxides heterogeneous catalysts	69
Table 3- 1. Physical and Chemical Properties of Heterogeneous Catalysts and Synthesized Ce-La-Zr/GO Catalyst	82
Table 3- 2. Physical and chemical properties of synthesised copper doped zirconia (Cu-ZrO) and copper, zirconia doped graphene (Cu-Zr/graphene) nanocomposite catalysts	84
Table 5- 1. <i>Experimental design variables and their coded levels.</i>	123
Table 5- 2. Experimental design matrix with the actual and predicted responses	121
Table 5- 3. Analysis of variance of developed model for BO conversion	123
Table 5- 4. Analysis of variance of developed model for BC yield	124
Table 5- 5. Optimisation constraints used to predict optimum conditions for 1,2-butylene carbonate	139
Table 6- 1. Experimental design variables and their coded levels	160
Table 6- 2. Experimental design matrix with the actual and predicted responses.	163
Table 6- 3. Analysis of variance (ANOVA) for response surface developed model	165
Table 7- 1. Experimental design variables and their coded levels	176

<i>Table 7- 2. Experimental design matrix with the actual and predicted responses</i>	177
Table 7- 4. Analysis of variance of developed model for BO conversion	183
Table 7- 5. Analysis of variance of developed model for BC yield.....	184

LIST OF ABBREVIATIONS

Al_2O_3	Aluminium oxide
AlCl_3	Aluminium chloride
AlO_4	Tetrahedra of alumina
ANOVA	Analysis of variance
BBD	Box-Behnken Design
BC	1,2-Butylene carbonate
BET	Brunauer-Emmett-Teller
BO	Butylene oxide
CaO	Calcium oxide
$\text{Ce}(\text{NO}_3)_3 \cdot 6\text{H}_2\text{O}$	Cerium(III) nitrate hexahydrate
Ce-La-Zr-O	Ceria and lanthana doped zirconia
CeO_2	Cerium oxide
Ce-Zr-O	Ceria doped zirconia

CH_2Cl_2	Dichloromethane
$(\text{CH}_3)_4\text{NOH}$	Tetramethylazanium hydroxide
CH_2O	Formaldehyde
CH_3OH	Methanol
CHFS	Continuous hydrothermal flow synthesis
CO	Carbon monoxide
CO_2	Carbon dioxide
COCl_2	Phosgene
Cs-P-Si oxide	Caesium–phosphorous–silicon mixed oxide
CuCl_2	Copper chloride
Cu-Ni	Copper-nickel
DMAP	4-Dimethylaminopyridine
DMC	Dimethyl carbonate
DME	Dimethyl ether
DMF	N,N-dimethylformamide
Et_4NBr	Ethyl-ammonium bromide

FID	Flame ionisation detector
FT-IR	Fourier transform infrared spectroscopy
GC	Gas chromatography
GO	Graphene oxide
Gt/y	Gigatonne per year
H	Hour
H ₂	Hydrogen
H ₂ O	Water
H ₂ O ₂	Hydrogen peroxide
H ₂ SO ₄	Sulphuric acid
H ₃ PO ₄	Phosphoric acid
HCl	Hydrochloric acid
HPLC	High performance liquid chromatography
K	Kelvin
K ₂ CO ₃	Potassium carbonate
KMnO ₄	Potassium permanganate

KOH	Potassium hydroxide
La ₂ O ₃	Lanthanum oxide
La–O	Lanthanum oxide
La–Zr–O	Lanthana doped zirconia
MCM-41	Molecular sieve
MeOH	Methanol
MgO	Magnesium oxide
Mg-Al oxide	Magnesium- aluminium mixed oxide
MoO ₃	Molybdenum trioxide
Mt/y	Megatonne per year
NaNO ₃	Sodium nitrate
Nb	Niobium
Nb ₂ O ₅	Niobium pentoxide
<i>n</i> -Bu ₄ NBr	Tetra- <i>n</i> -butyl ammonium bromide
NGP	Natural graphite powder
NiCl ₂	Nickel chloride

O ₂	Oxygen
OFAT	One-factor at a time analysis
OH	Hydroxide ion
PC	Propylene carbonate
PO	Propylene oxide
ppm	Parts per million
ppmv	Parts per million by volume
PVC	Polyvinyl chloride
Rh	Rhodium
RS	Raman spectroscopy
RSM	Response Surface Methodology
SBA-15	Mesoporous silica
SC	Styrene carbonate
scCO ₂	Supercritical CO ₂
SEM	Scanning electron microscopy
SiO ₂	Silica

SmOCl	Samarium oxychloride
SO	Styrene oxide
TBAB	Tetra-n-butyl ammonium bromide
TEM	Transmission electron microscopy
TiO ₂	Titanium oxide
V ₂ O ₅	Vanadium oxide
XPS	X-ray photoelectron spectroscopy
XRD	Powder X-ray diffraction
Zn	Zinc
ZnCl ₂	Zinc chloride
ZnO	Zinc oxide
Zr–O	Zirconium oxide
ZrO(NO ₃) ₂ ·6H ₂ O	Zirconium (IV) oxynitrate hydrate
ZrO ₂	Zirconium oxide
ZSM-5	Zeolite International
°C	Degree Celsius

% Percentage

LIST OF NOMENCLATURE

A_i	Area for the i th component
A_{is}	Area of internal standard
AR_i	Area ratio for the i th component
AR	Area ratio
C_i	Concentration of the i th component
C_{is}	Concentration of the internal standard
CR_i	Concentration ratio of the i th component
CR	Concentration ratio
Cu-Zr/GO	Copper-zirconia/graphene oxide synthesised <i>via</i> traditional wet impregnation
HTR300	Cu-Zr/GO Catalyst heat-treated at 573 K
HTR450	Cu-Zr/GO Catalyst heat-treated at 723 K
HTR600	Cu-Zr/GO Catalyst heat treated at 873 K
RF_i	Response factor for the i th component

RF

Response factor

CHAPTER 1

INTRODUCTION

CHAPTER 1: INTRODUCTION

1.1 Motivation

The earth's natural occurrence of carbon dioxide (CO₂) through carbon cycle from an aquatic and terrestrial environment are being compromised by anthropological activities of humankind. This is due to the continuous reliance on fossil fuels as a major source of energy producing CO₂ as a by-product that is being released to the atmosphere. Presently, the average atmospheric concentration of CO₂ in 2018 has increased rapidly from 280 ppm in pre-industrial times to approximately 410 parts per million (ppm) (NOAA, 2018). The rapid increase of CO₂ has been identified to be responsible for global climate change and also pose greater environmental challenges faced by scientists in recent times (Styring *et al.*, 2014b).

Carbon oxide (CO₂) plays an important role in every plant and animal process such as photosynthesis and respiration. It is found to be abundant and can be used as a nontoxic carbon source for the syntheses of organic carbonates. The utilization of CO₂ through cycloaddition reaction to epoxides to form organic carbonates offers a greener route to replace the conventional synthesis route of using phosgene, which produces harmful waste (Shaikh and Sivaram, 1996). Organic carbonates are important raw materials for polyurethane synthesis, alternatives to phosgene, and production of urea derivatives (Aresta and Dibenedetto, 2002). Furthermore, organic carbonates can be used as an additive to gasoline, green solvents, electrolytes for lithium batteries and thickeners for cosmetics (Adeleye *et al.*, 2014; North *et al.*, 2010; Saada *et al.*, 2015).

The conventional synthesis of organic carbonates is based on a few steps process such as the phosgene synthesis and reaction with alcohols. The outcomes of this process are moderate yield and several hazards that involve the use of highly toxic raw materials and production of acid waste. There is alternatives process that was commercialised by Texaco and the Japanese company to synthesise acyclic carbonate *via* cyclic carbonate with alcohol, however, the drawbacks were hazardous starting materials, multi-step synthesis, and production of ethylene glycol as a by-product (Tepzz, 2004).

There have been quite a few research efforts devoted to synthesise organic carbonate through the utilisation of carbon dioxide in order to contribute to the

reduction of atmospheric levels of CO₂ emission. These efforts include the synthesis of acyclic carbonate *via* cyclic carbonates, copolymerisation of epoxide, synthesis of cyclic carbonate in the presence of ionic liquids, onium salts, organocatalysts, metal porphyrin and related complexes, polyoxometalates, rhenium complexes, aluminum quinolate complexes, metal salen complexes, and metal oxides (North and Pasquale, 2009). The synthesis of these carbonates is highly influenced by the conditions of reaction, the types of catalysts and the substrates used for the synthesis.

Several academic works have been published on the synthesis of organic carbonates include ethylene carbonate (EC) (Cui *et al.*, 2004; Lu *et al.*, 2004), dimethyl carbonate (DMC) (Saada *et al.*, 2015; Tomishige *et al.*, 2001), 1,2-butylene carbonate (BC) (Leino *et al.*, 2013; Onyenkeadi *et al.*, 2017), propylene carbonate (PC) (Adeleye *et al.*, 2014; Du *et al.*, 2005) and, styrene carbonate (SC) (Kawanami and Ikushima, 2000; Zhu *et al.*, 2013). Although a few of these syntheses have been commercialised such as Yashentech's new dimethyl carbonate synthesis (see *Figure 1- 1*) using carbon dioxide and methanol as the only feedstock (Yashentech Corporation, 2014). This process provides the main advantage of significantly reducing the cost of production and the process also delivers an economically attractive route for carbon dioxide utilisation into commercial chemicals (Yashentech Corporation, 2014).

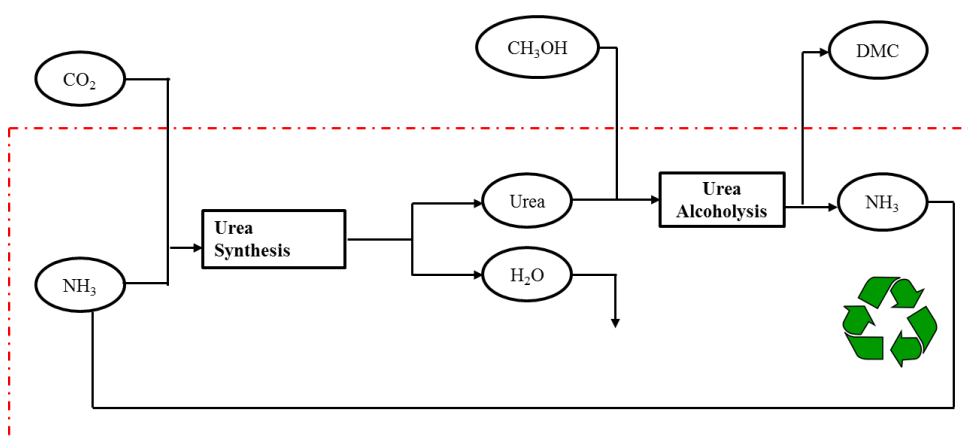


Figure 1- 1. Yashentech's process uses carbon dioxide and methanol to produce DMC (Yashentech Corporation, 2014)

The research showcase the use of different heterogeneous catalysts that include metal oxides (MgO, La₂O₃, ZrO₂, CeO₂, CuO₂) and mixed metal oxides (Ce-Zr-O,

La-Zr-O, Cu-Zr-O, Ce-La-ZrO, Ce-La-Zr/GO, Cu-Zr/GO) for the synthesis of cyclic carbonates such as 1,2-butylene carbonate (BC) and styrene carbonate (SC). The use of graphene oxide as a supported catalyst for mixed metal oxides and its properties such as mechanical strength (known as the strongest material ever tested) and electrical conductivity (conduct heat and electricity). Furthermore, in this research, the process of synthesising mixed metal oxide catalysts and catalysts characterisation have been discussed.

1.2 Carbon dioxide

Carbon dioxide (CO₂) is a triatomic molecule that is relatively an inert gas, which is neither flammable nor explosive and also a noncombustible compound. Thus, it is generally used as a fire extinguisher and an automatic fire suppression systems. CO₂ is also known to be asphyxiant and has a density (1.98 kg/m³ at 273K) greater than air. At room temperature and pressure, it is a gas while at atmospheric pressure it sublimates directly from a solid to a gas at 195 K.

Carbon dioxide occurs naturally in the earth's atmosphere as a result of forest fires, volcanic eruptions, and plant and animals. It is a key part of plant photosynthesis where green plants convert carbon dioxide and water into sugars. The natural carbon cycle of the land and ocean controls the level of carbon dioxide in the atmosphere hence regulate the temperature of the earth. The atmospheric earth's temperature pre industrialisation was 280 parts per million by volume (ppmv) and presently stood at approximately 410 ppm due to continuous burning of fossil fuel, which has upset the natural carbon cycle. As early as 19th-century scientists' recognised continuous accumulation of greenhouse gases in the atmosphere such as methane, water vapour, nitrous oxide chlorofluorocarbons, ozone, and carbon dioxide might affect the earth's temperature (greenhouse effect) leading to global warming. Carbon dioxide is one of the most prominent greenhouse gases that have been identified to cause the greenhouse effect. This is because of the long lifetime ability to absorb and re-emit infrared energy, which enables it to effectively heat-trapping gas. The consequences of continuous accumulation of carbon dioxide in the earth's atmosphere are global warming and climate change, which became a primary concern. Therefore, there is an urgent need among researchers to address the major cause of global warming. There are several ongoing research on how to

improve existing technologies or developing new approaches to CO₂ capture and storage (CCS) such as the use of absorption in amine and ammonia solutions, membrane separation, adsorption using molecular sieves and activated carbon, application of solid imidazolium-based polyionic liquid for CO₂ capture, CO₂ injection into cold geologic formation, and sequestration in deep saline aquifers and coal beds (Gibbins and Chalmers, 2008). The utilisation of CO₂ to value-added chemicals is also considered by researchers and found as one of the promising power tools to reduce the atmospheric concentration of CO₂, mitigate global warming and also used as a substitute for harmful chemicals. Although, the utilisation of CO₂ is already known in the mid-1800s where salicylic acid was synthesised from phenol and carbon dioxide by German scientists called Hermann Kolbe and Rudolf Schmitt (H.Frank, 1988). Other known CO₂ conversions are methanol from syngas enriched with CO₂ (Lee *et al.*, 2015) and the production of urea from ammonia and CO₂ (Krase and Gaddy, 1922). It is notable that CO₂ has been a useful valuable feedstock rather than waste, however, the uses of CO₂ as a feedstock has not been properly exploited until recently.

1.3 Sources of carbon dioxide (CO₂)

Carbon dioxide occurs from both natural and anthropogenic sources. The natural sources of CO₂ emission include ocean release, decomposition, and respiration while the anthropogenic sources involve human activities such as deforestation, cement production, and burning fossil fuel, for e.g. coal, oil, and natural gas (Gerlach, 2011).

Table 1. Percentage sources of CO₂ for both natural and anthropogenic sources
(Intergovernmental Panel on Climate Change, 2007)

<i>Natural Sources</i>	<i>Percentage contributions (%)</i>	<i>Anthropogenic sources</i>	<i>Percentage contributions (%)</i>
<i>Plant and animal respiration</i>	<i>28.56</i>	<i>Fossil fuel (gas, oil, and coal)</i>	<i>87</i>
<i>Ocean-atmosphere exchange</i>	<i>42.84</i>	<i>Deforestation and Land use</i>	<i>9</i>
<i>Soil respiration and decomposition</i>	<i>28.56</i>	<i>Industrial processes</i>	<i>4</i>
<i>Volcanic eruptions</i>	<i>0.03</i>		
<i>Total</i>	<i>100</i>	<i>Total</i>	<i>100</i>

1.3.1. Natural sources of carbon dioxide

The natural process of releasing carbon dioxide into the atmosphere involves the earth's oceans, plants, animals, soil, and volcanoes. Before the influence of industrial revolution, human sources of carbon dioxide level were much smaller than the natural emissions, which has been upset in carbon cycle balance by natural carbon sinks over thousand years ago (Houghton, 2005). The *Table 1* shows 42.48% of all natural source of carbon dioxide emissions comes from ocean-atmosphere exchange while 0.03%, 28.56%, 28.56% are from volcanic eruptions, plants and animals and soil respiration, respectively (Gerlach, 2011).

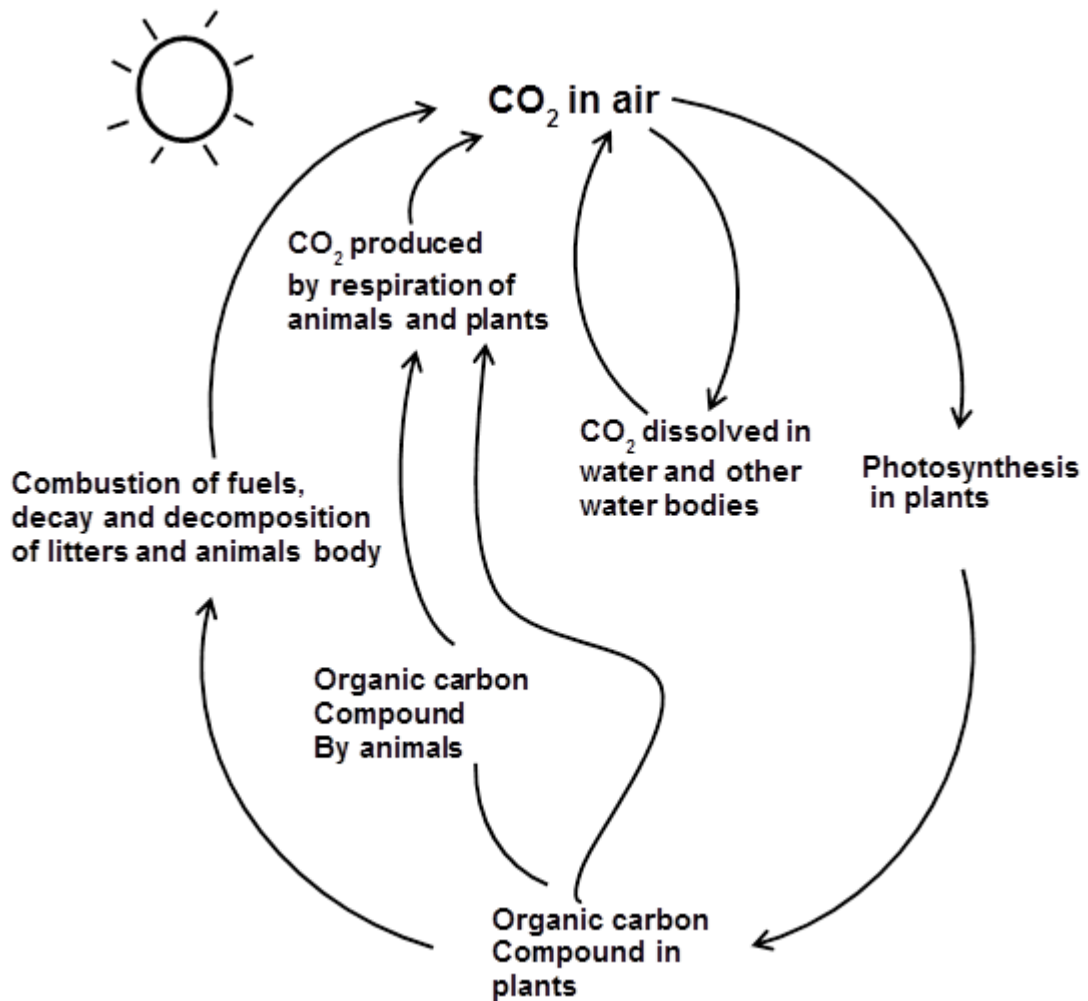


Figure 1- 2. Natural source of the carbon cycle. Adapted (National Oceanic and Atmospheric Administration, 2011)

1.3.2 Anthropogenic sources

The anthropogenic carbon dioxide sources were as a result of the continuous burning of fossil fuel to generate heat, steam, and electricity in the manufacturing industries as well as homes. There has been a significant growth of human sources of carbon dioxide emissions since the industrial revolution. The desire to live a comfortable life has led to human activities such as burning of gas, oil, coal as well as deforestation thereby increasing the concentration of carbon dioxide in the atmosphere.

The human-produced carbon dioxide emissions come from the burning of fossil fuels such as oil, natural gas, and coal with a share of 87%, while deforestation and other land hold about 9% and 4% for industrial processes such as cement manufacturing (see *Table 1*) (Le Quéré *et al.*, 2013, 2014).

1.4 Emissions of CO₂

The emissions of carbon dioxide have been steadily growing since the pre-industrial era reaching the level of 35.9 GT of 397 ppm in 2014 (Le Quéré *et al.*, 2015). The present CO₂ emission in 2018 is approximately 410 ppm from 280 ppm in the mid-1800s showing an average growth of ca. 2 ppm per year in the last 20 years. The report shows that the global total primary energy supply (TPES) has increased by 150% between 1971 and 2013 as a result of the world development and economic growth despite the huge surge of renewable development and nuclear energy sources (non-CO₂ emissions) have also been noticeable. This is as a result of the world energy supply that has been unchanged for over many decades and still in 2103 the use of fossil fuel accounts for approximately 87% of the world energy supply (Intergovernmental Panel on Climate Change (IPCC), 2005; Olivier *et al.*, 2011).

Undoubtedly, carbon dioxide emission is strongly linked to the combustion of fossil fuels. Petrochemical and chemical industry, cement industry and power plants are presently recognised as main sources of CO₂ emissions. Oil and coal have been the highest emissions of carbon dioxide till early 21st century where emission of CO₂ from oil superseded the emission of CO₂ from the use of coal. Although there was an upsurge of CO₂ emission from coal because of the higher consumption of coal to produce energy for industrial processes by developing countries such as China, India, and other Asia countries, which were found to have increased by 6,260 million metric tons collectively from 2005 to 2017 while the rest of the world collectively decreased by 220 million metric tons (IEA, 2015) (see *Figure 1- 3*).

The global coal emissions grew the most of any fuel from 2005–2017 period at 2.1% yearly while the natural gas-related emissions grew by 2.0% yearly, and petroleum-related emissions grew at 1.1% yearly. Further forecast for Coal-related emissions of CO₂ is expected to increase by 0.6% in 2018 and 2019. Petroleum-related emissions of CO₂ are projected to grow by 1.6% in 2018 but

drop by 0.2% in 2019. Natural gas-related emissions of CO₂ are projected to grow by 0.6% in 2018 and remain even in 2019 (EIA, 2017).

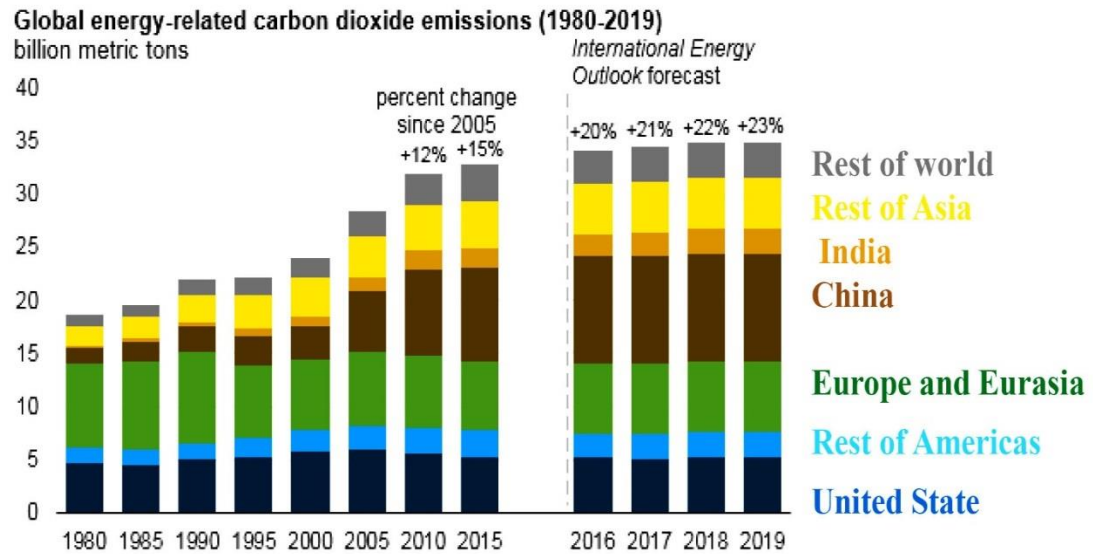


Figure 1- 3. Global emission of CO₂ from 1980 predicted to 2019. Source: U.S. Energy Information Administration, International Energy Statistics, International Energy Outlook, and Short-Term Energy Outlook

1.5 Policies of CO₂ emissions reduction

The general concept towards achieving effective solutions of CO₂ emission reduction policies is by understanding the global driving factors that influence the CO₂ emission. There is no doubt that the world population is growing and demand for energy has intensified thereby causing a severe increase in CO₂ emissions for the last few decades. It is evident that developed countries are responsible for the majority of greenhouse gases (GHG) emitted into the atmosphere over a century of years during the era of industrialisation. These countries are at the helm of greenhouse gases emission reduction policies. Furthermore, the developed countries prosper more from the era of industrialisation where more CO₂ emissions were prevalence. The fact still remains that in order to develop a sustainable way of CO₂ emission reduction in the earth's atmosphere all countries must be dedicated to meet the set target proposed.

Kyoto Protocol was the first international agreement for the GHG emissions reduction linked to the United Nations Framework Convention on Climate Change, adopted on 11 December 1997 and entered into force on 16 February 2005. The agreements were that the industrialised countries to reduce GHG emissions that includes (CO₂, N₂O, SF₆, CH₄, HFCs, PFCs) by 5% against 1990 levels during first commitment period (2008-2012). Although countries targets vary depending on the economic and political situation, for example, Germany target was -21%, France was 0% and the European Union was 8%. The second commitment period from 2013 to 2020 targets to reduce GHG emissions by 18% of the 1990 levels (Torrey, 2007). The second commitment period has not come into force because it requires two-thirds of the participating countries, which is 144 countries but only 49 countries have ratified Kyoto's protocol second commitment period as of 1st October 2015. Some of the biggest emitters (for example the United States) and other countries did not participate and that means it will require new international agreements (United Nations/Framework Convention on Climate Change, 2015).

A new international climate agreement was finalised in December 2015 at Paris during the United Nations Conference on Climate Change (COP21). These agreements will be applied from 2020 and involve the participation of developed and developing countries. The purpose of this agreement is to limit global temperature increase to less than 2 °C (United Nations/Framework Convention on Climate Change, 2015).

The European Union and its member states were able to meet the GHG emissions reduction commitments under the Kyoto Protocol of first commitment period easily because of their policies frameworks to develop low carbon economy and meet the long-term targets of reducing GHG emissions of about 80-95% of 1990 levels (Yin *et al.*, 2004). The first EU implementation target of the 20-20-20 policy of GHG reduction emissions is by 20%, which was higher than that of Kyoto Protocol agreements set. Having met the first target the European Union in 2014 set a new target for GHG emissions reduction by 40% with the respect to 1990 level for the 2030 year (EEA, 2016; Pérez-Fortes *et al.*, 2014; Yin *et al.*, 2004) (see *Figure 1- 4*).

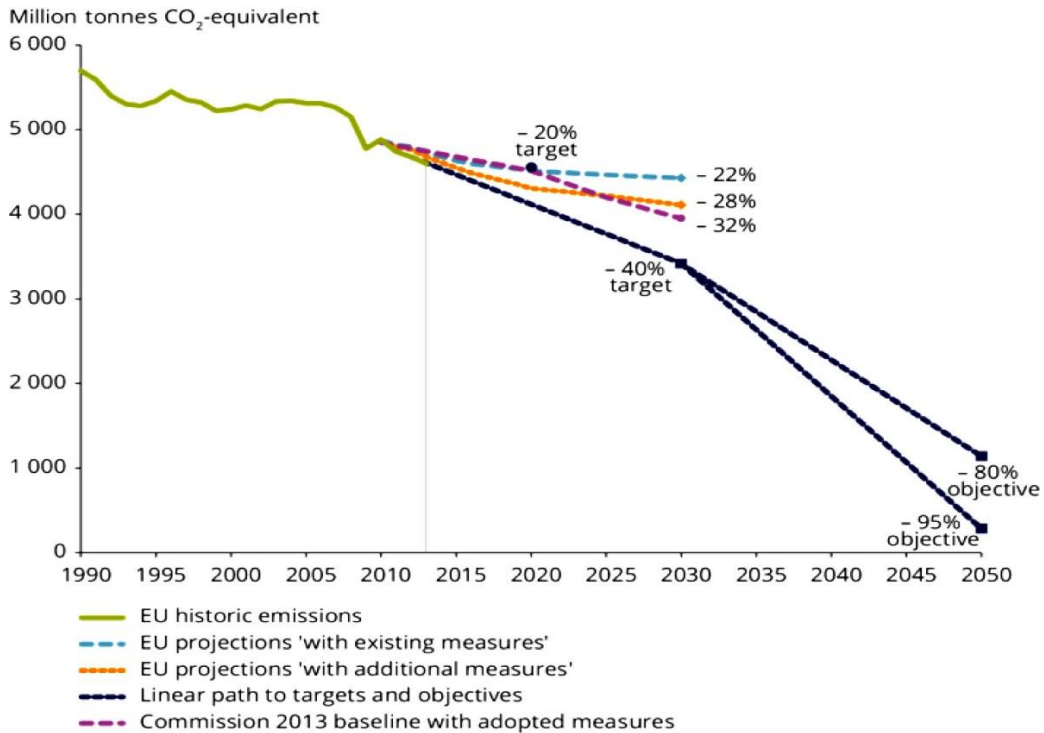


Figure 1- 4. Greenhouse gas emission trends (1990–2012), projections to 2030 and targets to 2050 (EEA, 2016).

1.6 Solutions for CO₂ emissions reduction

There are three strategical approaches to reducing CO₂ emission into the earth's atmosphere, which is energy consumption reduction, change in what we consume and change in attitude towards resources and waste (Hunt *et al.*, 2010). The well-developed countries are applying the first two strategies to reduce carbon consumption such as improving technologies with a higher efficiency that has resulted in decreasing consumption per capita and the use of renewables to replace fossil fuel-based energy source that includes solar, wind and biomass etc. Although the developed countries using carbon trading (cap and trade), which involves the use of financial incentives to reduce carbon dioxide emissions such as the use of a cap on the amount of CO₂ emissions and the least emitter of CO₂ could buy emission permits from those that have exceeded the allowable limit. Conversely, the change in attitude towards resources and waste are more significant that offers a key factor towards a sustainable development when compared to the first two strategies, which have limited capacity and could not be used as the only way of reducing CO₂ but one of the several approaches. There are known ways of reducing CO₂ emissions, which are carbon capture and

storage (CCS) and carbon capture and utilisation (CCU) (Cormos *et al.*, 2018; Styring *et al.*, 2011). These two methodologies of CCS technologies are aiming at capturing and subsequently storing waste CO₂ and the CCU is aiming at the synthesis of value-added chemicals. Besides, new technologies are currently being developed for CO₂ utilisation processes at such the use of both CCS and CCU are vital for the reduction of CO₂ emissions (Bennett *et al.*, 2014).

1.7 Developing attitude toward sustainability

Sustainability thrives on the concept of deriving a balance between three pillars such as an environment (signifies the planet), social (people) and economic (profit). These are the three main pillars that are required to be met without compromising the needs of the future generation (Krizmane *et al.*, 2016). Although, it is quite impossible that people would survive if there any no energy in recent times and the uses of energy drives industrial processes to produce products that make lives more habitable. The use of energy in process industries produce wastes that affect our planet and also cause global warming. Global warming is as a result of greenhouse gases emissions, mostly caused by continuous burning of fossil fuels, which have grave consequences, ones that are already becoming apparent. Therefore, there is a greater emphasis on developing an attitudinal change in achieving environmentally benign processes and more sustainable synthesis of greener chemicals.

The policies of CO₂ emissions reduction made in the Kyoto protocol and the Paris COP 21 submit on climate change have shown a step toward achieving a more sustainable environment. However, these policies made are not legally binding but every participated country has an obligation to meet those commitments and developing an attitude toward sustainability of CO₂ emissions reduction. The commitments to holding the average global temperature below 2°C will not only prevent global warming but save the planet and its habitats.

1.8 Research aims and objectives

The research aims and objectives of this study are as follows:

To extensively study the utilisation of CO₂ as a raw material for the synthesis of value-added chemicals that includes 1,2-butylene carbonate (BC), and styrene carbonate (SC). To further design and develop greener catalytic processes that

are sustainable for the production of SC and BC. These studies and development of greener processes that are sustainable for the synthesis of SC and BC have been achieved by using mixed metal oxides catalysts in the absence of organic solvent.

To investigate the performance of commercially available heterogeneous catalysts for the synthesis of BC and SC. A part of the research was conducted in collaboration with MEL Chemicals Ltd. The used heterogeneous catalysts are zirconium oxide (ZrO), magnesium oxide (MgO), cerium oxide (CeO), lanthanum oxide (LaO), ceria doped zirconia (Ce-Zr-O), lanthana doped zirconia (La-Zr-O), and ceria lanthana doped zirconia (Ce-La-Zr-O). Furthermore, graphene-based nanocomposite catalysts have been synthesised by using the conventional method and also continuous hydrothermal flow synthesis (CHFS) reactor e.g ceria, lanthana doped zirconia/graphene oxide (Ce-La-Zr/GO) and copper doped zirconia/graphene oxide (Cu-Zr/GO). The catalytic performance of these graphene-based inorganic nanocomposite catalysts for the synthesis of BC and SC has been studied.

To characterise the heterogeneous catalysts such as the metal oxides that include LaO, ZrO, CeO, GO and mixed metal oxides, which are Ce-Zr-O, La-Zr-O, Ce-La-Zr-O, Ce-La-Zr/GO, and Cu-Zr/GO using different characterisation techniques that include scanning electron microscopy (SEM), transmission electron microscopy (TEM), Brunauer- Emmett-Teller (BET), Raman spectroscopy (RS), X-ray photoelectron spectroscopy (XPS) and X-ray powder diffraction (XRD) analysis to study the morphology, molecular structure and physiochemical properties of the catalysts.

To investigate the effect of several parameters such as reaction temperature, heat treatment temperature, CO₂ pressure, reaction time, catalyst loading, and stirring speed in order to determine the optimum reaction conditions for the synthesis of BC and SC.

To investigate different reaction conditions for the synthesis of BC and SC using a direct synthesis of cycloaddition reaction of CO₂ to its respective epoxides in order to achieve a better yield and selectivity of the desired product. These reactions have been conducted in a high-pressure reactor (autoclave) in the presence of heterogeneous catalysts without any organic solvent.

To investigate the catalytic stability of the heterogeneous catalysts for the synthesis of BC and SC. Reusability studies have been conducted in a high-pressure reactor using a fresh catalyst to run an experiment and reused six times for the synthesis of BC and SC respectively to examine the long-term stability of the catalysts.

To limit and substitute the process complexity of using the homogeneous catalytic system with a greener direct route synthesis of the solvent-free heterogeneous catalytic system. This has been achieved experimentally involving a simple reaction procedure with a single separation process of the mixed metal oxides catalysts.

To replace the conventional processes of synthesising BC and SC with an effective heterogeneous catalytic process that requires no organic solvent. This has been achieved by using highly stable and active heterogeneous catalysts.

To use response surface methodology (RSM) to optimise the reaction conditions and validates the predicted model experimentally in order to maximise the yield of BC and SC. This predicted model has been validated experimentally and achieved optimum reaction conditions.

1.9 Novelty of the present study

There have been extensive reports of styrene carbonate (SC) synthesis through cycloaddition reaction of CO₂ and styrene oxide (SO) in the presence of organic solvent to enhance the rate of conversion and yield of SC. The use of solvents includes dimethylformamide (DMF), tetrahydropyran (THP), *tert*-butanol (tBA), zinc chloride (ZnCl₂) methanol (MeOH) etc and also most of the reported reactions for the synthesis of styrene carbonate have been facilitated with the use of cocatalysts such as tetrabutylammonium iodide (TBAI), 4-dimethylamino pyridine (DMAP), tetrabutylammonium bromide (TBAB), phenyltrimethylammonium tribromide (PTAT). These cocatalysts are used up in the system without being recovered. Presently, no researcher has reported the use of mixed metal oxide without the use of co-catalyst or an organic solvent for the synthesis of styrene carbonate. The novelty of this study is the use of Ce-La-Zr-O heterogeneous mixed metal oxides catalyst and also graphene-based inorganic nanocomposite catalysts to synthesise styrene carbonate without any addition of cocatalyst and an organic solvent for producing remarkable yields of

52% and 62% for Ce-La-Zr-O and Ce-La-Zr/GO respectively, which have never been reported. Furthermore, the use of response surface methodology (RSM) to develop regression models in the established significant process variables and predicting the optimised variables, which have been experimentally validated.

Presently there is no report on the direct synthesis of 1,2-butylene carbonate using heterogeneous catalyst apart from the conventional method, which produces toxic waste and uses harmful chemicals for the production of 1,2-butylene carbonate. However, the use of direct synthesis will not only offer a greener process but also contribute to limiting the emission of CO₂ into the atmosphere. Furthermore, the novelty is also the preparation of highly effective Cu-Zr/GO inorganic composite catalyst, which has never been reported for the synthesis of BC.

1.10 Thesis structure

The structure of the thesis is as follows:

CHAPTER 1: INTRODUCTION

This chapter, present the motivation for this research works. The background of CO₂, sources of CO₂, emissions of CO₂, policies of CO₂ emissions, policies of CO₂ emissions reduction, solutions for CO₂ emissions reduction and sustainability are extensively discussed. The aims and objectives of the research are also included in this section as well as the novelty of this research and the thesis structure.

CHAPTER 2: LITERATURE REVIEW

A detailed literature review of carbon dioxide (CO₂), its applications, properties, catalysis and organic carbonates are presented. This chapter presents an elaborate approach of CO₂ transformation to organic carbonate such as cyclic and polycyclic carbonates. Also focus on a detailed review of different synthesis route for styrene carbonate, 1,2-butylene carbonate, properties and industrial applications. This chapter also highlights various types of catalytic systems employed for the synthesis of styrene carbonate and 1,2-butylene carbonate.

CHAPTER 3: MATERIALS AND METHODS FOR CATALYSTS SYNTHESIS AND CHARACTERISATION

In this chapter, metal oxides, and mixed metal oxides synthesis through continuous hydrothermal flow synthesis (CFHS) reactor, conventional methods, Hummer's and Offa's method are presented. This is followed by the detailed presentation of physicochemical properties of the commercial catalysts and the synthesised catalysts. Furthermore, the BET surface area, scanning electron microscopy (SEM), transmission electron microscopy (TEM), X-ray photoelectron spectroscopy, X-ray diffraction and Fourier transform infrared spectroscopy (FT-IR) are discussed.

Chapter 4: GREENER SYNTHESIS OF 1,2-BUTYLENE CARBONATE FROM CO₂ USING GRAPHENE-INORGANIC COMPOSITE CATALYST

This chapter provides a detailed description of continuous hydrothermal flow synthesis of a green rapid, highly effective ceria, lanthana, zirconia doped graphene inorganic nanocomposite catalyst, which has been used for the synthesis of 1,2-butylene carbonate in cycloaddition reaction of CO₂ to 1,2 butylene oxide along with other heterogeneous catalysts. Catalysts preparation and characterisation have been presented. This is followed by a detailed explanation of experimental setup, experimental procedure and method of analysis. The results and discussions cover extensive discussions on reaction pathway, proposed reaction mechanism, effect of different heterogeneous catalysts, effect of mass transfer, effect of reaction time, effect of catalyst loading, effect of reaction temperature, effect of reaction temperature and effect of CO₂ pressure. Furthermore, the long-time stability of Ce-La-Zr/GO is presented by conducting reusability studies.

CHAPTER 5: SYSTEMATIC MULTIVARIATE OPTIMISATION OF 1,2-BUTYLENE CARBONATE SYNTHESIS VIA CO₂ UTILISATION USING GRAPHENE-INORGANIC NANOCOMPOSITE CATALYSTS

This chapter provides the modelling and optimisation of 1,2-butylene carbonate using Box Behnken Design (BBD) to study the single and several independent reaction variables (such as temperature, pressure, time and catalyst loading). Furthermore, multiple responses optimisation and optimum conditions validation are presented.

CHAPTER 6: GREENER SYNTHESIS OF STYRENE CARBONATE USING COMMERCIAL HETEROGENEOUS CATALYSTS (METAL OXIDE AND MIXED METAL OXIDE CATALYSTS)

This chapter gives a detailed background for synthesis of styrene carbonate; description of materials used, experimental methods, catalyst characterisation, and method of analysis are presented. Furthermore, results and discussion that covers reaction pathway, proposed reaction mechanism, effect of different heterogeneous catalysts, effect of mass transfer, effect of reaction time, effect of

catalyst loading, effect of reaction temperature and effect of CO₂ pressure are discussed. The response surface methodology (RSM) modelling and optimisation of the process are explained. The batch studies for catalyst stability and reusability studies are presented.

CHAPTER 7: A FACILE AND GREENER SYNTHESIS OF 1,2-BUTYLENE CARBONATE VIA CO₂ UTILISATION USING A NEW COPPER–ZIRCONIA /GRAPHENE CATALYST

This chapter presents a detailed description of a facile and greener synthesis of 1,2-butylene carbonate using a conventional synthesis of a new copper–zirconia /graphene catalyst at a lower reaction time. This is followed by a detailed discussion of catalyst characterisation results, description of the experimental set-up, pathway and proposed reaction mechanism. The effect of catalyst treatment, catalyst loading, reaction temperature, CO₂ pressure and reaction time are extensively evaluated. The re-usability study of Cu-Zr/graphene inorganic catalyst is presented in detail.

CHAPTER 8: CONCLUSIONS AND RECOMMENDATIONS FOR FUTURE WORK

In this chapter, conclusions of the overall research work and recommendations for future research work are summarised and outlined respectively.

CHAPTER 9: REFERENCES

This chapter shows all the used references from literature, which have been cited in this research work.

CHAPTER 10: APPENDICES

This chapter provides relevant materials and helpful information that support this research work.

CHAPTER 2

LITERATURE REVIEW

CHAPTER 2: LITERATURE REVIEW

2.1 Introduction

The natural carbon cycle has been upset by the continuous use of fossil fuel and its known consequence of continuous emission of carbon dioxide from the use of fossil fuel is climate change and global warming (Dincer *et al.*, 2013). Carbon dioxide has been recognised as one of the greenhouse gases responsible for the present environmental challenges, which can be used as a precursor to promote green chemical processes and environmental sustainability. The use of carbon dioxide as raw materials to synthesise value-added chemicals in the presence of heterogeneous catalyst will not only offer a green chemical process but also contribute to environmental sustainability, climate change and global warming prevention.

This chapter gives an overview of the carbon dioxide utilisation, focusing on organic carbonate syntheses. It reviews different homogeneous and heterogeneous catalytic processes in the presence of organic solvents reported in numerous research work. It analyses and reviews the advantages and disadvantages of the use of heterogeneous and homogeneous catalysts for the synthesis of organic carbonates. Furthermore, this chapter covers the method used to prepare the heterogeneous catalyst and its applications.

2.2 Carbon dioxide

Carbon dioxide (CO₂) is a triatomic molecule that is recognised as a non-toxic, inexpensive, renewable and widely abundant carbon source and attractive C1 building block for organic synthesis that can replace poisonous chemicals such as phosgene, carbon monoxide or isocyanates (Aresta and Dibenedetto, 2010). The carbon cycle of CO₂ occurs naturally in the aquatic and terrestrial environment in which the two known processes are photosynthesis and metabolism. The main sources of CO₂ emissions are coal, deforestation, fossil fuels and natural gas (Völker, 2008). The emissions of CO₂ through these major sources have increased the concentration of CO₂ in the atmosphere and kept on rising steadily in the last 200 years. In recent years, there has been increasing research in using CO₂ as starting material for the synthesis of value-added chemicals. Carbon dioxide (CO₂) is an inert linear triatomic molecule that is less

reactive at room temperature. The carbon atom of CO₂ is covalently bonded to two oxygen atoms *via* two double bonds and the central carbon atom is *sp*-hybridised. The activation of CO₂ can be achieved using highly reactive reactants such as epoxides and also the application of reducing agents such as amalgams, complex hydrides, and hydrogen.

2.2.1 Carbon cycle

The natural circulation of atmospheric CO₂ (see Chapter 1, *Figure 1- 2*) is integrated into two cycles. Firstly, the biological cycle of CO₂ that exists between photosynthesis and metabolism (respiration of living creature) and mineralisation of dead carbon-based material in equilibrium. Secondly, the chemical cycle that involves the exchange of atmospheric CO₂ and the deep oceans CO₂ with the sediments that are well balanced. The exchange between the soil and atmosphere is estimated at 200 Gt annually and 6.5 Gta⁻¹ of CO₂ from fossil fuels by human activities. Deforestation is estimated to have contributed to 2Gta⁻¹.

2.2.2 Physicochemical properties of carbon dioxide

Carbon dioxide is a colourless gas and occurs naturally in earth's atmosphere known as a trace gas. CO₂ gas becomes solid dry ice at normal room temperature and pressure that is below 194.5 K and turn to liquid only at a pressure above 5.1 bar. The triple point refers to the temperature and pressure at which the three phases (gas, liquid and solid) of CO₂ coexist in thermodynamic equilibrium. The triple point of CO₂ starts from 5.1 bar at 217 K and the supercritical state (sc-CO₂) behaves as a gas at a temperature higher than 304.1 K and pressure higher than 73.9 bar (Hewitt, 1996; Styring *et al.*, 2014a) (see *Figure 2- 1*). CO₂ in the supercritical state is an excellent medium promoting mass transfer in a process due to its low viscosity and high density. The low surface tension of supercritical CO₂ increases the rate of reaction and prevents catalyst coking. There are several properties of carbon dioxide that make it relevant to the process industry. CO₂ is also known to be an oxygen carrier and this enables it to be used in mild oxidation reactions (Bradshaw and Cook, 2001). *Table 2- 1* shows the physical and chemical properties of carbon dioxide.

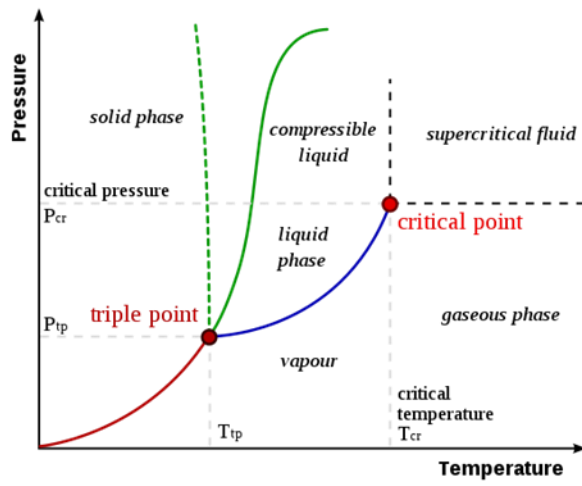


Figure 2- 1. CO₂ phase diagram

Table 2- 1. Physical and chemical properties of carbon dioxide (Styring *et al.*, 2014a)

<i>Physical and chemical properties of CO₂</i>	
<i>Molecular formula</i>	CO ₂
<i>Molecular weight</i>	44.0059 g/mol
<i>Critical temperature</i>	304.1 K
<i>Critical pressure</i>	73.9 bar
<i>Critical density</i>	467 kg/m ³
<i>Molar volume</i>	44.7 cm ³
<i>Composition</i>	C (27.29%) O (72.71%)
<i>Boiling point (1.013 bar)</i>	194.5 K
<i>Triple point temperature</i>	216.5 K
<i>Triple point pressure</i>	5.18 bar
<i>Solubility in water at STP</i>	1.716 vol/vol
<i>Gas density at STP</i>	1.976 kg/m ³
<i>Liquid density</i>	770 kg/m ³
<i>Solid density</i>	1560 kg/m ³
<i>Gas specific volume at STP</i>	0.506 m ³ /kg
<i>Number of electrons</i>	16
<i>Ionisation potential</i>	13.73 eV
<i>Electron affinity</i>	3.8 eV
<i>Bond length</i>	1.16 Å
<i>Bond Angles O=C=O</i>	180°

The C=O distance is 1.16 Å with a linear molecule, which contains two polar C=O bonds with a set of two orthogonal π orbitals. The potential energy of CO₂ is 13.7 eV with an electron affinity of 3.8 eV that makes it a poor electron donor and an electron acceptor. These make CO₂ very stable molecule and requires high energy to break the bond, highly active metal catalysts to activate the two different reaction sites present in the CO₂ molecule (Aresta *et al.*, 2015). The carbon atom of CO₂ is an electrophilic centre of Lewis acid character while the oxygen atoms are of nucleophilic centre of weak basic Lewis character. Several catalytic reactions need both acidic and basic centres to be activated for the easy

interaction of the metal oxide catalysts on carbon and oxygen atoms (Aresta *et al.*, 2015; Lu, 2015).

2.2.3 Carbon dioxide as a green solvent

The industrial use of organic solvents have environmental challenges and cost implications. Organic solvents are flammable, toxic and contributed to health problems as well as the severe environmental impacts as a result of its contribution to smog formation (Aresta and Dibenedetto, 2007). The quest to eradicate hazardous organic solvents and the zeal to discover valuable nonhazardous solvents is a key purpose of green processes. The application of CO₂ as a liquid or supercritical solvent mirrors an ideal green solvent's characteristics. CO₂ is abundant, cheap, renewable, nonflammable, nontoxic, environmentally benign compound and available in high purity at low cost and therefore can be used as a solvent (Loupy, 1999). The industrial use of CO₂ as a solvent is produced from numerous industrial processes including cement, fermentation, and fertilizer production. The purified generated CO₂ is cooled to the liquid state and compressed at 20 bar, which can be reused in various liquid and supercritical CO₂ processes.

Attention has been drawn to the potential use of supercritical CO₂ in green processes as a solvent in recent years due to its amazing properties that can be exploited by researchers for many useful industrial processes. These properties include low viscosity, high diffusivity and the density of supercritical CO₂ can be varied to suit desired purposes. This is achieved by slight changes in temperature or pressure around the critical point. The influences of supercritical CO₂ properties also include dissolving several non-polar compounds beyond its vapour pressure. Furthermore, CO₂ in its supercritical state can also dissolve into condensed phases and thereby reducing the surface tension and viscosity. These unique characteristics of supercritical CO₂ that includes low viscosity, variable density and high diffusivity have led to the wider use as a green solvent in diverse areas (for examples cleaning, extractions, impregnations and particle formation) (Nalawade *et al.*, 2006).

2.3 Applications of CO₂

Carbon dioxide is recognised as a valuable industrial gas that can find its applications in many areas in industries. The potential and current applications of CO₂ are illustrated in *Figure 2- 2* (McConnell, 2012).

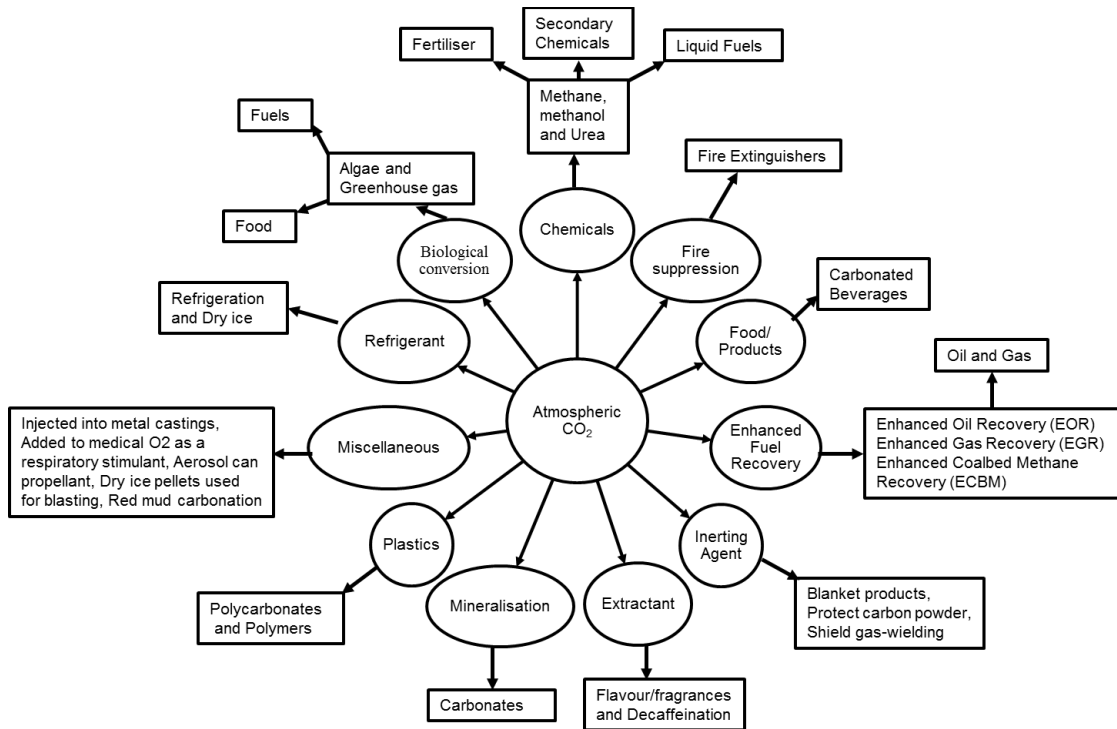


Figure 2- 2. The application of atmospheric CO₂ (McConnell, 2012)

The industrial current uses of carbon dioxide are significant and can be classified as the commercial application of CO₂ (this includes food production, preservation, storage, fire extinguisher, water treatment, refrigerant etc.), enhanced fossil fuel recovery (ECCR), biological, pharmaceuticals production, and chemical feedstock utilisation. Some of these applications after uses often contribute to the atmospheric carbon dioxide and thereby resulting in complication towards the genuine reduction of CO₂ emission. The obvious future applications are the use of biological and chemical conversion, which offers long-term CO₂ fixation.

2.3.1 Commercial applications of CO₂

The current commercial applications of CO₂ such as food production, preservation, storage, fire extinguisher, water treatment, the refrigerant is

relatively low compared to the emission of CO₂ into the atmosphere. Presently, the commercial application CO₂ is estimated around 15-20 Mt/year and this will increase over the coming decades depending on government policies (Hunt *et al.*, 2010).

The application of CO₂ into food and beverage industries include carbonate beers, soft drinks, wines and sparkling waters while another application in food production is packing under a controlled atmosphere, which limits food oxidation and microbial growth in the processed food. The carbonisation of beverages with CO₂ is known as the fermentation process. The industrial use of supercritical CO₂ for decaffeination of coffee is on a larger scale and also for the extraction of flavours and fragrances.

2.3.2 Enhanced fossil fuel recovery

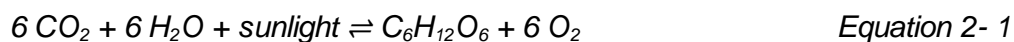
The application of CO₂ in enhanced fossil fuel recovery has been a known technique to extract coal, oil and natural gas as well as CO₂ storage. This method involves, the injection of CO₂ as a solvent into a depleted well (fossil fuel field) in order to increase the productivity of the extraction field. The primary function of the injected CO₂ solvent is to reduce the viscosity of the oil so that the oil can flow easily to the production well and CO₂ is stored permanently in the oil field when production is completed. This process is known to be relatively safe and increase the production rate.

Enhanced coal bed methane recovery (ECBM), enhanced oil recovery (EOR) and enhanced gas recovery (EGR) are the known enhanced recovery processes. The ECBM processes are similar to EOR and EGR. This method involves the injection of CO₂ into a depleted coal field with the purpose to enhance methane recovery, which can be exported or used for electricity generation. Although the ECBM is developing when compared to EOR and EGR, which are mostly used in advanced countries e.g. United States and the United Kingdom.

The enhanced fuel recovery technologies offer high CO₂ storage facilities. In 2010, the United State Department of Energy recorded an estimate of 0.56 Gt CO₂ consumed by EOR and the total storage capacity of CO₂ for oil and gas reservoirs is estimated to 138 Gt CO₂ (Curie, 2016). Conversely, this process not only shown to reduce the CO₂ emission but also increase the production of fossil fuels.

2.3.3 Biological uses of CO₂

There are natural biological uses of CO₂, however, the biological uses of CO₂ are primarily focused on the man-made created processes to produce biomass and biofuel using the principle of photosynthesis (refer to *Equation 2-1*) (Meylan *et al.*, 2015).



The application of CO₂ in horticulture provides greenhouses to maintain CO₂ concentration and improve plant growth. The use of CO₂, stimulate growth in marine organisms, which are a rich source of biomass for e.g., algae. The algae organisms can be used for biofuel production, which can produce energy on a larger scale. The biological uses of CO₂ are massive and it has been estimated ca. 1.8 tons of CO₂ is needed for the production of 1 ton of algal biomass (Martens *et al.*, 2017; Quadrelli *et al.*, 2011). Besides, this production requires a high volume of low quality of CO₂ and flue gases from power plants could be used.

2.3.4 Pharmaceuticals uses of CO₂

The use of CO₂ is receiving attention in the pharmaceutical processing industry. Several reported applications of CO₂ as a reaction medium provides huge potential for large-scale uses in the pharmaceutical industry such as particle formation with dense CO₂ and clean synthesis of drug compounds (Subramaniam *et al.*, 1997). The pharmaceutical industry uses spray drying technique for preparation of microcapsules, which is quite fast and prevents degradation of the product (Perumal, 2001). Although, the drawback of this technique is the production of powders with wide size distributions. The drawback, in the case of salting out a second liquid solvent that is added to the solution, is difficulty in controlling particle size and particle size distribution of precipitates and elimination of the organic solvent (Perumal, 2001). The use of supercritical CO₂ as solvents offers an alternative solution to the various problems encountered in traditional techniques. Supercritical CO₂ has important advantages when compared with several traditional solvents as it is non-toxic, non-flammable and inexpensive (Reverchon and De Marco, 2006). The use of

scCO₂ in pharmaceutical processing offers environmental advantage solvents elimination and products recovery with no residue left. Moreover, a dry solid product is easily obtained by the use of manipulating pressure (Jung and Perrut, 2001; Girotra *et al.*, 2013).

In modern medicine, about 5% CO₂ is added to pure oxygen to stimulate breathing and also used for stabilisation of O₂ and CO₂ balance in the blood. The use of CO₂ is commonly known as an insufflation gas for minimally invasive surgery (such as arthroscopy, endoscopy and laparoscopy) to expand and calm the body cavities in order to give better visibility of the surgical area. Furthermore, it can be used for respiratory stimulation during and after anaesthesia. CO₂ can be used for cryotherapy were moles, skin tags and wart can be removed. The high pressure of CO₂ is also used for sterilisation of medical equipment (Zhang *et al.*, 2006).

2.3.5 Utilisation of CO₂ as a chemical feedstock

The effect of CO₂ on global warming has generated lots of concern in the research community. This has led to researcher discovering that CO₂ recognised to be one of the greenhouse gases that cause global warming is no longer considered as a harmful pollutant but an important carbon source that is used as a value-added chemical (Darensbourg, 2010). The application of CO₂ as a chemical feedstock offers great potential with several advantages and industrial opportunities just as discussed in Chapter 2, section 2.3. Furthermore, *Figure 2-3* shows the current catalytic conversion of CO₂ into value-added chemicals and synthetic fuels. Some of the advantages CO₂ of utilisation offers over storage:

- The utilisation of CO₂ reduces the cost of transportation and storage system.
- It promotes the synthesis of valuable chemicals (such as organic carbonate) that can act as a substitute and replacement for existing toxic chemicals that produce harmful waste (e.g. phosgene).
- It promotes the positive public perception of companies engaging in the utilisation of CO₂ and it gives an edge to further drive the governmental policies of engaging in green technology.

- The companies market shares increase with the synthesis of new chemicals.

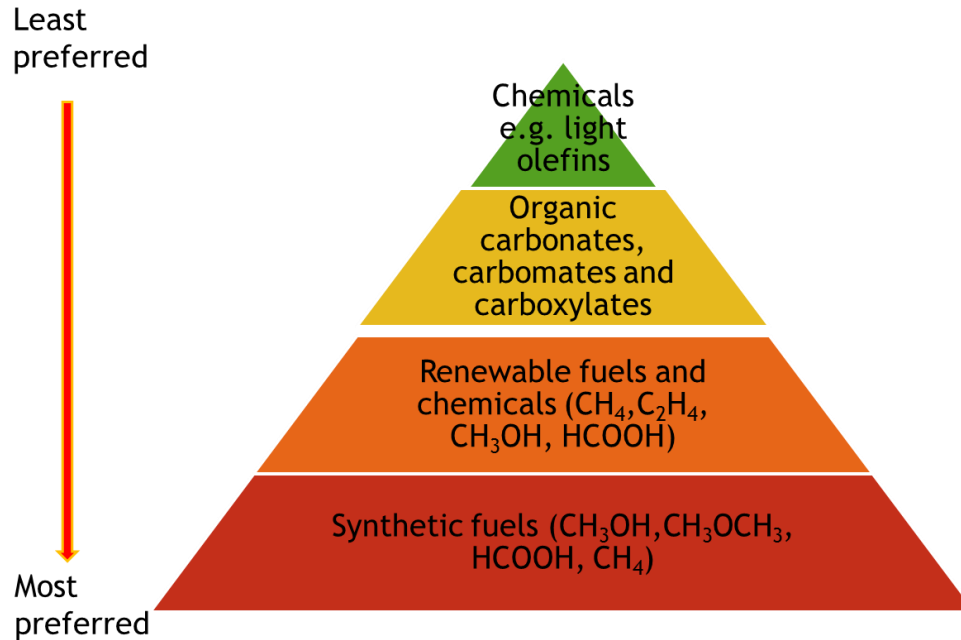


Figure 2- 3. Conversion of CO_2 into value-added chemicals and synthetic fuels hierarchy

Figure 2-3 shows the potential hierarchy process that involves the use of CO_2 on an industrial scale in the coming decade providing a new carbon-based economy. The conversion of CO_2 into synthetic fuels and renewable fuels are the most preferred.

Table 2-2. Utilisation of CO₂ (Aresta *et al.*, 2013)

Industry	Actual production	Usage (MtCO ₂ /y)	Future production	CO ₂ needed (MtCO ₂ /y)
Urea	155	114	180	132
Methanol	50	8	60	10
Dimethyl ether (DME)	11.4	3	>20	>5
Methyl tert-butyl ether (TBME)	30	1.5	40	3
Formaldehyde (CH ₂ O)	21	3.5	25	5
Organic carbonates	0.2	0.005	>2	0.5
Polycarbonates	4	0.01	5	1
Inorganic carbonates	200	50	250	70
Technological	-	28		80
Algae for biodiesel production	0.005	0.010	1	2
Total		200		299

Table 2-2 also shows the utilisation of CO₂ into chemicals and non-chemical applications range around 200 Mt/y as of 2013 (Aresta *et al.*, 2013). The potential process that involves the use of CO₂ on an industrial scale in the coming decade will provide a new carbon-based economy. The conversion of CO₂ into fuels and organic carbonates are predicted to play a major role in the management of CO₂ emission strategies. Although the conversion of CO₂ into fuel will be a huge market when compared to Organic carbonate because CO₂ emissions were as a result of energy produced from fossil fuel.

2.4 Organic carbonate

The formation of a stable organic carbonate is from a process of esterification of carbonic acid. The carbonic acid is not stable at room temperature, which is isolated in its pure form at a lesser temperature and characterised using spectroscopic techniques (Hage *et al.*, 1993). Carbonic acid is an important compound that promotes proton transfer reactions in a system containing carbonates either biological or geochemical (Millero *et al.*, 2002). Organic carbonate is the diesterification of carbonic acid where the functional group comprises two alkoxy groups from a carbonyl group. The type of substituents of the hydroxy groups is used to identify different types of organic carbonates. The simplest form of organic carbonates is dimethyl carbonate, which is produced in larger industrial scale *via* catalytic oxycarbonylation of methanol, which has

replaced the synthesis of many organic carbonates *via* unsafe phosgene or dimethyl sulphate route (Shaikh and Sivaram, 1992). The followings are the types of organic carbonates: acrylic carbonate, cyclic carbonate and polycarbonate.

2.4.1 Classification of organic carbonates

The organic carbonates can be classified into two saturated and unsaturated carbonates. The saturated carbonates include the aromatic, aliphatic and aliphatic-aromatic. The aliphatic consist of the linear, alicyclic and branched carbonate, while the aromatic comprises of simple carbonate, activated carbonated through substitution and cyclic carbonates. *Figure 2-4* gives comprehensive details of the classification of organic carbonates.

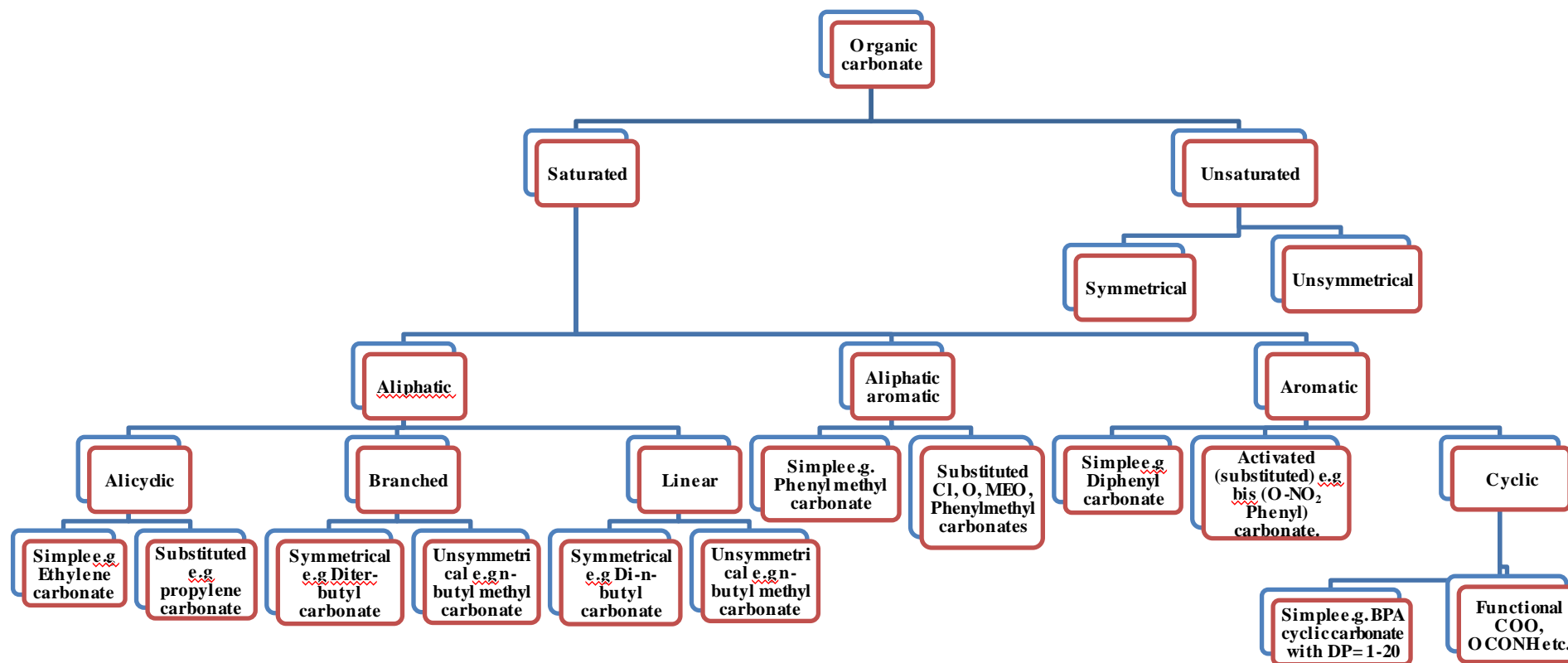


Figure 2- 4. Classification of organic carbonates (Shaikh and Sivaram, 1996)

2.4.2 Properties and application of 1,2-butylene carbonate and styrene carbonate

Cyclic carbonates are colourless liquid, almost insoluble in water and have a pleasant odour. In 1996, Shaikh and Sivaram stated that cyclic carbonates are soluble in organic solvent most especially polar solvent such as alcohols, aromatic hydrocarbons, ethers, esters and ketones. 1,2-Butylene carbonate is less soluble, but in water at room temperature of 298 K, only 7 g of 1,2-butylene carbonate dissolves in 100 g of water. Its molecular weight is 116.12 g/mol, the density at room temperature is 1.14 g/mL and boiling point is 523 K (Table 1). BC could be used extensively as chemical reactive intermediates that are the reaction with alcohols, amines and carboxylic acids for industrially synthesis of important compounds including plasticisers, polymers and surfactant (Clements, 2003; Xiaohua *et al.*, 2014). The BC application is not only limited to cure accelerator reactions in foundry sand binding but used to manufacture wood products and extraction of phenol formaldehyde (Huntsman Co-operaton, 2001). BC is an essential cyclic carbonate that is used as an alternative solvent for asymmetric hydrogenation (Schäffner *et al.*, 2009). Furthermore, BC is a valuable chemical used as an extractive solvent e.g. the extraction of phenol from industrial waste and toxic pollutant that are hazardous to environment and health (Schäffner *et al.*, 2010). In hydroformylation, BC solvent is used for catalyst separation from the reaction mixture and also used to produce lactone from the reaction of CO₂ and butadiene (Behr *et al.*, 2007).

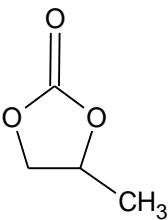
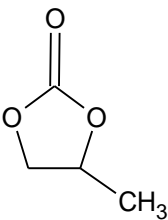
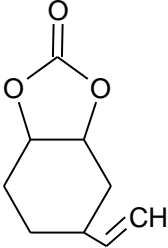
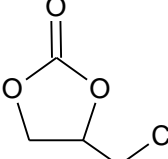
Table 2- 3 shows the physical properties of SC, at room temperature the density of SC is 1.25 g/mL with a molecular weight of 164.15 g/mol. SC is an important chemical in the processing industry, which can be used as a precursor for polymeric materials, intermediates in the production of pharmaceuticals and fine chemicals (Xiang *et al.*, 2009). SC solvent can be used as an electrolyte for producing lithium-ion batteries, which can serve as energy storage (Appaturi and Adam, 2013; Ravi *et al.*, 2015).

Table 2- 3. Physical properties of 1,2-butylene carbonate (BC) and styrene carbonate (SC)

Properties	BC	SC
Molar Mass (g/mol)	116.12	164.15
Boiling point K	523	627
Density (g/mL at 298 K)	1.14	1.25
Freezing point K	323	-
Flashpoint K	408	444.1
Melting point K	228	-

BC and SC can be synthesised by direct reaction of CO₂ to their respective epoxides (BO and SO) and they are biodegradable when released to the environment, which further support the view of the eco-friendly character of both carbonates. Table 2- 4, shows the applications of other cyclic carbonates.

Table 2- 4. Application of other cyclic carbonates.

Cyclic carbonates	Structure	Applications	References
Ethylene carbonate (EC)		It is used as a plasticizer, and as a precursor to vinylene carbonate, which is used in polymers and in organic synthesis. It is used as a green solvent for the modification of corn cob that is a lignocellulose residue from wet or dry milling processes during ethanol production, industrial and food. It is also used as a reactive intermediate for the formation of alkoxylation, carbamate and transesterification	(Bhanage <i>et al.</i> , 2003; Chamú-Muñoz <i>et al.</i> , 2015; Vollmer <i>et al.</i> , 2004)
Propylene carbonate (PC)		Used as a solvent for stripping of paint, degreasing, cleaning application and for producing cosmetic as well as medication, It is used as an intermediate chemical for the synthesis of dimethyl carbonate, polyurethane and polycarbonate	(Adeleye <i>et al.</i> , 2014; Aresta and Dibenedetto, 2007)
4-vinyl-1-cyclohexene carbonate (VCHC)		It is used as an antifoam agent for antifreezing, additive and plasticizers as well as intermediate for producing glycerine carbonate, methoxymethyl carbonate.	(Lee <i>et al.</i> , 2008)
Epichlorohydrin carbonate (CMEC)		It is used as pesticides, insecticides and disinfectants	(Aresta and Dibenedetto, 2010; Burton <i>et al.</i> , 2010)

2.4.3 Methods of organic carbonate synthesis

There are several known methods of organic carbonate synthesis. These are as follows:

- Phosgenation synthesis

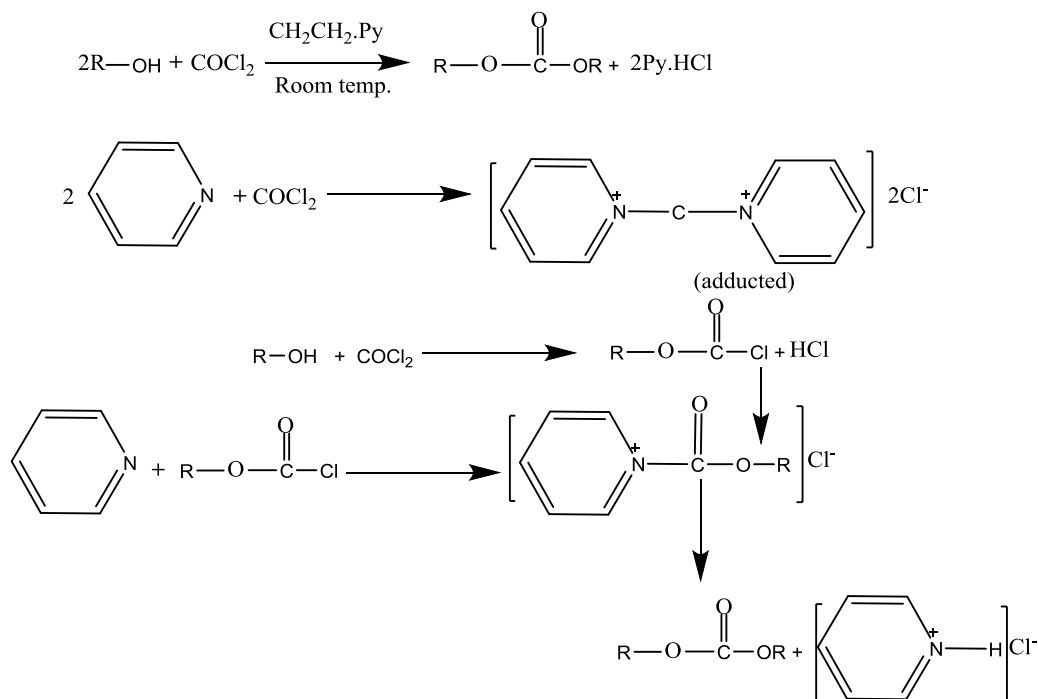
- The reaction of urea with alcohols or phenols
- Oxidative carbonylation of alcohols and phenols
- The transesterification of carbonate
- Carbonate interchange reaction
- The synthesis of organic carbonates by CO₂ utilisation

2.4.3.1 Phosgenation synthesis

The phosgenation process involves the use of alcohols or phenols, which are dissolved in an inert anhydrous solvent of excess pyridine (another substitute can be nitrogen based bases) and phosgenated at below ambient temperature. The use of pyridine as the base is to form an ionic adduct when reacted with phosgene. The formed ionic adduct is more reactive than the chlorocarbonic acid esters. Symmetric carbonates are synthesised in one step while unsymmetrical are produced by two-step reaction and these processes account for most of the synthesis of organic carbonates (*Scheme 2- 1*) (Shaikh and Sivaram, 1992).

Aromatic hydroxy compounds are regarded as slow reaction with phosgene when compared with aliphatic hydroxy compounds. This is because the more acidic hydroxy a compound contains the less reactive toward phosgene (e.g. halogenated phenol react slower than phenol). The direct reaction of the hydroxy compound with phosgene in the absence of an organic base requires higher temperature from 323 K to 423 K and can result to low yields of carbonates with unreacted chlorocarbonates as well as the formation of unwanted products (Babad and Zeiler, 1973).

The advantages of this phosgenation method of synthesis give higher yields, the most possibility to synthesise functionalised and activated carbonates although the obvious drawbacks are the application of toxic chemicals like pyridine and phosgene, the neutralisation of excess used pyridine and by-products removal (Eckert, 2011).

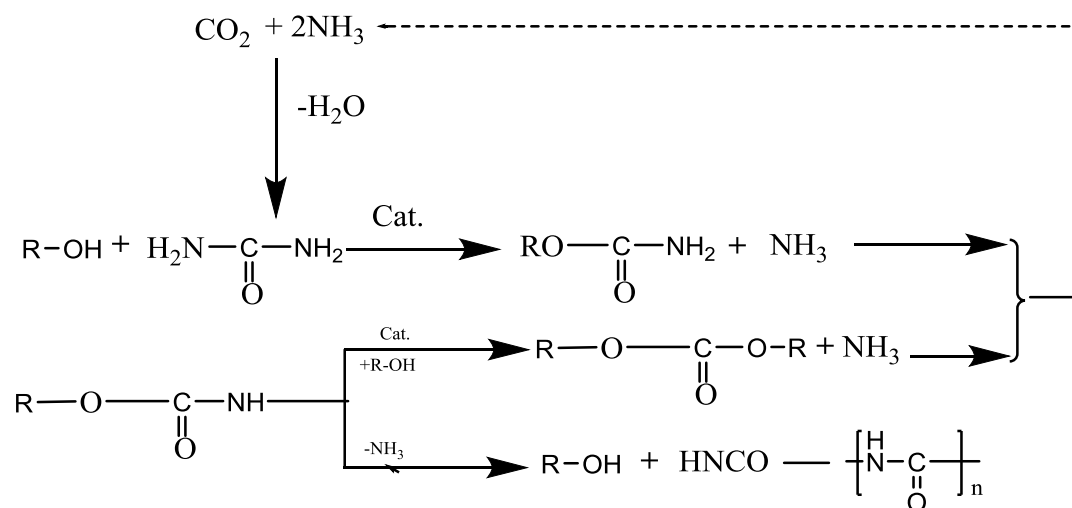


Scheme 2- 1. Cyclic carbonates synthesis using phosgene in presence of pyridine and dichloromethane solvent.

2.4.3.2 The reaction of urea with alcohols or phenols

The synthesis of carbamates is conducted through the reaction of urea and alcohols in the presence of metal salts such as lead acetate, zinc acetate. These carbamates syntheses were discovered by Paquin in 1946 where metal salts were used in the reaction of urea and alcohols. These carbamates can further react to produce carbonates in the presence of co-catalyst known as triphenylphosphine producing by-products of isocyanuric, ammonia and similar compounds. The produced ammonia can be recycled and used as a catalyst for synthesis of carbonate (Scheme 2- 2). Some known catalysts used in the production of urea are dibutyl dimethoxide, dibutyltin oxide and triphenyltin chloride gives high yields while some of the used heterogeneous catalysts include aluminium trioxide and antimony trioxide (Peng *et al.*, 2008; Shaikh and Sivaram, 1996). The usual reaction temperature is carried out at 423- 468 K for 4 h and at 468 – 493 K depending on the type of catalytic system used. For example, the reaction of urea with aromatic hydroxy compounds was investigated by Shaikh under the process condition temperature of 423 – 468 K for 4.5 h using a different combination of catalysts. A thermally unstable aryl carbonate was

achieved as an intermediate and decomposed to isocyanuric acid and phenol. Although the formation of stable aryl carbonate is also affected by the type of catalyst, the nature of substituent, and reaction medium. The electron donating groups facilitated by the further formation of aryl carbonate and decelerated by electron withdrawing groups but in a nonpolar solvents (dibutyl ether) decomposition continues much slower when compared with a polar solvent that including DMF, NMP and HMPA. The bases of pyridine and triethylamine enhance decomposition while weak acid resulted to slow decomposition and mineral acids causes' fast decomposition. Dimethyl carbonate can be produced using methanol and urea.



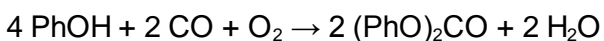
Scheme 2- 2. Two stages synthesis of carbonates from urea.

2.4.3.3 Oxidative carbonylation of alcohols and phenols

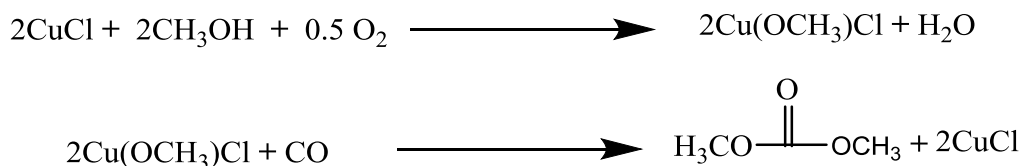
The reactions of alcohols and carbon monoxide are effectively promoted by the use of transition metal and post-transition metal compounds to form dialkyl carbonates. Palladium, mercury or copper-based catalysts are used in oxidative carbonylation of alcohol but the most catalysts used in this method are palladium and mercury-based catalysts but the reaction does not reduced metal, which can not directly be reoxidised (Gabriele *et al.*, 2006). Moreover, copper is known as the only species that can be directly re-oxidised. This is due to the reactivity of copper that prompt the redox cycle of the catalyst.

In 1980, Romano and coworker discovered the use of copper salt such as copper chloride as a catalyst to synthesise dimethyl carbonate by oxidative carbonylation of methanol. The processes are of two steps, which cuprous chloride oxidised to cupric methoxy chloride and later reduced to form dimethyl carbonate and regenerate cuprous chloride in the presence of carbon monoxide (*Scheme 2- 3*) (Nam *et al.*, 2013; Romano *et al.*, 1980).

Dimethyl carbonate is one of the few carbonates that is produced industrially by oxidative carbonylation of methanol such industries include Ube Industries Limited, Dow Chemical and Enichem Synthesis (J.Tsuji, 2005). *Scheme 2- 3* shows the oxidative carbonylation of phenols catalysed by palladium and *Scheme 2- 4* shows the oxidative carbonylation of methanols catalysed by copper.



Scheme 2- 3. Oxidative carbonylation of phenols catalysed by palladium

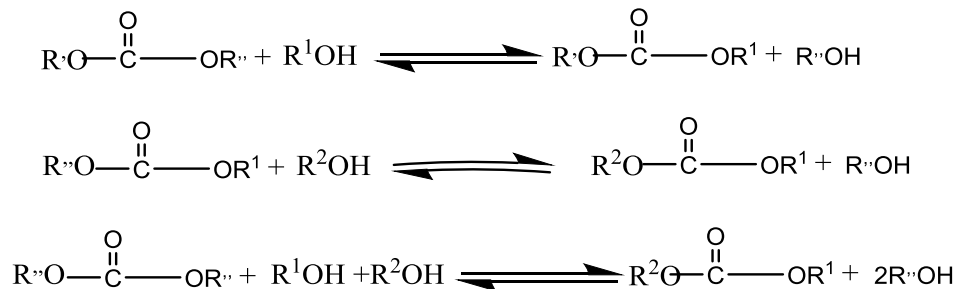


Scheme 2- 4. Oxidative carbonylation of methanols catalysed by copper.

There have been other attempts to synthesise diaryl carbonate by direct oxidative of phenols with the condensation of CO₂ or CO. The oxidation of phenols with CO and O₂ is carried by the use of palladium compounds, alkyl ammonium halide and an organic base at 373 -473 K for 1 – 3 h. This leads to the formation of diphenyl carbonate ranging from 4-30% yield with high selectivity (Shaikh and Sivaram, 1992).

2.4.3.4 Transesterification of carbonate

The carbonate transesterification is known to be an interchange reaction of carbonate when a catalytic process of one carbonate is being converted to another carbonate *via* the reaction of an alcohol with the existing carbonate. The formation of the carbonate is as a result of the more nucleophilic alcohol displaces the less nucleophilic compound, in other words, aliphatic alcohol will substitute phenols from aryl carbonates. More also if both compounds exhibit similarity in nucleophilicity the more volatile alcohol will be replaced by the less volatile alcohol. Hence, dialkyl carbonates and phenols are produced from the lower mass alcohols diaryl carbonates, although higher mass alcohol reacts with the lower mass of dialkyl carbonates to obtain the higher mass of dialkyl carbonates (*Scheme 2- 5*). The use of distillation is applied to eliminate the lower boiling alcohol. For this process, carbonate interchange reaction takes place in stages to form an intermediate of a mixed carbonate. There are several examples of this transesterification of carbonate under the different reaction conditions.



Where R[·] = alkyl, aryl or substituted alkyl or aryl; R¹, R² = Alkyl, aryl, same or different

Scheme 2- 5. Carbonate synthesis by carbonate transesterification.

2.4.3.5 Direct synthesis of cyclic carbonates by CO₂ utilisation

Over the years, there has been rapid significant innovation and development of reaction methodologies based on CO₂ utilisation as feedstock to produce cyclic carbonates through the direct synthesis of epoxides and CO₂ under the desired reaction conditions. The chemistry of CO₂ has been deliberated as a monomer in polymerisation and polycondensation reactions with oxiranes to effectively synthesise cyclic carbonate in the presence of catalysts. The use of catalysts

such as metal oxides (Yano *et al.*, 1997), mixed metal oxides (Saada *et al.*, 2018), metal-organic framework (Ji *et al.*, 2018), onium salts (Siewniak *et al.*, 2014), organic base salts, metal complexes, ionic liquids (Jadhav *et al.*, 2016), salen metals and alkali halides or alkylammonium halides (Darensbourg *et al.*, 1996) have been reported for the synthesis of cyclic carbonates based on cycloaddition reaction of carbon dioxide to epoxides and these could not only contribute CO₂ emissions reduction but offer a new approach to synthesise valuable chemicals that is eco-friendly from the viewpoint of Green Chemistry.

Yano *et al.* (1997) synthesised styrene carbonate using MgO and N, N-dimethylformamide (DMF) and achieved a moderate yield of 60% at 423 K, 80 bar of CO₂ pressure for a reaction time of 15 h. The synthesis of styrene carbonate was also carried out by Kawanami and Ikushima in 2000 from a direct synthesis of styrene oxide and CO₂ using only DMF as both catalysts and solvent under a supercritical pressure of CO₂ (scCO₂). The yield of 85% was achieved when compared with the use of CO₂ gas at the same conditions, 29% yield of SC was obtained (Kawanami and Ikushima, 2000) but a similar experiment was also carried out by Aresta in 2003, using CO₂ gas and DMF as both catalysts and solvents under the reaction conditions of 408 K, 30 bar for 12 h. An improve of 37% yield was achieved from 29% yield of SC conducted by Kawanami and Ikushima (Aresta, 2003). The improvement was as a result of reaction conditions and it was found that the solubility of the substrate in the solvent and catalyst were significant factors in controlling the reaction.

Gigante and coworkers investigated the use of polymeric Al(salen) complexes of polystyrene (Al(salen)PS) and polyethylene glycol bis-methacrylate(Al(salen)PEA) with an organic base of N-methylimidazole to produce styrene carbonate. The use of polymeric Al(salen)PEA complex gave 78% yield of SC and 89% SO conversion at 353 K and 100 bar (Alvaro *et al.*, 2005).

Arai and his group develop high efficient catalyst system of zinc bromide (ZnBr₂) and quaternary ammonium iodide (*n*-Bu₄NI) to study the binary activity of the catalyst on the synthesis of SC under the supercritical condition of CO₂ pressure in a direct reaction of SO and CO₂. The yield and selectivity of SC were found to be ~100% at the reaction condition of 353 K for half an hour. The further individual catalyst of ZnBr₂ and *n*-Bu₄NI was used separately and resulted not to be productive when compared used as combined catalysts (Sun *et al.*, 2005b).

In 2007, Shim and coworkers examined the use of quaternary onium salts of tetraalkylphosphonium and tetraalkylammonium halides in 1-butyl-3-methylimidazolium tetrafluoroborate (bmimBF₄) ionic liquid. It was discovered that the use of tetrabutylphosphonium bromide (Bu₄PBr) in the presence of bmimBF₄ gave 99.4% yield of styrene carbonate at a reaction temperature of 393 K, CO₂ pressure of 140 bar and reaction time of 2 h. As it was reported that tetrabutylphosphonium bromide (Bu₄PBr) exhibited high activity when compared to other tetrabutylphosphonium halides and also hinted that the catalytic activity improves as CO₂ pressure was increased (Choon *et al.*, 2007).

Yokoyama and coworkers investigated the use of zinc catalysts immobilized on soluble imidazolium styrene copolymers to synthesize styrene carbonate from CO₂ and styrene oxide. Among zinc catalysts (Zn/PS-IL[X], X = Br⁻, Cl⁻, BF₄⁻, and PF₆⁻) supported on imidazolium–styrene copolymers, Zn/PS-IL[Br] gave a 97.5% yield of styrene carbonate under the reaction condition of 393 K, 30 bar for 8 h. It was reported that styrene oxide when compared to ethylene oxide and propylene oxide is more demanding to convert to styrene carbonate. This is because of its less reactive β-carbon atom and hence, require a high reaction temperature and long reaction time for CO₂ cycloaddition reaction with styrene oxide (Qiao *et al.*, 2009).

In 2010, Arai and group reported the use of cheap quaternary ammonium salts such as tetrabutylammonium iodide (TBAI), tetrabutylammonium chloride (TBACl) and tetrabutylammonium bromide (TBAB) as effective homogeneous catalysts for the direct reaction of CO₂ and epoxides using without organic solvent and also with an organic solvent of tertbutyl hydroperoxide (TBHP). Low yield 33-39% of styrene carbonate were obtained when TBHP was used as an oxidant at a reaction condition of 353 K, 10-150 bar for 6 h. It was contradicting when compared with other reports that an increase in CO₂ pressure reduces the rate of reaction for cyclic carbonate formation (Fujita *et al.*, 2010).

A facile and efficient synthesis of SC was reported by Nelson and Adam (2013) using mesoporous MCM-411-Imi/Br catalyst in the absence of organic solvent and achieved 99.1% selectivity and 97.7% yield of SC under the reaction condition of 30 bar CO₂ pressure, 373 K for 4 h. It was reported that the synergistic effect of the strong nucleophilicity of Br⁻ and amine in the catalyst leads to the maximum selectivity. Although there was a formation of a by-product

of styrene glycol, which was due to the interaction of water molecule trapped within the catalyst silica matrix, which promoted the formation of the by-products, which were eliminated completely by the increase in CO₂ pressure from 60 bar to 100 bar. The catalyst was reused several times without any significant loss in the activity of the catalyst (Appaturi and Adam, 2013).

Tong Au and coworkers used high efficient hydroxyl ionic liquid grafted onto cross-linked divinylbenzene polymer (PDVB-HEIMBr) to synthesize cyclic carbonate from epoxides and CO₂. Styrene carbonate and 1,2-butylene carbonate yield of 99.5% and 79% were obtained respectively. The reaction condition of 413 K reaction temperature, 20 bar CO₂ pressure for 4 h. The effects of reaction temperature, time and initial CO₂ pressure on product yield suggested that the synergetic effect between the bromide ions and the hydroxyl groups facilitates the coupling reaction (Dai *et al.*, 2013).

Jasiak *et al.* (2016) used nanogold ionic liquid catalyst to synthesize SC from styrene and CO₂. The developed catalyst of gold nanoparticles immobilised on multi-walled carbon nanotube (Au/CNT) of diameter of 6 nm was used for epoxidation. The optimal process condition of 393 K reaction temperature and 12 bar of CO₂ pressure in the presence of 1-butyl-3-methylimidazolium bromide [bmim]Br-ZnBr₂ system and obtained 60% yield of styrene carbonate. After the reaction, Au/CNT could be easily separated and still maintain its catalytic activity.

Nevertheless, it is very clear that the CO₂ plays a crucial role in the formation of cyclic carbonates but due to CO₂ is thermodynamic stable, it will require an organic solvent, which is never recovered from the processes or longer reaction time to eliminate the thermodynamic limitation. Although the use of supercritical state of CO₂ improves the mass transfer efficiency of the reactants and enhances the activation of CO₂ molecules, thereby shifting the reaction equilibrium to the product side to overcome the thermodynamic limitations of the reaction in the presence of suitable catalysts.

Homogeneous catalysts have been extensively employed because of its outstanding catalytic activity, mild reaction conditions, and selectivity. However, these catalysts suffer difficulty of isolation. The use of heterogeneous catalytic systems overcome these problems since they can be effectively recovered from a reaction mixture in simple separation technique. Largely, heterogenisation is

achieved by grafting the active sites on solid materials including inorganic supports, polymers and hybrid materials. Silica, alumina, active carbon, ceria, polystyrene, polyvinylpyrrolidone are typical examples. The synthesis of cyclic carbonates using highly active mixed metal oxides catalyst is gaining more attention in recent times. Although, there have been few studies showing the use of mixed metal oxides catalysts without the use of organic solvents (Adeleye *et al.*, 2015; Saada *et al.*, 2015). The use of graphene oxide as a supported catalyst has been identified to have improved the performance of mixed metal oxides catalysts (Saada *et al.*, 2018).

2.5 Catalysis

2.5.1 Classification of catalysis

Catalysis can be categorised into three separate groups: bio-catalysis, homogeneous catalysis and heterogeneous catalysis. Bio-catalyst exists naturally in most of living organism as enzymes or bacteria. Homogeneous catalyst exists in the same phase with the reactant with no boundary existent example includes organic solvents, metal onium, metal halide and on another hand, heterogeneous catalyst exist in phase boundary separates the catalyst from the reactant (Somorjai, 1979). Heterogeneous catalysts are mostly in solid state that acts on substrates in a liquid or gaseous reaction mixture (Öhlmann, 1999a). The subsequent sections will discuss this classification of catalysis.

2.5.2 Bio-catalysis

The process in which the natural catalyst such as protein enzymes perform a chemical transformation on the organic compound is known as bio-catalytic processes. Bio-catalysis is an important aspect of catalysis and has been used widely to make small drugs in the pharmaceutical industry (Seibert and Tracy, 2014). Most of the living organisms' processes depend on the use of enzymes that consist of proteins and the amino acids, which are linked by bonds called peptide bonds and these bonds form the enzyme's structure. Enzymes use four types of interactions that are electronic interactions, hydrogen bonding, hydrophobic interactions and Van der Waals interactions to bind its substrates.

The bond between the active site and substrate is relatively weak and could not prevent enzymes' catalytic cycle if the bond is strong (Hagen *et al.*, 2006).

2.5.3 Homogeneous catalysis

In homogeneous catalysis, the catalyst, which is normally in a liquid state and the reaction mixture is in the same phases. The use of homogeneous catalyst offers a better result over the use of the heterogeneous catalyst in terms of yield and selectivity but the drawback is obviously the difficulty of separation and recovery of the catalyst. The past decade has recorded significant utilisation of CO₂ for the synthesis of organic carbonate using homogeneous catalysts. The uses of homogeneous catalysts have been investigated and developed for the synthesis of organic carbonate metal halides, salen, organic base, salts etc.

There are several reports on the use of homogeneous catalysts such as metal halide or onium salt, ionic liquid, salen and organic base for the synthesis of cyclic carbonates in the past decade.

2.5.3.1 The synthesis of cyclic carbonate in the presence of metal halide or onium salts

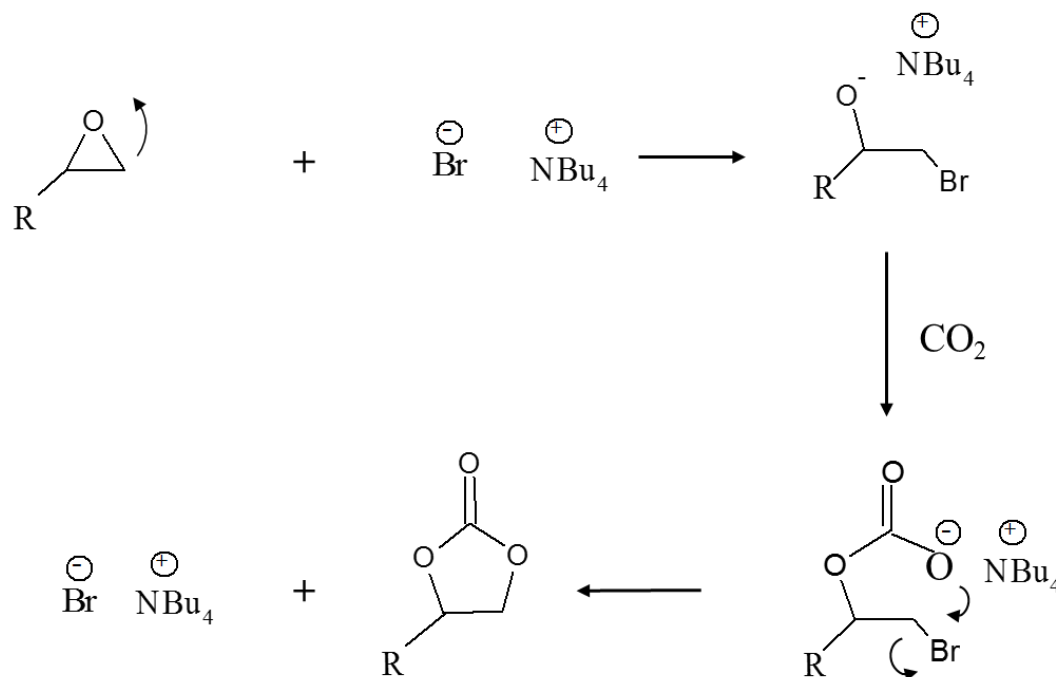
Metal halides are compounds that exist between metals and halogens, which some are covalently bonded. Onium salts are very cheap and valuable homogeneous catalysts for the synthesis of cyclic carbonates. Caló and co-worker (2002) demonstrated the use of tetrabutylammonium halides as solvent and catalysts to synthesise cyclic carbonates. They further showed how epoxide dissolved in molten tetraalkylammonium halides to convert into cyclic carbonates under atmospheric pressure (Caló *et al.*, 2002a). The rate of reaction depends on the structure of the cation and nucleophilicity of the halide ions shown in *Scheme 2- 6*. The use of catalyst system based on NiCl₂/PPh₃ in the presence of TBAB and zinc powder as a reducing agent produced an excellent yield greater than 99% at 25 bar, 393 K with turn over frequency of 3544 h⁻¹. Park *et al.* (2008) investigated the addition of CO₂ to butyl glycidyl ether in the presence of tetraalkylammonium salts and found that the catalytic activity improved as the length of the alkyl groups increased but beyond C8 did not produce any beneficial effect. Work by Gonzalez *et al.* demonstrated high catalytic activity for cyclic carbonate formation turn over the frequency of 293 h⁻¹, in the presence of

solid supported RuCl_3 with SiO_2 , or tetraethylammonium bromide as the support, at 353 K and under supercritical conditions. (Gomes et al, 2008).

The use of propylene oxide as a substrate to synthesise cyclic carbonate from terminal epoxides using silica-supported quaternary ammonium salt catalyst under supercritical CO_2 condition was investigated by He and his group (2006). The use of propylene oxide as a substrate, an initial survey was carried out in which a range of unsupported and silica-supported tetra-butylammonium halide salts was tested for activity. The reaction conditions used CO_2 at 80 bar with 1 mmol% catalyst at 423 K for 10 h. All four of the silica supported salts produced. (Wang et al, 2006).

Sakakura et al. (2002) reported the use of samarium oxychloride as a catalyst for the addition of CO_2 to propylene oxide, obtaining quantity conditions 1 bar, 393 K with a turn over frequency of 1.3 h^{-1} .

Sun et al. (2004) investigated the synthesis of SC using tetraalkylammonium halides as a catalyst in the presence of an oxidant of tertbutyl hydroperoxide and achieved a moderate yield of 33% at reaction conditions of 353 K, 150 bar for 6 h. It was highlighted that the increase of CO_2 pressure inhibits further cycloaddition reaction of CO_2 to epoxide. In 2010, Fujita and co-workers improved the yield from 33% to 39% with the lower pressure of 10 bar while the other reaction condition remains the same. (Fujita et al., 2010).



Scheme 2- 6. The cycloaddition reaction mechanism (Miao et al., 2008).

2.5.3.2 Synthesis of cyclic carbonate in the presence of an ionic liquid

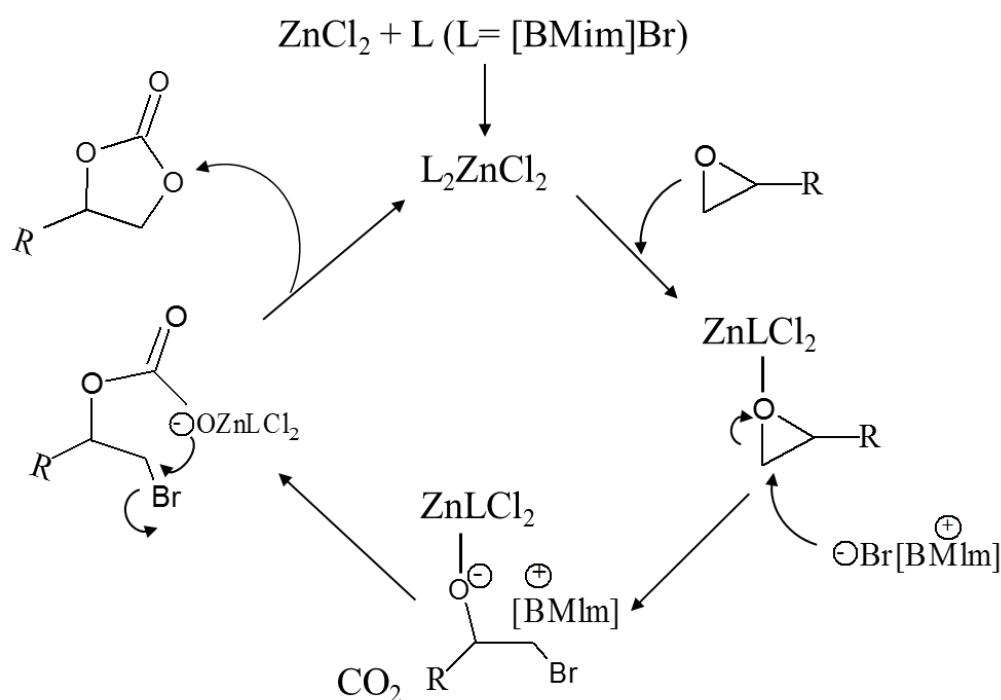
There have been several reports over the last decade on the use of ionic liquid to synthesize cyclic carbonates with higher yields. The unique use of an ionic liquid such as catalyst has been widely reported. The direct synthesis of styrene carbonate was investigated by Aria and his co-worker (Sun et al., 2004). He used Bu_4NBr as a catalyst and TBHP as an oxidant to achieve 38% yield of styrene carbonate under the reaction conditions of 1 bar, 353 K for 6 h (Sun et al., 2004). The same group further improved the yield of styrene carbonate to 100% at 353 K, for 1 h using Bu_4NBr and ZnBr_2 as the catalysts but only 28% was obtained as the yield when Bu_4NBr was used as a catalyst only (Sun et al., 2005).

Yokoyama and his group (2007) achieved 85% yield of styrene carbonate under the reaction conditions of 30 atm, 383 K for 2 h using an ionic liquid 1-butyl-3-methylimidazolium (BMIm), 1-ethyl-3-methylimidazolium (EMIm) and urea hydrogen peroxide (UHP) as catalysts while methyltrioxorhenium (MTO) as an oxidant. The formation of styrene carbonate has been achieved through one pot multi-step synthesis using styrene as the beginning of the process. Although

using the same procedure at 353 K, the yield of 55% of styrene carbonate was achieved (Ono et al., 2007).

Deng and Peng (2001) also reported the use of 2.5 mol% of 1-butyl-3-methylimidazolium on the synthesis of propylene carbonate under the reaction conditions of 25 atm, 383 K for 6 h with a turn over frequency of 6.6 h^{-1} and achieved 67% conversion while a higher TOF of 15 h^{-1} was achieved for 1.5 mol%. Furthermore, Kim et al. (2003) explored the use of ZnBr_2 with ionic liquids as catalysts and achieved improvements in the yields with the same reaction conditions apart from the use of higher pressure. Xia and his group uses a similar system of Zinc salts such as (ZnBr_2 and ZnCl_2) with BMIm on the synthesis of propylene carbonate through cycloaddition reaction of CO_2 to propylene oxide and achieved 98% yield with TOF 5580 h^{-1} while the ZnCl_2 with BMIm gave 95% yield of propylene carbonate and a TOF of 5410 h^{-1} under the reaction conditions of 373 K, 15 atm for 1 h. *Scheme 2- 7* shows the possible reaction mechanism for the synthesis of PC.

Ikushima and co-worker (2003) found a rapid and effective synthetic method of synthesis of propylene carbonate using supercritical CO_2 (scCO_2). The catalyst used was 1-octyl-3-methylimidazolium tetrafluoroborate and achieved almost 100% yield, 100% selectivity within 5 min while the TOF value was about 77 times larger than those results reported before their investigation. They found that the phase behaviour of high pressure under the same reaction conditions marks an increase in the concentration of the reactants (Kawanami *et al.*, 2003).



Scheme 2- 7. Catalytic cycle for ZnCl₂ facilitated addition of CO₂ to epoxides in the presence of the ionic liquid [BMIm]Br adapted from (North and Pasquale, 2009).

2.5.3.3 Cyclic carbonate synthesis catalysed by salen catalysts

The use of salen complexes was inspired by Jacobsen's success from the application of asymmetrical ring opening reaction of epoxides. Salen ligands are synthesised by the condensation of diamine and salicylaldehyde, which may be chiral or achiral. Salen ligands are easy to synthesise in contrast to porphyrins and its ease of modification has prompted an increasing interest in salen as a ligand for many different catalytic systems. There are varieties of complexes that salen ligand can form with both metal and transition metals used as catalysts for several types of reaction. Salen complexes have several metals of +3 oxidation state, which have been found to catalyse cycloaddition reaction of CO₂ to epoxides, in particular, Co, Cr, Al, Mn and Zn.

Cobalt (salen) complexes (Co(III)(salen)) complexes are known for stereo-controlled polycarbonates synthesis from CO₂ and epoxides. These complexes

produce cyclic carbonates at specific reaction conditions. Jacobsen and his group demonstrated the use of Cobalt (III) salen complexes as a catalyst that can serve as ring opening of epoxides with several nucleophiles (Jacobsen et al., 2000). Zhang and group (2004) accomplished enantioselective cycloaddition reaction of CO₂ to propylene oxide using Co(III)(salen) (Lu et al., 2004). The use of a binary catalyst system based on chiral Co(III)(salen)O₂CCCl₃ with TBAB produced a high TOF of 245 h⁻¹ at 15 atm, room temperature and derived 50% enantiomeric excess in the product. There was a decrease in the TOF from 245 h⁻¹ to 27 h⁻¹ of cyclic carbonates when TBAB was replaced by TBACl. Although there was a significant improvement in enantioselectivity excess from 50% to 70% at a low temperature of 273 K yet at a loss of activity (Lu et al., 2004).

Jing et al. (2007) synthesised propylene carbonate from CO₂ and propylene oxide using a combination of Co(III)(salen)O₂CCCl₃ complex with PTAT and obtained a high yield of TOF of 706 h⁻¹ at room temperature, 4 atm but exhibited poor enantioselectivity. Paddock et al. (2004) also reported the use of Co(III)(salen)O₂CCCl₃ complex and DMAP combination, which was highly reactive for the synthesis of propylene carbonate. The synthesis reaction conditions were 373 K, 10 atm in dichloromethane and the reaction produced a high TOF of 120 h⁻¹. Zhang et al. (2009) also demonstrated the use of asymmetric cycloaddition reaction of CO₂ to epoxide was achievable when using Co(III)(salen) with cinchona alkaloids as cocatalysts (Zhang et al., 2009).

Many other groups such as Kruper (Kruper and Dellar, 1995), Holmes (Mang and Cooper, 2000), and Darensbourg (Darensbourg et al., 2004) have investigated and developed copolymerisation of epoxides and CO₂ using chromium (III) salen as a catalyst. This development is as a result of its stability and low toxicity. Although He and coworker first use *n*-Bu₄NBr as a cocatalyst for chromium(III) salen catalyst to synthesise ethylene carbonate at 15-16 MPa of pressure at 373 K and achieved a TOF of 1320 h⁻¹ (He et al., 2002). Paddock and Nguyen (2004) synthesised propylene carbonate from cycloaddition reaction of CO₂ to propylene oxide using chromium(III) salen complexes in the presence of DMAP as cocatalyst under the reaction conditions 373 K and 4 atm. High TOF of 916 h⁻¹ was obtained but fell to 3 h⁻¹ when the reaction temperature was operated at room temperature. Paddock and Nguyen (2004) discovered that long reaction time is needed to achieve a satisfactory yield. Shen et al. (2003) use

binaphthydiamino salen type catalyst such as binaphyldiamon salen type catalyst. The yield achieved for propylene carbonate was 80 and 91% in the presence of the catalyst and 2 equiv of DMAP or Et₃N at 373 K. Darensbourg's group (2004) investigated the use of chromium (III) salen chlorine complexes and toluene as a solvent to synthesise under the reaction conditions of 25 atm and 313 K. It was discovered that similar reaction conditions of the use different epoxide gave alternating copolymers. Furthermore, the use of solid supported Cr(III)(salen)Cl. Complexes with tributylamine were found to promote styrene carbonate synthesis (Alvaro et al., 2004).

The use of aluminium in place of chromium as the Lewis acidic centre could improve the better the couple reaction of CO₂ and epoxides. He and Lu (2002) synthesised ethylene carbonate using Al (III)(salen)Cl complexes catalyst with TBAB as cocatalyst at 383 K, 160 atm and achieved a TOF of 220 h⁻¹ (Lu et al., 2002). Alvaro et al. (2005) developed an active solid supported Al(III)(salen)Cl complex for the synthesis of styrene carbonate using the supercritical pressure of 100 atm and reaction temperature of 353 K. North and co-worker (2007) reported the synthesis of cyclic carbonates from CO₂ and epoxides using dimeric aluminum (salen) complexes and TBAB as a cocatalyst under solventless conditions. It was found that the system showed a unique activity as CO₂ pressure at room condition could be used alongside a low reaction temperature of 298 K, leading to the formation of styrene carbonate when styrene oxide as a substrate. It was found that 63% conversion after 3 h and 98% conversion after 24 h (North et al. 2007). The kinetic studies carried out by North and his group found out that the reaction was in the first order in dimeric aluminium (salen) complexes catalyst as well as being in a second order in TBAB (North and Pasquale, 2010).

Manganese(III) salen complexes (Mn(III) salen)I was used as a catalyst to synthesise propylene carbonate under supercritical conditions and obtained 90% yield exhibiting a TOF 203 h⁻¹ at 413 K and 200 atm. Under the same conditions, 31% yield of styrene carbonate was obtained, although the TOF was 213 h⁻¹ (Jutz et al., 2009). There was further improvement of 96% yield of styrene carbonate when SiO₂ immobilised (Mn(III) salen)Br used as catalyst under the same conditions, exhibiting a TOF of 196 h⁻¹. The catalyst activity remains stable after

the 3rd run, based on the kinetic study using FT-IR spectroscopy that revealed the nature of epoxide strongly influence the reaction rate (Jutz et al., 2009).

2.5.3.4 Cyclic carbonate synthesis catalysed by organo-catalyst systems

In the quest for developing a green chemical synthesis for cyclic carbonates, researcher major goal is to develop an ideal catalyst that would promote environmentally benign and improve productivity. There are several reports on organocatalytic systems that involve the use of dimethylaminopyridine (DMAP) as a catalyst for the synthesis of propylene carbonate formation. Jones and Shiels (2007) found from the extensive study of DMAP derivatives could be immobilised on silica and produce a heterogeneous that convert 85% of epoxide for 4 h at 393 K under 17 atm. Moreover, the result improved to 92% yield under 34 atm (Shiels and Jones, 2007).

2.5.4 Heterogeneous catalysis

Heterogeneous catalysis is a type of catalysis that the catalyst usually is solid form occupies a different phase from the reactant and product. The advantage of this type of catalysis over homogeneous catalysis is the ease of separation of the catalysts. Heterogeneous catalysis occurs in three catalytic process stages, which are: First, the physisorption (weak adsorption) or chemisorption (strong adsorption that include bond weakening or breaking of the reactant), which is the adsorption of the reactant at the surface of the catalyst active sites leading to the interaction of the reactants on the surface of the catalysts, which is the second stage. The final stage is the desorption of the products from the surface of the catalyst to form a new molecule that reacts and attach (Deikus and Bechhofer, 2011; Öhlmann, 1999b).

Adsorption of reactants on the catalyst surface provides easy reaction between the reactants and leads to difficulty of desorption of product from the surface of the catalyst (Schlögl, 2015). *Table 2- 5* has shown several advantages of heterogeneous catalysis over homogeneous catalysis.

Table 2- 5. Heterogeneous and homogeneous catalysts comparison

<i>Parameters</i>	<i>Heterogeneous Catalysts</i>	<i>Homogeneous Catalysts</i>
<i>Application</i>	<i>Widely used</i>	<i>Limited to certain processes</i>
<i>Catalyst phase</i>	<i>Usually Solid (Metals, Metal oxides or mixed metal oxides)</i>	<i>Metal complex</i>
<i>Recyclability</i>	<i>Easy</i>	<i>Difficult</i>
<i>Selectivity</i>	<i>Variable</i>	<i>Usually high (gives high yield)</i>
<i>Solvent</i>	<i>Free of solvent (not required)</i>	<i>Solvent needed (Often required)</i>
<i>Stability</i>	<i>Highly stable at high temperature</i>	<i>Decomposed</i>

The last 25 years have shown the applications heterogeneous catalysts in chemical processes have become an important tool to promote environmentally friendly and actualises green chemistry. These chemical processes include the use of metal oxides and mixed metal oxides to synthesise cyclic carbonates.

2.5.4.1 Supported catalysts

There has been a continued rise in the use of supported catalysts for the synthesis of cyclic carbonate through the reaction of CO₂ and epoxides. Supported catalysts are of industrial interest in recent times and are at the heart of researchers since most of the supported catalysts are made by metal ions or transition metals attached to polymers. The supported catalyst is known to have a high surface area and usually, they are mainly in solid form (Li *et al.*, 2011; Liu, 2017). The large surface area of supported catalyst offers a base in which the catalyst could be distributed over. Although in every catalytic reaction the support may be inert or participate and the various kind of supports includes alumina, carbon, silica and polymers, which have been reported for organic carbonate synthesis. The use of supported catalysts provides the technological advantages of better morphology control, density, less reactor fouling and high polymer bulk (Fujita and Makio, 2007).

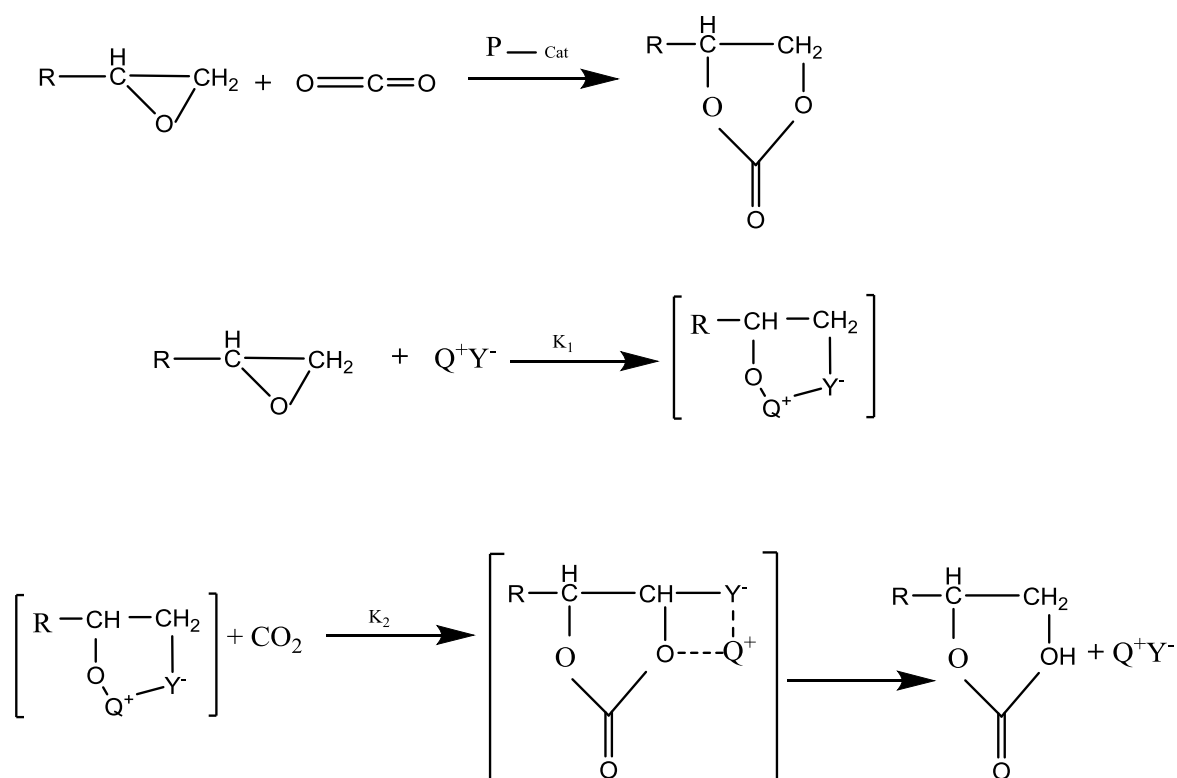
2.5.4.1.1 Polymer-supported catalysts

The use of polymer support, which is catalytically immobilised onto a catalyst system through chemical bonds or weaker interactions that include hydrogen bonds or donor-acceptor interactions is known as polymer-supported catalyst (Hodge, 1986; MacHin, 1970). The uses of polymer-supported catalysts are mostly built on polymers network in beads appearance. Its advantages are the ability to be separated from reaction mixture and be reused several times (Benaglia *et al.*, 2003). *Scheme 2- 8* shows the reaction mechanism of polymer-supported catalysts.

Baj and coworkers use polymer-supported catalysts made up of two effective components of quaternary onium salts and aqueous solutions of metal salts to synthesise cyclic carbonates from CO₂ and epoxides. The synthesis of propylene carbonate from CO and PO using Tributylmethylammonium chloride immobilized on polystyrene cross-linked with divinylbenzene (PS-TBMAC) was investigated by the Baj's group and obtained 48% after 4 h at 383 K and low pressure of ~ 8.9 atm. This was improved by the use of cocatalyst zinc iodide (ZnI₂) to 76% PC yield and reaction time was shortening to 3 h. Furthermore, the combination use of PS-TBMAC and aqueous ZnI₂ solution gave an increase of 91% PC yield after 2h (Siewniak *et al.*, 2014). The same reaction conditions and polymer-supported catalysts were used to synthesis styrene carbonate from cycloaddition reaction of CO₂ to styrene oxide (SO) and 71% yield was achieved (Siewniak *et al.*, 2014). The presence of the cocatalyst ZnI₂ act as a Lewis acid, which was involved in the activation of the epoxide and the further addition of water to the reaction system also helped in activating the opening epoxide ring whilst hydrolysis the reaction of epoxide (Kim *et al.*, 2014).

Cui *et al.* (2015) synthesised cyclohexane carbonate catalysed by polymer-supported catalysts of polystyrene-divinylbenzene cross-linked resin supported with zinc chloride catalysts in the presence of cocatalyst of tetrabutylammonium (TBAB). The catalyst of diethylene glycol as a connecting arm and 2-aminopyridine (PS-DEG-2ap-ZnCl₂) showed the optimal catalytic performance of 95.18% yield of cyclohexane carbonate under the optimal conditions of 393 K, ~49 atm for 6 h.

Wang et al. (2016) synthesised cyclic carbonates using polymer-supported ionic liquids of styrene functionalised quaternary ammonium chloride salts derived from trimethylamine, triethylamine, triethanolamine, imidazole and copolymerised with divinylbenzene (DVB). The use of imidazolium-based PSIL, which was solvothermal copolymerisation of 1,3-bis(4-vinyl benzyl)imidazolium chloride and DVB that was denoted as PSIL(IMD) from the cycloaddition reaction of CO₂ to PO gave 99.9% of PC yield at 403 K, ~20 atm for 5 h.



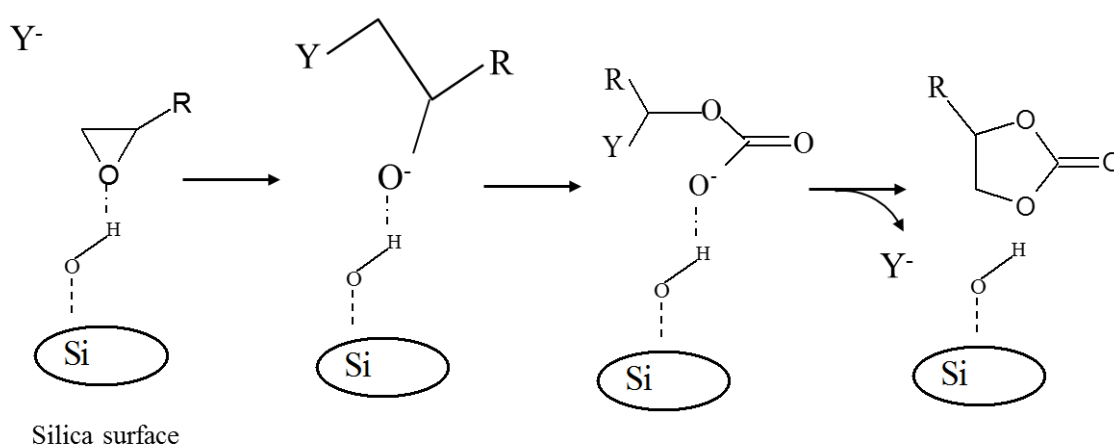
Scheme 2- 8. Reaction mechanism of polymer-supported catalysts (Shaikh and Sivaram, 1996).

2.5.4.1.2 Silica supported catalyst

Wang et al. 2006 synthesised cyclic carbonates from carbon dioxide and epoxides *via* supercritical conditions over silica supported quaternary ammonium salts. The silica-supported tetra-*n*-butyl ammonium bromine (*n*-Bu₄NBr/SiO₂) was used to synthesise propylene carbonate under the reaction conditions 1 mmol% catalyst loading, 423 K, ~ 79 atm for 10 h and achieved 97% yield of PC. The *n*-Bu₄NBr/SiO₂ solid catalyst could be recovered easily by a simple filtration, which

can be rinsed and dried and was reused for four different runs with a slight loss of its catalytic activity. Wang and his group suggested that the application of $n\text{-Bu}_4\text{NBr/SiO}_2$ catalyst could offer a new direction for investors interested to develop continuous fix bed flow reactor that will be solvent-free and product driven.

The use of silica supported phosphonium halides as an acid-based bifunctional heterogeneous catalyst for the reaction of CO_2 and epoxides was demonstrated by Sakakura and coworkers. The group found that the Si-OH groups on the silica surface activated the epoxide and then undergoes a nucleophile attack by the halide anion (Y^-) (Scheme 2- 9, section A) that resulted into the ring opening (Scheme 2-4, section B) and cyclic carbonate is formed by the insertion of CO_2 into the ring opened epoxide (Scheme 2- 9, section C-D). The insertion of CO_2 into intermediate becomes the rate-determining step of CO_2 pressure less than 50 atm.

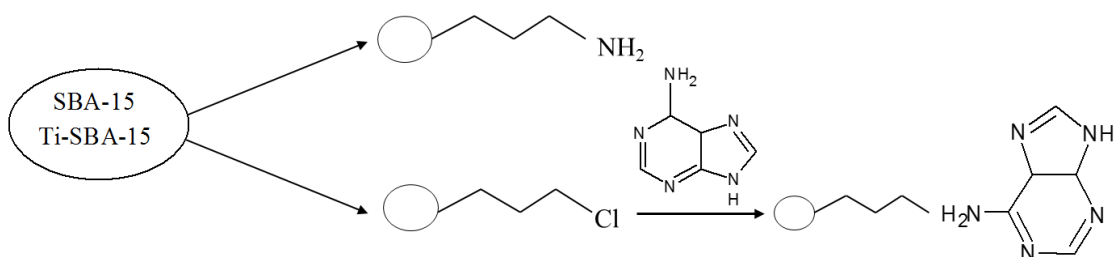


Scheme 2- 9. The possible reaction mechanism for cyclic carbonates syntheses over silica supported phosphonium halides catalysts (Motokura et al., 2009).

Motokura et al. (2009) discovered from Sakakura's group that stability of counter anions improves in the existence of large delocalised counter cations with resonance forms and hence, developed silica supported aminopyridinium halides for the transformations of epoxides to cyclic carbonates under atmospheric pressure of CO_2 . The use of silica supported 4 pyrrolidinopyridinium iodide ($\text{SiO}_2\text{-1(I)}$) catalyst was used to synthesise styrene carbonate in the absence of an organic solvent or additives under 1 atm, 373 K for 20.5 h and achieved 89%

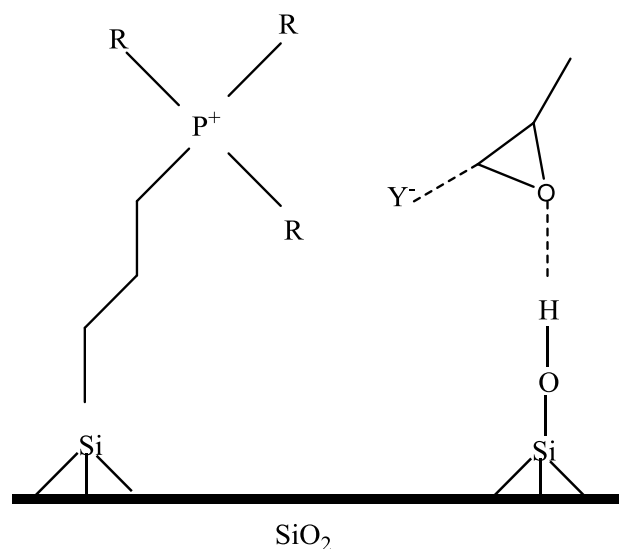
yield. The catalytic activity reduced when silica supported 4 pyrrolidinopyridinium bromide ($\text{SiO}_2\text{-1(Br)}$) or silica supported 4 pyrrolidinopyridinium chloride ($\text{SiO}_2\text{-1(Cl)}$) was used instead to 79% and 19% respectively. Although the yield of styrene carbonate was greater than 70% when supported alkylamino pyridinium but the application of silica supported tetraalkylammonium iodide gave 89% yield of styrene carbonate and more conversion of 94% of styrene oxide whereas for ($\text{SiO}_2\text{-1(I)}$) conversion of styrene oxide was 91%. The reusability test for both performing catalysts was conducted by Baba's group and found that it could be reused three times without any appreciable loss of activity of the catalysts (Motokura *et al.*, 2009).

Although, the first report on the use of silica-immobilized tetraalkyl phosphonium bromide for a flow reactor was reported by Takahashi's and coworkers (Yasuda *et al.*, 2006). The *Scheme 2- 10* shows how phosphonium bromide was immobilised on silica, which was used to synthesise PC using 10 MPa of CO_2 for more than 1000 h achieved yield above 80% by the increase of reaction temperature from 363 K to 433 K. The increase in temperature suggested leaching of the phosphonium bromide from the support might have occurred but the selectivity of PC was over 99.9%. They further showed the synergistic effects of immobilisation of phosphonium halides on silica from the batch experimental reaction and found that the TOF of the immobilised phosphonium halides was greater than 300 times when compared to phosphonium halides that were used homogeneously. Moreover, the enhancement in the activity on polystyrene from the immobilisation was not observed but that of the support on silica was ascribed to the activation of epoxide through the acidic surface silanol groups and halide anion of the immobilised phosphonium salts was observed (*Scheme 2- 11*). The best active immobilized catalyst could convert PO to PC at 373 K, 10 MPa of CO_2 for a low reaction time of 1 h.



Scheme 2- 10. Immobilization of adenine and propylamine on Ti-SBA-15 or SBA-15 (Fujita *et al.*, 2014).

The preparation of immobilized phosphonium halide catalysts using aluminosilicate, silica, and basic alumina as the support materials was done by Ema's group (Sakai *et al.*, 2008). The use of silica supported catalysts was found to perform better when compared to aluminosilicate, and basic alumina (silica > aluminosilicate > basic alumina) as the support materials for the CO₂ cycloaddition reaction to epoxyhexane (Dai *et al.*, 2010). Scheme 2- 11 shows the acidity of the OH group on the support surface and also illustrates the cooperative activation mechanism. The enrichment of the activity by the immobilization was also observed with imidazolium and aminopyridinium halides (Motokura *et al.*, 2009). Hence, the effects of the immobilization interaction on inorganic materials having surface hydroxyl groups are communal. The number of surface hydroxyl groups, the mean pore size and the total pore volume of the immobilised catalysts were found to be a crucial determining factor of the performance of the catalysts (Udayakumar *et al.*, 2009).



Scheme 2- 11. Activation of an epoxide molecule on silica immobilised phosphonium halides (Fujita *et al.*, 2014).

The synthesis of styrene carbonate was synthesised by Sartorio's group using silica-molecular sieve supported catalysts with silica-supported guanidine (MCM-41-MTBD) catalyst. This catalyst was prepared by covalently bonding of molecular sieve (MCM-41) and-methyl-1,5,7-triazabicyclo[4,4,0]dec-5-ene, (MTBD) and used to synthesise styrene carbonate. The yield of SC achieved and SO conversion was 90% and 98% respectively. The reaction condition used for this synthesis was 413 K and 50 bar of CO₂. The yield of styrene carbonate was reduced when homogeneous counterpart (MTBD) was used. MCM-41-MTBD catalyst performed better and is desirable because of its numerous advantages such as ease of separation and can be reused more than 3 times and maintain its stability (Barbarini *et al.*, 2003). The use of SiO₂-supported quaternary ammonium and imidazolium salts as a catalyst for cycloaddition reaction of PO and CO₂ was investigated by He and coworkers and reported 99% yield and selectivity of PC in the presence SiO₂/imidazolium salt ([C4-mim]⁺[BF₄]⁻) catalyst (Wang *et al.*, 2006).

Similarly, in 2006, Zhang *et al.* investigated the use of silica (SiO₂) supported organic base catalysts (SiO₂/MTBD) to synthesise PC and achieved 99% conversion of PO and 99% yield of PC at 423 K reaction temperature and 20 bar of CO₂ pressure. Furthermore, the use of adenine-modified microporous silica (Ti-SBA-15-pre-Ade) catalyst was investigated by Ratnasamy's group for PC

synthesis and achieved 81% yield of PC, 95% conversion of PO and 100% selectivity under the reaction temperature of 393 K and 69 bar of CO₂ pressure (Srivastava *et al.*, 2005).

Gao *et al.* (2015) uses silica supported zinc glutarate catalyst prepared *via* a rheological phase reaction with a reaction medium of toluene to synthesise polypropylene carbonate from copolymerisation of CO₂ and propylene oxide and obtained alternating an increase in yield of poly(propylene carbonate) (PPC) with the carbonate content of above 97 % and the M_ns of above 10, 000 g/mol from 12.7 kg polymer/mol Zn of ZnGA to 25.6 of ZnGA/SiO₂.

2.5.4.2 The synthesis of cyclic carbonates using metal oxide catalysts

There are several reports on metal oxide catalysts used to synthesise cyclic carbonates that are showing promising results. These promising results were as a result of the use of organic solvents. These organic solvents have helped to lower the reaction conditions and also improve product selectivity. The acidic and basic properties of metal oxide allow ease interaction of polarisable species such as CO₂. The adsorption of CO₂ onto metal oxides is a known process with several examples reported in the literature including infrared studies on MgO, CaO, CeO₂, La₂O₃, ZrO₂, TiO₂, ZnO and BeO. As a result, activation of CO₂ by metal oxides, ease of catalyst recovery and product separation has prompted much work on the development of metal oxide catalysts. (Yamaguchi *et al.*, 1999). He and his group used tin catalyst under supercritical CO₂ to synthesise propylene carbonate direct from propylene glycol (Du *et al.*, 2005). Furthermore, the synthesis of cyclic carbonates from diol and urea was demonstrated by Sun and his group using metal oxides as catalysts (Li *et al.*, 2006). The yield of 93% of ethylene carbonate was obtained using zinc oxide as catalyst under the atmospheric condition of CO₂ at 423 K for 3 h. It was found that extending the time to improve the yield of the cyclic carbonate (Li *et al.*, 2006).

Bhanage *et al.* (2001) prepared and conducted an experiment on cheap metal oxides such as Al₂O₃, CaO, CeO₂, La₂O₃, MgO, ZnO and ZrO in the presence to N,N-dimethylformamide (DMF) to synthesise cyclic carbonates (Table 2-4, entries a-g). Among the metal oxides, La₂O₃ exhibited the highest yield (54%) for propylene carbonate (Table 2- 6, entry d), whilst MgO showed highest selectivity (92%), (Table 2- 6, entry e) at reaction condition of 423 K, 80 bar for 15 h. Yano

et al. (1997) had performed similar experiment using MgO and obtained higher PC and SC yield when compared to the results reported by Bhanage et al. (2001) when using MgO as catalyst and DMF as solvent (*Table 2- 6*, entry h and i). The discrepancies in results might be as a result of MgO and DMF concentrations as well as the difference in reaction conditions.

Table 2- 6 show the use of metal oxide catalysts that have been supported by an organic solvent to synthesise cyclic carbonates. It has been observed that the mixed oxides with the presence of organic solvents have achieved a better yield and selectivity. The use of these organic solvents does not promote green chemistry. However, the synthesis of styrene carbonate using solvent free catalyst promote green chemistry but the yield and selectivity obtained are lower to catalytic system with the use of organic solvent. The use of an organic solvent is toxic and not environmentally friendly. These drawbacks associated with the use of organic solvents are: difficulty in products separation, process complexity, influence the formation of different isomers, affect reaction rates and mechanisms.

The development of mixed metal oxides catalysts to synthesise cyclic carbonates in the absence of any organic solvent have drastically improved the yield and selectivity of the products (see Table 2-7). There is more room for improvement in order to achieve a higher yield and selectivity. One of such improvements is catalyst modifications, which will improve the acid and basic sites of the catalyst.

Table 2- 6. Catalytic performance of several metal oxide catalysts for the synthesis of cyclic carbonates.

Entry	Catalyst	Epoxide	Reaction conditions				Results		References
			Solvent	Pressure bar	Temperature K	Time h	Selectivity %	Yield %	
a	Al ₂ O ₃	PO	DMF	80	423	15	6.6	6.6	(Bhanage et al., 2001)
b	CaO	PO	DMF	80	423	15	8.1	0.8	(Bhanage et al., 2001)
c	CeO ₂	PO	DMF	80	423	15	76.9	17.5	(Bhanage et al., 2001)
d	La ₂ O ₃	PO	DMF	80	423	15	74.5	54.1	(Bhanage et al., 2001)
e	MgO	PO	DMF	80	423	15	92	32.1	(Bhanage et al., 2001)
f	MgO	PO	DMF	20	408	12	-	41	(Bhanage et al., 2001)
g	ZrO ₂	PO	DMF	80	423	15	50.8	10.9	(Bhanage et al., 2001)
h	MgO	PO	DMF	20	408	12	-	41	(Yano et al., 1997)
i	Mg-Al oxide	PO	DMF	5	393	24	97.7	88	(Yamaguchi et al., 1999)
j	Nb ₂ O ₅	PO	DMF	50	423	12	-	88	(Aresta et al., 2003a)
k	Zn-Si oxide	PO	TBAB	45	293	6	100	100	(Ramin et al., 2006)
l	Cs-P-Si oxide	PO	-	80	473	8	96	94	(Yasuda et al., 2006)
m	DMF	SO	-	79	423	15	-	85	(Kawanami and Ikushima, 2000)
n	MgO	SO	DMF	80	423	15	17.2	15.8	(Bhanage et al., 2001)
o	MgO	SO	DMF	20	408	12	-	60	(Yano et al., 1997)
p	Mg-Al oxide	SO	DMF	5	373	15	97.8	90	(Yamaguchi et al., 1999)
q	Nb ₂ O ₅	SO	DMF	50	408	12	-	80	(Aresta et al., 2003a)

PO: propylene oxide; SO: styrene oxide; TBAB: Tetra-n-butyl ammonium bromide.

2.5.4.3 The synthesis of cyclic carbonate using mixed metal oxide catalysts

The use of mixed metal oxides of Mg-Al was used to synthesise propylene carbonate and obtained 88% yield at 393 K and 3 atm. The same catalyst and reaction condition was used for the synthesis of styrene carbonate and 38% yield was obtained with TOF less than 4 h (Yamaguchi *et al.*, 1999).

In 2006, Sakakura used caesium, phosphorous, silicon mixed-oxide (Cs-P-Si) to synthesise propylene carbonate at 80 atm and 473 K. Cs-P-Si catalyst gave 50% yields. Yuan *et al.* (2008) reported the use of magnesium hydroxychloride (Mg(OH)Cl) and potassium iodide heterogeneous catalyst under a free solvent condition to synthesise propylene carbonate and styrene carbonate. The obtained yield for propylene carbonate was 98% with TOF of 17 h⁻¹ and styrene carbonate was 75% with a TOF of 8 h⁻¹ under the same reaction condition of 393 K and 60 atm.

Dai and Au recently used a composite oxide material composed of zinc, aluminium and magnesium to synthesis cyclic carbonate from epoxide and CO₂. The highest yield obtained was 89% of propylene carbonate from the reaction of CO₂ and epoxide, which was achieved after 12 h from reaction conditions of 25 atm and 393 K in the presence of triethylamines as an additive. The catalyst was recovered and reused five times during which no reduction in activity of the catalyst was observed. It was also observed that the catalyst active site contains both Lewis acidic of Aluminium and basic of Zinc, Magnesium groups, which were important for the simultaneous activation of the epoxide and CO₂ (Dai *et al.*, 2010).

The use of zinc-based hydroxyapatite catalyst in the presence of DMAP as a cocatalyst gave a high yield of styrene carbonate of 89% under the process condition of 100 atm and 373 K with TOF of 308 h⁻¹ (Mori *et al.*, 2004). In 2006, Baiker *et al.* used zinc-based catalysts supported on silica with TBAB as a cocatalyst for the synthesis of propylene carbonate and achieved a low yield of 19.2%. The low yield was as a result of a low catalyst loading when the amount of catalyst was increased from 2.5 wt% to 7 wt% ZnO/SiO₂ the yield reached 100% after 6 h at 393 K (Grunwaldt *et al.*, 2006).

Adeleye *et al.* (2014) synthesised propylene carbonate using a mixed metal oxide of ceria, lanthana doped zirconia under a free solvent and achieved 64% yield of

propylene carbonate. The reaction conditions for this process were 443 K, 79 atm for 20 h. It was noted that the increase in time is significant on the reactivity of the reactant and the catalysts in order to achieve a high yield and conversion. The catalyst was reused for five different runs and still achieved the same results, which show that the catalyst retains its catalytic performance.

The use of graphene oxide as a supported heterogeneous catalyst was investigated by Saha's group for the synthesis of propylene carbonate. Ceria, lanthana, zirconia doped graphene inorganic nanocomposite catalyst *via* continuous hydrothermal flow synthesis (CHFS) reactor was used to improve the synthesis of propylene carbonate to 74% yield. The optimum reaction condition was found to be 443 K, 69 atm and 10% (w/w) catalyst loading for 20 h. The catalyst reusability was investigated and found that it could be reused several times without losing its catalytic activity (Adeleye *et al.*, 2015).

Saha's group further exploited the use of graphene oxide as a supported heterogeneous catalyst to synthesise dimethyl carbonate (DMC). The novel catalyst used was ceria, zirconia oxide doped graphene and achieved 33% yield of DMC from methanol (MeOH) and carbon dioxide (CO₂) using 1,1,1, trimethoxymethane (TMM) as a dehydrating agent in a high-pressure reactor. The process reaction condition was at 383 K, 269 atm and 10% (w/w) catalyst loading for 16 h. The long-time stability of the catalyst was investigated and reported that it can be reused several times and still retains its catalytic activity (Saada *et al.*, 2015). In 2017, the use of graphene oxide supported heterogeneous catalysts of Ce-La-Zr-O was further investigated to synthesise 1,2-butylene carbonate *via* direct synthesis of the cycloaddition reaction of CO₂ to 1,2 epoxy butane and gave 64% yield. The process reaction conditions were found to be 408 K, 74 atm and catalyst loading of 10% (w/w) for 20 h (*Table 2-7*) (Onyenkeadi *et al.*, 2017).

Furthermore, in 2018, Saha's group developed a novel catalyst of tin, zirconia doped graphene *via* CHFS reactor, which was used to improve the direct synthesis of DMC through the reaction of propylene carbonate (PC) and methanol (MeOH) with molar ratio of 10:1, reaction temperature of 443 K, catalyst loading of 2.5% (w/w) for 4 h. This reaction achieved ~76% yield of DMC and ~72% conversion of PC. Optimisation of DMC synthesis was investigated by Saha's group using Box Bekhein Design (BBD) of response surface methodology

(RSM) and obtained the maximum predicted responses of 85.1% PC conversion and 81% yield of DMC at 12.33:1 MeOH: PC molar ratio, 446.7 K, 2.9% (w/w) catalyst loading and 4.08 h. These results were later validated experimentally and achieved ~78% yield of DMC and ~82% PC conversion at reaction condition of 12.3: 1 MeOH : PC molar ratio, reaction temperature of ~447 K, catalyst loading of 2.9% (w/w) and ~4.1 h (Saada *et al.*, 2018). The use of CHFS reactor to synthesise heterogeneous catalyst has been identified by Saha's group to give a better performance when compared to the traditional method of synthesising catalysts. One of the CHFS reactor advantages over traditional method identified was the reaction variables (e.g., temperature and pressure) that could influence the particle properties can be controlled independently. Another advantage highlighted was the presence of superheated water (673 K, 237 atm) used by CHFS reactor gives rapid precipitation and controlled growth in the fastest reaction time with anticipated chemical and physical characteristics. Some of CHFS reactor advantages include rapid synthesis, highly tunable and controllable way of synthesis of nano-material sparticle size < 500 nm (Kafizas *et al.*, 2009). There have been several reports that described the use of CHFS reactor as efficient, environment kindly and easy to use for the catalyst synthesis (Kellici *et al.*, 2010). However, Saha's group identified the major setback of CHFS was the high temperature of 673 K and pressure of 237 atm, which could likely pose danger and advised adequate safety measure should be taken to check such potential danger.

There has been a great deal of recent interest in the well-exfoliated graphene oxide (GO) product. In particular, GO sheets have been considered as a promising precursor for the bulk production of graphene-based materials through various reduction methods (Park and Ruoff, 2009a). Therefore, in parallel to the rapid progress of research in graphene materials, industrial-scale production of GO has emerged (Zhu *et al.*, 2012). GO, which can undergo deoxygenation upon thermal annealing, has long been known to be thermally unstable. The most attractive property of GO is that it can be (partly) reduced to graphene-like sheets by removing the oxygen-containing groups with the recovery of a conjugated structure. The reduced GO (rGO) sheets are usually considered as one kind of chemically derived graphene. In the so-called thermal "reduction", GO is actually undergoing disproportionation reactions, in which some of the partially oxidised sp^3 carbon atoms become fully oxidised to carbonaceous gases such as CO_2 and

the rest reduced to sp^2 graphene product (Cote *et al.*, 2012). However, the energy released from the deoxygenation of GO can also be harnessed to drive new reactions for creating graphene-based hybrid materials (Kim *et al.*, 2010). Various studies have shown that prolonged heat treatment of graphene oxide from 200 °C above becomes graphene and the colour turned black from brown (Kim *et al.*, 2010; Schniepp *et al.*, 2006, 2007).

The use of graphene as a supported heterogeneous catalyst has been identified to have improved the synthesis of cyclic carbonate due to the special qualities that are endowed with distinctive properties, for example, graphene at room temperature is known to have an excellent thermal conductivity of 3000 – 5000 W/(MK), electron mobility over 15,000 cm^2/Vs , which makes it unique in electric conductivity, very high specific surface area of about 2630 m^2g^{-1} and excellent catalytic properties (Park *et al.*, 2008). Since the discovery of a single atomic layer of two-dimensional carbon of nanomaterial that is relatively close to the ubiquitous graphite. Graphene in recent times has shown a wider application in energy storage, photoelectric, drug carrier, electronic information, semiconductor materials etc. (Pan *et al.*, 2017).

Graphene has been presented as the miracle of the 21st century. It has perfect sp^2 hybrid carbon structure, periodic structure and enormous conjugated bonding system with endless repetition in two dimension plane. The thickness of graphene of 0.334 nm makes it the thinnest material in the world. Graphene derivative includes graphene oxide in which carbon monolayer linked with carbonyl, carboxyl, epoxy groups and hydroxyl randomly thereby creating a lattice of amorphous and heterogeneous (Ren *et al.*, 2018).

The structure of graphene is obtained from the graphite oxide layering *via* ultrasonic process and stimulating water soluble solution of graphite oxide (Park and Ruoff, 2009b). There is no doubt that the application of graphene has become a promising material such as clean energy devices (Stoller *et al.*, 2008), nanoelectronic devices (Drnovšek, 2018), transparent conductive films (Park and Ruoff, 2009b), nanocomposite formulation (Jang and Zhamu, 2008), biochemical, physical and chemical sensors (Fowler *et al.*, 2009). Sensing applications of graphene sheets have experienced rapid usage in the last decade as it is used as transducers, most for gas sensing platforms (Gutés *et al.*, 2012).

The graphene is initially decorated with metal nanoparticles to increase sensitivity, limit of detection and selectivity of these properties. The decorating process is performed by electrochemical reduction of the metal ion *via* graphene flakes produced from graphene oxide or using an external reducing agent such as light while in other cases the formation of nanoparticles of metal is obtained by chemical reduction of the metal salts with the help of reducing agent (Sundaram *et al.*, 2008). The graphene is thereby decorated by adsorption of the formed nanoparticles in the solution (Li *et al.*, 2011).

The use of graphene oxide as a precursor to producing graphene-based heterogeneous catalysts through chemical vapour decomposition (CVD) using continuous hydrothermal flow synthesis (CHFS) reactor has been reported by Adeleye *et al.* (2015). This technique was also used by Saada *et al.* (2015) to produce graphene-based heterogeneous catalysts to synthesise dimethyl carbonate. This technique has been adopted to produce a graphene-based heterogeneous catalyst for the synthesis of 1,2-butylene carbonate.

2.6 Critical features of a high performing catalyst for cyclic carbonate synthesis

There have been several routes reported for the synthesis of cyclic carbonates including oxidative carboxylation of alkenes (Eghbali and Li, 2007; Sun *et al.*, 2005a, 2009; Wang *et al.*, 2008), oxidative carbonylation of alcohol and phenol (Ronchin *et al.*, 2009), reaction of urea and phenol or alcohol (Li *et al.*, 2008; Shaikh and Sivaram, 1996; Wang *et al.*, 2012) and phosgene and oxetanes (Aresta and Dibenedetto, 2004; Gupta, 2015; Krone and Klingner, 2005; Wijte *et al.*, 2011). These processes of cyclic carbonates syntheses use toxic materials and produced harmful by-products that are carcinogenic, which could pose a severe health challenge and a threat to the environment. These drawbacks in conventional approaches remain a major problem in recent times.

Recently, studies have shown that the use of catalysts have not only facilitated the process of greener organic carbonates synthesis but also enhanced the selectivity of the desired products and fulfilled the requirements for the sustainability of the greener chemical process. Various homogeneous catalytic processes have been studied extensively including an ionic liquid (Sun *et al.*, 2004a, 2004b, 2005b), salen metal complex (He *et al.*, 2009; Paddock and

Nguyen, 2004; Paddock *et al.*, 2004), salt and metal halide (Caló *et al.*, 2002; Feng *et al.*, 2016; Fujita *et al.*, 2010) for the synthesis of cyclic carbonate through the catalytic reaction of CO₂ and epoxides. However, these processes have suffered various drawbacks due to high cost of catalyst production, difficulty in separation of product from the reaction mixture, complexity of processes, extensive usage of co-solvent, potential production of toxic species, limitation of catalyst reusability and instability of the catalyst under room condition (Liu *et al.*, 2015a).

In recent years, a variety of heterogeneous catalysts have been developed through process of immobilizing or grafting of ionic liquid and salts into polymers, molecular sieve (MCM-41), magnesium oxide (MgO), and aluminium oxide (Al₂O₃) (Eghbali and Li, 2007; Yano *et al.*, 1997) to form solid materials in order to solve the drawbacks associated with using homogeneous catalysts. These techniques have shown an improvement in catalytic activity and better product selectivity for the synthesis of cyclic carbonates. There are several reports about diminishing activity of the immobilized heterogeneous catalyst when using solvents to achieve a better yield and therefore, could not pass the reusability test (Xu *et al.*, 2015).

The development of solvent-free heterogeneous catalytic system plays a significant role in greener process route for valuable chemical synthesis and offers numerous benefits. These benefits include reduction of process complexity, ease of catalyst separation, improved thermal stability, elimination of toxic and hazardous by-products. Moreover, it provides easier handling, safer storage, safer disposal, and introduce efficient reusability over the homogeneous counterpart (Adeleye *et al.*, 2015). This aptly makes solvent free heterogeneous catalytic system more economically viable and more attractive process that eliminates the risk to human health and the environment (Cavell *et al.*, 2010). There are other limitations of solvent-free heterogeneous catalytic system, which require a significant amount of catalyst of loading, high temperature, reaction time and lack of reactor design flexibility (Liu *et al.*, 2015b; Marvaniya *et al.*, 2011).

Recent reports on the use of mixed metal oxides for the synthesis of cyclic carbonates are showing promising results in terms of eliminating the drawbacks presented by the use of homogeneous catalysts. Tomishige and Kunimori (2002) had prepared CeO₂-ZrO₂ solid mixed metal oxides heterogeneous catalyst, which

gave a better activity under high calcination temperature. This was as a result of acid and basic properties of $\text{CeO}_2\text{-ZrO}_2$. Jiang (Jiang *et al.*, 2003) had also reported that $\text{H}_3\text{PW}_{12}\text{O}_{40}$ modified ZrO_2 had improved better catalytic activity than application of metal oxide ZrO_2 . The introduction of CeO_2 and La_2O_3 to ZrO_2 increases the amount of moderately acidic and basic sites, which then favours the activation of SO and CO_2 and improves the catalytic activity of SC synthesis.

Previous studies from Saha's group on the use of graphene supported heterogeneous catalyst has identified the improvement of the acid and basic sites of the mixed metal oxides catalysts. These improvements were identified to be as a result of different catalyst supports, different composition of metal oxide catalysts on acidic-basic surface properties and redox properties as well as using continuous hydrothermal flow synthesis reactor for catalysts synthesis.

Considering the above, one can acknowledge that despite many research efforts, the current pathways proposed to achieve better yield and selectivity of cyclic carbonates suffer from various setbacks which are summarised below.

- The use of homogeneous catalytic processes have suffered several setbacks due to high cost of catalyst production, difficulty in separation of product from the reaction mixture, complexity of processes, extensive usage of co-solvent, potential production of toxic species, limitation of catalyst reusability and instability of the catalyst under room condition.
- The use of several techniques such as immobilizing, grafting of ionic liquid and salts into polymers and molecular sieve to form solid heterogeneous materials have improved the limitation suffered by homogenous catalysts but unfortunately, there are several reports about diminishing of the catalyst activities. Some of these catalysts cannot withstand high temperature reaction.
- The use of organic solvent and heterogeneous metal oxide catalysts have shown remarkable yield and selectivity but have failed to promote green processes.
- It has been identified that bond distance provides CO_2 compound with unique properties, where it is hard to be activated and requires high energy to transform into another compound (Fujita *et al.*, 2014).
- The development of solvent free heterogeneous catalytic system promotes green processes. However, the use of a significant amount of

catalyst loading, high pressure, high temperature, longer reaction time and lack of reactor design flexibility have been identified (Marvaniya et al., 2011).

Examining all these shortcomings, more research efforts and deeper insight into developing solvent free heterogeneous catalysts that would address all these shortcomings are essential.

Table 2- 7. The synthesis of cyclic carbonates via mixed metal oxides heterogeneous catalysts

Reactants	Catalysts	Products	Temp (K)	PCO ₂ (Bar)	Time (h)	Conversion (%)	Yield (%)	Selectivity (%)	References
PO/CO ₂	Ce-La-Zr-O	PC	443	80	20	74	64	87	Adeleye et al., 2014
PO/CO ₂	Ce-La-Zr/GO(HT-500)	PC	443	70	20	86	82	94	Adeleye et al., 2015
MeOH/CO ₂	Ce-Zr/GO	DMC	383	275	16	58	33	57	Saada et al., 2015
BO/CO ₂	Ce-La-Zr/GO	BC	408	75	20	84	64	76	(Onyenkeadi et al., 2017)
MeOH/PC	Zr-Sn/GO	DMC	433	-	4	76	72.1	95	Saada et al., 2018
MeOH/CO ₂	Cu-Ni	DMC	383	12	10	7.8	6.9	88	Bain et al., 2009
Urea/1,2-propanediol	Zn-Mg	PC	443	-	0.5	-	94.8	-	Zhang et al., 2015

2.7 Conclusions

This chapter is a detailed literature review on carbon dioxide, applications of carbon dioxide, catalysis, organic carbonates and its applications that includes the various ways of syntheses of cyclic carbonates such as styrene carbonate and 1,2-butylene carbonate. Moreover, the process conditions and parameters such as temperature, pressure, catalyst loading and reaction time were evaluated and discussed.

The literature review has comprehensively demonstrated the growing attention of the synthesis of organic carbonates *via* the use of homogeneous and heterogeneous catalysts. The use of homogeneous and heterogeneous catalytic systems has been broadly considered and evaluated with the keen interest of CO₂ emissions reduction *via* utilisation to produce value-added chemicals. Heterogeneous catalytic systems have been found to be the best from the environmental and green chemistry point of view, especially metal oxides and mixed metal oxides catalysts.

The use of mixed metal oxides catalysts has shown a greater advantage for the synthesis of cyclic carbonates in the absence of organic solvents. Although, there is a need for more work to be done to improve the reaction time. Unlike the use of other heterogeneous catalysts, which have achieved much better yield with the help of organic solvents in a lesser time. The use of organic solvents helps to overcome the thermodynamic limitation of the reaction. It is essential to develop a novel catalyst that will not only improve the yield and selectivity of cyclic carbonates but also facilitate the reduction of the reaction time of the process and there no doubt that it requires more effort.

The development of novel heterogeneous catalytic processes will offer a new direction for the commercialisation of the green eco-friendly process of cyclic carbonates syntheses and also economically viable when compared with traditional routes.

CHAPTER 3

MATERIALS AND

METHODS FOR

CATALYSTS SYNTHESIS

AND

CHARACTERISATION

CHAPTER 3: MATERIALS AND METHODS USED FOR CATALYSTS SYNTHESIS AND CHARACTERISATION

3.1 Introduction

The quest for developing a greener and sustainable process for CO₂ emissions reduction requires the use of heterogeneous catalytic process to replace existing homogeneous catalytic processes. The use of metal oxides that include (lanthanum oxide (La₂O₃), cerium oxide (CeO₂), zirconium oxide (ZrO₂), magnesium oxide (MgO), graphene oxide (GO), copper oxide (CuO) and some mixed metal oxides such as magnesium doped aluminium oxide (MgO/Al₂O₃), lanthana doped zirconia (La₂O₃/ZrO₂), ceria doped zirconia (CeO₂/ZrO₂), copper doped zirconia (CuO/ZrO₂), ceria, lanthana doped zirconia (CeO₂-La₂O₃/ZrO₂), ceria, lanthana, zirconia doped graphene (CeO₂-La₂O₃-ZrO₂/GO), and copper, zirconia doped graphene (CuO-ZrO₂/GO) as heterogeneous catalysts. The use of continuous hydrothermal flow synthesis (CHFS) reactor (Figure 3-1) was explored for the synthesis of all metal oxides used to produce ceria, lanthana doped zirconia (CeO₂-La₂O₃/ZrO₂) and ceria, lanthana, zirconia doped graphene (CeO₂-La₂O₃-ZrO₂/GO) except copper doped zirconia (CuO/ZrO₂) and copper, zirconia doped graphene (CuO-ZrO₂/GO), which were synthesised using conventional means. The graphene oxide was synthesised using modified Hummers and Offerman's method and the rest of the catalysts were commercially purchased. The synthesised catalysts and commercially purchased catalysts were further characterised using scanning electron microscopy (SEM), transmission electron microscopy (TEM), Raman spectroscopy, X-ray powder diffraction (XRD), X-ray photoelectron spectroscopy (XPS) and Brunauer–Emmett–Teller (BET) surface area measurement.

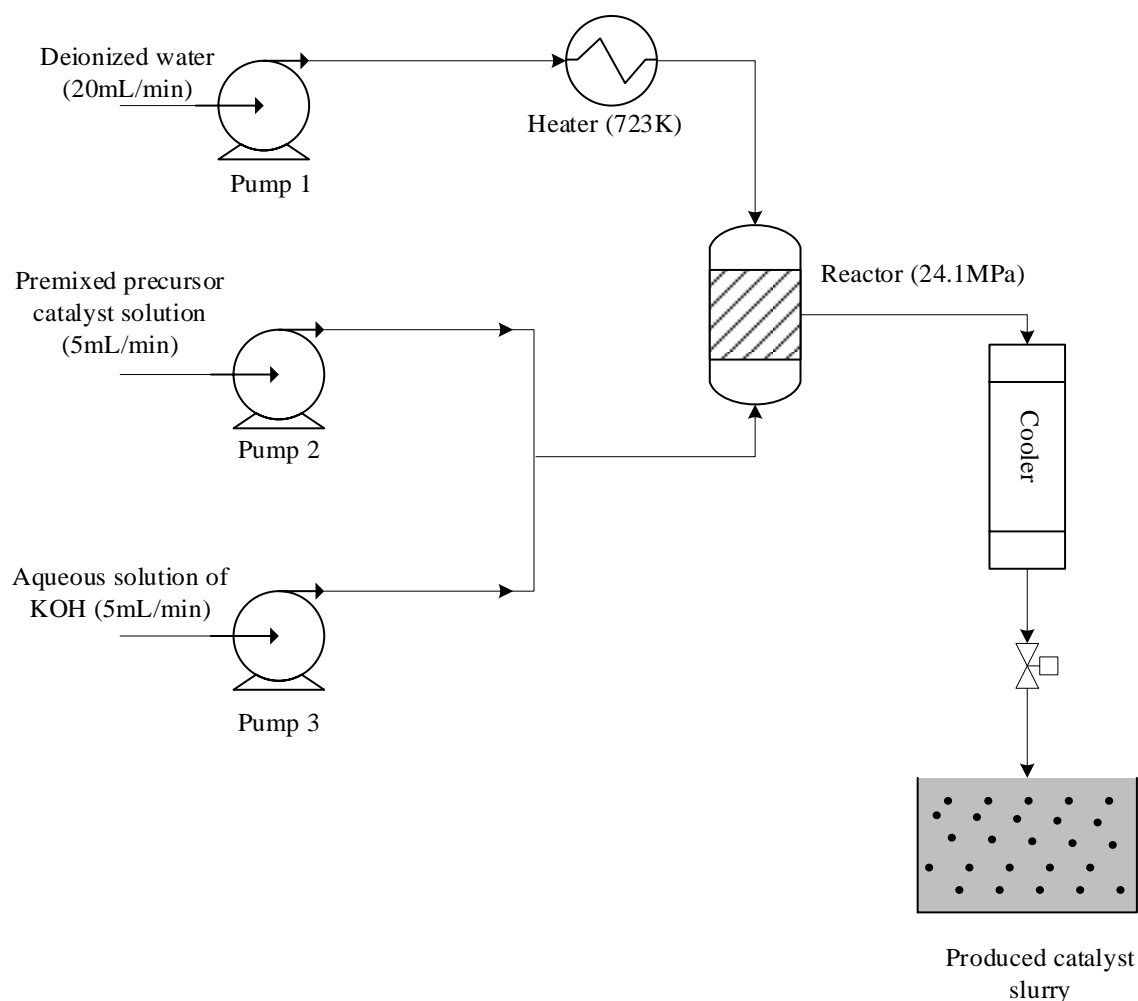


Figure 3- 1. Schematic of a CHFS reactor set up used for catalyst production

3.2 Metal oxides and mixed metal oxides synthesis

The following metal oxides and mixed metal oxides such as graphene oxide (GO) lanthanum oxide (La_2O_3), zirconium oxide (ZrO_2), lanthana doped zirconia ($\text{La}_2\text{O}_3/\text{ZrO}_2$), ceria doped zirconia ($\text{CeO}_2/\text{ZrO}_2$), ceria, lanthana doped zirconia ($\text{CeO}_2\text{-La}_2\text{O}_3/\text{ZrO}_2$) and ceria, lanthana, zirconia doped graphene ($\text{CeO}_2\text{-La}_2\text{O}_3\text{-ZrO}_2/\text{GO}$), copper oxide (CuO) and copper, zirconia doped graphene ($\text{CuO-ZrO}_2/\text{GO}$) were synthesised.

3.2.1 Graphene oxide synthesis

3.2.1.1 Materials

Natural graphite powder (NGP), hydrochloric acid (HCl), sulphuric acid (H_2SO_4), sodium nitrate, potassium hydroxide pellet (KOH), hydrogen peroxide (H_2O_2), acetone ($\text{C}_3\text{H}_6\text{O}$), and potassium permanganate (KMnO_4) were purchased from Fisher Scientific UK Ltd.

3.2.1.2 Graphene oxide synthesis procedure

Hummers and Offeman improved method (*Figure 3- 2, Figure 3- 3 and Figure 3- 4*) was used to prepare GO from NGP using KMnO_4 as an oxidizing agent (Hummers and Offeman, 1958). 1.25 g of NaNO_3 and 1.25 g of NGP were added into 57.5 mL of H_2SO_4 , which was stirred continuously with a magnetic stirrer in an ice bath for 15 min. 10 g of KMnO_4 was added to the black slurry mixture gradually under a continuous stirring, which was left for 15 min. The resulting dark green mixture was transferred to an oil bath at 313 K and stirred at 600 rpm for 90 min. The deionised water of 100 mL was added slowly to the dark green mixture for about 15 min then 15 mL of hydrogen peroxide (H_2O_2) was added in a dropwise manner for about 5 min followed by another 100 mL of deionised water, which was added to the mixture for about 15 min. The resulting light brown mixture was kept at 363 K and stirred continuously at 600 rpm for 15 min. The mixture was cooled to room temperature and the product was centrifuged (5000 rpm, 5 min per cycle). The centrifuged product was washed with diluted HCl (10 mL of HCl in 80 mL deionised water) four times and deionised water three times in order to remove impurities. The GO was freeze-dried for 24 hrs.

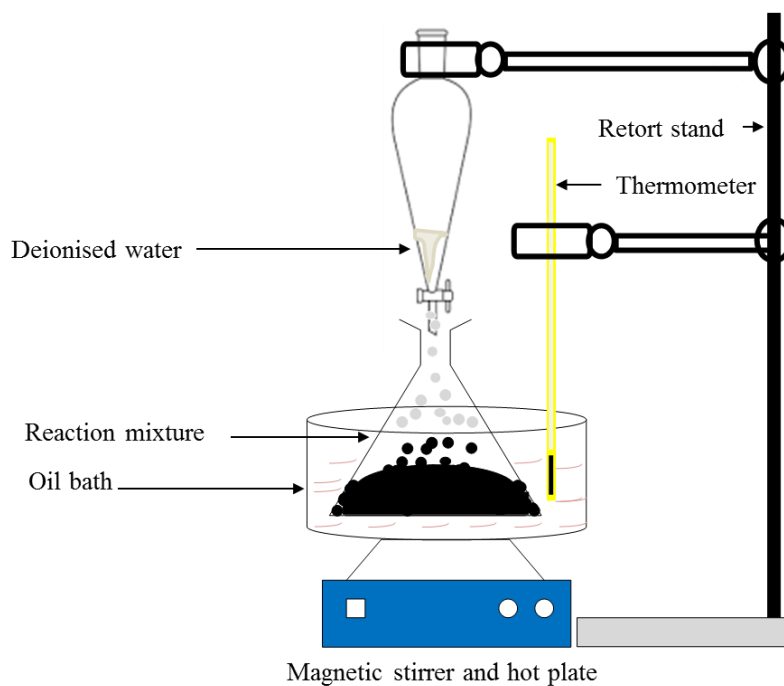


Figure 3-2. The schematic of experimental set-up for graphene oxide preparation

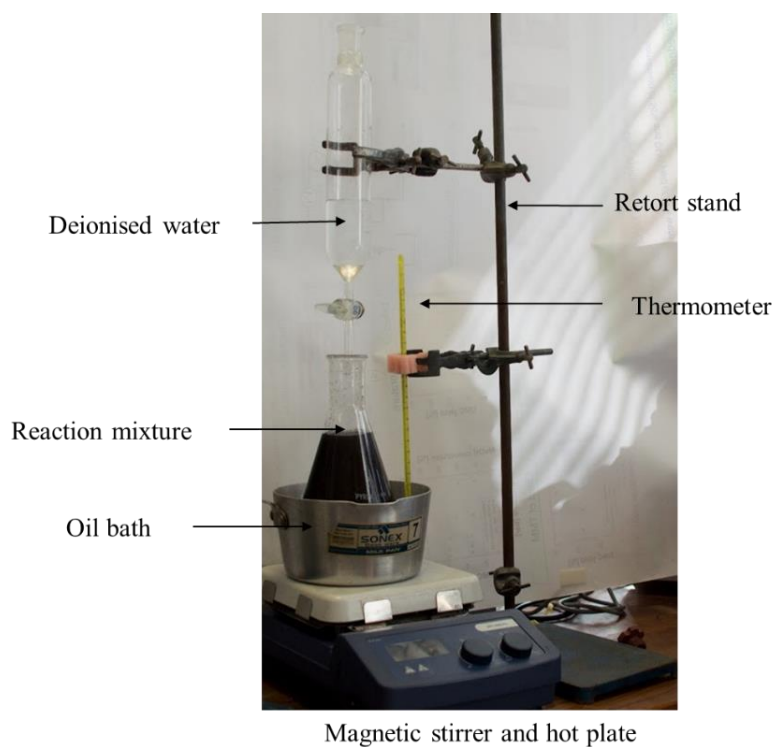


Figure 3-3. An image of the experimental set-up for graphene oxide preparation

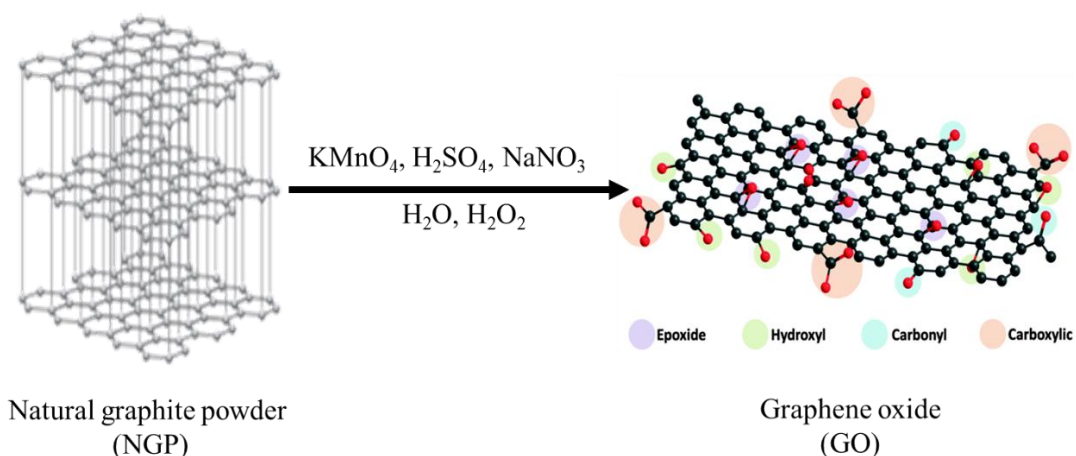


Figure 3- 4. A schematic representation of graphite powder transformation to graphene oxide (GO)

3.2.2 Lanthanum oxide synthesis

3.2.2.1 Materials

The precursor materials used for the synthesis include lanthanum (III) nitrate hexahydrate, $\text{La}(\text{NO}_3)_3 \cdot 6\text{H}_2\text{O}$ and potassium hydroxide (KOH).

3.2.2.2 Lanthanum oxide synthesis procedure

The metal salts of $\text{La}(\text{NO}_3)_3 \cdot 6\text{H}_2\text{O}$ and 1M of KOH were pumped at a flow rate of 5 mL/min into a reactor from the pump 2 and pump 3 respectively (Figure 3- 1). The resultant metal salts mixture co-currently meet with de-ionised water pumped from pump 1 at a flow rate of 20 mL/min, which was superheated to 723 K at 24.1 MPa in the reactor. This led to the formation of La_2O_3 (aqueous suspension) in a continuous manner, which was cooled down and collected with the aid of a back pressure regulator. The catalyst slurry was centrifuged (6000 rpm) and the solid particles were collected. These solid particles were washed twice with de-ionised water and freeze-dried for 24 h. The synthesised catalyst was labelled La-O (Figure 3- 5a).

The same procedure was carried out for the synthesis of cerium oxide and zirconia oxide with the use of the following metal salts cerium (III) nitrate hexahydrate, $\text{Ce}(\text{NO}_3)_3 \cdot 6\text{H}_2\text{O}$ and zirconium (IV) oxynitrate hydrate,

ZrO(NO₃)₃·6H₂O respectively as a precursor. The catalyst of CeO₂ was then labelled Ce-O and ZrO₂ was also labelled Zr-O (*Figure 3- 5 b*).



Figure 3- 5. Image of (a) lanthana oxide (La-O) and (b) zirconia oxide (Zr-O)

3.2.3 Lanthana doped zirconia oxide synthesis

3.2.3.1 Materials

The precursor materials used for the synthesis include lanthanum (III) nitrate hexahydrate, La(NO₃)₃·6H₂O and zirconium (IV) oxynitrate hydrate, ZrO(NO₃)₃·6H₂O and potassium hydroxide (KOH).

3.2.3.2 Lanthana doped Zirconia Oxide synthesis procedure

The metal salts of La(NO₃)₃·6H₂O and ZrO(NO₃)₃·6H₂O premixed solution of a ratio 11: 89 respectively were pumped at a flow rate of 5 mL/min into a reactor from the pump 2 and 1M of KOH was pumped from pump 3 at the same flow rate (*Figure 3-1*). The resultant metal salts mixture co-currently meet with de-ionised water pumped from pump 1 at a flow rate of 20 mL/min, which was superheated to 723 K at 24.1 MPa in an in-house built reactor upon, which the formation of La_xZr_{1-(x+y)}O₂ occurs in a continuous manner. This aqueous suspension was cooled down and collected with the aid of a back pressure regulator. The catalyst slurry was centrifuged (6000 rpm) and the solid particles were collected. These solid particles were washed twice with de-ionised water and freeze-dried for 24 h. The synthesised catalyst was heat treated at 973 K for 4 h and labelled as La-Zr-O (*Figure 3- 6a*).

The procedure was repeated for the synthesis of ceria doped zirconium oxide with the use of metal salts cerium (III) nitrate hexahydrate, $\text{Ce}(\text{NO}_3)_3 \cdot 6\text{H}_2\text{O}$ and zirconium (IV) oxynitrate hydrate, $\text{ZrO}(\text{NO}_3)_2 \cdot 6\text{H}_2\text{O}$ at an atomic ratio of 16:84 respectively as a precursor. The catalyst of CeO_2 doped ZrO_2 was then labelled Ce-Zr-O (Figure 3- 6b).

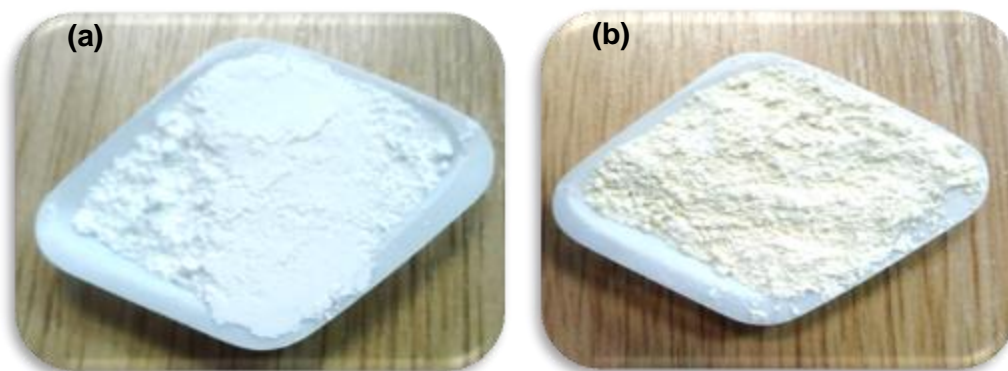


Figure 3- 6. Image of (a) lanthana doped zirconium oxide (La-Zr-O) and (b) ceria doped zirconium oxide (Ce-Zr-O)

3.2.4 Copper doped zirconia oxide synthesis

3.2.4.1 Materials

A control reaction using a traditional wet impregnation method was conducted for the synthesis of Cu-Zr-O catalyst. Copper (II) nitrate hydrate ($\text{Cu}(\text{NO}_3)_2 \cdot 2.5\text{H}_2\text{O}$) and zirconium(IV) oxynitrate hydrate ($\text{ZrO}(\text{NO}_3)_2 \cdot 6\text{H}_2\text{O}$) were used as metal precursors.

3.2.4.2 Copper doped zirconia oxide synthesis procedure

The catalyst was prepared using a conventional method where 2.5 g of $\text{Cu}(\text{NO}_3)_2 \cdot 2.5\text{H}_2\text{O}$ and 3.75 g of $\text{ZrO}(\text{NO}_3)_2 \cdot 6\text{H}_2\text{O}$ were added to 250 mL of deionised water and continuously stirred using a magnetic stirrer for 15 min. A solution of 30 mL of 8 M sodium hydroxide (NaOH) solution was added dropwise to the mixture while maintaining a vigorous agitation. The mixture was heated at 353 K using an oil bath for 1 h and was then cooled down to room temperature. The solid catalyst was separated using a centrifuge (6000 rpm, 5 min per cycle). The prepared catalyst was washed twice with deionized water using centrifuge (6000 rpm, 25 min per cycle) and dried at 323 K for 24 h.

3.2.5 Copper–zirconia/graphene inorganic composite synthesis

3.2.5.1 Materials

The traditional wet impregnation method was employed for the synthesis of Cu-Zr/GO using copper (II) nitrate hydrate ($\text{Cu}(\text{NO}_3)_2 \cdot 2.5\text{H}_2\text{O}$), zirconium(IV) oxynitrate hydrate ($\text{ZrO}(\text{NO}_3)_2 \cdot 6\text{H}_2\text{O}$) and GO were used as metal precursors.

3.2.5.2 Copper–zirconia/graphene inorganic composite synthesis using the conventional method

The catalyst was prepared using a traditional wet impregnation method for the synthesis of Cu–Zr/graphene inorganic composite catalyst. Copper (II) nitrate hydrate ($\text{Cu}(\text{NO}_3)_2 \cdot 2.5\text{H}_2\text{O}$) and zirconium(IV) oxynitrate hydrate ($\text{ZrO}(\text{NO}_3)_2 \cdot 6\text{H}_2\text{O}$) were used as metal precursors. 1 g of GO was dispersed in 50 mL of deionized water by ultrasonic vibration for 1 h. The mixture was removed from the ultrasonic bath and 0.5 g of ($\text{Cu}(\text{NO}_3)_2 \cdot 2.5\text{H}_2\text{O}$) and 0.75 g of $\text{ZrO}(\text{NO}_3)_2 \cdot 6\text{H}_2\text{O}$ were added to the GO suspension and continuously stirred using a magnetic stirrer for 12 min. 6 mL of 8 M sodium hydroxide (NaOH) solution was added dropwise to the mixture while maintaining a vigorous agitation. The mixture was heated at 80 °C using an oil bath for 1 h and was then cooled down to room temperature. Cu–Zr/GO inorganic composite catalyst was separated using a centrifuge (5000 rpm, 25 min per cycle). The prepared catalyst was washed twice with deionised water and dried at 323 K for 24 h. The dried Cu–Zr/GO nanocomposite catalyst (*Figure 3-7e*) was treated at different temperatures (i.e., 573 K, 723 K, 873 K) under nitrogen for 2 h. The catalyst was cooled down for 2 h before it was used to conduct experiments. The samples synthesised and heat treated (573 K, 723 K and 873 K) using this method were labelled as HTR300, HTR450 and HTR600 respectively.

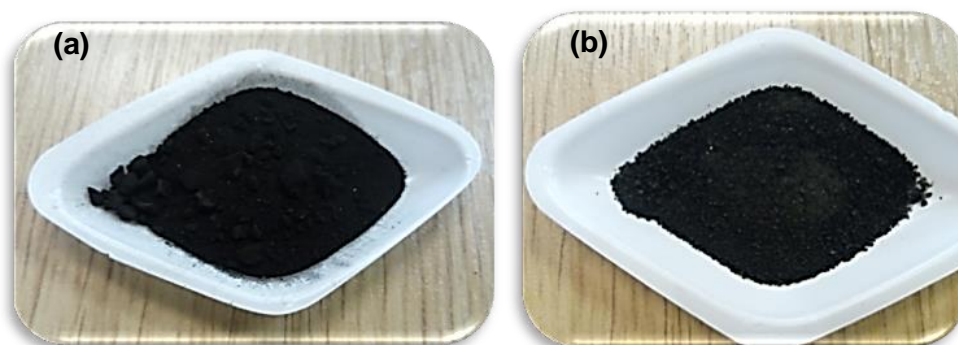


Figure 3- 7. Photographic image of (a) copper, zirconia doped graphene (Cu-Zr/GO) and (b) Heat treatment of copper, zirconia doped graphene at 723 K (HTR450).

3.2.6 Ceria-lanthana doped zirconia oxide synthesis

3.2.6.1 Materials

The materials used for the synthesis of ceria-lanthana doped zirconia oxide were an aqueous solution of KOH, deionised water, $\text{Ce}(\text{NO}_3)_3 \cdot 6\text{H}_2\text{O}$, $\text{La}(\text{NO}_3)_3 \cdot 6\text{H}_2\text{O}$ and $\text{ZrO}(\text{NO}_3)_2 \cdot 6\text{H}_2\text{O}$

3.2.6.2 Ceria-lanthana doped zirconia oxide synthesis via CHFS

The salts solution of zirconium ($\text{ZrO}(\text{NO}_3)_2 \cdot 6\text{H}_2\text{O}$), lanthanum ($\text{La}(\text{NO}_3)_3 \cdot 6\text{H}_2\text{O}$) and cerium ($\text{Ce}(\text{NO}_3)_3 \cdot 6\text{H}_2\text{O}$) were premixed at a desired atomic ratio of 80:15:5 respectively. These solutions were pumped using pump 2 likewise the aqueous solution of KOH from pump 3 at a flow rate of 5 mL/min as shown in *Figure 3-1*. The mixture of KOH and metal salts solutions then meet superheated deionised water at a temperature of 723 K, pressure of 24.1 MPa in a ¼ inch countercurrent reactor (kellici et al, 2014), which leads to the formation of $\text{Ce}_x\text{-La}_y\text{-Zr}_{(x+y)}\text{O}_2$ in a continuous way. The vertical cooler was used to cool down the aqueous suspension and the slurries were collected using a back pressure regulator. The slurry was centrifuged (6000 rpm) in order to separate the solid catalyst from the mixture. These solid particles (catalysts) were washed twice with deionised water and freeze-dried for 24 h. The synthesised catalyst was heat treated at 973 K for 4 h and labelled as Ce-La-Zr-O (*Figure 3- 8a*)

3.2.7 Ceria-lanthana-zirconia oxide/graphene nanocomposite synthesis

3.2.7.1 Materials

The following materials GO, Ce-La-Zr-O (15:5:80), an aqueous solution of KOH, and deionised water were used for the synthesis of ceria-lanthana-zirconia oxide/graphene (Ce-La-Zr/GO) nanocomposite catalyst.

3.2.7.2 Preparation of ceria-lanthana-zirconia/graphene nanocomposite synthesis *via* CHFS

CHFS experiment was conducted using a reactor with a basic design that has been reported earlier (Chaudhry et al., 2006; Kellici et al., 2010; Saada et al., 2015; Yan et al., 2010). CHFS simplified schematic of which is shown in Figure 3.1, mainly consists of three high-pressure pumps (utilised for delivery of the water and desired precursors), countercurrent reactor, cooler and back pressure regulator. In a typical experiment, each pre-mixed aqueous solution of $\text{Ce}(\text{NO}_3)_3 \cdot 6\text{H}_2\text{O}$, $\text{La}(\text{NO}_3)_3 \cdot 6\text{H}_2\text{O}$ and $\text{ZrO}(\text{NO}_3)_2 \cdot 6\text{H}_2\text{O}$ (with a total metal ion concentration of 0.2 M) Ce:La:Zr nominal atomic ratios (15:5:80) and pre-sonicated aqueous solution of GO (4 $\mu\text{g}/\text{mL}$) were pumped (*via* Pump 2) to meet a flow of KOH (1 M, delivered *via* Pump 3) at a T-junction (*Figure 3- 1*). The molar ratio of metal salt mixture $\text{Ce}^{3+}/\text{La}^{3+}/\text{Zr}^{4+}$ to GO was 1:1. This mixture meets superheated water (delivered *via* Pump 1 through the heater) at 24.1 MPa of 723 K inside an in-house built countercurrent reactor whereupon the formation of Ce-La-Zr/GO occurred continuously. The aqueous suspension was cooled through a vertical cooler and slurries were collected from the exit of the back pressure regulator (BPR). The product was separated *via* centrifugation (5000 rpm), washed with deionised water twice and then freeze-dried for 24 h (*Figure 3- 8b*).

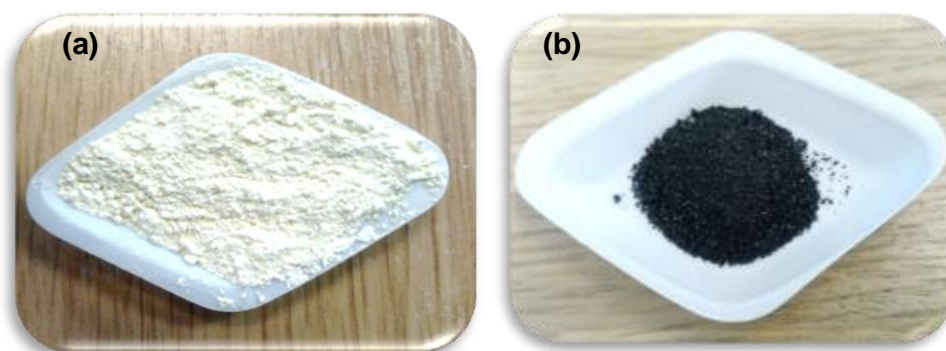


Figure 3- 8. Image of (a) ceria,lanthana, doped zirconia doped (Ce-La-Zr-O) and (b) ceria,lanthana, zirconia doped graphene (Ce-La-Zr/GO).

3.3 Physicochemical properties of heterogeneous catalysis

Table 3- 1 shows the physical and chemical properties of some of the commercially available catalysts and the synthesised catalysts used for this research work. These catalysts include Zr-O, GO, La-O, La-Zr-O, Ce-Zr-O, Ce-La-Zr-O and Ce-La-Zr/GO. Table 3-1 shows that Zr-O has the largest surface area of $310 \text{ m}^2 \text{ g}^{-1}$, which indicates the larger active surface contact for reactants while La-O offers less surface contact because it has the least surface area of $22 \text{ m}^2 \text{ g}^{-1}$. The surface area of GO is $124 \text{ m}^2 \text{ g}^{-1}$, La-Zr-O is $75 \text{ m}^2 \text{ g}^{-1}$, Ce-Zr-O is $70 \text{ m}^2 \text{ g}^{-1}$, Ce-La-Zr-O is $55 \text{ m}^2 \text{ g}^{-1}$ and Ce-La-Zr/GO is $115 \text{ m}^2 \text{ g}^{-1}$. Ce-La-Zr/GO catalyst has the smallest pore volume of $0.047 \text{ cm}^3 \text{ g}^{-1}$, which was relatively similar to GO catalyst of $0.049 \text{ cm}^3 \text{ g}^{-1}$ and Zr-O catalyst has the largest pore volume of about $0.45 \text{ cm}^3 \text{ g}^{-1}$.

Table 3- 1. Physical and Chemical Properties of Heterogeneous Catalysts and Synthesized Ce-La-Zr/GO Catalyst

Catalyst Properties	Catalyst						
	Zr-O	GO	La-O	La-Zr-O	Ce-Zr-O	Ce-La-Zr-O	Ce-La-Zr/GO
Physical form	White powder	Black powder	White powder	White powder	Pale-yellow powder	Pale-yellow powder	Black powder
Composition (%)	ZrO ₂ : 95±5	O: 24.64 C: 75.36	La ₂ O ₃ : 100	La ₂ O ₃ : 10±1 ZrO ₂ : 90±1	CeO ₂ : 18±2 ZrO ₂ : 82±2	CeO ₂ : 17±2 La ₂ O ₃ : 5±1 ZrO ₂ : 78±3	Ce: 2.98 La: 1.19 O: 34.99 C: 47.29 K: 0.8 Zr: 12.75 115
BET surface area (m ² g ⁻¹)	310	124	22	75	70	55	115
Pore volume (cm ³ g ⁻¹)	0.45	0.049	0.015	0.22	0.2	0.29	0.047
Particle size (nm)	5000	-	100	5000	30000	1700	5.78±3.9
Operating Temperature (K)	673	443 ^b	2578	673	673	673	443 ^b

Manufacturer data and ^bmeasured data (GO and Ce-La-Zr/GO)

3.4 Micrometrics Analysis

Brunauer-Emmett-Teller (BET) surface area measurements were performed on a Micromeritics Gemini VII analyser (nitrogen adsorption and desorption method) on the following heterogeneous catalysts: GO, Ce-La-Zr/GO, Cu-ZrO, Cu-Zr/GO (labelled AP) and corresponding heat treated catalysts at 723 K (labelled as HTR450) and 873 K (labelled as HTR600). Particle size analysis was performed using ImageJ particle size analysis software. The pore size distribution and pore volume were obtained using the Barrett–Joyner–Halenda (BJH) method.

The most commonly used technique to measure surface area is Brunauer-Emmett-Teller (BET) method (Naderi, 2015). This method determines the surface area based on the amount of gas adsorbed. Liquid nitrogen is the adsorptive gas used to determine the BET surface area at a constant temperature. The total amount of the gas adsorbed can be used to calculate the amount of adsorbed gas molecules that would produce a monolayer of the sample's surface at the desired pressure. The BET surface area of the heterogeneous catalysts presented in *Table 3-1* have been measured.

About 1 g sample was positioned in a sample tube and degassed for about 60 min at 393 K in order to remove moisture and impurities from the sample's surface. The tube sample was cooled down to room temperature and connected to liquid N₂ parallel to an empty reference tube. The sample tube and reference empty tube were lowered into Dewar (containing liquid N₂). Initially, the setting was run without loading a sample while subsequent runs were conducted with samples. Each catalyst was degassed at 373.15 K for 5 h prior to analysis using a Micromeritics FlowPrep 060 sample degas system. The five-point analysis was employed and the BET equation was used for calculation.

BET specific surface area (SSA) of Cu-ZrO, AP, HTR450 and HTR600 synthesised *via* traditional wet impregnation method are presented in *Table 3-2*. The trends observed in SSA and particle size are reported in *Figure 3-9*. Cu-ZrO has the largest BET surface area of 121 m²g⁻¹ and total pore volume of 0.28 cm³g⁻¹. It is prominent that the catalyst sample of AP shows a high SSA of 67 m²g⁻¹, which decreased to SSA of 41 m²g⁻¹, when heat treated at 723 K and shows further reduction when heat treated at 873 K to SSA of 33 m²g⁻¹. This reduction may be attributed to an increase in the particle size as confirmed by TEM data (*Table 3-2*). All catalysts are in mesoporous range (2-50 nm). The pore

volume of AP, HTR450 and HTR600 catalysts are $0.151 \text{ cm}^3\text{g}^{-1}$, $0.095 \text{ cm}^3\text{g}^{-1}$, and $0.105 \text{ cm}^3\text{g}^{-1}$ respectively.

Table 3- 2. Physical and chemical properties of synthesised copper doped zirconia (Cu-ZrO) and copper, zirconia doped graphene (Cu-Zr/graphene) nanocomposite catalysts.

<i>Catalyst Properties</i>	<i>Catalyst</i>			
	<i>Cu-ZrO</i>	<i>AP</i>	<i>HTR450</i>	<i>HTR600</i>
<i>Physical form</i>	<i>Black powder</i>	<i>Black powder</i>	<i>Black powder</i>	<i>Black powder</i>
<i>BET surface area ($\text{m}^2 \text{g}^{-1}$)</i>	121	67	41	33
<i>TEM Mean particle size (nm)</i>	18.0 ± 6.5	6.71 ± 1.12	6.92 ± 1.32	7.81 ± 1.57
<i>Pore volume ($\text{cm}^3 \text{g}^{-1}$)</i>	0.28	0.151	0.095	0.105
<i>Average pore diameter (nm)</i>	4.5	2.5	2.1	2.2
<i>True Density (g cm^3)</i>	4.4	3.05	2.7	3.1
<i>Atomic composition (%) (XPS)</i>	Cu: 2.98 O: 36.17 C: - Zr 3d: 11.75 Na 1s : 12.1	Cu: 1.11 O: 48.98 C: 30.40 Zr 3d: 5.75 Na 1s:13.75	Cu: 0.49 O: 21.98 C: 59.42 Zr 3d: 4.15 Na 1s:11.15	Cu: 0.47 O: 19.99 C: 64.38 Zr 3d: 4.05 Na 1s: 9.75

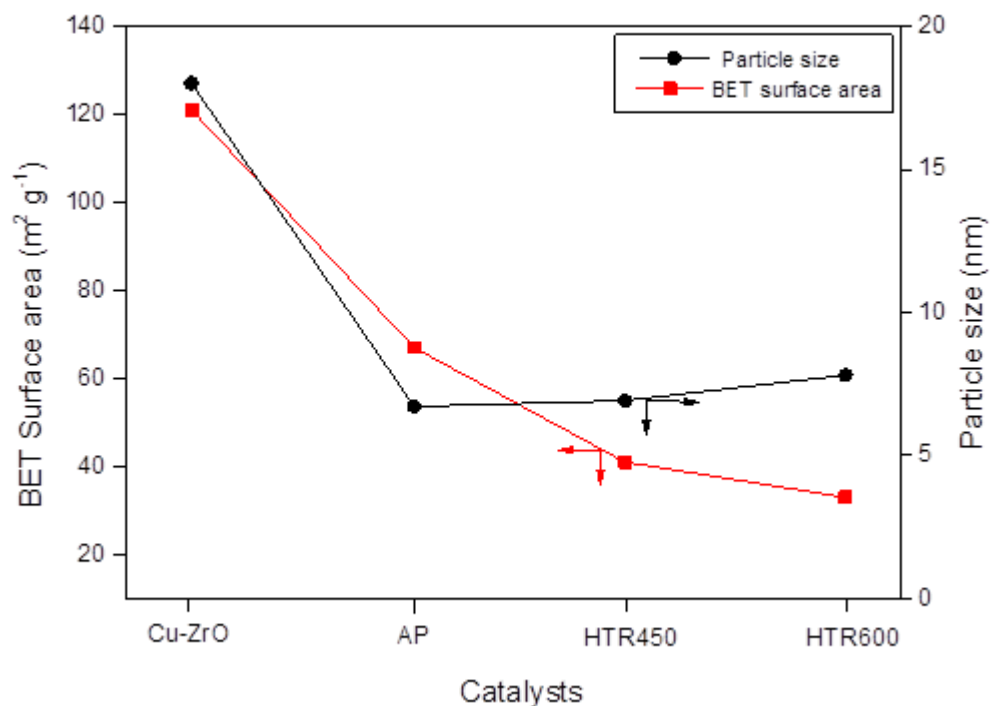


Figure 3- 9. BET surface area and particle size trends of AP and the corresponding heat-treated Cu-Zr/graphene nanocomposite catalysts.

$$\text{BET adsorption isotherm equation} = \frac{1}{V_a \left(\frac{P}{P_0} - 1 \right)} = \frac{P(C-1)}{C P_0 V_m} + \frac{1}{V_m C} \quad \text{Equation 3- 1.}$$

$$S_{\text{total}} = \frac{v_m N s}{V} \quad \text{Equation 3- 2.}$$

$$S_{\text{BET}} = \frac{S_{\text{total}}}{a} \quad \text{Equation 3- 3.}$$

Where

V_a =Volume of the adsorbed gas.

P_0 = The saturation pressure of adsorbates at the temperature of adsorption.

P = Equilibrium pressure

C = BET constant

V_m =Volume of the monolayer of adsorbed gas

S_{total} = Total surface science

N = Avogadro's number

s = The adsorption cross-section of the adsorbing species

V = Molar volume of the adsorbate gas

a = Mass of the solid sample or adsorbent

S_{BET} = Specific surface area

3.5 Electron microscopy (EM)

This is a type of microscopy that uses beams of electrons to generate an image of an examined specimen. It produces higher magnifications, has a greater resolving power and revealing smaller objects in finer details when compared with a light microscope (Kogure, 2013). There are two different types of electron microscopes and all uses electromagnetic or electrostatic lenses to control the path of electrons. The design of an electromagnetic lens is a coil of wire around the outside tube known as a solenoid through which current is passed through and that creates an electromagnetic field. Electron beams pass through the solenoid down to the column of EM to the samples and the faster the electrons travel, the shorter its wavelength becomes (Kogure, 2013). The sensitivities of electrons to magnetic fields make it easy to control by changing the current through the lenses. The technique of electron microscopy reveals the formation of the particle size, shape and compositions. Scanning electron microscopy (SEM) and Transmission electron microscopy (TEM) care the two types of Electron microscopy.

3.5.1 Scanning electron microscopy (SEM)

The scanning electron microscopy (SEM) involves the application of a microscope, which uses electrons instead of light to build a three-dimensional image of higher magnification. This mainly works by scanning the surface of the sample in a raster pattern with a focused beam of electrons and detecting an image from the reflected electrons from and off the sample's surfaces (Han *et al.*, 2018).

In this study, analysis of GO, Zr-O, La-O, Ce-Zr-O, La-Zr-O, and Ce-La-Zr-O catalysts were carried out using FEI inspect F and Quanta 3D FEG with a gold plated sample holder. These catalysts structural images are shown in Chapter 6, section 6.3.

3.5.2 Transmission electron microscope (TEM) analysis

The TEM uses a high voltage electron beam emitted by a cathode and produced from magnetic lenses. It uses electrons in place of light as a source to the targetted image. These electron beams are transmitted partially through the thin slice of the sample and carry information about the structure of the sample to the other side (Paredes, 2014). The image is then magnified by series of magnetic lenses until is recorded by smashing on the fluorescent screen, photographic plate or light-sensitive sensor for example charge-couple device (CCD) camera (McNeill, 2012). The detected image by CCD is displayed in real time on the computer. This is particularly good for learning as it has shown the component that the sample is made up to form the structure and a valuable tool for analysis in several professional fields, especially in material science due to its high resolution. The use of TEM for analysis is often time-consuming when preparing a sample of a thin layer that is electron transparent.

The TEM used to analyse GO, Ce-La-Zr-GO, AP, HTR450 and HTR600 was JEOL 2100FCs with a Schottky Field Emission Gun transmission electron microscope (200 kV accelerating voltage). The collected catalyst sample was dispersed in deionised water ultrasonically, then a drop of the suspension was placed on a carbon-coated copper grid (Holey Carbon Film, 300 mesh Cu, Agar Scientific, Essex, UK). The particle distribution sizes were calculated from the images of the catalysts that were attained in transmission mode using J software Images. The presence of the mixed metal oxide support on graphene becomes darker because of the higher density. This is further explained in details in Chapter 4 and 7 in the catalyst characterisation section.

3.6 X-ray photoelectron spectroscopy (XPS) analysis

The simplicity of X-ray photoelectron spectroscopy (XPS) and results obtained for several oxidation states of the catalyst under analysis makes it the most

widely used surface analysis technique at a relative depth of 10 nm. XPS can also be used to study the dispersion of the supported catalyst (Chorkendorff and Niemantsverdriet, 2003) and uses a photoelectric effect technique. The sample is exposed to X-ray photons, which interacts with the inner electrons' shell and the atom ionises to produce an ejected free photoelectron (Figure 3- 10).

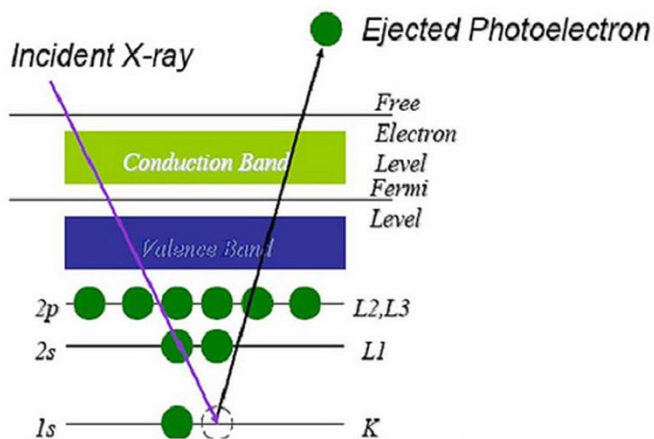


Figure 3- 10. An X-ray photoelectron spectroscopy. Adapted from (Chorkendorff and Niemantsverdriet, 2003)

$$E_k = h\nu - E_b - \Phi \quad \text{Equation 3- 4}$$

Where:

E_k = Kinetic energy

h = Planck's constant

ν = Radiation frequency

E_b = Electron binding energy

Φ = The work function of the material

Equation 3- 4 can be used to calculate the kinetic energy of the emitted photoelectrons. E_b is dependent on the atom's chemical bonding that makes XPS important to identify the atom's oxidation state. XPS instruments comprise of the sample stage, X-ray source, the analyser of the photoelectrons and electron detector.

The XPS measurement of GO, Ce-La-Zr/GO, AP, HTR450 and HTR600 catalysts were performed on Kratos Axis ultra DLD photoelectron spectrometer utilising monochromatic Al $K\alpha$ source, operating at 144W. The catalysts samples were placed using conductive carbon tape and data were collected in the hybrid mode of operation *via* electrostatic and magnetic lenses. The survey and narrow scans were carried out at a pass energy of 40 and 160 eV respectively. These samples spectra were collected under the base pressure of the system of ca. 1×10^{-9} Torr rising to ca. 4×10^{-9} Torr and take off angle of 90° . The C (1s) line from the resulting spectra was calibrated at 284.8 eV.

XPS analysis was employed to investigate the changes in the concentration of copper and zirconium in the lattice, their oxidation states and the chemical states of as-prepared (AP) catalyst and corresponding HTR450 and HTR600 heat-treated catalysts. XPS percentage (%) atomic composition showed that GO predominantly consists of oxygen and carbon atoms (C:O/3:1) and Ce-La-Zr-GO catalysts consist of metals (Ce - cerium, La – lanthanum and Zr – zirconium), K – potassium, C - carbon and O – oxygen atoms as shown in *Table 3- 1*. XPS percentage (%) atomic composition showed that is copper, zirconia doped graphene nanocomposite catalysts consist of metals (Cu-copper and Zr-zirconia), Na – sodium, C - carbon and O – oxygen atoms as shown in *respectively*.

Table 3- 2. XPS analysis revealed that the metal ratios for all samples are all very similar.

3. 7 X-ray powder diffraction (XRD) analysis

XRD is a powerful analytical technique that is commonly used for identification of a crystalline substance and generate information on the dimensions of the unit cell (Cassetta, 2014). The XRD consists of a sample holder, an X-ray tube, and an X-ray detector. The pattern of XRD pure powder sample is just like a fingerprint of substance morphology and each substance has its own diffraction pattern characteristic. At the cathode ray tube, the X-rays are generated and hitting the samples with electrons, which dislodge the inner shell electrons of the samples, thereby producing X-rays spectra. These spectra have several

components and the most used are K_{α} and K_{β} K_{α} having in parts of $K_{\alpha 1}$ and $K_{\alpha 2}$ $K_{\alpha 1}$. When X-ray beam strikes a crystalline sample, they scatter and generate a diffraction pattern that is being detected by an X-ray detector. Bragg's equation (see Equation 3.5) is used to measure the distance between the planes (Figure 3- 11)

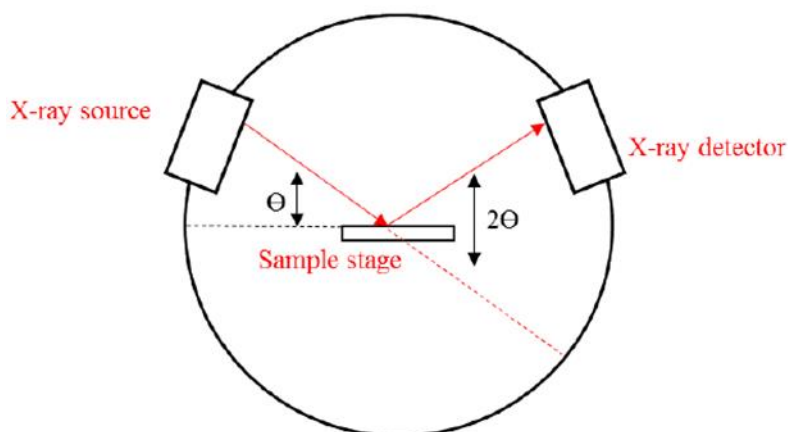


Figure 3- 11. Basic set up of an X-ray Diffractometer. Adapted from (Alsaiani, 2017)

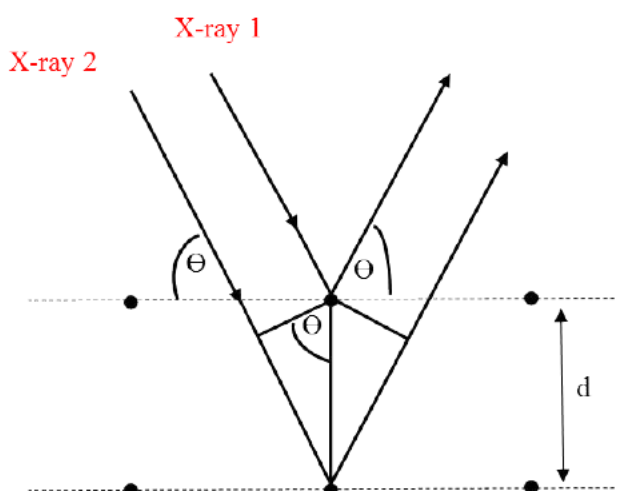


Figure 3- 12. The interaction of X-rays within a crystal surface. Adapted from (Cassetta, 2014).

The XRD patterns of Zr-O, La-O, Ce-Zr-O, La-Zr-O, and Ce-La-Zr-O were investigated on a Siemens D5000 X-ray powder diffractometer analyser operated

at $\Theta/2\Theta$ geometry. The XRD patterns of GO, Ce-La-Zr/GO (prepared *via* CHFS reactor), AP, HTR450 and HTR600 were obtained on a Stoe StadiP transmission diffractometer using a 0.7093-angstrom wavelength of Mo radiation set at 50 kV 30 mA *via* Germanium 111 monochromatic crystal of $K_{\alpha 1}$. The prepared samples were sandwiched between two polymer sheets clamping into an aperture holder of 3 mm and the X-ray beam was rotated. Dectris Mythen 1 K silicon strip position sensitive detector (PSD) were used to collect data at 2Θ by scanning from 2° to 45° at 0.5° steps per 30 seconds while resolution step of the data is 0.015° . The alignment of diffractometer was tested with the LaB_6 standard.

3.8 Fourier transform infrared spectroscopy (FT-IR) analysis

The FT-IR analysis is usually used to generate an infrared spectrum of absorption or emission of different materials in liquid, gas or solid state. When an infrared (IR) radiation is passed through a sample, some radiation passes through while some radiation is absorbed by the sample. The detector generates a spectrum from the detected resulting signal, which represents a molecular fingerprint of the sample. The use of IR spectroscopy promotes effectual positive identification of all materials *via* qualitative analysis. Moreover, the peak sizes of the spectrum relate to the number of materials existing in the sample.

The use of FT-IR is highly accurate in generating results and requires no calibration. It is a nondestructive technique and processing time is fast when compared to scanning spectrometer. FT-IR consists of five main parts, which are the sample, IR source, interferometer, detector and computer (*Figure 3- 13*).

Firstly, a background spectra measurement of a blank sample in the beam was taken due to the requirement for a relative scale in absorption intensity. The IR spectra analysis were carried out on some of the heterogeneous catalysts using FT-IR – 660 Plus FT-IR spectrometer (JASCO). Acetone was used to clean the sample holder and the sample was placed in the sample holder. The scans were carried out between 500 and 4000 cm^{-1} and the data were collected.

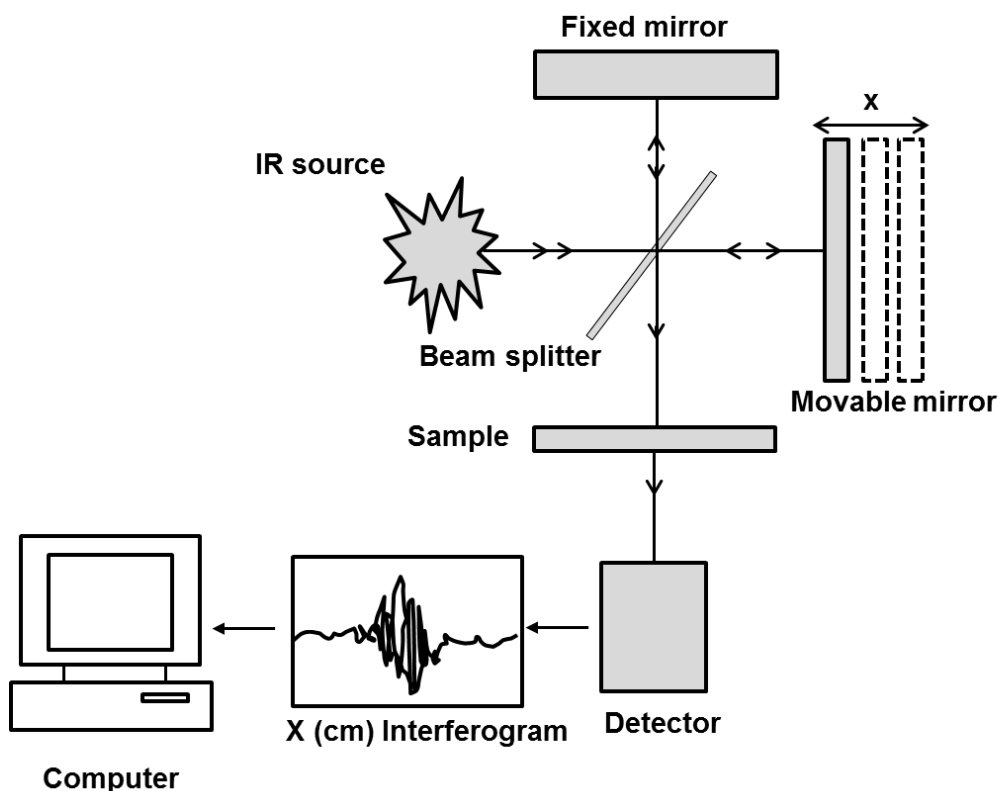


Figure 3- 13. Schematic sketch of the essential features of a Fourier transform infrared (FTIR) spectrometer.

3.9 Conclusions

Several heterogeneous catalysts were successfully synthesised using a continuous hydrothermal flow synthesis (CHFS) reactor and traditional wet impregnation method while the graphene oxide was prepared by modified Hummer and Offerman (1958) method. The methods used for catalysts characterisation such as Brunauer–Emmett–Teller (BET) surface area measurement, scanning electron microscopy (SEM), transmission electron microscopy (TEM), X-ray powder diffraction (XRD), X-ray photoelectron spectroscopy (XPS) and Fourier transform infrared spectroscopy were extensively discussed.

CHAPTER 4

GREENER SYNTHESIS OF 1,2-BUTYLENE CARBONATE VIA CO₂ USING GRAPHENE- INORGANIC NANOCOMPOSITE CATALYST

CHAPTER 4: GREENER SYNTHESIS OF 1,2-BUTYLENE CARBONATE FROM CO₂ USING GRAPHENE-INORGANIC NANOCOMPOSITE CATALYST

4.1 Introduction

1,2-Butylene carbonate, one of the cyclic carbonates, is a valuable chemical of great commercial interest. It is an excellent reactive intermediate material used in industry for the production of plasticisers, surfactants, and polymers and can also be used as a solvent for degreasing, paint remover, wood binder resins, foundry sand binders, lubricants as well as a potential solvent for lithium battery as energy generation because of its high polarity property (Aresta and Dibenedetto, 2002; Alves et al., 2017). The significance of 1,2-butylene carbonate synthesis will not only contribute to CO₂ emission reduction that causes global warming, but will also contribute to a value-added chemical production for industrial usage.

Several metal oxide catalysts have been developed and assessed for the effective synthesis of cyclic carbonates such as magnesium oxide (MgO) (Fujita et al., 2014), graphene oxide (GO) (Xu et al., 2015), zirconium oxide (ZrO₂) (Dai et al., 2009), cerium oxide (CeO₂) (Dai et al., 2009), lanthanum oxide (La₂O₃) and a mixed metal oxide such as ceria doped zirconia oxide (Ce-ZrO₂) (Saada et al., 2018). Furthermore, it has been identified that the use of support can enhance the dispersion of the active sites, the stability of catalyst, and consequently offer, improvements of the catalytic properties of the material.

Recent studies have shown numerous materials have been extensively used as suitable supports such as activated carbon, silica, molecular sieves, metal oxides and graphene oxide (Huang and Tan, 2014). However, there are no studies that have shown the synthesis of 1,2-butylene carbonate using a supported heterogeneous catalyst.

In this chapter, we report the use of graphene derivative (ceria-lanthana-zirconia/graphene nanocomposite) as high-quality catalyst material (highly stable and active) prepared *via* controlled, easily scalable continuous hydrothermal flow synthesis (CHFS). The use of CHFS reactors over conventional means gives independent control over reaction variables such as temperature, flow rate and pressure (Zhang et al., 2009). The process of CHFS involves the continuous

mixing of supercritical water stream with an aqueous precursor/flow (typically metal salts) to produce spontaneous precipitation of nanoparticles with desirable composition and properties.

The catalytic activities of the CHFS synthesised Ce-La-Zr/GO inorganic nanocomposite has been assessed using a new, greener and sustainable process for the direct synthesis of 1,2-butylene carbonate from CO₂ with 1,2-butylene oxide. Several heterogeneous catalysts and graphene oxide as the supported heterogeneous catalyst have been used to synthesise 1,2-butylene carbonate through direct synthesis of 1,2-butylene oxide and carbon dioxide in a high-pressure reactor under different reaction conditions. Effect of various parameters and factors such as catalysts loading, reaction temperature, reaction time, CO₂ pressure has been studied. Catalyst reusability studies have been carried out to investigate the stability and reusability of the catalyst for the synthesis of BC.

4.2 Materials

Natural graphite powder (NGP), hydrochloric acid (HCl), sulphuric acid (H₂SO₄), sodium nitrate, potassium hydroxide pellet (KOH), hydrogen peroxide (H₂O₂), acetone (C₃H₆O), octane (C₈H₁₈) and potassium permanganate (KMnO₄) were purchased from Fisher Scientific UK Ltd. Methanol (CH₃OH), cerium(III) nitrate hexahydrate (Ce(NO₃)₃·6H₂O), lanthanum (III) nitrate hexahydrate (La(NO₃)₃·6H₂O), zirconium (IV) oxynitrate hydrate (ZrO(NO₃)₂ · xH₂O), 1,2-butylene oxide (C₄H₈O), 1,2-butylene carbonate (C₅H₈O₃) were purchased from Sigma–Aldrich Co. LLC, UK. The catalysts used for the experiments were magnesium oxide (MgO), zirconium oxide (ZrO₂), cerium oxide (CeO₂), lanthana oxide (La₂O₃), lanthana doped zirconia (La-ZrO₂), lithium doped zirconia (Li-ZrO₂), ceria doped zirconia (Ce-ZrO₂) and ceria, lanthana doped zirconia (Ce-La-ZrO₂). The above-mentioned catalysts were supplied by MEL Chemical Company Ltd except for magnesium oxide, which was purchased from Sigma Aldrich. The liquid CO₂ cylinder (99.9%) equipped with a dip tube was purchased from BOC Ltd., UK. All chemicals were used without further pre-treatment or purification.

4.3 Preparation and characterisation of ceria-lanthana-zirconia oxide/graphene nanocomposite synthesis *via* CHFS

4.3.1 Graphene oxide (GO) preparation

An improved method of Hummers and Offeman (Hummers and Offeman, 1958) was used to prepare GO from NGP using KMnO₄ as an oxidizing agent. 1.25 g of NaNO₃ and 1.25 g of NGP was added into 57.5 mL of H₂SO₄, which was stirred continuously with a magnetic stirrer in an ice bath for 15 min. 10 g of KMnO₄ was added to the black slurry mixture gradually under a continuous stirring, which was left for 15 min. The resulting dark green mixture was transferred to an oil bath at 313 K and stirred at 600 rpm for 90 min. The deionised water of 100 mL was added slowly to the dark green mixture for about 15 min then 15 mL of hydrogen peroxide (H₂O₂) was added in a dropwise manner for about 5 min followed by another 100 mL of deionised water. The resulting light brown mixture was kept at 363 K and stirred continuously at 600 rpm for 15 min. The mixture was cooled to room temperature and the product was subject to centrifugation (5000 rpm, 5 min per cycle). The product was washed with diluted HCl (10 mL of HCl in 80 mL deionised water) four times and deionised water three times in order to remove impurities. The GO was freeze-dried for 24 hrs.

4.3.2 Preparation of ceria-lanthana-zirconia/graphene nanocomposite synthesis *via* CHFS

CHFS experiment was conducted using a reactor with a basic design that has been reported earlier (Chaudhry et al., 2006; Kellici et al., 2010; Yan et al., 2010; Saada et al., 2015). CHFS simplified schematic of which is shown in Figure 4.1, mainly consists of three high-pressure pumps (utilised for delivery of the water and desired precursors), countercurrent reactor, cooler and back-pressure regulator. In a typical experiment, each pre-mixed aqueous solution of Ce(NO₃)₃.6H₂O, La(NO₃)₃.6H₂O and ZrO(NO₃).6H₂O (with a total metal ion concentration of 0.2 M) Ce:La:Zr nominal atomic ratios (15:5:80) and pre-sonicated aqueous solution of GO (4 µgm/L) were pumped (*via* Pump 2) to meet a flow of KOH (1 M, delivered *via* Pump 3) at a T-junction (see *Figure 4- 1*). The molar ratio of metal salt mixture Ce³⁺/La³⁺/Zr⁴⁺ to GO was 1:1. This mixture meets superheated water (delivered *via* Pump 1 through the heater) at 24.1 MPa of 723 K inside an in-house built countercurrent reactor whereupon the formation of Ce-

La-Zr/GO occurred continuously (Lester et al., 2006; Cabañas et al., 2007). The aqueous suspension was cooled through a vertical cooler and slurries were collected from the exit of the back-pressure regulator (BPR). The product was separated *via* centrifugation (5000 rpm), washed with de-ionised water twice and then freeze-dried.

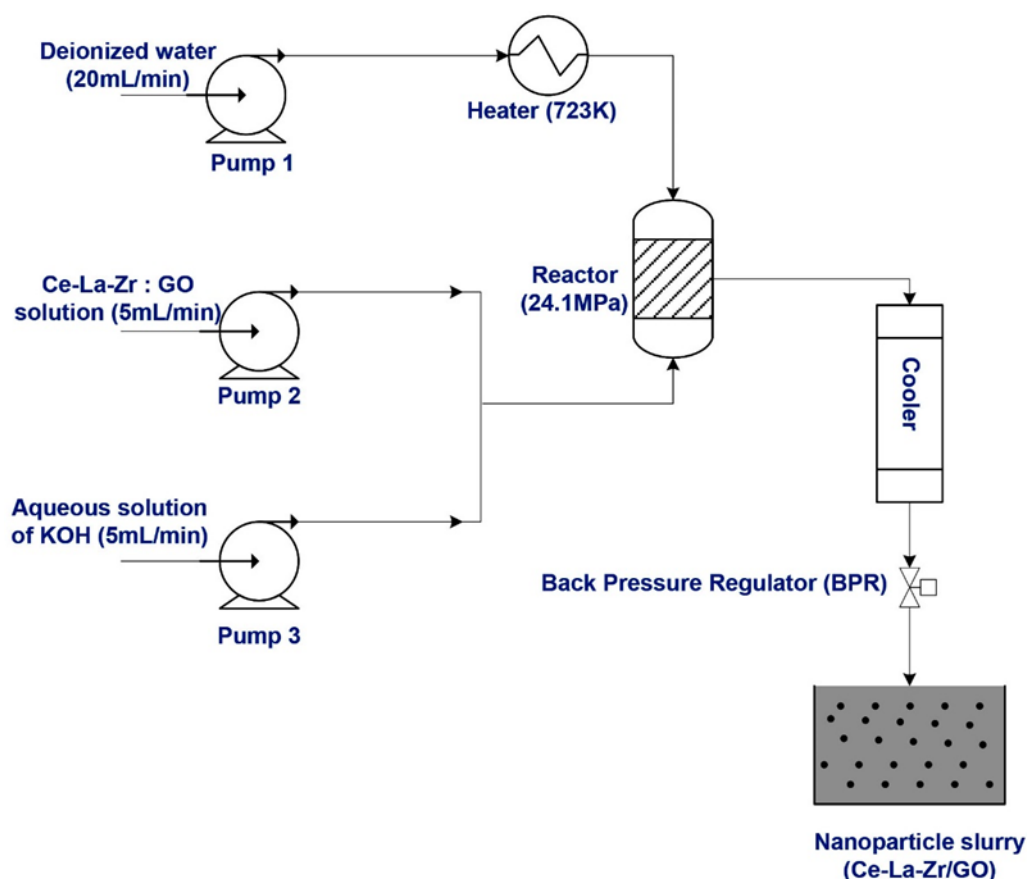


Figure 4- 1. Schematic of a CHFS reactor set up used for the production of Ce-La-Zr/GO inorganic nanocomposite catalyst.

4.4 Experimental procedure for the synthesis of 1,2-butylene carbonate (BC)

The synthesis of BC was carried out in a 25 mL stainless steel high-pressure reactor (Model 4590, Parr Instrument Company, USA) equipped with a mechanical stirrer, thermocouple (type J) and a heating mantle and controller (model 4848) (Figure 4- 2). The reactor was charged with a required amount of

BO and catalyst. The high-pressure reactor was heated to the required temperature and continuously stirred at a known stirring speed. Supercritical fluid pump (model SFT-10, Analytix Ltd., U.K) was used to inject CO₂ at a desired pressure from the cylinder to the reactor and left for a specified time. After the reaction, the reactor was quenched using an ice bath to room temperature to stop the reaction. The reactor was depressurized, and the reaction mixture was filtered. The recovered catalyst was washed with acetone and dried in an oven while the products were analysed using gas chromatography (GC) equipped with a flame ionization detector (FID) with a capillary column using toluene as an internal standard. The effect of various parameters that include catalyst types, catalyst loading, CO₂ pressure, reaction temperature and reaction time was studied for the optimisation of the reaction conditions. Catalyst reusability studies were also conducted to assess the stability of the catalyst for synthesis of BC.

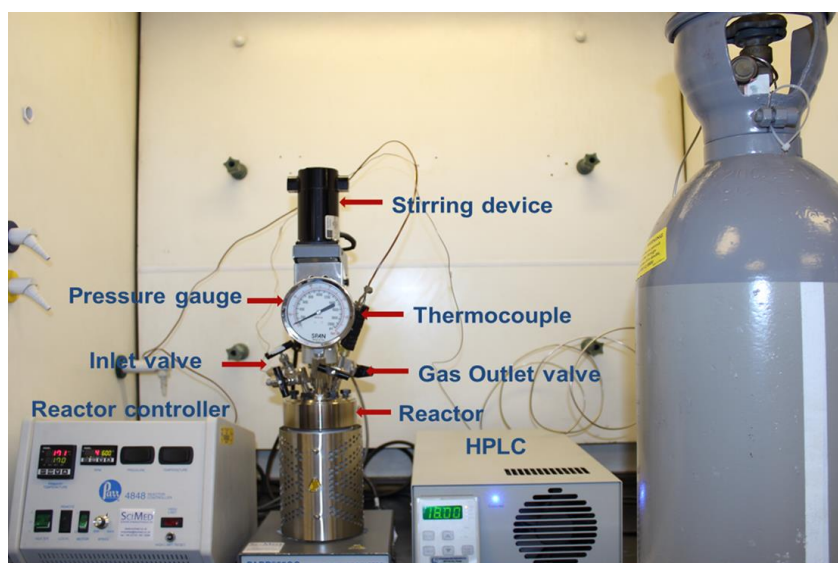


Figure 4-2. Batch experimental set-up for the synthesis of styrene carbonate.

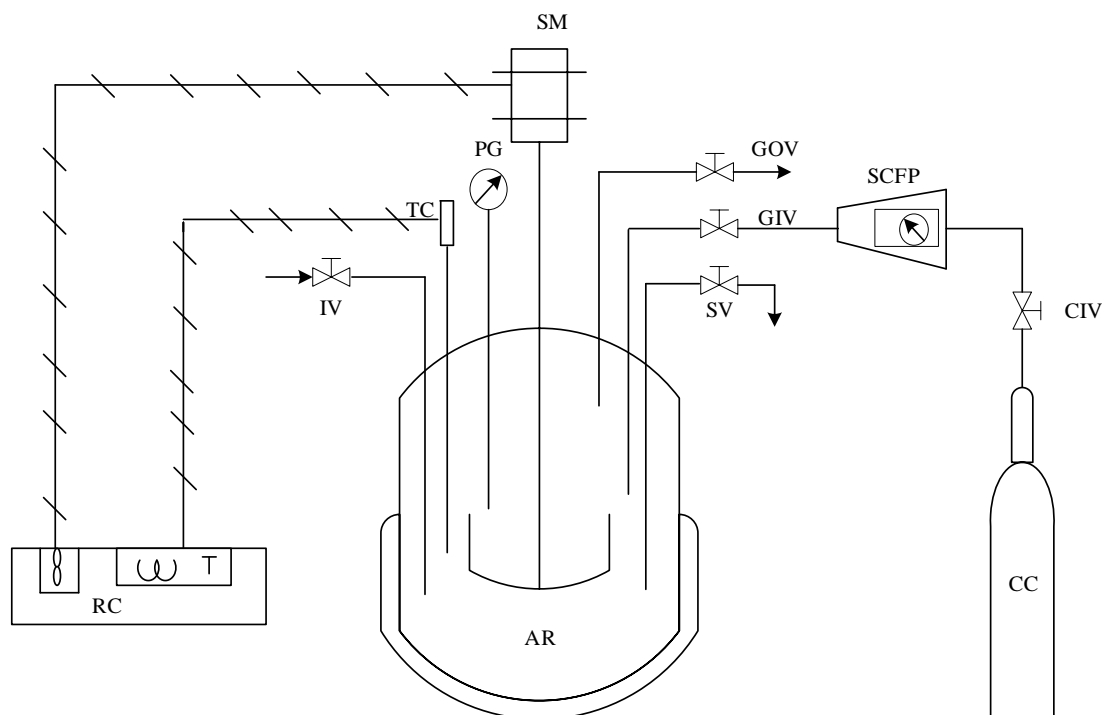


Figure 4- 3. Schematic representation of the experimental set-up for the synthesis of styrene carbonate using a high-pressure reactor (Autoclave reactor). Key: AR, Autoclave reactor; RC, reactor controller; IV, inlet valve; TC, thermocouple; PG, pressure gauge; SM, stirring motor; GOV, gas outlet valve; GIV, gas inlet valve; SV, sampling valve; SCFP, supercritical fluid pump; CIV, CO₂ inlet valve; CC, CO₂ cylinder.

4.5 Method of analysis

The separation and identification of experimental samples were done by Shimadzu gas chromatography (GC). The GC was equipped with a capillary column of dimension (30m x 320 μ m x 0.25 μ m) and flame ionization detector (FID) as the detector. High purity (99.9%) helium was used as carrier gas at a flow rate of 1 mL/min. The injection and detector temperatures were maintained isothermally at 553 K. A split ratio of 50:1 and the injection volume of 0.5 μ L were chosen as a part of the GC method. A ramp method was used to differentiate all the components present in the sample mixture and the initial temperature was set at 323 K. An autoinjector was used to inject the sample for analysis. The oven's temperature was set at 323 K for 5 min after the sample injection, which was then ramped to 553 K at the rate of 25 K/min. The total run time for each sample was ~

14min. After each run, the oven's temperature was cooled down to 323 K for successive sample runs. Octane was used as an internal standard. A chromatograph of sample mixture analysed using GC revealed that octane, BO and BC peak occurred at residence times of ~4, ~7 and ~12 respectively.

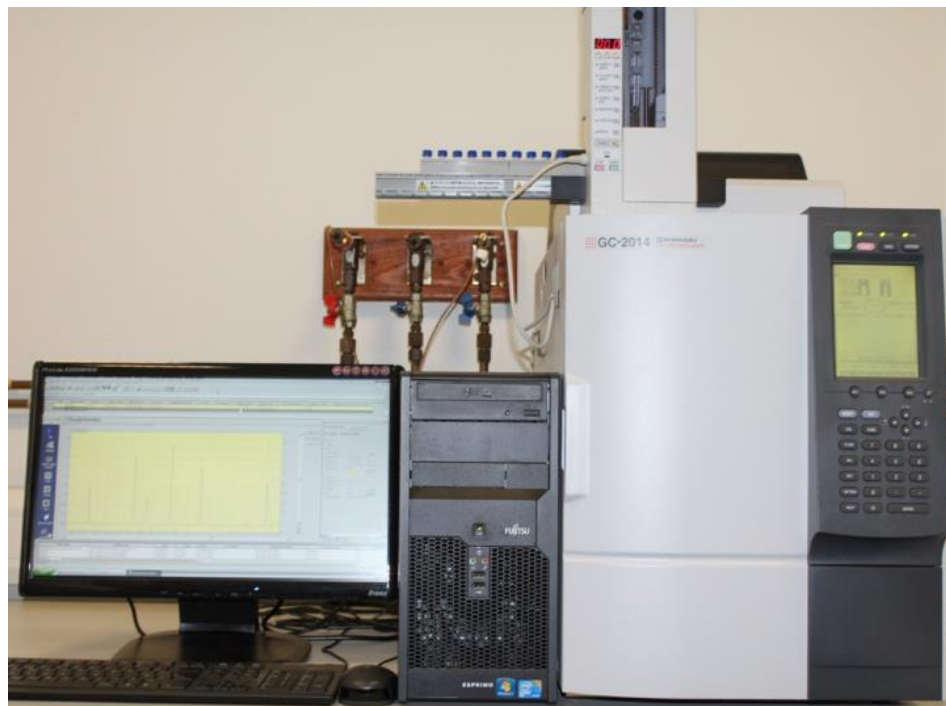


Figure 4- 4. Shimadzu gas chromatography (GC-2014) used for samples analysis.

4.5.1 Internal standardisation

An internal standard is used in the quantitative analysis of a reaction mixture. This analytical technique involves the use of comparison responses from an unknown compound in the sample to the response of reference standards added to the sample extract before injection. In concept, it requires a constant amount of the internal standard added to every sample, both the calibrators and unknowns and instead of establishing the calibration on the absolute response of the peak height, the ratio of the area and internal standard are used.

4.5.1.1 Selection of internal standards

The followings are the guidelines toward the selection of an internal standard:

- The internal standards should not be similar in analytical behaviour to the compound of interest.
- The internal standard must be miscible with samples that need to be analysed.
- The elute of the used internal standard must be near to the desired product or before the last sample in order to limit processing time. (saving energy).
- The internal standard must be stable and under the set conditions.
- The method of measurement of the internal standard should be demonstrated by the analyst that it would not be affected by target analytes or by matrix interferences.

4.5.1.2 Benefits of internal standardisation

- It accounts for routine variation in the response system of the chromatographic.
- It accounts for the variations in the exact volume of sample extract introduced into the system of the chromatographic.
- The retention times of the target compound and the internal standard can be used to obtain the relative retention time (RRT) of the target compound and can as well be used to compensate the shifts for small retention time.

4.5.1.3 Disadvantages

The common disadvantage of internal standard calibration is that the internal standards used must not be the same compounds that are found in the samples, which will be analysed because this will produce an unambiguous response to the chromatographic detector system.

4.5.2 Calibration method

In analytical chemistry, a calibration curve is a general method of determining the concentration of an unknown substance by comparing it with a set of known sample concentration and this process is called a calibration method. There are

three known methods to develop calibration curves, which are the standard addition, internal standards and external standards.

The internal standards were used by producing the calibration curves. These were achieved by preparing several standard solutions of known reactant, product, and an internal standard of toluene. A known volume of each of the prepared standard was injected into the GC and a chromatograph was obtained for each of the injected samples. The concentration ratio of each component (C_i) to the internal standard (C_{is}) was calculated in *Equation 4.1*. The peak area's ratio for each component (A_i) to the internal standard (A_{is}) was calculated as shown in *Equation 4.2*. This formed the calibration curve of concentration ratio against the area ratio of all the components. The slope of the curve is known to be the response factor. The response factor is for calculating the conversion and yield can be determined using *Equation 4.3*.

$$\text{Concentration ratio (CR)} = \frac{\text{Concentration of the } i^{\text{th}} \text{ component (} C_i \text{)}}{\text{Concentration of internal standard (} C_{is} \text{)}} \quad \text{Equation 4.1}$$

$$\text{Area ratio (AR)} = \frac{\text{Area of the } i^{\text{th}} \text{ component (} A_i \text{)}}{\text{Area of internal standard (} A_{is} \text{)}} \quad \text{Equation 4.2}$$

$$\text{Response factor of the } i^{\text{th}} \text{ component (} RF_i \text{)} = \frac{\text{Area ratio (} AR_i \text{)}}{\text{Concentration ratio (} CR_i \text{)}} \quad \text{Equation 4.3}$$

$$\text{The equation of a straight line is } y = mx + c \quad \text{Equation 4.4}$$

Equation 4.3 was linearised. Therefore we have

$$AR_i = RF_i \times CR_i \quad \text{Equation 4.5}$$

Where y is the concentration ratio (CR_i), m the slope is the response factor of the i^{th} component (RF_i) and x is the area ratio (AR_i).

Plots of concentration ratio against area ratio of all the components were plotted to determine response factors. These response factors were used to calculate all

the unknown compositions of the high-pressure reactor reaction mixture using Equation 4.5.

4.5.3 Chromatogram and calibration curves

The mixture of toluene and the reaction products from cycloaddition reaction of CO₂ to BO were injected into Shimadzu GC-2014 gas chromatograph. The typical response to the synthesis of 1,2-butylene carbonate is shown in *Figure 4-5*.

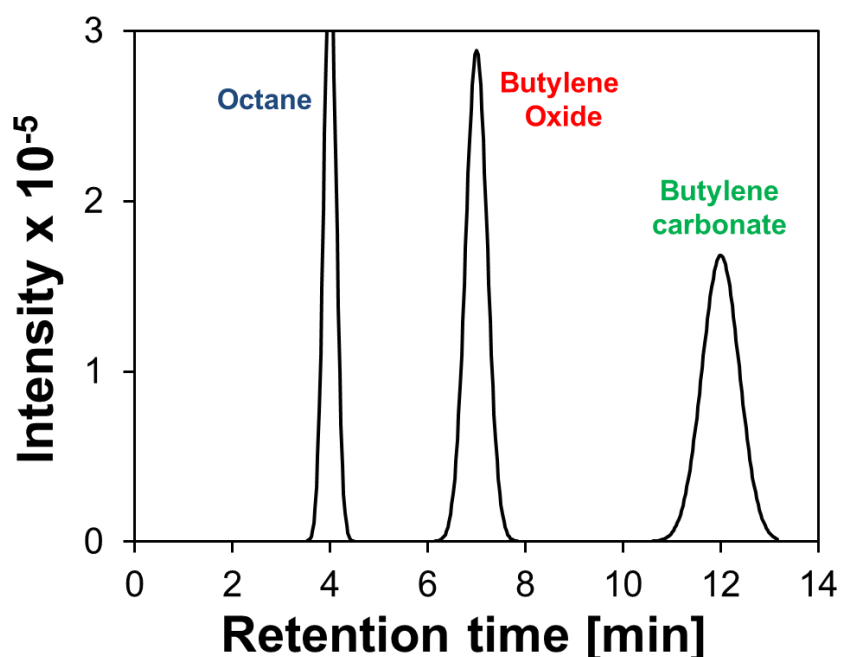


Figure 4- 5. A typical chromatogram of a reaction mixture analysed by a Shimadzu GC-2014 gas chromatograph.

Octane peak emerged at first at the response time of ~4 min followed by BO at the response time of ~7 min and BC at the response time of ~12 min. The total run for each sample for this study was 14 min

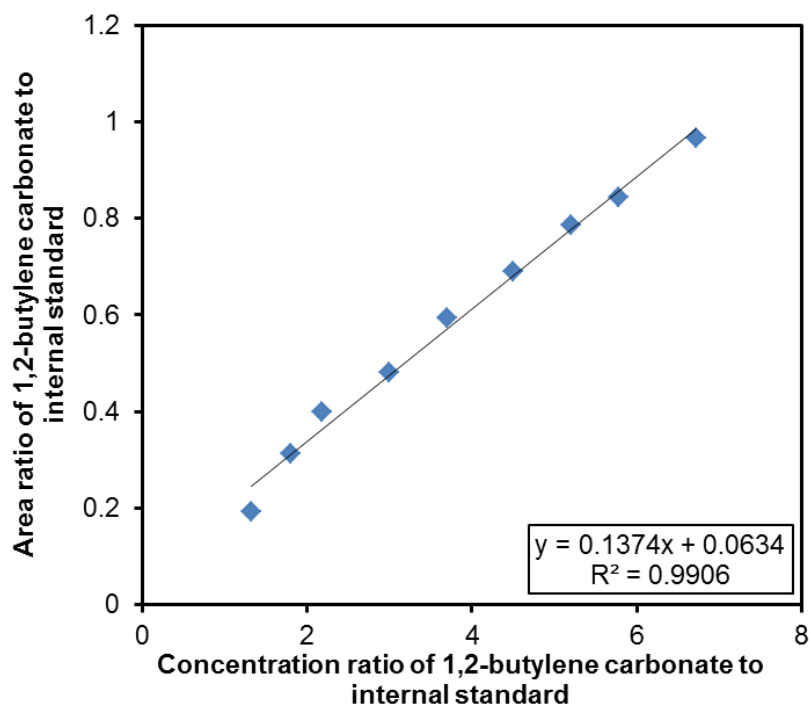


Figure 4- 6. Calibration curve for response factor of BC using OC as an internal standard.

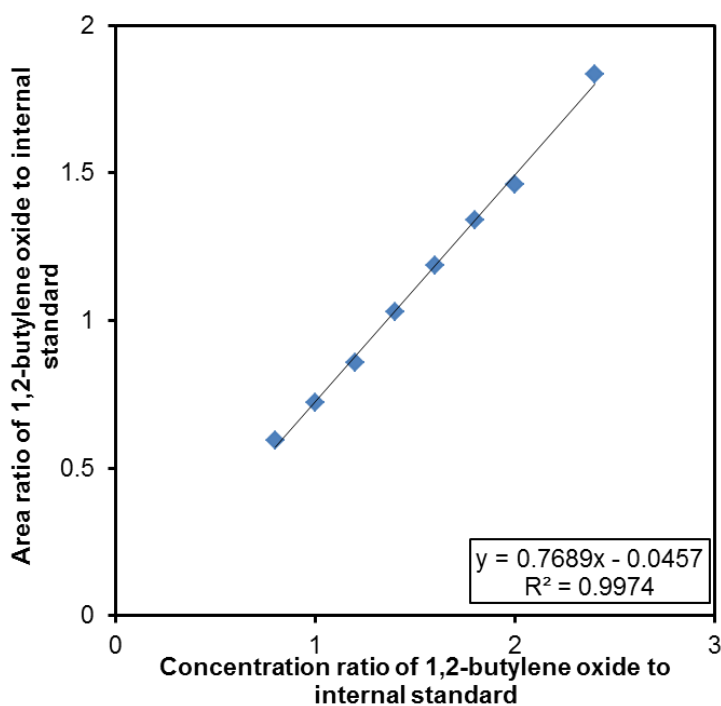


Figure 4- 7. Calibration curve for response factor determination of BO using OC as an internal standard.

Figure 4-6 and 4-7 shows the calibration curves for BC and BO as prepared respectively. The standard solutions for BC (CBC), BO(CBO) and (COC) were prepared based on known concentration samples. These samples were injected into the GC and a chromatogram was obtained for each of the samples. The peaks area ratios of the three samples were used to calculate the area ratio and response factors for BC and BO. The response factors for BC and BO were 0.1374 and 0.7689, respectively and were generated within the specific range of concentrations used to develop the calibration curves. The interpolation can only be used in the region over which the data have been fitted for both calibration curves.

4.5.4 Determination of BO conversion, BC yield, and selectivity

The conversion of BO, the yield of BC and selectivity were determined using Equation 4.5 and Equation 4.6 respectively.

$$\text{BO Conversion (\%)} = \frac{\text{Initial moles of BO} - \text{Moles of BO remaining}}{\text{Initial moles of BO}} \times 100 \quad \text{Equation 4.5}$$

$$\text{BC Yield (\%)} = \frac{\text{Moles of products formed}}{\text{Initial moles of BO}} \times 100 \quad \text{Equation 4.6}$$

$$\text{Selectivity (\%)} = \frac{\text{BC Yield (\%)}}{\text{BO Conversion (\%)}} \times 100 \quad \text{Equation 4.7}$$

Equation 4.5 was used to calculate the BO conversion (%) from the difference of the initial moles of BO and moles of BO remaining to the initial moles. The resultant result was multiplied by 100% to get the BO conversion in percentage.

Equation 4.6 was used to calculate the BC yield (%) from the ration of moles of the products formed to the initial moles of BO. The resultant result was multiplied by 100% to have the BC yield in percentage. Equation 4.7 was used to calculate the selectivity (%) from the ratio of BC yield (%) to the BO conversion (%). The resultant result was multiplied by 100% to get the selectivity in percentage.

4.6 Results and discussion

4.6.1 Reaction pathway

The active acidic and basic site on the surface of mixed metal oxide catalyst plays a vital role in the synthesis of a cyclic carbonate and influences the selectivity of the product massively (Klaewkla *et al.*, 2011). The reaction pathway for the synthesis of BC from the reaction of BO and CO₂ in the presence of the heterogeneous catalyst is shown in *Figure 4- 8a*. The proposed reaction mechanism in which the metal atom M consists of Lewis acid site and an oxygen atom O consists of Lewis basic site is shown in *Figure 4-8b*. The reaction was initiated by adsorption of CO₂ on the basic site of the metal oxide catalyst to form a carboxylate anion and BO was activated by adsorption on the acidic site. The previous report has also suggested the parallel requirement of both Lewis base activation of the CO₂ and Lewis acid activation of the epoxide (Szent-gyorgyi, 2006). The carbon atom of BO is attacked by a carboxylate anion that leads to the ring opening of BO to form an oxyanion species and this was also supported by Adeleye *et al.* (2015). BC formed as a product through desorption from the dissociation of metal oxide (catalyst) from the oxyanion species leads to a ring closure (Dai *et al.*, 2009). The side products associated with the reaction of BO and CO₂ includes an isomer of BO and oligomers of BC, which were below the detection limit of the GC-FID used in the analysis.

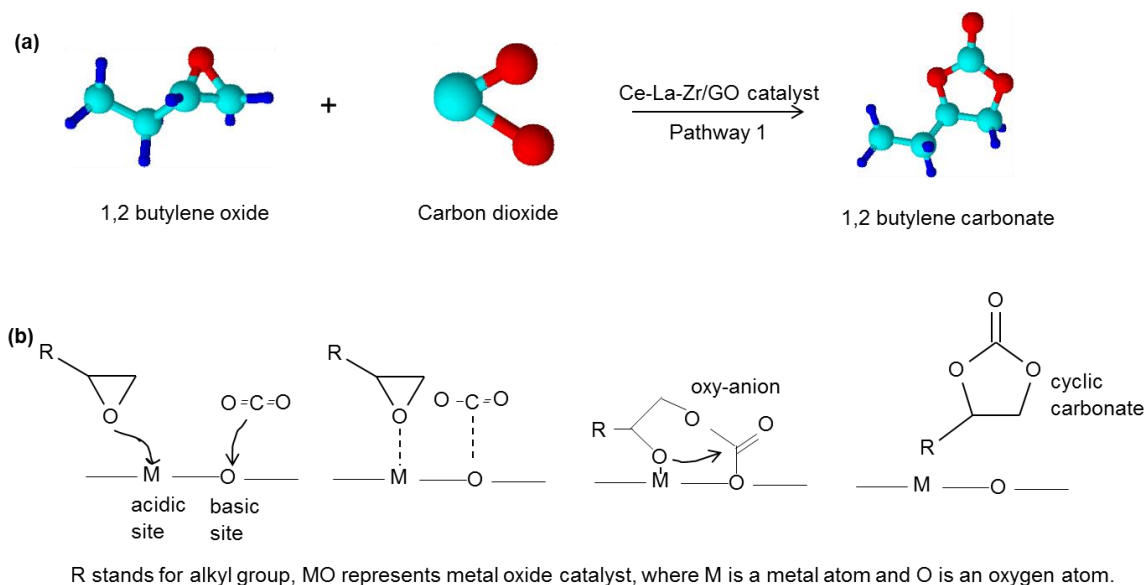


Figure 4- 8. Synthesis of 1,2-butylene carbonate (BC) using a heterogeneous catalyst. (a) Reaction scheme and (b) Plausible reaction mechanism.

4.6.2 Proposed reaction mechanism

The proposed reaction mechanism is of three-step stages. Step 1 shows the initiation by adsorption of BO and CO₂ on the mixed metal oxide catalyst (Figure 4- 9) while step 2 shows the ring opening of BO to form an oxy-anion specie (Figure 4- 10) and step 3 shows the closure of the ring and desorption of BC (Figure 4- 11). Figure 4- 9 to Figure 4- 11 shows the proposed reaction mechanism in which the metal atom M consists of Lewis acid site and an oxygen atom O consists of Lewis basic site. Cycloaddition reaction was initiated by adsorption of CO₂ on the basic site of the metal oxide catalyst to form a carboxylate anion and BO was activated by adsorption on the acidic site. The carbon atom of BO was attacked by a carboxylate anion that leads to the ring opening of BO to form an oxyanion species. Dissociation of metal oxide (catalyst) from the oxyanion species leads to ring closure and desorption of BC as a product. The side products associated with cycloaddition reaction of CO₂ and BO include an isomer of BO and oligomers of BC, which was below the limit of the GC-FID used in the analysis.

Step (1): Adsorption of 1,2 butylene oxide (BO) and CO₂ onto Ce-La-Zr/GO

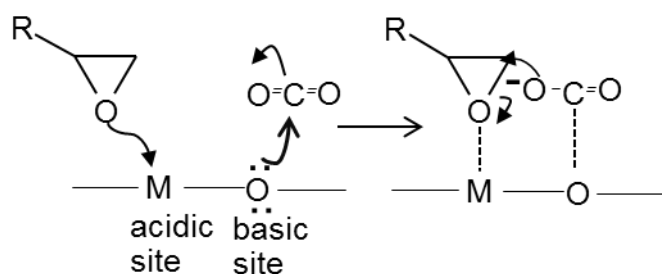


Figure 4- 9. Initiation by adsorption of BO and CO₂ on Ce-La-Zr/GO.

Step (2): Formation of oxy-anion specie through the opening of the ring

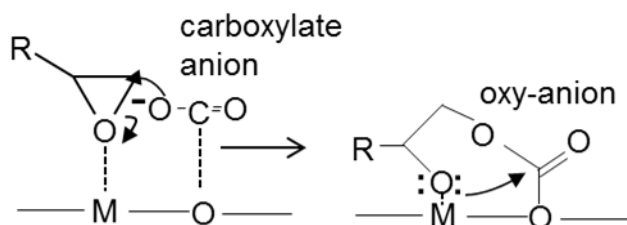


Figure 4- 10. Ring opening of BO to form oxy-anion specie.

Step (3): Desorption of BC and closure of the ring

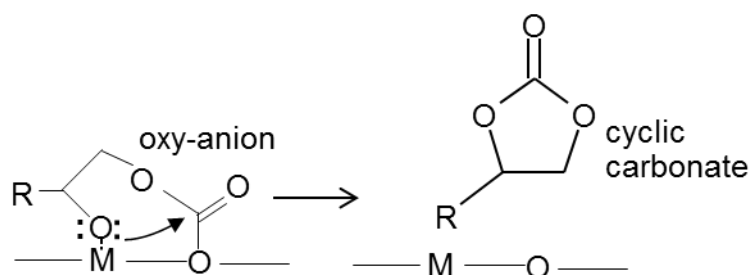


Figure 4- 11. Ring closure and desorption of 1,2-butylene carbonate

4.6.3 Catalyst characterisation

In this work, a rapid, single step, Continuous Hydrothermal Flow Synthesis (CHFS) approach was used for the synthesis of nanocomposite inorganic. Figure 4- 12 shows a schematic representation of the synthesised Ce-La-Zr/GO inorganic nanocomposite. The Ce-La-Zr/GO inorganic nanocomposite was

produced from 0.2 M (total concentration) of a pre-mixed aqueous solution of cerium, lanthanum and zirconium nitrate (Ce³⁺: La³⁺: Zr⁴⁺ at 15: 5: 80 atomic ratios) and GO (synthesised *via* improved Hummer's method) under alkaline conditions (KOH, 1M)

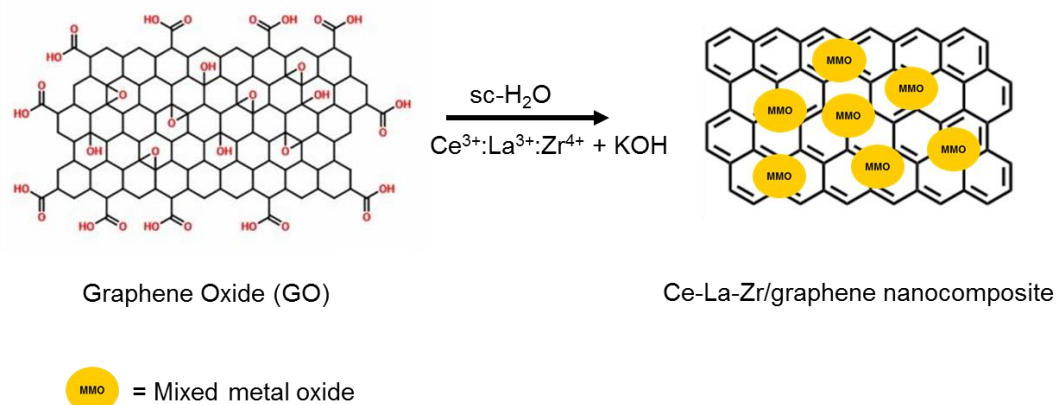


Figure 4- 12. A schematic representation of the synthesized Ce-La-Zr/GO nanocomposite.

The transmission electron microscopy (TEM) images of GO and Ce-La-Zr/GO catalysts are shown in *Figure 4-13* with Ce-La-Zr/GO catalyst exhibiting a mean particle size of 5.78 ± 1.56 nm (refer to *Table 3- 1*). Additionally, for comparative purposes, commercially available catalysts were also used for preliminary work and some of their characteristics shown in *Table 3- 1* (Chapter 3, section 3.3).

X-ray powder diffraction (XRD) shown in *Figure 4- 14* was employed to assess the phase crystallinity of CHFS as-prepared catalysts Ce-La-Zr/GO and GO (starting precursor). The XPS pattern of the nanocomposite matched with $Zr_{0.84}Ce_{0.16}O_2$ (ICDD standard card No. 38-1437) structure as indicated in the previously reported research (Dincer *et al.*, 2015). The composition, oxidation states and chemical states of the as-synthesised materials were examined and analysed by X-ray photoelectron spectroscopy (XPS). *Figure 4- 15* shows the XPS analysis of the metal ratio of Ce-La-Zr/GO and the spin-orbit splitting of the $La_{3d5/2}$ peak (ca. 4.5eV) indicating La_2O_3 phase for the latter. The spectra of samples revealed strong peaks corresponding to cerium, lanthanum, zirconium, oxygen and carbon. The hydrothermal process is effective in reducing GO as reported in by Kellici *et al.* (2017). The C1s XPS spectra of Ce-La-Zr/GO made

hydrothermally revealed the reduction of the peak intensities of the oxygen-containing functional group (epoxide, carboxyl and hydroxyl), which is associated with GO as starting material. The XPS analysis further revealed the presence of mixed Ce(III) and Ce (IV) species as evidenced by the peak at ca. 900 eV (Bêche et al., 2008). The XPS spectrum of the state Zr 3d core level shows a strong spin-orbit doublet due to ZrO₂ at 182.2 eV while at state 183.4 eV is due to Zr-OH bonds. The Zr-OH is supported by large O1s component at 531.4 eV. The presence of suboxides is eliminated at these lower binding energies (ca 179-181 eV).

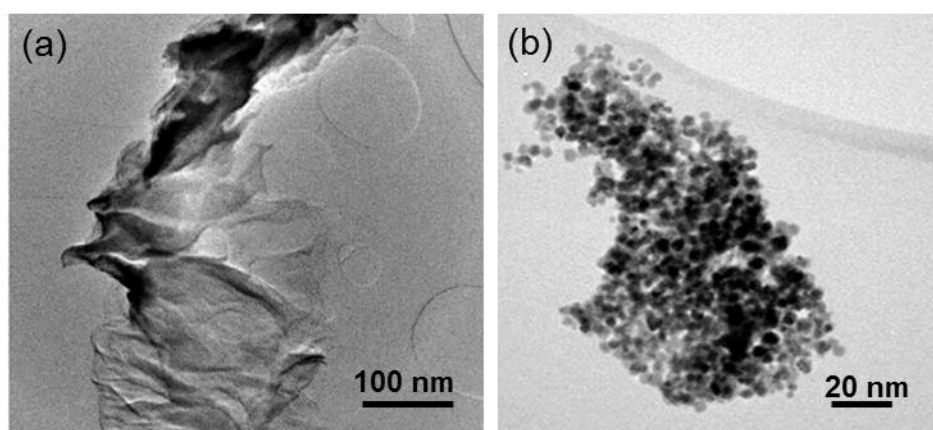


Figure 4- 13. Transmission electron microscopy (TEM) images of (a) graphene oxide and (b) ceria, lanthana and zirconia graphene oxide (Ce-La-Zr/GO).

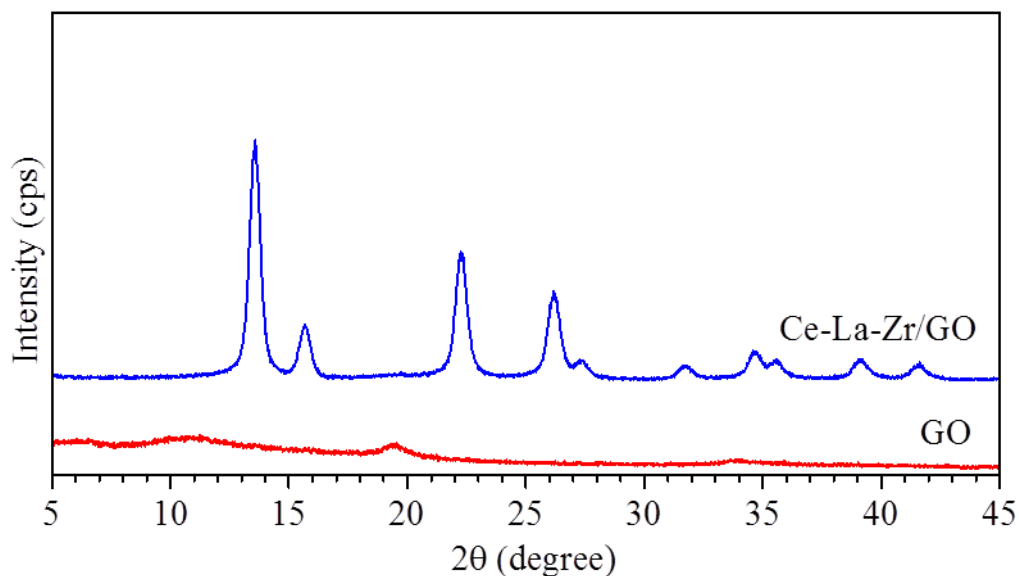


Figure 4- 14. X-ray diffraction (XRD) patterns of ceria-lanthana - zirconia/graphene oxide (Ce-La-Zr/GO), and graphene oxide (GO) catalysts.

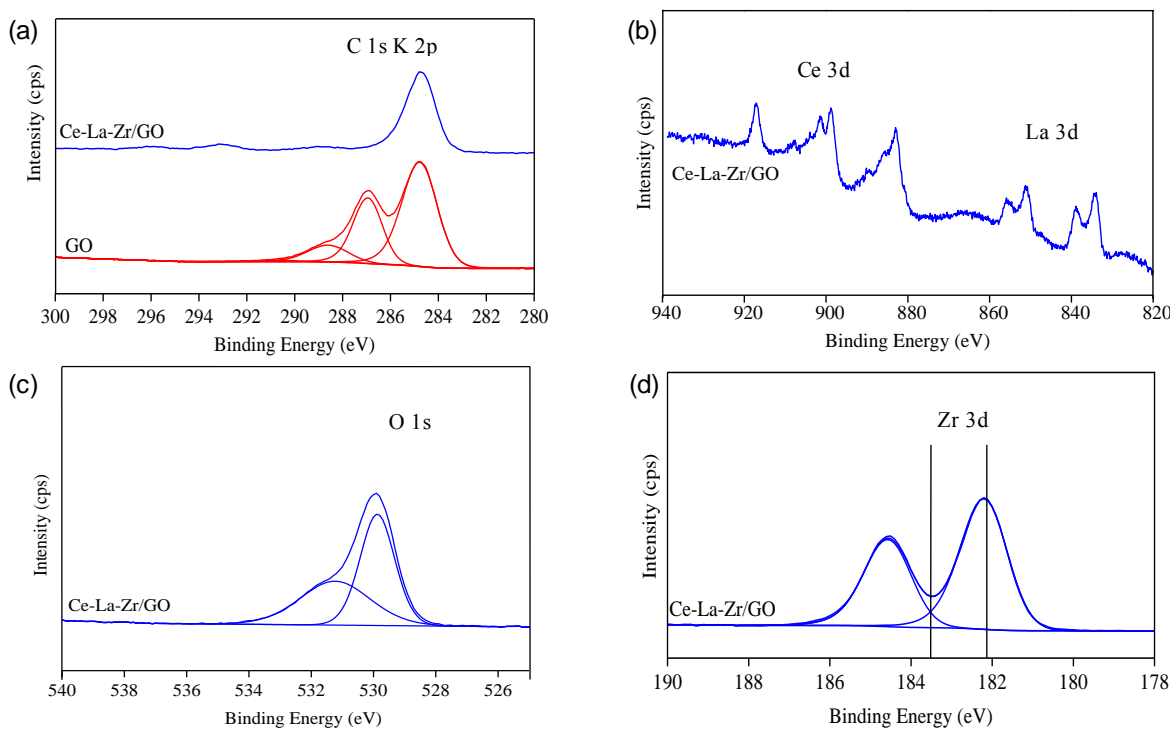


Figure 4- 15. X-ray photoelectron spectroscopy (XPS) spectra showing (a) deconvoluted C 1s (b) Ce 3d and La 3d region (c) O 1s region and (d) Zr 3d region for CHFS synthesized Ce-La-Zr/GO catalysts.

4.6.4 Effect of mass transfer in heterogeneous catalytic reactions

In a heterogeneous catalytic reaction, the effect of mass transfer is very significant due to the reactants being in different phase from the solid catalyst unlike the homogeneous catalytic reaction, (where the reactant, catalyst, and yield are in the same phase), thereby making the effect of mass transfer between phases nearly negligible. Mass transfer plays a vital role in the reaction rate, the conversion of reactant and formation of product (yield) (Klaewkla et al., 2011). The activity of a solid catalyst towards the selectivity of the desired product depends on the characteristics of the catalyst and prevailing conditions. This characteristics of the catalyst include active site, molecular structure, pore size, porosity, surface area and particle size. The prevailing conditions at the boundaries of a solid catalyst include pressure, temperature, and superficial velocity.

The understanding of the effect of mass transfer in cycloaddition of CO₂ to BO in the presence of heterogeneous catalytic reaction offers a better understanding toward designing a new catalyst based on the limiting resistance for both internal and external mass transfer on the variable reaction parameters. Mass transfer of the reactants occurs from the bulk fluid to the external surface of the catalyst and diffuses from the external surface through the pores within the catalyst to the catalytic surface of the pores, in which the reaction occurs (Szent-gyorgyi, 2006; Dou et al., 2017). However, the external mass transfer resistance could be limited through the control of various parameters such as pressure, temperature and stirring speed. Furthermore, the understanding of catalytic reactions could limit the effect of mass transfer process during a chemical reaction and thereby shift the equilibrium towards the selectivity of the desired product.

The synthesis of BC through cycloaddition of CO₂ to BO was carried out using different stirring speed of 300 - 500 rpm. The results in *Figure 4- 16* shows that the conversion of BO and yield of BC were found to be the approximately same as there were no significant changes in the conversion and yield. The conversion of BO and yield of BC were found to be 84% and 64%, respectively with an experimental error of $\pm 2\%$. This confirmed that the external mass transfer resistance is negligible for the stirring speed from 300 rpm to 500 rpm under the related reaction conditions. Furthermore, the influence of internal mass transfer resistance is also negligible, and this is attributed to the size of the catalyst of 5-

26 nm range, the average pore diameter of Ce-La-Zr/GO nanocomposite catalyst, which was 2.16 nm and falls in the mesoporous region i.e. 2–50 nm reported by Clerici and Kholdeeva (Clerici and Kholdeeva, 2013). Moreover, the absence of internal and external mass transfer resistance using different stirrer speed and different size fractions of ion-exchange resins as catalysts for the synthesis of n-hexyl acetate has been reported by Patel and Saha (Patel and Saha, 2007). The stirring speed of 300 rpm has been selected and used to conduct a further investigation for cycloaddition of CO₂ to BO for the synthesis of BC as a result of energy efficiency and cost. Therefore, it can be concluded that there was no effect of mass transfer resistances on the synthesis of BC using Ce-La-Zr/GO catalyst at 300 rpm.

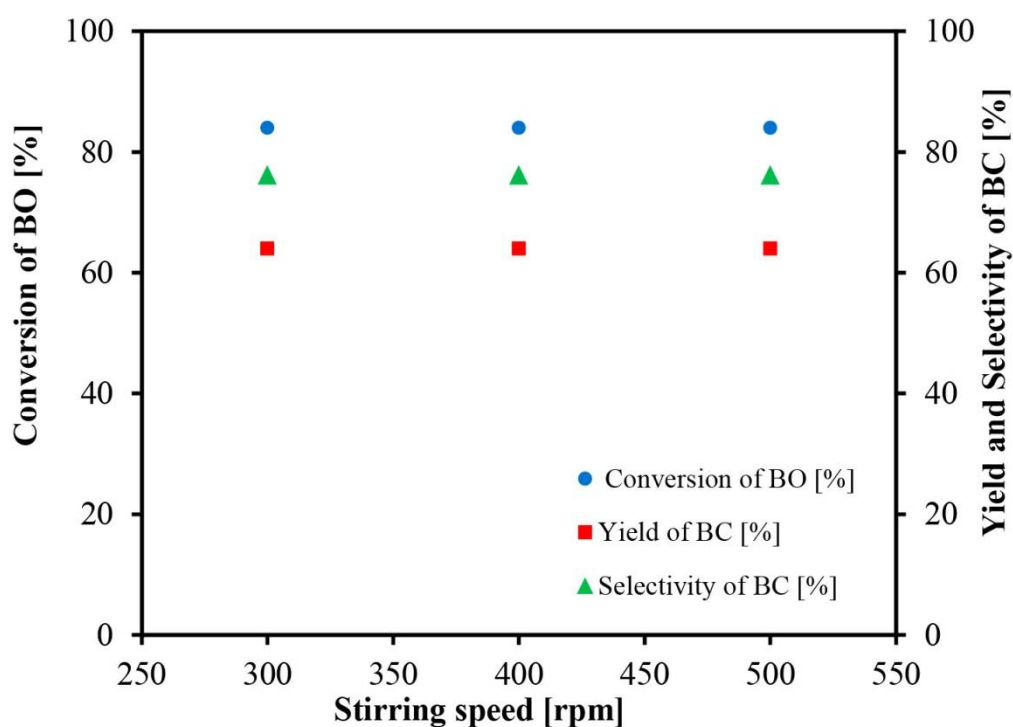


Figure 4- 16. Effect of mass transfer resistance on conversion of 1, 2 butylene oxide (BO) against yield and selectivity of 1,2-butylene carbonate (BC). Experimental conditions: Catalyst - Ce-La-Zr/GO; Catalyst loading - 10% (w/w); CO₂ pressure - 75 bar; Reaction temperature - 408 K; Reaction time - 20 h.

4.6.5 Effect of different heterogeneous catalysts

The study of various heterogeneous catalysts such as catalytic activity, conversion, yield and selectivity were conducted in order to establish the best performing metal oxide or mixed metal oxide catalyst for the synthesis of BC

through the cycloaddition reaction of CO₂ to BO using a high-pressure reactor. Figure 4- 17 shows the results of different (commercially available) heterogeneous catalysts as well as Ce-La-Zr/GO (synthesised *via* CHFS) on the conversion of 1,2 butylene oxide, the yield and selectivity of 1,2-butylene carbonate. The experiments were conducted using the optimum reaction conditions. Ce-La-Zr/GO catalyst gave an improved conversion of BO (84%) and highest BC yield (64%) and selectivity (76%) at optimum reaction conditions of reaction temperature 408 K, CO₂ pressure 75 bar, reaction time 20 h, stirring speed 300 rpm and catalyst loading of 10% (w/w).

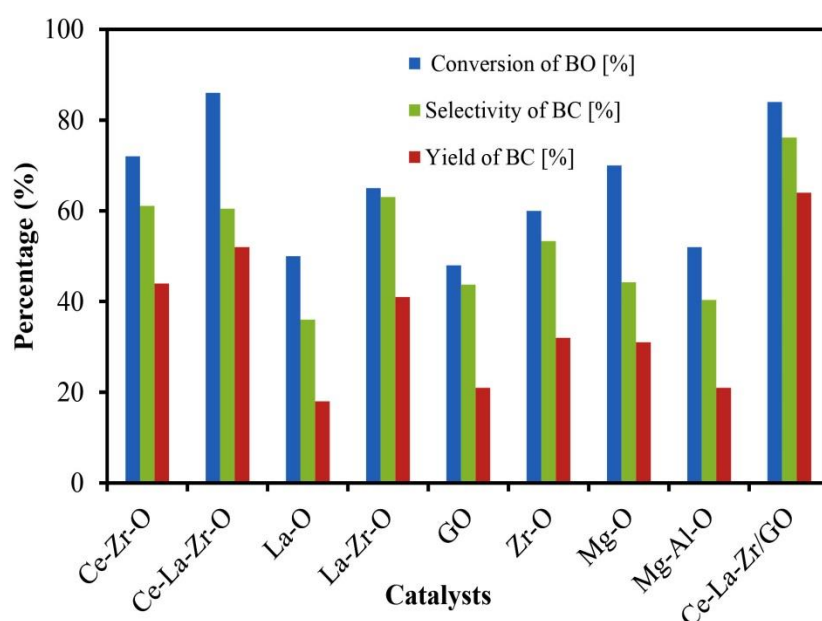


Figure 4- 17. Effect of different metal oxide, and mixed metal oxide heterogeneous catalysts as well as prepared GO *via* Hummer's method and Ce-La-Zr/GO inorganic nanocomposite *via* CHFS on conversion of BO against yield and selectivity of BC. Experimental conditions: Catalyst - Ce-La-Zr/GO; Catalyst loading - 10% (w/w); CO₂ pressure - 75 bar; Reaction temperature - 408 K; Reaction time; 20 h; Stirring speed - 300 rpm.

4.6.6 Effect of catalyst loading

The influence of different catalysts loading (w/w) ranging from 5% - 15% have been studied for the synthesis of BC *via* cycloaddition reaction of CO₂ to BO as

shown in *Figure 4- 18*. It has been observed that with an increase in catalyst loading (w/w) from 5% to 10%, BO conversion was increased from 48% to 84%, and the yield of BC increased rose from 18% to 64% (see *Figure 4- 18*). However, with an increase in catalyst loading (w/w) from 10% to 12.5%, there were no significant changes in the conversion of BO and yield of BC, although the separation of the product becomes difficult as the catalyst loading goes beyond 10% (w/w). Furthermore, there were no significant changes in the responses as the catalyst loading exceeded 10% (w/w), except for 15% (w/w) catalyst loading where it was observed that there was a slight drop in the yield of BC. The trends observed were as a result of five different catalysts loading experiments conducted, e.g, 2.5% [w], 5% [w], 7.5% [w], 10% [w], 12.5% [w] and 15% [w]. These results obtained from different catalysts loading revealed that from 2.5% [w] to 7.5% [w] catalysts loading requires more active sites of the catalysts to be loaded. The observed trend in the graph revealed that there is a corresponding increase in conversion of styrene oxide. At 10% [w] catalyst loading, the conversion of styrene oxide also increased, but beyond 10% [w] to 15% [w] catalyst loading, there were no significant changes. This suggests that the required active sites for styrene oxide conversion is sufficient at 10% [w] catalyst loading. However, beyond 10% [w] the active sites become excess for the reaction, thereby making separation of the product difficult (separation of the product takes more time as it goes beyond 10% [w] catalyst loading). This observed trend of catalyst loading behaviour is also similar to that reported by Adeleye et al. (2014). This shows that the active sites required for the reaction of BO and CO₂ to produce BC were sufficient at 10% (w/w) catalyst loading when taking the experimental error of $\pm 2\%$ into consideration. Therefore, based on this study, it can be concluded that at the reaction conditions of 408 K, 75 bar and 20 h, 10% (w/w) catalyst loading is the optimum amount of catalyst needed for this reaction.

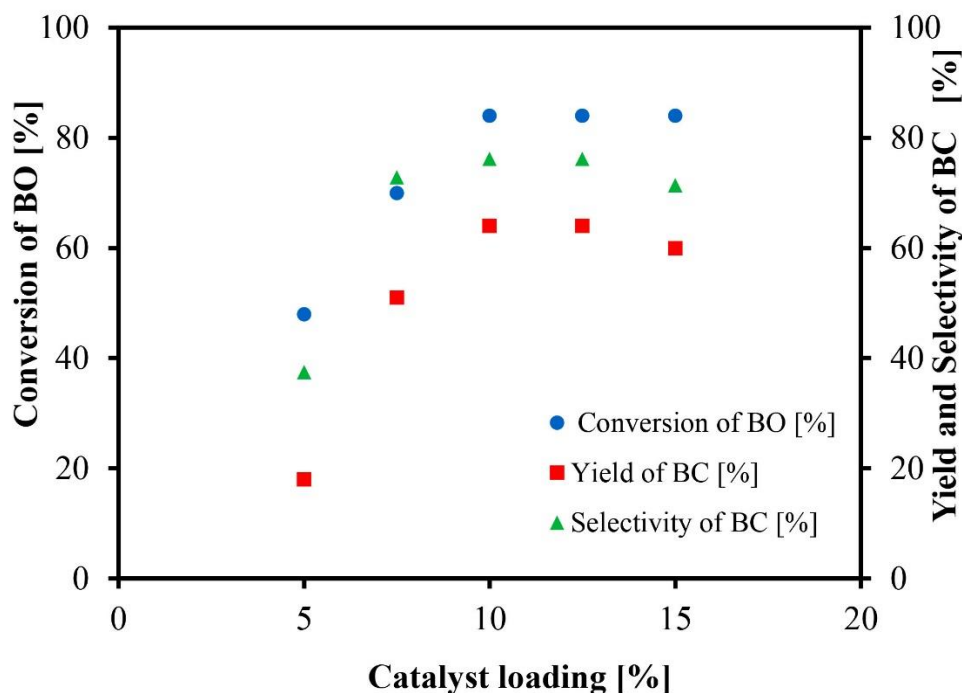


Figure 4- 18. Effect of catalyst loading on conversion of BO against yield and selectivity of BC. Experimental conditions: Catalyst - Ce-La-Zr/GO; Catalyst loading - 10% (w/w); CO₂ pressure - 75 bar; Reaction temperature; 408 K; Reaction time; 20 h, Stirring speed – 300 rpm.

4.6.7 Effect of reaction time

Several experiments were carried out using different reaction time ranging from 16 h to 24 h with a target to conclude the importance of reaction time on the synthesis of BC. The different reaction time of 16 h, 20 h and 24 h at constant reaction conditions of 408 K, 75 bar and 10% catalyst loading for Ce-La-Zr/GO were investigated. Figure 4- 19 shows that the reaction time affects both BO conversion and BC yield significantly. It increases both responses (i.e. BO conversion and BC yield) from the range between 16 and 20 h, while beyond 20 h the conversion of BO and yield of BC remains unchanged, which were 84% and 64% respectively. In contrast, at the reaction time of 16 h, the conversion of BO was 71% and BC yield was 64% while at the reaction time of 20 h, it increases to 84% and 64% respectively. In this study, it is evident that optimum reaction time is 20 h under otherwise identical reaction conditions.

In contrast, at the reaction time of 16 h, the conversion of BO was 71%, and BC yield was 64% while at the reaction time of 20 h, it increases to 84% and 64% respectively. In this study, it is evident that optimum reaction time is 20 h under otherwise identical reaction conditions.

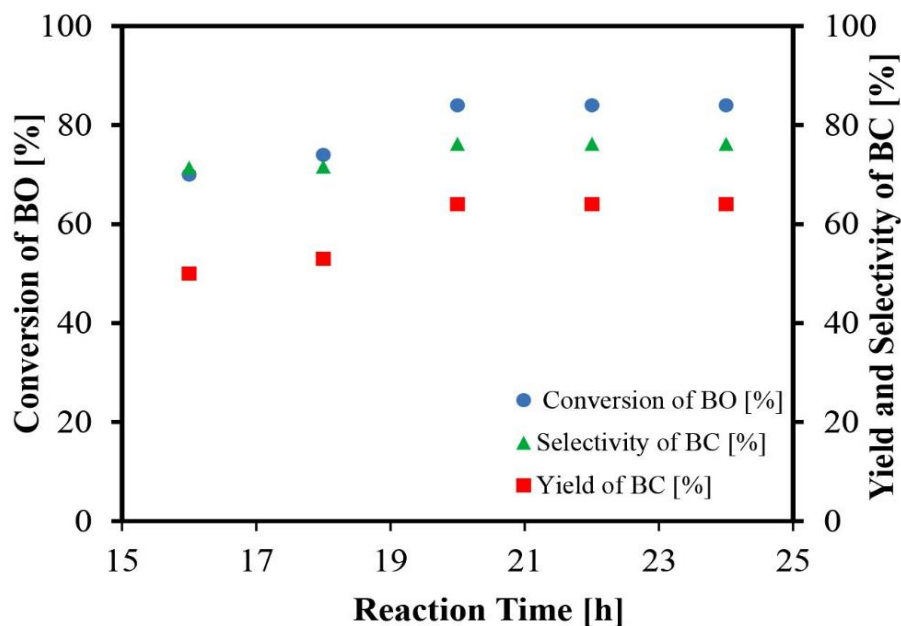


Figure 4- 19. Effect of reaction time on conversion of BO against yield and selectivity of BC. Experimental conditions: Catalyst - Ce-La-Zr/GO; Catalyst loading - 10% (w/w); CO₂ pressure - 75 bar; Reaction temperature; 408 K; Stirring speed – 300 rpm

4.6.8 Effect of reaction temperature

In this study, the synthesis of BC through the reaction of BO and CO₂ were carried out at a different reaction temperature from 368 K to 408 K in order to establish the effect of reaction temperature on BO conversion, BC on yield and selectivity. The reaction conditions for this study were set at 10% (w/w) catalyst loading, the CO₂ pressure of 75 bar for 20 h. As it was expected, the higher the temperature, the more the conversion of BO into carbonates isomers and oligomers (see *Appendix 1- 1*). These isomers and oligomers can be identified using gas chromatography-mass spectrometry. At a set CO₂ pressure of 75 bar within the studied temperature ranges (368 K to 408 K), CO₂ is in a supercritical state. Therefore, there is an absence of partial pressure in the reaction because

all the reactions occur in the supercritical region of carbon dioxide. *Figure 4- 20* shows the temperature dependence on the yield and selectivity of BC.

It was observed from *Figure 4- 20* that there was a corresponding increase in conversion of BO, BC yield and selectivity as temperature increases from 368 K to 408 K, however, further increase of temperature from 408 K to 430 K, there was a significant drop of BC yield from 64% to 58%. The selectivity drops from 76% to 64% whilst its BO conversion increases from 84% to 90%. These results are in good agreement with similar work published by Adeleye et al. (2014). Based on this study, 408 K was found to be the optimum reaction temperature for the synthesis of BC.

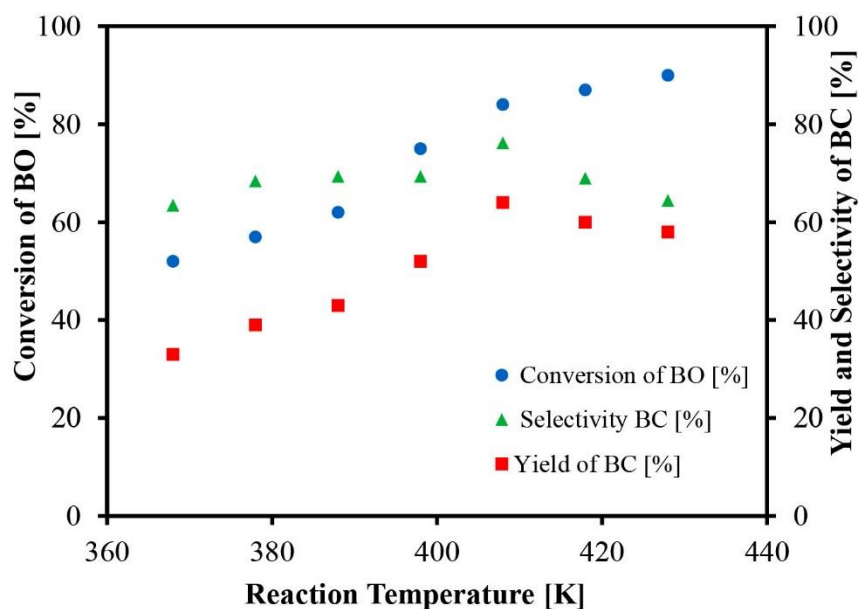


Figure 4- 20. Effect of reaction temperature on conversion of BO against yield and selectivity of BC. Experimental conditions: Catalyst - Ce-La-Zr/GO; Catalyst loading - 10% (w/w); CO₂ pressure - 75 bar; Reaction time; 20 h; Stirring speed – 300 rpm.

4.6.9 Effect of CO₂ pressure

The use of CO₂ pressure is very significant for the synthesis of BC through the reaction of BO and CO₂. It has been reported that application of CO₂ in the supercritical state can influence reaction system positively and improve the mass transfer efficiency of the reactants, thereby, creating a shift in the reaction equilibrium, which tends to open up the thermodynamic limitation of the reaction (Baiker, 1999; Zou et al., 2004). The effect of CO₂ pressure on BO conversion and BC yield were investigated to determine the optimum CO₂ pressure for the cycloaddition reaction of CO₂ to BO. These experimental studies were carried out in a high-pressure reactor at 408 K with CO₂ pressure ranging from 55 bar to 105 bar for 20 h and the obtained experimental results were shown in *Figure 4- 21*. It was observed in *Figure 4- 21* that an increase in CO₂ pressure from 55 bar to 75 bar increases the BO conversion and the BC yield. As a result, selectivity increased rapidly from 58% to 76%, however, beyond 75 bar there were further increase in BO conversion but the yield of BC dropped slightly. This can be explained by the pressure effect on the concentrations of CO₂ and epoxide in the reaction (Xiong et al., 2013). Furthermore, the drop in yield could also be attributed to the form of by-products such as oligomers and isomers, which were below the detection limit of GC-FID used in the analysis and therefore yields of the by-products were not calculated. Based on the experimental results of the investigation, it can be concluded that the optimum CO₂ pressure for this reaction is 75 bar. This study shows the supercritical condition of CO₂, there is an improvement in polarity and solubility of BO conversion as the reaction pressure increases.

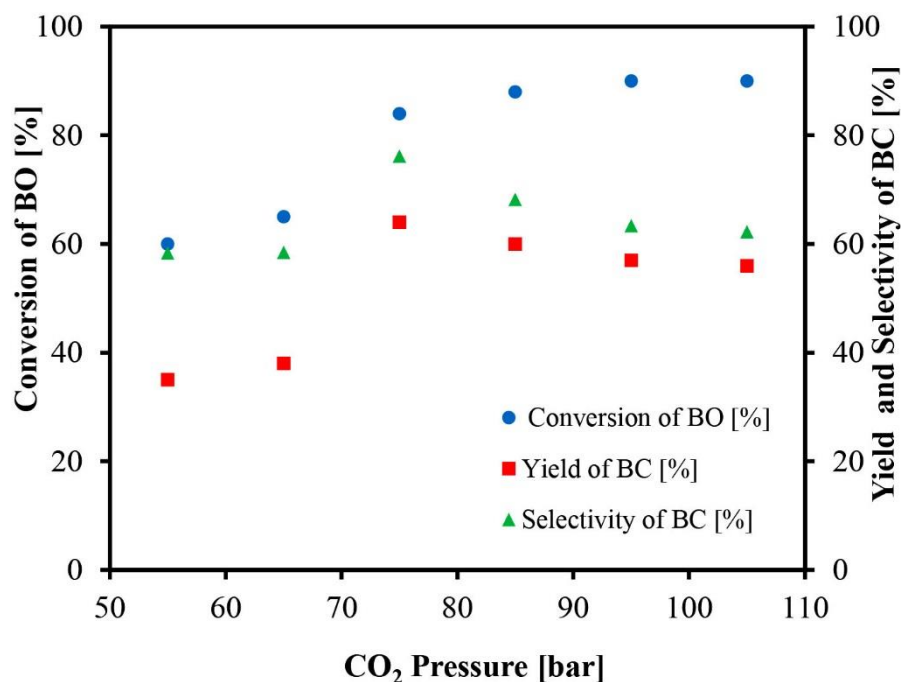


Figure 4- 21. Effect of reaction CO₂ pressure on conversion of BO against yield and selectivity of BC. Experimental conditions: Catalyst - Ce-La-Zr/GO; Catalyst loading - 10% (w/w); Reaction temperature – 408 K; Reaction time; 20 h; Stirring speed – 300 rpm.

4.6.10 Catalyst reusability studies

One of the vital characteristics of an industrial catalyst is the ability to regenerate without losing its catalytic activity and also providing resistance to deactivation. The heterogeneous catalyst reusability experiments were conducted to investigate the catalytic activity of the best performed heterogeneous catalyst. Ceria-lanthana-zirconia/graphene nanocomposite reusability test was investigated in different runs. The experiments were carried out in a high-pressure reactor at optimum reaction conditions of temperature 408 K, the CO₂ pressure of 75 bar, fresh 10% (w/w) catalyst loading of Ce-La-Zr/GO for 20 h. The first used catalyst was recovered by filtration from the reaction mixture and washed with acetone, which was dried in an oven for 12 h at 323 K. The catalyst was later reused for 5 different runs subjected to the same reaction conditions and as it can be observed in Figure 4- 22 that the conversion of BO, yield and selectivity of BC were approximately the same with an experimental error of $\pm 2\%$ (Appendix A- 1). It can be concluded that Ce-La-Zr/GO catalyst still maintains similar catalytic activity after several runs.

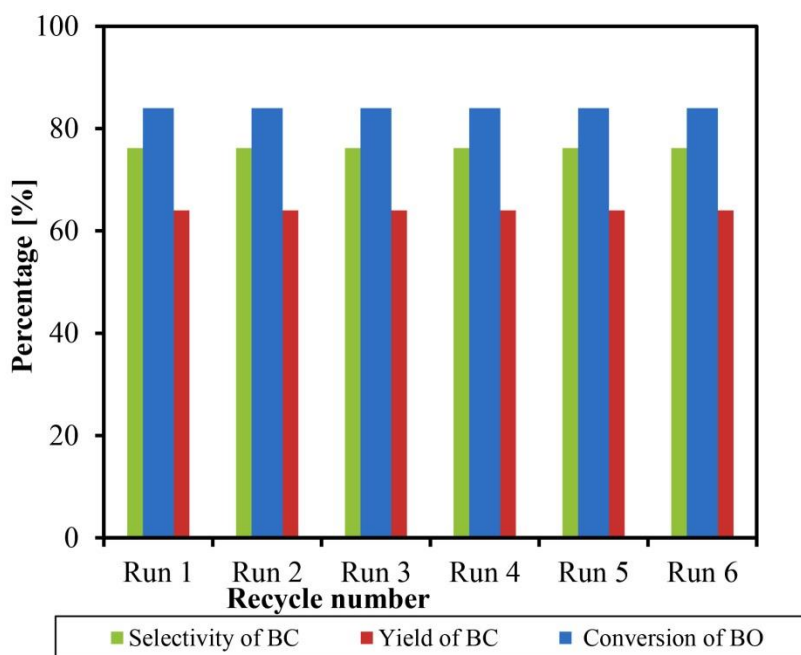


Figure 4- 22. Catalyst reusability studies on conversion of BO against yield and selectivity of BC. Experimental conditions: Catalyst - Ce-La-Zr/GO; Catalyst loading - 10% (w/w); Reaction temperature – 408 K; CO₂ pressure - 75 bar; Reaction time; 20 h; Stirring speed – 300 rpm

4.7 Conclusions

The synthesis of BC through cycloaddition reaction of CO₂ and BO has been successfully carried out using a high-pressure reactor in the presence of various heterogeneous catalysts without any solvent. It was observed that supercritical state of CO₂ influence reaction system positively and improve the mass transfer efficiency of the reactants. The experimental results revealed that among the used heterogeneous catalysts, ceria-lanthana-zirconia/graphene oxide (Ce-La-Zr/GO) catalyst was found to be the best-performed catalyst and the optimum reaction condition was found at 408 K, 75 bar CO₂ pressure, 10% (w/w) catalyst loading and 20 h reaction. Ce-La-Zr/GO catalyst was easily recycled and reused several times without any reduction in its catalytic performance.

CHAPTER 5

RESPONSE SURFACE METHODOLOGY (RSM) MODELLING AND OPTIMISATION OF 1,2- BUTYLENE CARBONATE

CHAPTER 5: SYSTEMATIC MULTIVARIATE OPTIMISATION OF 1,2-BUTYLENE CARBONATE SYNTHESIS VIA CO₂ UTILISATION USING GRAPHENE-INORGANIC NANOCOMPOSITE CATALYSTS

5.1 Introduction

Developing an efficient and effective process for the fixation of CO₂ through utilisation to form value-added chemicals such as propylene carbonate, styrene carbonate and 1,2-butylene carbonate taking account of energy usage warrant optimisation. The optimisation of a process is the bedrock of saving cost by maximising all the used resources in order to achieve optimal results (Bezerra *et al.*, 2008). This process promotes the reduction of waste, maximising production output and that would effectively reduce CO₂ emissions.

Unadventurously, the optimisation of process parameters reveals the response effect of each process parameter at a time. On the application of the traditional method, only the investigated response is varied at one factor at a time (OFAT), where the other factors are at a constant level. This disseminates the effect of a single factor on the response where the optimum value of each parameter is only valid at a constant value of the other parameters (Montgomery, 2006). Accordingly, the experimental design using either full or partial factorial design has been developed to overcome the aforementioned optimisation restrictions and to define the real optimum conditions by varying all the process parameters simultaneously. In addition, using an experimental design technique avoid the essential need for performing a large number of experiments that consume chemicals and materials (Baş and Boyacı, 2007).

In recent times, several experimental design techniques have been implemented for process optimisation including response surface methodology (RSM), Taguchi method, artificial neural network (ANN) and Fuzzy modelling (Aghbashlo *et al.*, 2017; Omrani *et al.*, 2018). RSM is a powerful optimisation process that has been extensively used to optimise different applications processes (Aboelazayem *et al.*, 2018a; Anitha *et al.*, 2016; Bo *et al.*, 2015; Sillanpää *et al.*, 2018). RSM is used to combine the effect of process variables with the assistance of fewer experimental data (Khuri and Mukhopadhyay, 2010). Thus, this method is the most effective and efficient that has proven to have reduced cost and less labour intensive.

RSM method employs the use of a mathematical algorithm on the results produced from the designed experiments. It is also used to develop regression models and to validate them using several statistical techniques (Witek-Krowiak *et al.*, 2014). The application of RSM could be summarised for development of mathematical model representing the process variables function in the process response, illustrate the effect of process variables and their interactions on the response and optimise the process variables to achieve the desired goal for the process response (Chi *et al.*, 2012).

In this study, a systematic multivariate optimisation has been implemented for the synthesis of BC using a graphene-based heterogeneous catalyst. The effect of each process variables including temperature, pressure, reaction time and catalyst loading has been evaluated on process response. RSM using BBD has been used to investigate the effect of process variables and their interactive effect on the response. A quadratic model has been developed representing the interrelationship between process variables and each response. The developed mathematical models have been validated using analysis for variance (ANOVA). The developed optimum conditions have been validated statistically and experimentally.

5.2 Experimental design

RSM has been used to design the experiments *via* BBD, which is based on three levels for each process variable. The three levels represent the maximum, minimum and the average range of each variable. Four independent variables have been studied including temperature, pressure, catalyst loading and time that have been coded as A, B, C and D, respectively. In this study, the levels of the independent variables have been coded as -1, 0 and 1 as shown in *Table 5- 1*.

Table 5- 1. Experimental design variables and their coded levels

Factor	Code	Levels		
		-1	0	+1
Temperature (°C)	A	100	135	170
Pressure (bar)	B	60	75	90
Catalyst loading (w/w)	C	5	10	15
Time (h)	D	16	20	24

Twenty-nine runs have been performed in a randomised manner to minimise the effect of unexplained inconsistency in the responses (Jaliliannosrati *et al.*, 2013). The analysed reaction variables are temperature (A, °C), pressure (B, bar), catalyst loading (C, w/w) and time (D, h) while reaction responses are BO conversion (Y_1 , %) and BC yield (Y_2 , %). The results of the experimental runs have been reported in an uncertainty matrix as shown in *Table 5- 2*.

Table 5- 2. Experimental design matrix with the actual and predicted responses

Ru n	Tempera ture (°C) (B)	Press ure (bar) (C)	Catalyst loading (w/w)	Time (min) (D)	Actual BO Conver sion %	Predicted BO Conversi on %	Actual BC Yield %	Predict ed BC Yield %
1	170	75	15	20	86	87.96	64	64.38
2	135	75	10	20	84	84.00	64	64.00
3	135	90	10	24	90	97.29	65	66.04
4	135	75	15	16	69	67.83	35	35.46
5	100	75	5	20	54	55.79	23	24.88
6	135	60	10	24	75	72.96	40	41.04
7	135	90	10	16	70	75.79	35	36.21
8	135	60	5	20	66	58.87	37	33.50
9	100	60	10	20	42	46.33	16	14.62
10	135	60	10	16	68	64.46	35	36.21
11	135	90	15	20	88	91.37	65	66.50
12	135	75	5	24	67	68.17	33	32.29
13	135	90	5	20	86	81.21	36	35.00
14	135	60	15	20	77	78.04	44	43.00
15	135	75	10	20	84	84.00	64	64.00
16	170	90	10	20	86	81.67	45	46.13
17	135	75	15	24	89	85.33	65	64.29
18	170	75	5	20	54	59.29	26	28.88
19	170	75	10	16	68	62.38	38	33.33
20	100	75	15	20	58	56.46	31	30.38
21	100	75	10	16	52	52.88	23	24.33
22	170	75	10	24	90	85.38	64	60.67
23	135	75	10	20	84	84.00	64	64.00
24	100	75	10	24	58	59.88	29	31.67
25	100	90	10	20	90	82.67	55	51.13
26	135	75	10	20	84	84.00	64	64.00
27	170	60	10	20	75	82.33	54	57.63
28	135	75	10	20	84	84.00	64	64.00
29	135	75	5	16	52	55.67	26	26.46

5.3 Statistical analysis

The mathematical model was defined *via* multiple regression analysis using the general quadratic model as shown in Equation (5.1).

$$Y = b_o + \sum_{i=1}^n b_i x_i + \sum_{i=1}^n b_{ii} x_i^2 + \sum_{i=1}^{n-1} \sum_{j>1}^n b_{ij} x_i x_j + \varepsilon \quad (\text{Equation 5- 1})$$

where Y is the predicted response (i.e. BO conversion and BC yield), b_o is the model coefficient constant, b_i , b_{ii} , b_{ij} , are coefficients for intercept of linear, quadratic, interactive terms respectively, while x_i , x_j are independent variables ($i \neq j$). n is a number of independent variables and ε is the random error.

The adequacy of the predicted models was checked by several statistical validations including coefficient of correlation (R^2), adjusted coefficient of determination (R^2_{adj}) and the predicted coefficient of determination (R^2_{pred}). The statistical significance of the predicted models was analysed by ANOVA using Fisher's test, i.e. F-value and p-value, at 95% confidence interval. Design Expert 11 software (Stat-Ease Inc., Minneapolis, MN, USA) was used to perform the initial experimental design, model prediction, statistical analysis and optimisation.

5.4 Development of regression model

The responses for randomised experiments in terms of BO conversion and BC yield have been reported as shown in *Table 5- 3*. It has been observed from the experimental results that BO conversion ranges from 42 to 90%, while BC yield ranges from 16 to 65%. Multiple regression analysis of the experimental data has been performed using Design Expert software. The software has fitted four models for each response i.e. linear, two factors interactions (2FI), quadratic and cubic polynomials. Amongst the predicted fitted models for each response, the model with the highest fitting has been chosen based on several statistical validations. It has been observed that the experimental data of both responses are highly fitting with the quadratic polynomial models. Accordingly, two quadratic models have been developed representing the empirical relationship between process responses (BC yield and BO conversion) and reaction variables as shown in *Equations 5.2 and 5.3*.

$$Y_1 = 84.00 + 8.75 A + 8.92 B + 7.33 C + 7.50 D - 9.25 AB + 7.00 AC + 4.00 AD - 2.25 BC + 2.25 BD + 1.25 CD - 11.63 A^2 + 0.87 B^2 - 7.50 C^2 - 7.25 D^2 \text{ (Equation 5- 2)}$$

$$Y_2 = 64.00 + 9.50 A + 6.25 B + 10.25 C + 8.67 D - 12.00 AB + 7.50 AC + 5.00 AD + 5.50 BC + 6.25 BD + 5.75 CD - 14.50 A^2 - 7.13 B^2 - 12.38 C^2 - 12.00 D^2 \text{ (Equation 5- 3)}$$

Where, Y_1 and Y_2 represent response variables including BO conversion and BC yield, respectively. While A , B , C , and D represent the independent variables i.e. temperature, pressure, catalyst loading and time, respectively. Further, AB , AC , AD , BC , BD and CD represent the interaction between independent variables. Finally, A^2 , B^2 , C^2 and D^2 represent the excess of each independent variable.

The developed models have demonstrated the effect of each independent variable, variables interactions and excess of each variable on the response. The positive sign of each variable coefficient represents the synergetic effect of the variable on the response, however, the negative sign represents the antagonistic effect on the response.

5.5 Models adequacy checking

The models have been examined for adequacy to inspect the fitting accuracy of the predicted results with the experimental results. Different statistical validation techniques have been applied to investigate the accuracy of the predicted models. The significance of the predicted models and the independent variables have been examined using ANOVA at 95% confidence level as shown in *Table 5- 2* and *5-3*. The main test that could examine the significance of the model and the variables is the p-value, where the value smaller than 0.05 of this test indicates the significance of the examined parameter.

Table 5- 3. Analysis of variance of developed model for BO conversion

	Sum of square	df	Mean Square	F Value	p-value	Significance
<i>Model</i>	5194.09	14	371.01	11.31	< 0.0001	HS
<i>A-Temperature</i>	918.75	1	918.75	28.02	0.0001	HS
<i>C-Pressure</i>	954.08	1	954.08	29.10	< 0.0001	HS
<i>C-Catalyst Loading</i>	645.33	1	645.33	19.68	0.0006	S
<i>D-Time</i>	675.00	1	675.00	20.58	0.0005	S
<i>AB</i>	342.25	1	342.25	10.44	0.0060	S
<i>AC</i>	196.00	1	196.00	5.98	0.0283	S
<i>AD</i>	64.00	1	64.00	1.95	0.1842	NS
<i>BC</i>	20.25	1	20.25	0.62	0.4451	NS
<i>BD</i>	42.25	1	42.25	1.29	0.2754	NS
<i>CD</i>	6.25	1	6.25	0.19	0.6691	NS
<i>A²</i>	876.59	1	876.59	26.73	0.0001	S
<i>B²</i>	4.97	1	4.97	0.15	0.7030	NS
<i>C²</i>	364.86	1	364.86	11.13	0.0049	S
<i>D²</i>	340.95	1	340.95	10.40	0.0061	S
<i>Residual</i>	459.08	14	32.79			
<i>Lack of Fit</i>	459.08	10	45.91	0.44	0.56	NS
<i>Pure Error</i>	0.000	4	0.000			
<i>Cor Total</i>	5653.17	28				

Table 5- 4. Analysis of variance of developed model for BC yield

	Sum of square	df	Mean Square	F Value	p-value	Significance
Model	7446.55	14	531.90	68.68	< 0.0001	HS
A-Temperature	1083.00	1	1083.00	139.85	< 0.0001	HS
C-Pressure	468.75	1	468.75	60.53	< 0.0001	HS
C-Catalyst Loading	1260.75	1	1260.75	162.80	< 0.0001	HS
D-Time	901.33	1	901.33	116.39	< 0.0001	HS
AB	576.00	1	576.00	74.38	< 0.0001	HS
AC	225.00	1	225.00	29.05	< 0.0001	HS
AD	100.00	1	100.00	12.91	0.0029	S
BC	121.00	1	121.00	15.62	0.0014	S
BD	156.25	1	156.25	20.18	0.0005	S
CD	132.25	1	132.25	17.08	0.0010	S
A ²	1363.78	1	1363.78	176.11	< 0.0001	HS
B ²	329.29	1	329.29	42.52	< 0.0001	HS
C ²	993.34	1	993.34	128.27	< 0.0001	HS
D ²	934.05	1	934.05	120.62	< 0.0001	HS
Residual	108.42	14	7.74			
Lack of Fit	108.42	10	10.84	1.35	0.325	NS
Pure Error	0.000	4	0.000			
Cor Total	7554.97	28				

Where HS, S and NS represent highly significance, significance and non-significance.

As shown in *Table 5- 3* and *5.4*, both developed models are highly significant with a p-value of < 0.0001. In addition, the lack of fit analysis, which indicates the failure of the model in fitting the experimental data showed the non-significant result. This illustrates the accuracy of the models in predicting the experimental results. In addition, the values of R^2 , R^2_{adj} , R^2_{pred} have been evaluated for BO yield model as 0.99, 0.978 and 0.943, respectively. The value of adequacy precision, which indicates the ratio between the predicted response and the relative error (signal to noise ratio) has been assessed for both models. The values greater

than 4 for the adequacy precision is favourable. The adequacy precision test has reported 12.37 and 25.92 for both BO conversion and BC yield models, respectively. A plot representing the experimental actual data *versus* predicted date shown in *Figure 5- 1*. The similarity between the predicted and actual data ensures the accuracy and the adequacy of the predicted models.

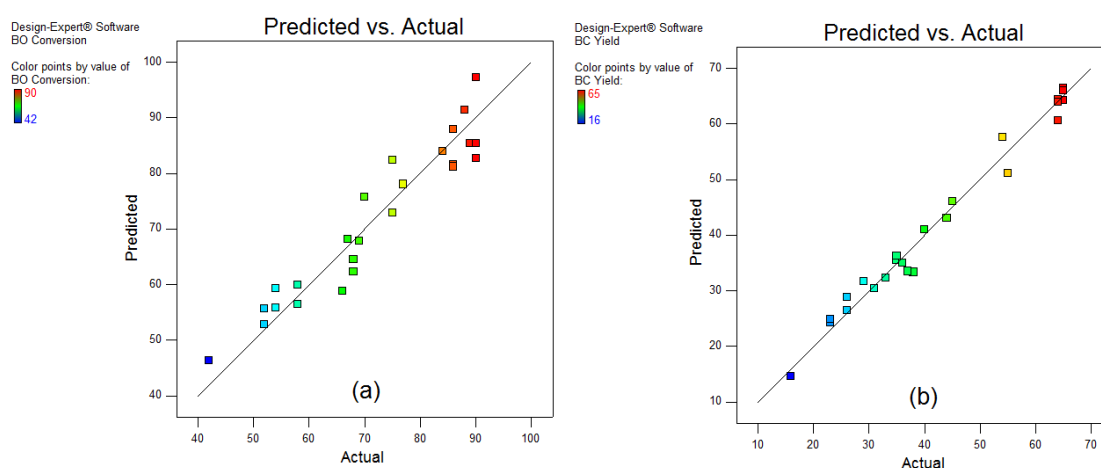


Figure 5- 1. Predicted *versus* actual values for (a) BO conversion model (b) and BC yield model

In order to rely on the conclusions conveyed from the statistical adequacy checking using ANOVA, the assumptions of the ANOVA should be examined. These assumptions could be summarised in residuals normality, residuals randomisation and homoscedasticity (equal variance) of residuals (Aboelazayem *et al.*, 2018b). The first assumption, which is the normality of the residuals has been investigated using the normality plot for both models as shown in *Figure 5- 2*. It has been observed that the residuals are approximately fitted to a straight line. This confirms the normality of the models' residuals, which validate the first assumption of ANOVA. Secondly, the randomisation of the residuals has been assessed using a plot between the residuals *versus* predicted responses values as shown in *Figure 5- 3*. The random distribution of the residuals without following any specific trend assure the validity of the second assumption of ANOVA. Finally, the homoscedasticity of residuals has been checked using a plot between the residuals and the actual experimental values at each level. One of

the independent variables, i.e. temperature, has been used as an example to ensure the variance equality at each level as shown in *Figure 5- 4*. The homoscedasticity of residuals has been validated with the observed similar range of residuals at each level.

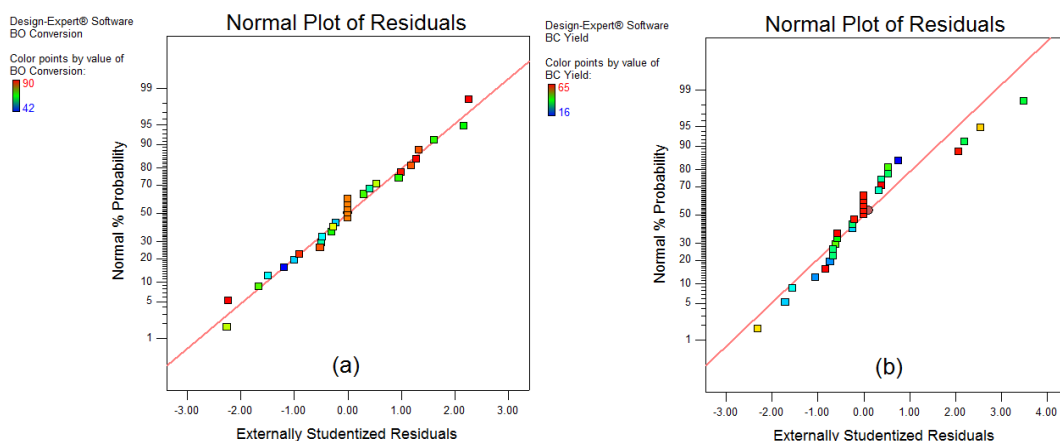


Figure 5- 2. The normal plot of residuals for (a) BO conversion model and (b) BC yield model

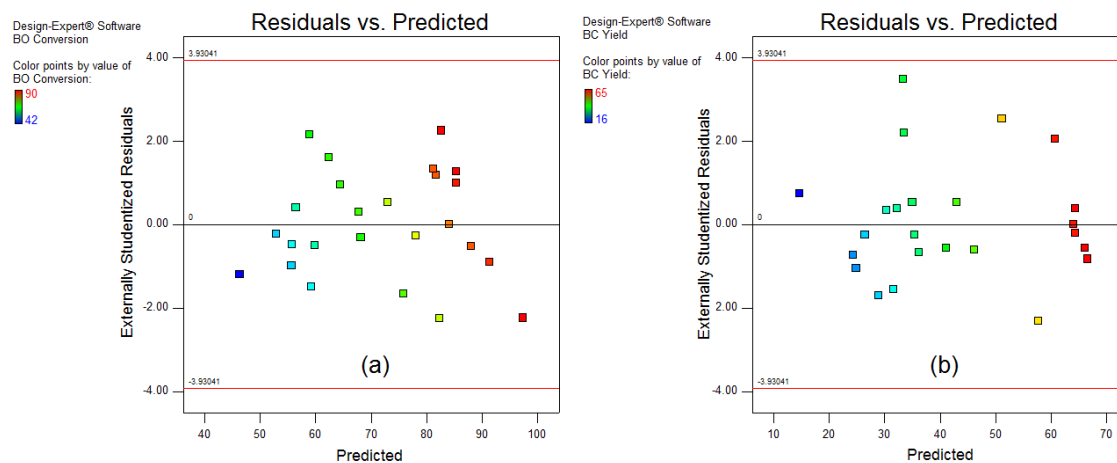


Figure 5- 3. The plot of residuals versus predicted response for (a) BO conversion model and (b) BC yield model.

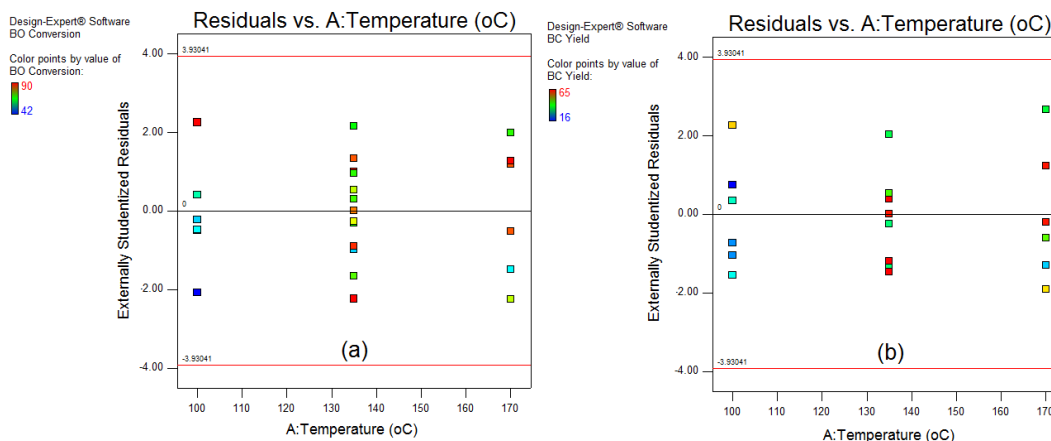


Figure 5- 4. The plot of residuals versus predicted values of temperature variable for (a) BO conversion model and (b) BC yield model.

In summary, the predicted models have been checked for adequacy using various methods where they have shown high accuracy in predicting the experimental data. ANOVA has been used to assess the significance of the models. In addition, the ANOVA assumptions have been examined in order to assure its results. Finally, the predicted models' results have been compared with the previously determined OFAT experiments reported by Onyenkeadi et al. 2018. The similarity between predicted and actual experimental values at a wide range of a number of OFAT experiments has proved the significance and the adequacy of the predicted regression models.

5.6 Effect of process variables and their interactions

In this section, the effect of each process independent variable on the process responses have been investigated. In addition, the interactive effect of different independent variables on the responses has been highlighted.

5.6.1 Effect of individual variables on responses

The effect of the independent variables on the reaction responses i.e. BO conversion and BC yield has been assessed using the developed validated models. These results have been compared with the experimental data obtained using OFAT reported elsewhere (Onyenkeadi *et al.*, 2018). A similar effect of the process variables has been observed on each process response as shown in

Figure 5- 5 to Figure 5- 8. The in-depth discussion of the effect of individual variables has been reported elsewhere (Onyenkeadi *et al.*, 2018)

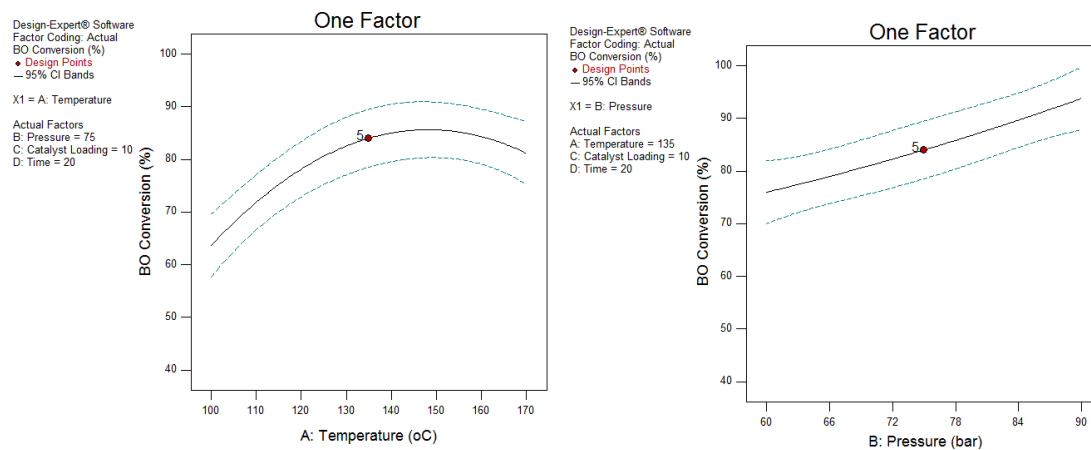


Figure 5- 5. The plot showing the effect reaction temperature and pressure on BO conversion

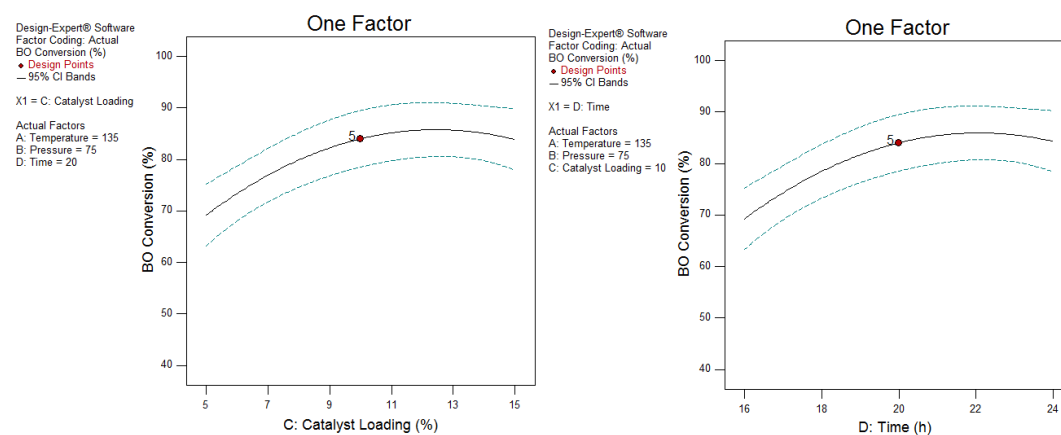


Figure 5- 6. The plot showing the effect of catalyst loading and reaction time on BO conversion

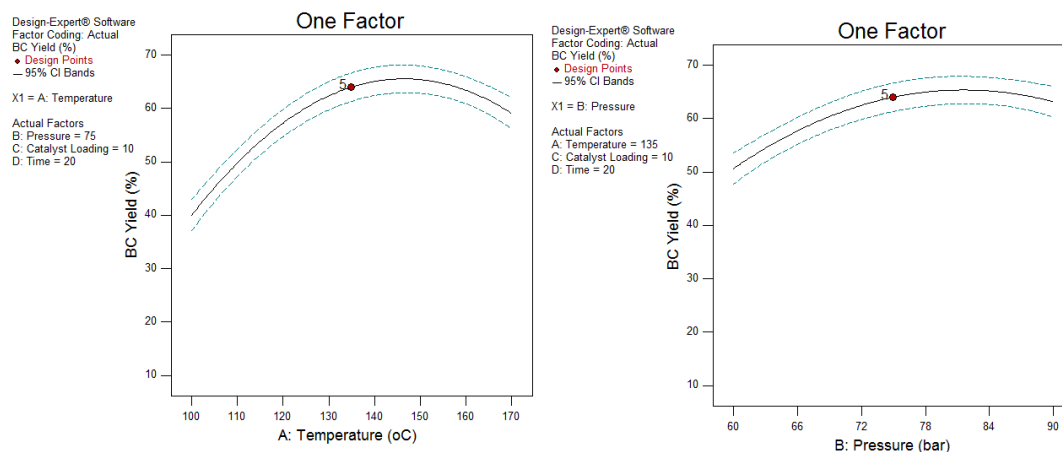


Figure 5- 7. The plot showing the effect of reaction temperature and pressure on BC yield

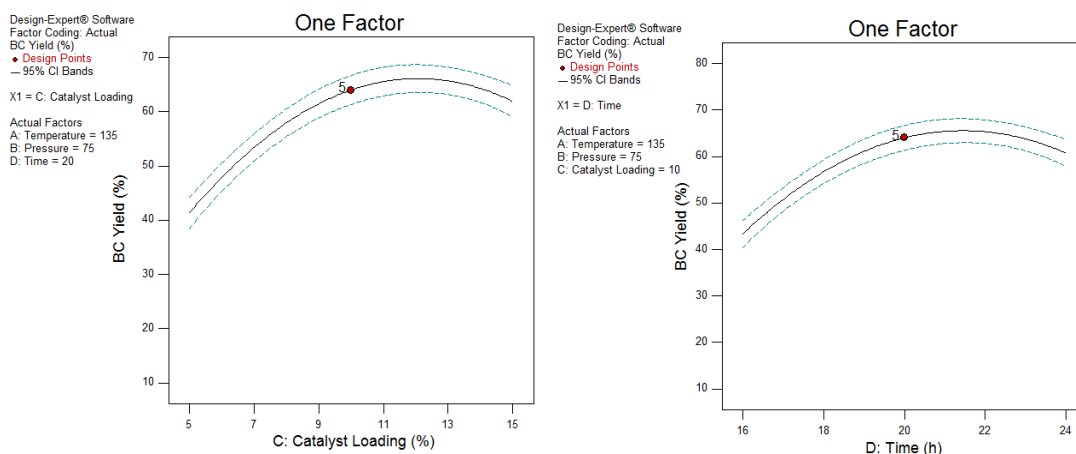


Figure 5- 8. The plot showing the effect of catalyst loading and reaction time on BC yield

5.6.2 Effect of variables interaction on responses

In this section, the effect of independent variables interactions have been illustrated and discussed. The investigation of the interactive effect of variables on the responses is important as the effect of some variables on the response would change at different levels of other variables. Hence, the interactive effect has a direct influence on the process optimisation. Further, Figure 5-9 illustrates the significance of reaction temperature and pressure on BO conversion. At low reaction temperature, the increase in pressure from 60 bar to 90 bar increases the conversion rate of BO from 70% to 90% whereas there was a slight drop of temperature beyond 150 °C. Although in Figure 5-10 there has been a

corresponding drop in the yield as the temperature increased beyond 150 °C, it is quite evident that at reaction temperature goes higher than 150 °C, causes a linear decrease in both BO conversion and BC yield. This decrease is probably due to the equilibrium nature of the cycloaddition reaction of BO and CO₂ where higher reaction temperatures can shift the equilibrium to the reactant side and results in a reduction to the yield of BC, which is similar to the work published by Saada et al. 2018 and Rasal et al. 2018. Conversely, at higher reaction temperature the pressure was constant from 75 bar to 85 bar after which there was a slight drop in the BC yield of 1.25%. Hence, it can be observed that the optimum reaction temperature is 135 °C and pressure is 75 bar.

The effect of catalyst loading and reaction time on BO conversion (see *Figure 5-11*) shows an increase in catalyst loading that leads to a corresponding rapid increase in the BO conversion, however, BO conversion is steady at catalyst loading goes beyond 10% (w/w) until 14% (w/w). Similarly, the effect of time on BO conversion reflects the same pattern beyond 20 h where it remains constant. Furthermore, *Figure 5-12* shows that BC yield was constant from 20 h upward and at 10% (w/w) catalyst loading, although there was a noticeable drop in the BC yield when the catalyst loading was 15% (w/w) and reaction time of 24 h. This significant drop can be attributed to the formation of oligomers and isomers, which were below the flame ionisation detection limits. For this study, all further OFAT experiments were conducted at 75 bar, 135 °C, 10% (w/w) catalyst loading and for 20 h. The optimum reaction conditions are within the range of the literature published (Adeleye *et al.*, 2014; Liu *et al.*, 2017; Sakakura and Kohno, 2009; Yamaguchi *et al.*, 1999).

5.6.2.1 Interactive effect of reaction temperature and pressure

It has been observed from Figures 5-9 and 5-10 that the effective reaction temperature has a positive effect on process responses until a specific value, and then the responses decrease at a higher temperature. Similarly, the effect of reaction pressure on BC yield has an increasing effect from 60 bar to 84 bar and beyond 84 bar there was a slight drop in BC yield. However, the effect of the reaction pressure has an increasing effect on the BO conversion. These observations have been made by changing one variable while keeping the other variables at a constant value. Alternatively, the interactive effect of reaction temperature and pressure on the reaction responses has different observations.

As illustrated in Tables 5-3 and 5-4, the interaction between temperature and pressure (AB) has a highly significant effect on both responses. This has been clearly observed in Figures 5-9 and 5-10, where the effect of temperature on both responses varies with pressure and *vice-versa*.

As shown in Figures 5-9 and 5-10, the effect of reaction temperature at 60 bar has an increasing effect on both responses (BO conversion and BC yield) until around 150 °C, and beyond 150 °C the effect of temperature is insignificant on the BC yield. However, the effect of reaction temperature at 90 bar is totally different on both responses where there is an increasing effect on both responses until 135 °C where there is no noticeable improvement in BC yield rather a drop in the response of BC yield as the temperature is increased at 90 bar. This shows that the temperature has a negative effect on both responses at higher values. Besides, the effect of pressure at 100 °C on both responses shows an increased effect on BO conversion and BC yield. However, the effect of pressure at 170 °C has a decreasing effect on both responses. These observations exemplify the importance of studying the interactive effect as the effect of process variables should not be recognised only at the constant value of other variables. The response surfaces are shown in *Figure 5- 9* and *Figure 5- 10* could be used to determine accurate optimum process conditions.

Design-Expert® Software

Factor Coding: Actual

BO Conversion (%)

● Design points above predicted value

● Design points below predicted value



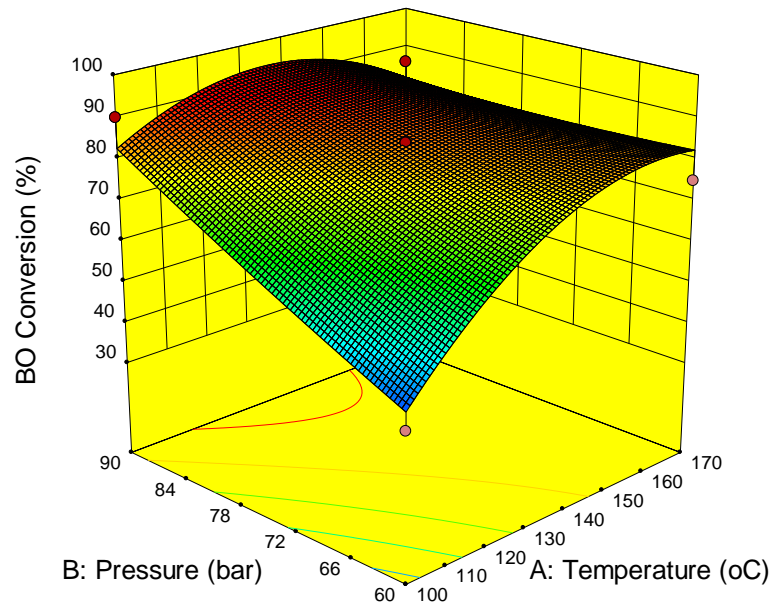
X1 = A: Temperature

X2 = B: Pressure

Actual Factors

C: Catalyst Loading = 10

D: Time = 20



Design-Expert® Software

Factor Coding: Actual

BO Conversion (%)

● Design Points



X1 = A: Temperature

X2 = B: Pressure

Actual Factors

C: Catalyst Loading = 10

D: Time = 20

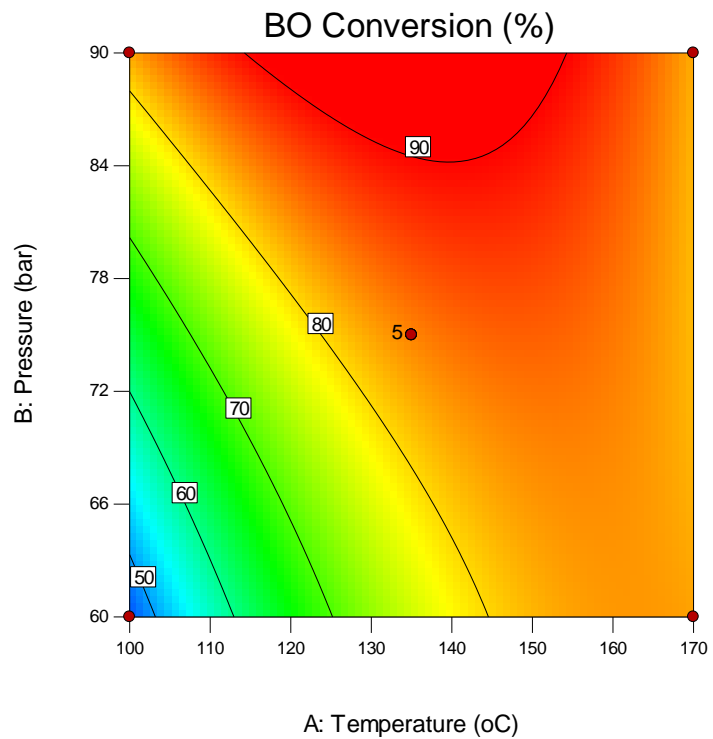


Figure 5- 9. 3D response surface and contour plot of reaction temperature and pressure versus BO conversion.

Design-Expert® Software

Factor Coding: Actual

BC Yield (%)

- Design points above predicted value
- Design points below predicted value



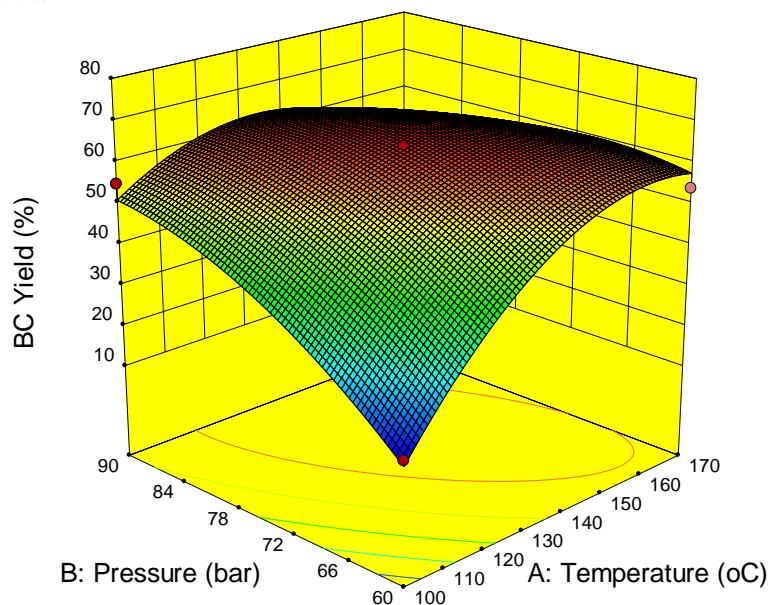
X1 = A: Temperature

X2 = B: Pressure

Actual Factors

C: Catalyst Loading = 10

D: Time = 20



Design-Expert® Software

Factor Coding: Actual

BC Yield (%)

- Design Points



X1 = A: Temperature

X2 = B: Pressure

Actual Factors

C: Catalyst Loading = 10

D: Time = 20

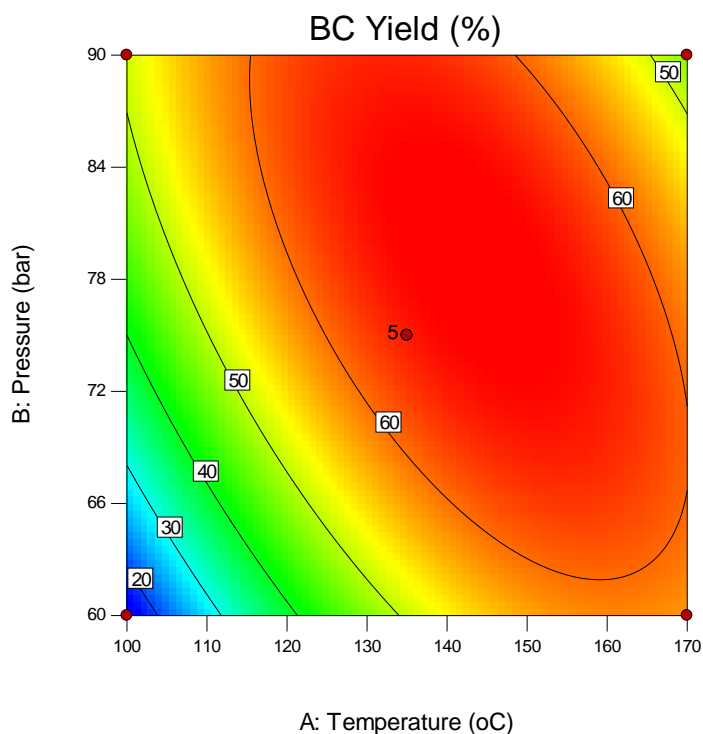


Figure 5- 10. 3D response surface and contour plot of reaction temperature and pressure versus BC yield.

5.6.2.2 Interactive effect of catalyst loading and reaction time

Based on the results obtained from ANOVA as illustrated in Table 5- 3, show that the interactive effect of catalyst loading and reaction time (CD) has an insignificant effect on BO conversion. This insignificant effect elucidates that the effect of catalyst loading on BO conversion is constant and does not change at different levels of reaction time. This has been illustrated in *Figure 5- 11*, where the effect on catalyst loading on BO conversion at 16 h is the same at 24 hr.

On the other hand, the interactive effect of catalyst loading and reaction time has a highly significant effect on BC yield as reported in *Table 5- 4*. It has been observed in the increasing effect of catalyst loading at a reaction time of 16 h has an increasing effect on BC yield until about 11% (w/w), which later decreases as the catalyst loading is increased (*Figure 5- 12*). However, the effect of catalyst loading on BC yield at 24 h is different. This shows an increasing effect on BC yield until about 13% (w/w) where there is a drop in BC yield. Therefore, catalyst loading beyond 13% (w/w) has an insignificant effect on BC yield. Similarly, the effect of reaction time on BC yield depends on the value of catalyst loading.

Design-Expert® Software

Factor Coding: Actual

BO Conversion (%)

● Design points above predicted value

○ Design points below predicted value

90

42

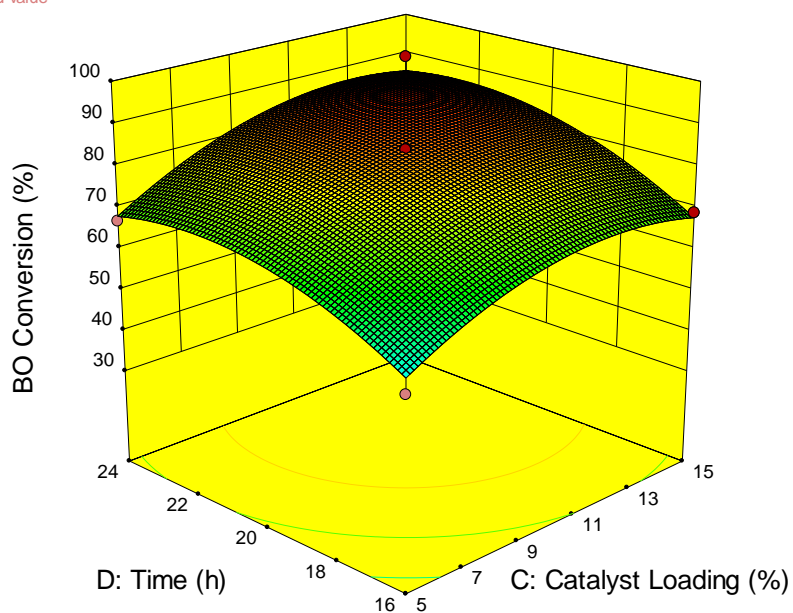
X1 = C: Catalyst Loading

X2 = D: Time

Actual Factors

A: Temperature = 135

B: Pressure = 75



Design-Expert® Software

Factor Coding: Actual

BO Conversion (%)

● Design Points

90

42

X1 = C: Catalyst Loading

X2 = D: Time

Actual Factors

A: Temperature = 135

B: Pressure = 75

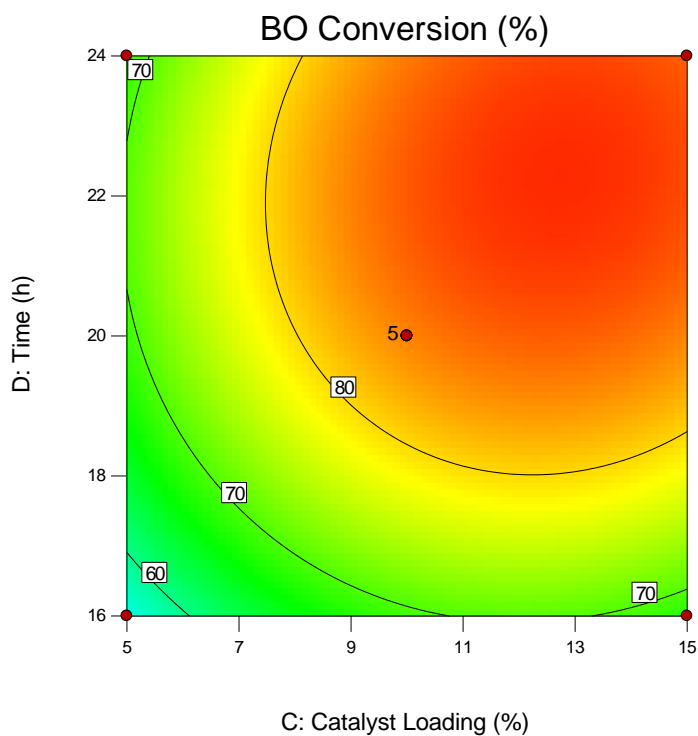


Figure 5- 11. 3D response surface and contour plot of catalyst loading and reaction time versus BO conversion.

Design-Expert® Software

Factor Coding: Actual

BC Yield (%)

● Design points above predicted value

○ Design points below predicted value

65

16

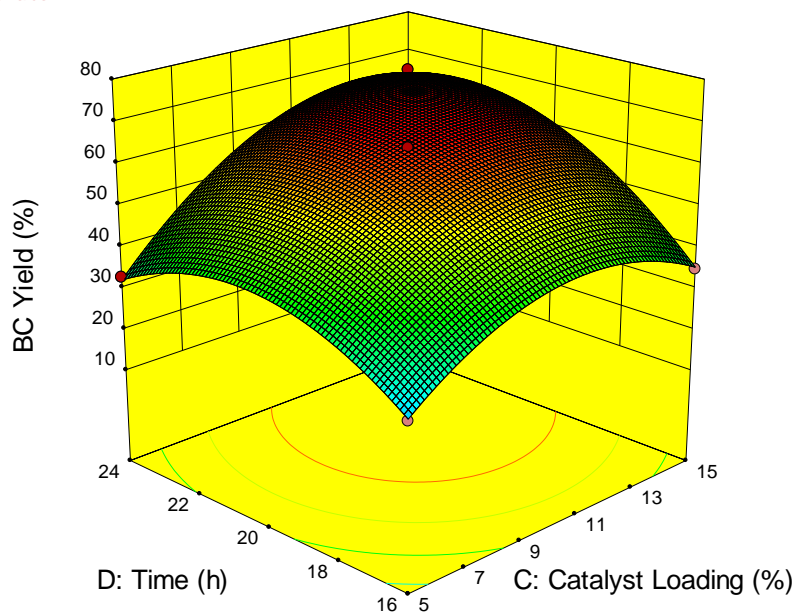
X1 = C: Catalyst Loading

X2 = D: Time

Actual Factors

A: Temperature = 135

B: Pressure = 75



Design-Expert® Software

Factor Coding: Actual

BC Yield (%)

● Design Points

65

16

X1 = C: Catalyst Loading

X2 = D: Time

Actual Factors

A: Temperature = 135

B: Pressure = 75

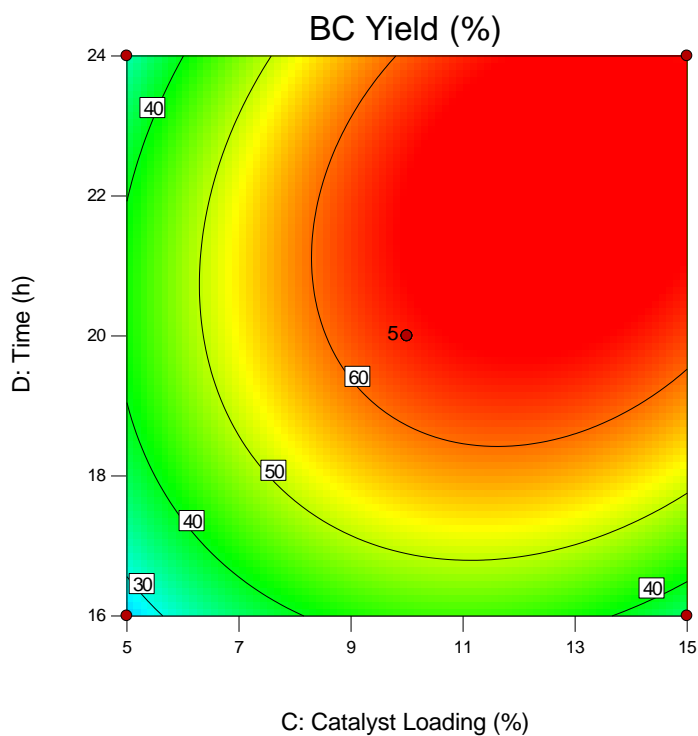


Figure 5- 12. 3D response surface and contour plot of catalyst loading and reaction time versus BC yield.

5.7 Process optimisation

One of the main advantages of using RSM is the applicability to perform process variables optimisation based on favourable targets. The optimisation targets have been set to maximise the process productivity. Accordingly, both responses have been targeted to reach the maximum value. However, the reaction variables including reaction temperature and time have been targeted to a minimum value as they consume a huge amount of energy that is not favourable economically and environmentally. In addition, the catalyst loading has been set without a specific target based on the efficient catalyst reusability. A summary of the optimisation targets for independent variables and responses is given tabulated in *Table 5- 5*. Using Design-Expert software, a numerical feature has been set to estimate the combination of the process parameters to achieve the required targets.

Consequently, 50 solutions have been generated by the software for optimum combinations, where the combination with the highest desirability has been chosen. The predicted optimum conditions have been reported at 135 °C, 90 bar, 15% catalyst loading and 20 h. These conditions have resulted in BO conversion and BC yield are 91.4% and 66.5%, respectively. This optimisation process has considered all the interactive effects between the independent variables and their effect on the responses.

In order to assess the accuracy of the predicted conditions, an experimental validation has been performed at the developed conditions. The experiments have resulted in similar results as predicted where the relative errors of the predicted results from the experimental data are 1.45% and 1.52% for BO conversion and BC yield, respectively. The similarity between the predicted and experimental results at the optimum conditions has validated the predicted optimum conditions.

Table 5- 5. Optimisation constraints used to predict optimum conditions for 1,2-butylene carbonate

Factor	Code	Goal	Limits	
			Lower	Upper
Temperature (°C)	A	Minimise	100	170
Pressure (bar)	B	In range	60	90
Catalyst loading (%)	C	In range	5	15
Time (h)	D	Minimise	16	24
BO conversion	Y ₁	Maximise	60	95
BC yield	Y ₂	Minimise	30	70

5.9 Conclusions

The systematic multivariate optimisation of 1,2-butylene carbonate synthesis via CO₂ utilisation using graphene-inorganic nanocomposite catalysts has been successfully carried out in a high-pressure reactor and the experimental results have been optimised RSM. The reaction parameters that include pressure, reaction temperature, catalyst loading and reaction time have been established as important variables affecting reaction responses using OFAT method. The regression models of BO conversion and BC yield have been developed by the use of RSM in the established significant variables. The use of OFAT method at the optimum reaction conditions at 75 bar, 135 °C, 10% (w/w) catalyst loading in 20 h reaction time gave a conversion of BO and BC yield of 84% and 64%, respectively. Conversely, the use of RSM numerical optimisation identified the optimum conditions to be 90 bar, 408 K, 15% (w/w) catalyst loading in 20 h reaction time and with BC yield of 66.5% and BO conversion of 91.4%. The predicted optimum conditions have been validated experimentally with 1.45% and 1.52% relative error for both BO conversion and BC yield, respectively. Ce-La-Zr/GO catalyst has been recycled easily and reused several times without any reduction in its catalytic performance. This detailed and systematic study clearly illustrates an efficient and greener route for 1,2-butylene carbonate synthesis using Ce-La-Zr/GO catalyst via CO₂ utilisation.

CHAPTER 6

GREENER SYNTHESIS OF STYRENE CARBONATE USING COMMERCIAL HETEROGENEOUS CATALYSTS (METAL OXIDE AND MIXED METAL OXIDE CATALYSTS

CHAPTER 6: GREENER SYNTHESIS OF STYRENE CARBONATE USING COMMERCIAL HETEROGENEOUS CATALYSTS (METAL OXIDE AND MIXED METAL OXIDE CATALYSTS)

6.1 Introduction

Styrene carbonate (SC) is an essential cyclic carbonate that can be used as an electrolyte for making lithium-ion batteries and also can be utilized as a feedstock to produce other useful organic carbonates (Wang et al., 2007; Ulusoy et al., 2011; Pescarmona and Taherimehr, 2012).

It has been established from the literature that most processes of cyclic carbonates syntheses uses toxic materials and produce harmful by-products that are carcinogenic, which could pose a severe health challenge and a threat to the environment. The drawback in these processes (conventional approaches) remains a major problem in recent times. Recently, studies have shown that the use of catalysts have not only facilitated the process of greener organic carbonates synthesis but also enhanced the selectivity of the desired products and fulfilled the requirements for the sustainability of the greener chemical process.

The development of solvent-free heterogeneous catalytic processes to replace homogeneous catalytic processes used extensively for the synthesis of styrene carbonate (SC) through the catalytic reaction of CO₂ and styrene oxide that includes an ionic liquid (Sun et al., 2004a, 2004b, 2005b), salen metal complex (Paddock and Nguyen, 2004; Paddock et al., 2004; He et al., 2009), salt and metal halide (Caló et al., 2002; Fujita et al., 2010; Liu et al., 2015a; Xu et al., 2015; Feng et al., 2016) will eliminate and improve the homogeneous catalytic processes' drawbacks. The elimination of these drawback includes high cost of catalyst production, difficulty in separation of product from the reaction mixture, complexity of processes, extensive usage of co-solvent, potential production of toxic species, limitation of catalyst reusability and instability of the catalyst under room condition (Liu et al., 2015a; Xu et al., 2015).

The development of solvent-free heterogeneous catalytic system not only plays a significant role in greener process route for valuable chemical synthesis but offers numerous benefits including reduction of process complexity, ease of catalyst

separation, improved thermal stability, elimination of toxic and hazardous by-products. Moreover, it provides easier handling, safer storage, safer disposal, and introduce efficient reusability over the homogeneous counterpart (Adeleye et al., 2015). This aptly makes solvent free heterogeneous catalytic system more economically viable and more attractive process that eliminates the risk to human health and the environment (Anastas, 2009). Although, there are other limitations of solvent-free heterogeneous catalytic system, which requires a significant amount of catalyst loading and lack of reactor design flexibility (Marvaniya et al., 2011; Liu et al., 2015c).

Response Surface Methodology (RSM) has been identified as a collection of mathematical and statistical techniques that can be used for optimising, developing and improving different processes. It is capable to develop high regression equation illustrating an empirical relationship between selected parameters and responses through a series of experimental runs (Ondari Nyakundi and Padmanabhan, 2015; Yuan et al., 2015). RSM is a significant tool to investigate the interaction between process parameters and quantitatively illustrate the effect of each parameter on the process responses (Gönen and Aksu, 2008; Zhong et al., 2012). It is extensively used in different chemical process optimisation and analysis where it minimises the number of experiments and provides comprehensive analysis conclusion. Due to the lack of research studies on SC synthesis using RSM, one factor at a time (OFAT) analysis has been applied as a startup for the experimental design. It has been used to determine the appropriate effective range of process parameters by varying only one parameter while keeping other parameters at a constant value (Kim et al., 2007; Liu et al., 2010; Duan et al., 2014).

In this study, the synthesis of SC from cycloaddition reaction of SO and CO₂ has been examined. Different heterogeneous catalysts such as magnesium oxide (MgO), titanium silicate (TiOSiO₄), zirconium oxide (ZrO₂), cerium oxide (CeO₂), lanthana oxide (La₂O₃), lanthana doped zirconia (La-Zr-O), ceria doped zirconia (Ce-Zr-O) and ceria, lanthana doped zirconia (Ce-La-Zr-O) have been investigated to determine the best performing catalyst on SO conversion and SC yield, in addition, to affirming its reusability test. One factor at a time (OFAT) test for different reaction parameters i.e. reaction temperature, pressure, time, catalyst loading and stirring rate have been analysed to determine their effects on

reaction responses and to conclude their levels that have a significant effect on the reaction response. RSM using Box-Behnken (BBD) has been used to optimise SC synthesis process. The reaction temperature, pressure, time and catalyst loading have been considered as independent variables for the reaction while SO conversion and SC yield have been chosen as reaction responses. Analysis of variance (ANOVA) has been used to investigate the significance of the developed regression models representing all independent variables function in each response variable.

6.2 Materials

Styrene oxide (97%w/w), toluene (99.8%w/w), and n-pentane (99.8%) (w/w) were procured from Sigma-Aldrich Co. LLC. The catalysts used for the experiments were magnesium oxide (MgO), titanium silicate (TiOSiO_4), zirconium oxide (ZrO_2), cerium oxide (CeO_2), lanthana oxide (La_2O_3), lanthana doped zirconia (La-Zr-O), ceria doped zirconia (Ce-Zr-O) and ceria, lanthana doped zirconia (Ce-La-Zr-O). MgO and TiOSiO_4 catalysts were purchased from Sigma-Aldrich while other catalysts were supplied by MEL Chemicals Company. The catalysts were used without further purification. The liquid CO_2 cylinder equipped with a dip tube was purchased from BOC Ltd., UK. Supercritical fluid (SCF) pump (model: SFT-10) was procured from Analytix Ltd., UK. A Parr high-pressure stainless steel autoclave reactor (model: 5500) of 25 mL capacity equipped with a reactor controller (model: 4848) was purchased from SCIMED (Scientific and Medical Products Ltd.), UK.

6.3 Catalyst characterisation

The commercial use of heterogeneous catalysts such as metal oxide and mixed metal oxide catalysts are commonly employed for the synthesis of cyclic carbonates. Such metal oxides include MgO, Ce-O, La-O, Zr-O and mixed metal oxide catalysts doped zirconium oxides includes Ce-Zr-O, La-Zr-O, and Ce-La-Zr-O have been assessed and analysed based on their activity and selectivity towards styrene carbonate synthesis. SEM, XRD, and Raman spectroscopy were used to investigate the characterization of heterogeneous catalysts. SEM was used to determine the morphology of the solid catalyst, while XRD and Raman spectroscopy were used to determine the structural characteristic of the heterogeneous catalyst.

These solid catalysts (except La-O, which was procured from Sigma-Aldrich Co. LLC) used in this research were prepared by proprietary processes developed by MEL Chemicals Ltd., the UK that has been optimised to create specific particle size distributions and different textural properties (surface area and pore volume). SEM analysis was carried out using FEI Inspect F and Quanta 3D FEG with a gold plated sample holder. XRD patterns were investigated on a Siemens D5000 X-Ray Powder Diffractometer analyser operates in $\theta/2\theta$ geometry. Raman spectra were recorded using a Renishaw Ramascope 1000 (model: 52699) analyser.

Table 3- 1 in chapter 3, shows the physical and chemical properties of heterogeneous catalysts of Zr-O, La-O, La-Zr-O, Ce-Zr-O and Ce-La-Zr-O. The physical appearance of Zr-O, La-O, and La-Zr-O are white powder while Ce-La-Zr-O and Ce-Zr-O are pale yellow powder.

The BET surface area of Ce-La-Zr-O, Ce-Zr-O, La-Zr-O, La-O, and Zr-O catalysts are $55 \text{ m}^2 \text{ g}^{-1}$, $70 \text{ m}^2 \text{ g}^{-1}$, $22 \text{ m}^2 \text{ g}^{-1}$, $75 \text{ m}^2 \text{ g}^{-1}$, and $310 \text{ m}^2 \text{ g}^{-1}$, respectively. This shows that Zr-O has the largest BET surface area, while the least is La-O. Furthermore, the La-O catalyst has the least particle size and pore volume of $0.1 \mu\text{m}$ and $0.015 \text{ cm}^3 \text{ g}^{-1}$ respectively. Ce-La-Zr-O, Ce-Zr-O, La-Zr-O and Zr-O catalysts exhibited pore volume of $0.29 \text{ cm}^3 \text{ g}^{-1}$, $0.2 \text{ cm}^3 \text{ g}^{-1}$, $0.22 \text{ cm}^3 \text{ g}^{-1}$ and $0.45 \text{ cm}^3 \text{ g}^{-1}$ respectively.

Figure 6- 1 to *Figure 6- 5* shows the Scanning electron microscopy images of Ce-La-Zr-O, Ce-Zr-O, La-Zr-O, La-O and Zr-O catalysts. *Figure 6- 1* revealed the image of Zr-O catalyst that shows different grain-like surface. *Figure 6- 2* revealed the four-sided grain-like surface image of La-O catalyst while the SEM image of La-Zr-O catalyst has aggregated smooth circular surface (*Figure 6- 3*) and the SEM image of Ce-La-Zr-O in is well-dispersed circular smooth surface (*Figure 6- 5*). The use of dopants (lanthana and ceria) indicated to have a strong influence on the morphology of the catalyst

The Raman spectra of Ce-La-Zr-O, Ce-Zr-O, La-Zr-O, La-O and Zr-O catalysts can be seen in (*Figure 6- 6*). The broad and high-intensity peaks appeared at wavelengths (λ) of 640 cm^{-1} and 1080 cm^{-1} , signify the presence of Zr-O and La-O as the principal substance of the catalysts. Although La-O at the wavelength (λ) 640 cm^{-1} has no peak the broad peak was in agreement with Zr-O catalyst

reported by Liu et al. 2010, while Ce-Zr-O catalyst showed larger and higher intensity peaks at a wavelength (λ) of 640 cm^{-1} as compared to Ce-La-Zr-O, La-Zr-O, and Zr-O catalysts. The surface area of the dopant Zr-O could have contributed to the stronger intense peaks of Ce-Zr-O.

Figure 6- 7, shows the XRD patterns of the Ce-La-Zr-O, Ce-Zr-O, La-Zr-O, La-O and Zr-O. The dopant (ceria and lanthana) have a stronger interaction with zirconia. The catalyst La-O and Zr-O catalysts peaks show low intensity at $2\theta = 23^\circ, 28^\circ, 30^\circ, 31^\circ, 40^\circ, 44^\circ, 50^\circ, 60^\circ$ and 66° when compared to Ce-La-Zr-O catalyst's higher intensity peaks at $2\theta = 32^\circ, 34^\circ, 39^\circ, 54^\circ$ and 63° . Ce-Zr-O and La-Zr-O catalysts have high-intensity peaks appeared at $2\theta = 29^\circ, 32^\circ, 34^\circ, 50^\circ$ and 60° .

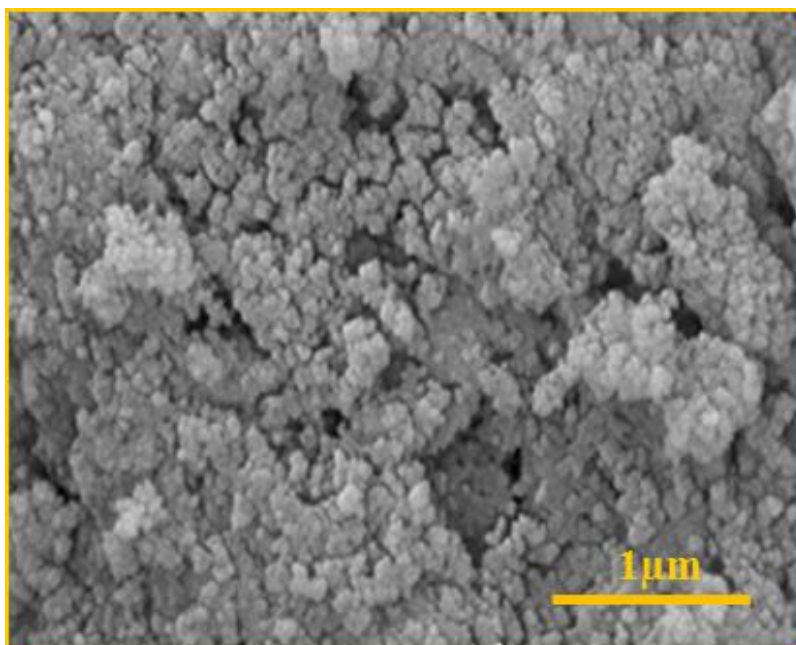


Figure 6- 1. Scanning electron microscopy (SEM) image of zirconium oxide (Zr-O) catalysts

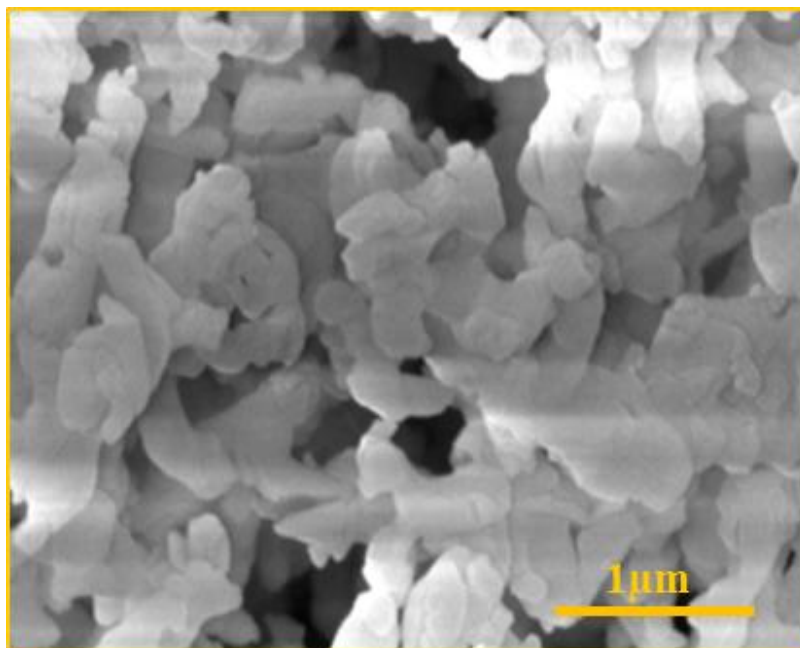


Figure 6- 2. Scanning electron microscopy (SEM) image of lanthanum oxide (La-O).

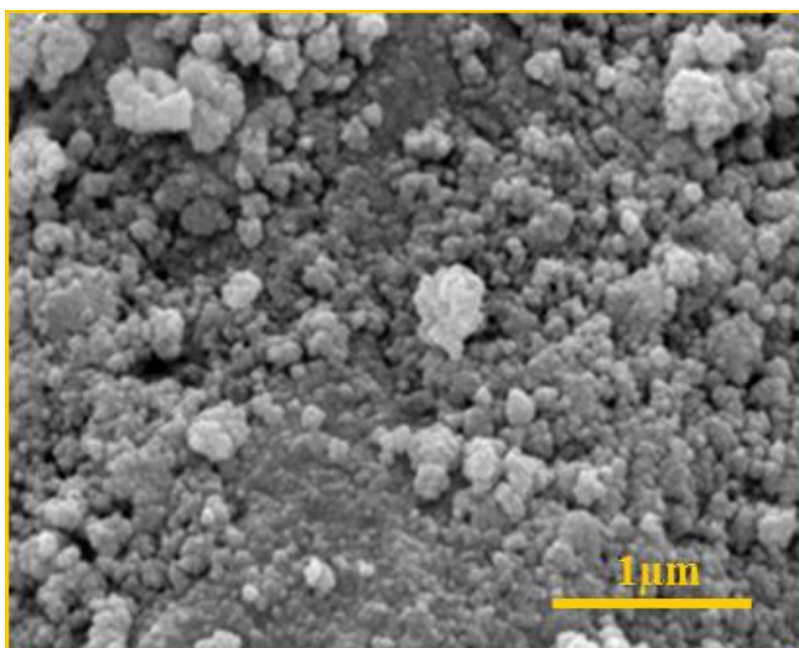


Figure 6- 3. Scanning electron microscopy (SEM) image of lanthana doped zirconia (La-Zr-O)

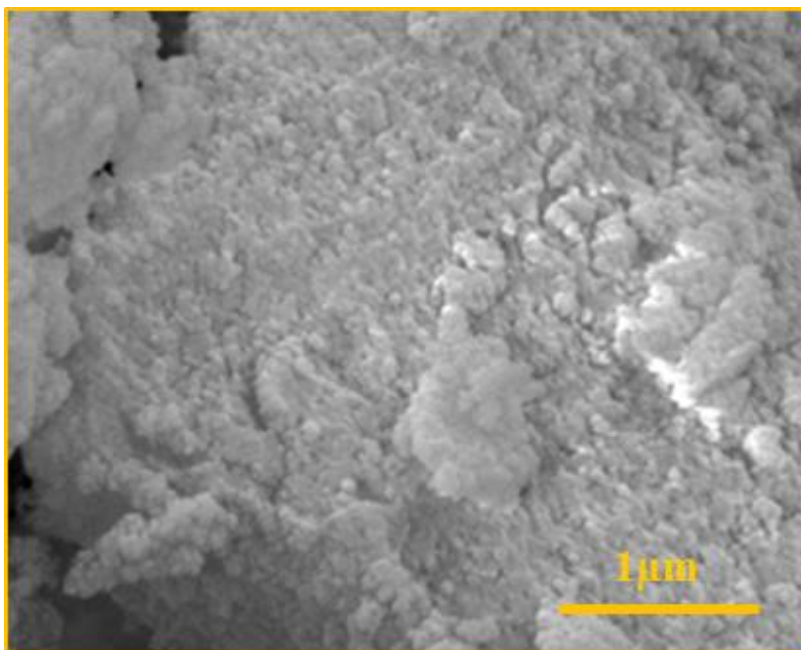


Figure 6- 4. Scanning electron microscopy (SEM) image of ceria doped zirconia (Ce-Zr-O).

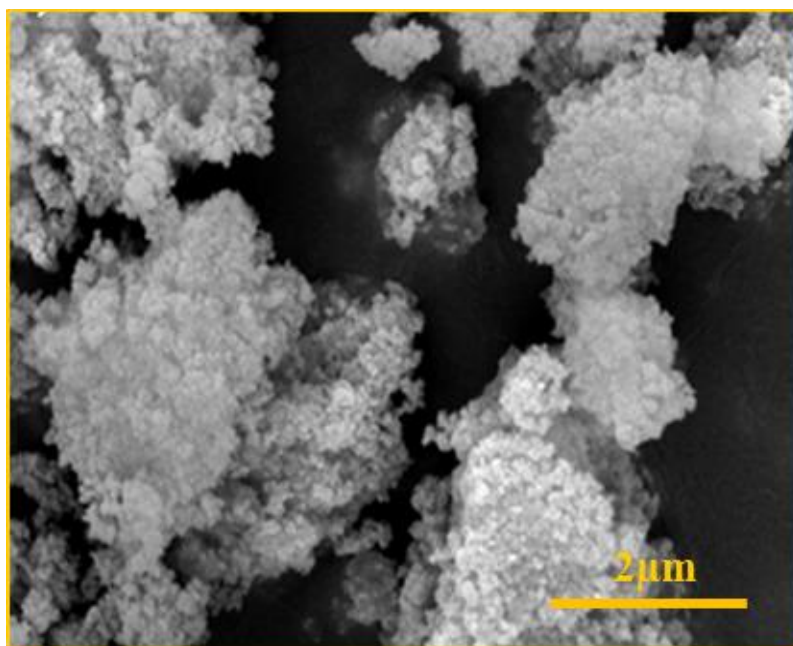


Figure 6- 5. Scanning electron microscopy (SEM) image of ceria and lanthana doped zirconia (Ce-La-Zr-O)

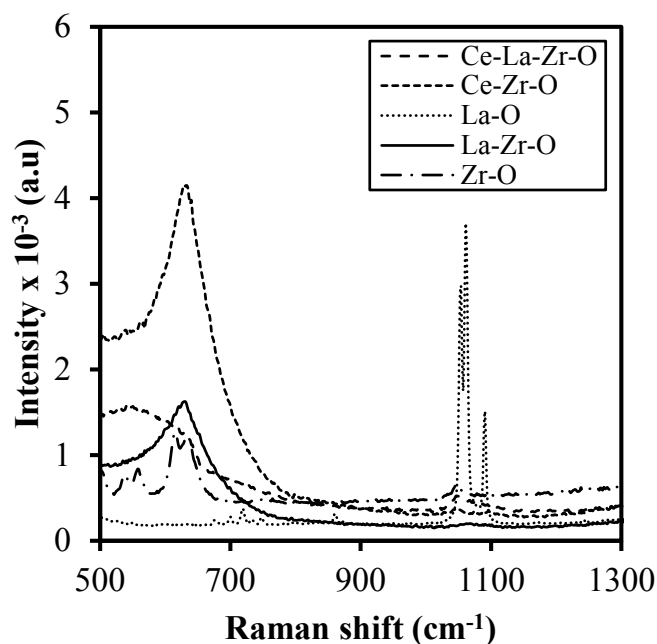


Figure 6- 6. Raman spectra of ceria and lanthana doped zirconia (Ce-La-Zr-O), ceria doped zirconia (Ce-Zr-O), lanthanum oxide (La-O), lanthana doped zirconia (La-Zr-O) and zirconium oxide (Zr-O) catalysts.

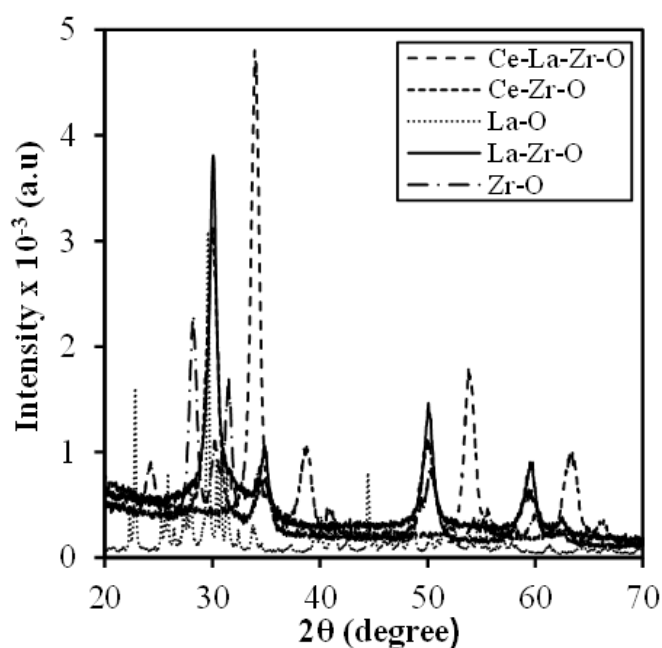


Figure 6- 7. X-ray diffraction (XRD) patterns of ceria and lanthana doped zirconia (Ce-La-Zr-O), ceria doped zirconia (Ce-Zr-O), lanthanum oxide (La-O), lanthana doped zirconia (La-Zr-O) and zirconium oxide (Zr-O) catalysts.

6.4 The synthesis of SC *via* cycloaddition reaction of CO₂ to SO

The synthesis of SC was carried out in a 25 mL stainless steel high-pressure autoclave details of which have been reported previously (Adeleye *et al.*, 2014) equipped with a stirrer, thermocouple and a heating mantle and controller. The reactor was charged with a required amount of SO and catalyst. The reactor was heated to the required temperature and continuously stirred at a known stirring speed. The supercritical fluid pump was used to pump CO₂ at a desired pressure from the cylinder to the reactor and left for a specified time. The time at which the liquid CO₂ was charged into the reactor was taken as the starting time (t=0). After the reaction, the reactor was cooled down to room temperature using an ice bath.

The reactor was depressurized and the reaction mixture was filtered. The recovered catalyst was washed with acetone and dried in an oven while the products were analysed using gas chromatography (GC) equipped with a flame ionization detector (FID) with a capillary column using octane as an internal standard. The effect of various parameters such as catalyst types, catalyst loading, CO₂ pressure, reaction temperature and reaction time was studied for the optimisation of the reaction conditions. Catalyst reusability studies were also conducted to assess the stability of the catalyst for the synthesis of SC.

6.5 Method of analysis

GC Shimadzu 2014 equipped with FID and a capillary column of dimensions (30 m x 250 μ m x 0.25 μ m) was used to analyse the filtrate collected from the reactor. The carrier gas was helium with a high purity of 99.9%, and the helium gas flow rate was set at 0.95 mL min⁻¹. The column's initial temperature was set at 323 K for 5 min after sample injection while the isothermal temperature of the injection and detector was maintained at 513 K. The column temperature was increased to 527 K at the rate of 293 K min⁻¹. The total run time for each sample was ~16 min. The ramp method was used to distinguish all the components present in the sample mixture and a split ratio of 75:1 used as part of the GC ramp method. The filtered product sample was injected by autosampler whose injection volume was set at 0.1 μ L and n-pentane was used as a solvent for pre and post-injection needle rinsing. The successive filtrate samples were run when the column temperature was cooled back to 323 K. Toluene was used as an internal standard to quantify all components present in the sample mixture. The chromatogram of the sample mixture analysed by the use of Shimadzu GC-2014

shown the peak of toluene at a residence time of ~7 min followed by SO peak at ~12 min, and SC peak at ~15.5 min, while the side products were below the limit of the GC-FID used in the analysis, and therefore specific yields of the by-products were not calculated. This observation is parallel to the work published by Adeleye et al. (2014).

6.6 Results and discussion

6.6.1 Reaction pathway

The synthesis of SC through the cycloaddition of CO₂ to SO in the presence of Ce-La-Zr-O catalyst and isomerization of SO as shown in *Figure 6-8*.

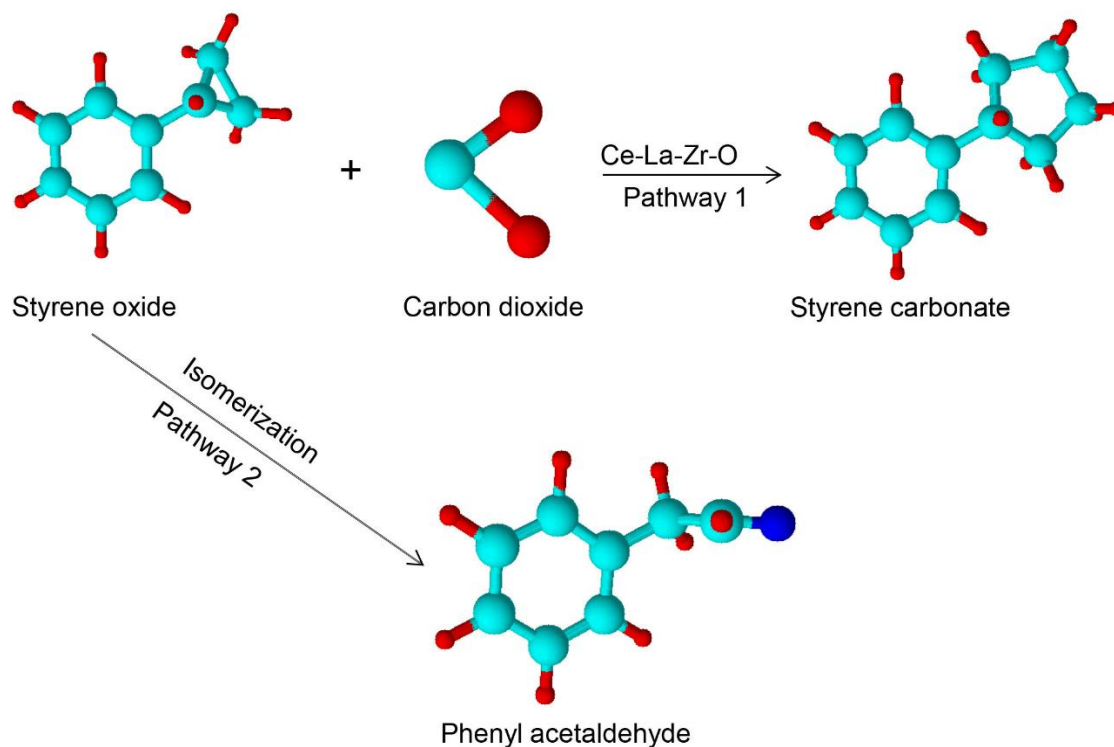


Figure 6- 8. The pathway 2 is the isomerisation of SO into phenylacetaldehyde, which is an industrially important intermediate for fine chemical synthesis. The reaction could occur under mild conditions at 25 – 70°C. The pathway 1 is for SC synthesis via cycloaddition reaction of CO₂ to SO in the presence of Ce-La -Zr-O catalyst.

6.6.1 Effect of different heterogeneous catalysts

Various heterogeneous catalysts were investigated to ascertain the best performing metal oxide or mixed metal oxide catalyst for the synthesis of SC through analysing their catalytic activity on conversion, yield and selectivity. *Figure 6- 9* shows the result of different heterogeneous catalysts on the conversion of styrene oxide, the yield, and selectivity of SC. Ce-La-Zr-O catalyst gave the highest conversion of SO (84%) and highest SC yield (52%) and selectivity (61%) at conditions of reaction temperature 408 K, CO₂ pressure 75 bar, reaction time 20 h, stirring speed 300 rpm and catalyst loading of 10% (w/w). Similarly, Mg-Al-O, La-Zr-O, Zr-O and MgO catalysts gave a yield of styrene carbonate of 25%, 21%, 18% and 16% respectively, while the selectivity of Zr-O is higher apart from Ce-La-Zr-O. The presence of Zr-O has a significant effect on the catalytic activity of Ce-La-Zr-O catalyst for the cycloaddition reaction of SO and CO₂. The presence of cerium oxide (Ce₂O₃) and lanthana oxide (La₂O₃) to Zr-O catalyst opens up the bond of SO for cycloaddition of CO₂ at desired operating conditions. Furthermore, increases the amount of moderately acidic and basic sites, which then favours the activation of SO and CO₂ and improves the catalytic activity of SC synthesis. We could, therefore, speculate the presence of the dopants have a substantial effect on the rate of conversion of SO and yield of SC. Hence, it could be concluded that the addition of Ce₂O₃ and La₂O₃ to Zr-O catalyst gave a better selectivity and higher yield. Based on this study, Ce-La-Zr-O catalyst was found to be the best-performed catalyst for the synthesis of SC and all further studies were conducted using Ce-La-Zr-O catalyst.

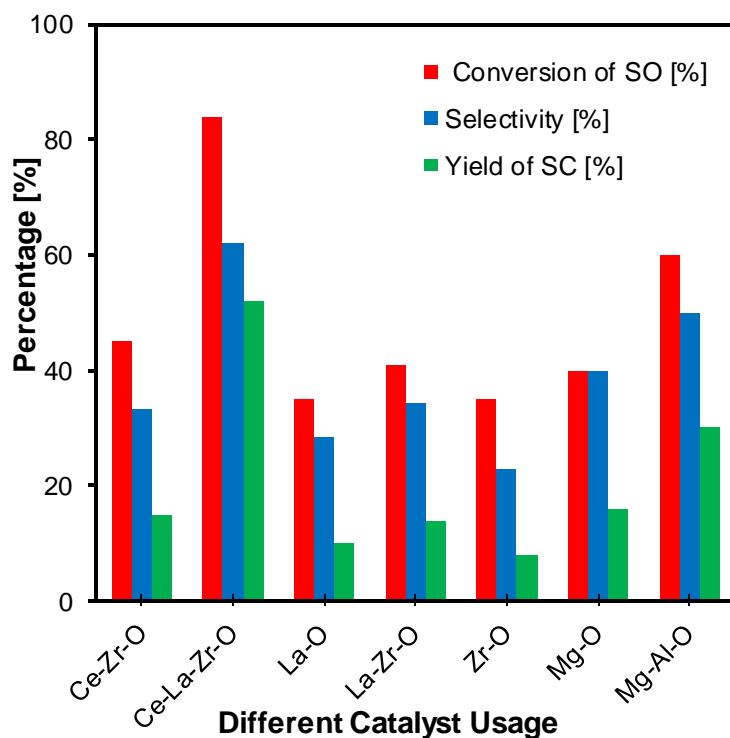


Figure 6- 9. Effect of different catalysts on conversion of styrene oxide (SO), selectivity and yield of styrene carbonate (SC). Experimental conditions: Catalyst loading – 10% (w/w); reaction temperature 408 K; CO₂ pressure 75 bar; reaction time 20 h; stirring speed 300 rpm.

6.6.2 Effect of mass transfer

The effect of mass transfer for homogeneous catalytic reaction, substances such as reactant, catalyst, and yield are in the same phase, thereby making the effect of mass transfer between phases nearly negligible, unlike heterogeneous catalytic reaction where the reactants are in a different phase of the solid catalyst, making the effect of mass transfer significant. The study of the effect of mass transfer was conducted in order to understand the activity of heterogeneous catalyst during a chemical reaction. The activity of a solid catalyst towards the selectivity of the desired product depends on the morphology of the catalyst that includes (active site, molecular structure, pore size, porosity, surface area and particle size) and prevailing conditions at the boundaries of solid catalyst such as (pressure, temperature, and superficial velocity). Mass transfer of the reactants first takes place from the bulk fluid to the external surface of the catalyst and the reactants then diffuse from the external surface through the pores within the catalyst to the catalytic surface of the pores, in which the reaction occurs

(Bhanage *et al.*, 2001; Patel and Saha, 2007), but varying parameters such as pressure, temperature and stirring speed can help to limit the external mass transfer resistance.

However, the understanding of catalytic process could limit the effect of mass transfer process during a chemical reaction and thereby shift the equilibrium towards the selectivity of the desired product. The synthesis of SC through cycloaddition reaction of CO₂ to SO was carried out at the different stirring speed of 300 – 500 rpm. The results are shown in *Figure 6- 10* that there were no significant changes in conversion of SO and yield of SC at a different stirring speed starting from 300 – 500 rpm. This shows that external mass transfer resistance is negligible in this study. Furthermore, the influence of internal mass transfer resistance is also negligible, and this is attributed to the size of the catalyst, the pore diameter, which ranges from 0.1 – 30 µm and 2.7 – 21.1 nm respectively. This is in agreement with the pore diameter of the catalyst particles is in the mesoporous region i.e. 2 – 50 nm as reported by Clerici and Kholdeeva (Beckman, 2004). Moreover, Patel and Saha reported that the absence mass transfer resistance for both internal and external mass transfer resistances using different stirrer speed and different size fractions of ion-exchange resins as catalysts for the synthesis of n-hexyl acetate (Patel and Saha, 2012).

It has been concluded that the effect of mass transfer resistances on the synthesis of SC is not significant using a Ce-La-Zr-O catalyst. Accordingly, mass transfer variable has been excluded from further optimisation experiments where it has been fixed at the minimum value, which is 300 rpm.

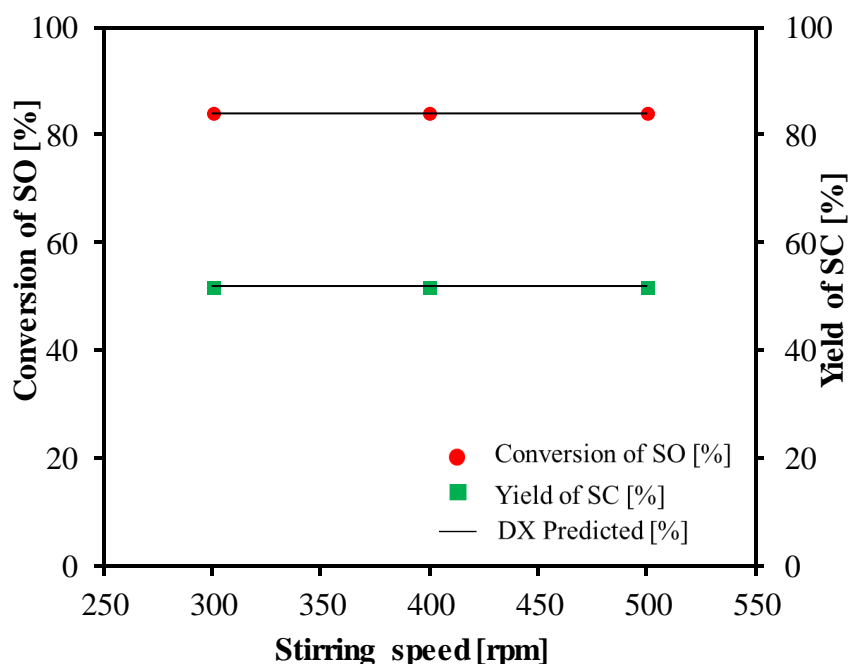


Figure 6- 10. Effect of mass transfer resistance on conversion of styrene oxide (SO) against yield of (SC). Experimental conditions: Catalyst – ceria and lanthana doped zirconia (Ce-La-Zr-O); catalyst loading 10% (w/w); reaction temperature 408 K; CO₂ pressure 75 bar; reaction time 20 h.

6.6.3 Effect of reaction time

Several experiments were carried out using different reaction time ranging from 16 h to 24 h with a target to conclude the importance of reaction time on the synthesis of SC. The experiments have performed with a different reaction time of 16 h, 20 h and 24 h at constant reaction conditions of 408 K, 75 bar and 10% catalyst loading for Ce-La-Zr-O. Figure 6- 11 shows that reaction time affects both SO conversion and SC yield significantly. It increases both responses from the range between 16 and 21 h, while beyond 21 h it has a negative impact by slightly decreasing both responses.

In contrast, at the reaction time of 20 h, the conversion of SO was 84%, and SC yield was 52% while at the reaction time of 16 h, it decreases to 70% and 45% respectively. This clearly shows that optimum reaction time is 20 h under otherwise identical reaction conditions. It is also evident that reaction time is variable affecting reaction responses. Consequently, it has been included within

the significant variables for further optimisation steps using RSM within specified 3-levels of 16, 20 and 24 coded as -1, 0, 1, respectively.

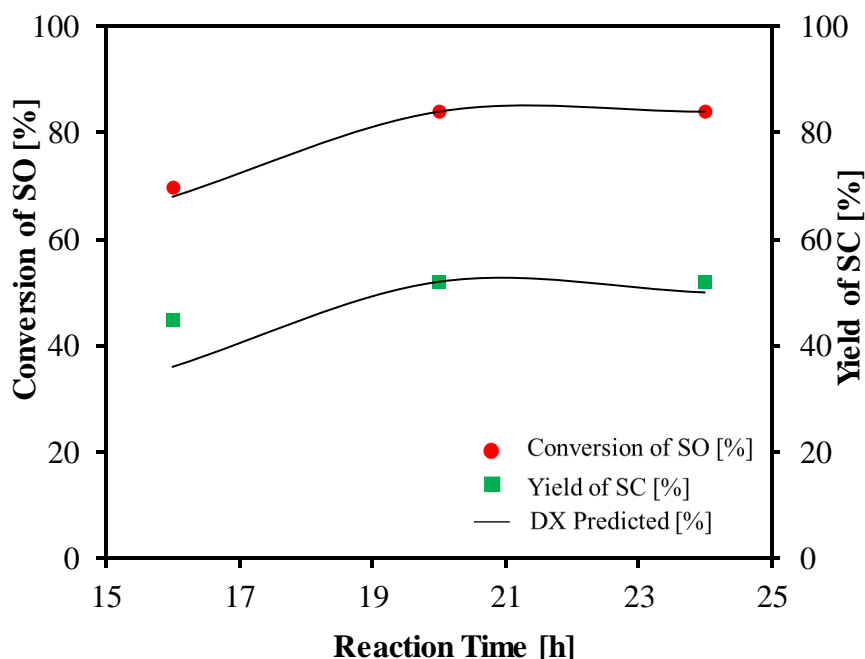


Figure 6- 11. Time dependence and prediction by design expert (DX) model on conversion of styrene oxide (SO) against yield of styrene carbonate (SC). Experimental conditions: Catalyst – ceria and lanthana doped zirconia (Ce-La-Zr-O); catalyst loading 10% (w/w); reaction temperature 408 K; CO₂ pressure 75 bar; stirring speed 300 rpm.

6.6.4 Effect of catalyst loading

The performance of different catalysts loading (w/w) ranging from 2.5% - 15% have been investigated for the synthesis of SC *via* the reaction of SO and CO₂ as shown in *Figure 6- 12*. It can be seen that with an increase catalyst loading (w/w) from 2.5% to 10%, SO conversion was increased from 35% to 84%, and the yield of SC rose from 15% to 52%. However, with an increase in catalyst loading (w/w) from 10% to 15%, there was a slight increase in the conversion of SO and yield of SC although the separation of the product becomes difficult as the catalyst loading goes beyond 12.5% (w/w). Furthermore, there were no significant changes in the responses as the catalyst loading exceeded 12.5% (w/w). This shows that the active sites required for the reaction of SO and CO₂ to produce

SC were sufficient at 10% (w/w) catalyst loading when taking the experimental error of $\pm 2\%$ into consideration. Therefore, based on this study, it can be concluded that at fixed reaction conditions at 408 K, 75 bar and 20 h, 10% (w/w) catalyst loading is the optimum amount of catalyst needed for this reaction. Accordingly, catalyst loading (w/w) has been concluded as a significant variable affecting reaction responses and it has been included for further experimental optimisation using RSM within specified levels between 2.5 to 15 % (w/w).

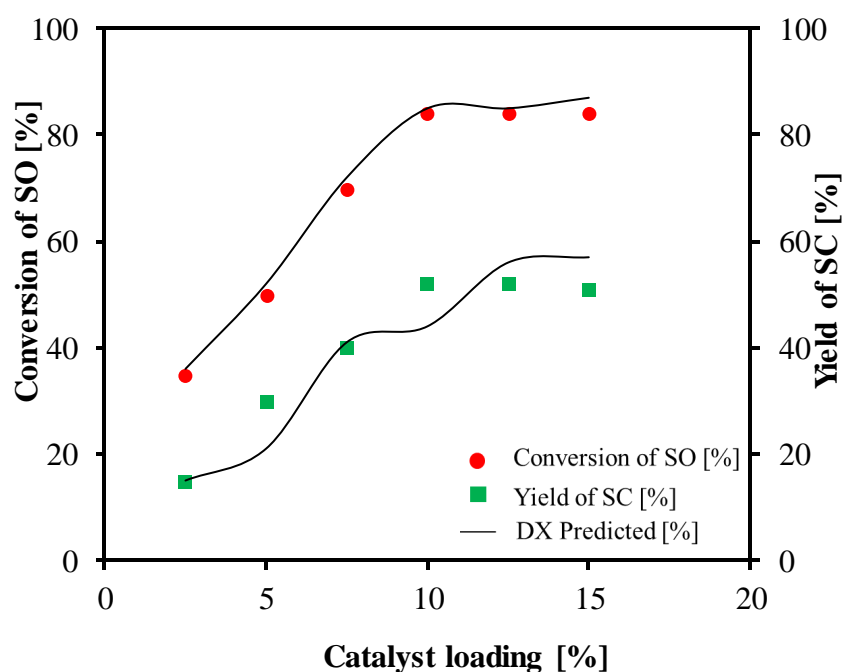


Figure 6- 12. Catalyst loading dependence and prediction by design expert (DX) model on the conversion of styrene oxide (SO) against the yield of styrene carbonate (SC). Experimental conditions: Catalyst – ceria and lanthana doped zirconia (Ce-La-Zr-O); reaction temperature 408 K; CO₂ pressure 75 bar; reaction time 20 h; stirring speed 300 rpm.

6.6.5 Effect of reaction temperature

The heterogeneous catalytic reaction of SO and CO₂ were carried out at a different reaction temperature from 368 K - 443 K. The reaction conditions for this study were set at constant conditions of 10% catalyst loading, 75 bar CO₂ pressure and 20 h. As it was expected, the higher the temperature, the more the conversion of SO into carbonates, isomers and oligomer. *Figure 6- 13* shows that the yield and selectivity of SC are dependent on the reaction temperature.

It can be observed from *Figure 6- 13* that there is a corresponding increase in conversion of SO, SC yield, and selectivity as the temperature increases from 368 K to 408 K. However, at further increase of temperature from 408 K to 443 K, there is less significant drop of SC yield from 52% to 51%, whilst the corresponding SO conversion increases from 84% to 90%.

The slight decline in the yield of styrene carbonate and further conversion of styrene oxide could be as a result of partial decomposition of the product that leads to the formation of oligomers, which was also suggested by Bhanage et al. (2001). From these results, it can be concluded that the 408 K is the optimum temperature for this exothermic reaction at constant reaction conditions of 75 bar, 20 h and 10% catalyst loading. Accordingly, reaction temperature has been included within the significant variables affecting reaction responses and has been considered for further optimisation using RSM.

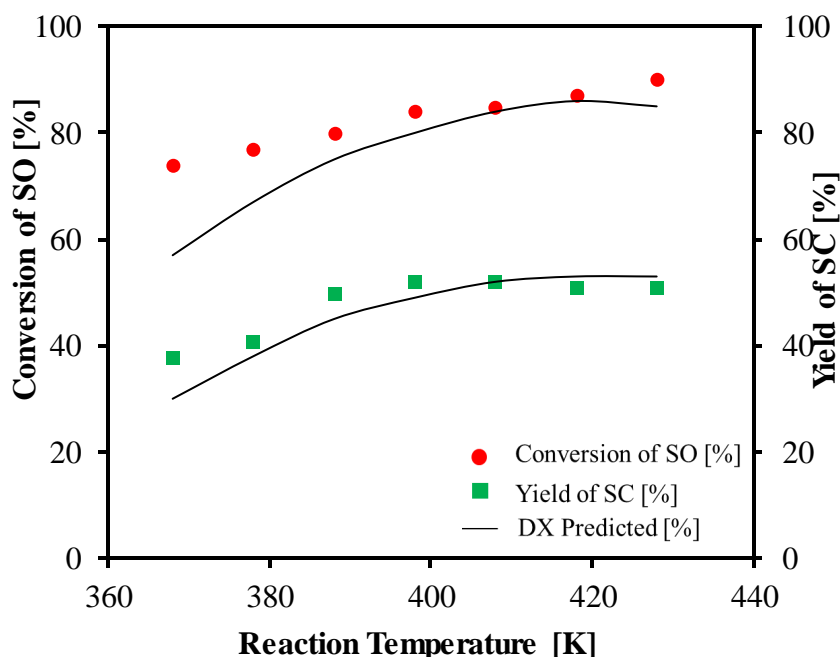


Figure 6- 13. Temperature dependence and prediction by design expert (DX) model on conversion of styrene oxide (SO) against yield of styrene carbonate (SC). Experimental conditions: Catalyst – ceria and lanthana doped zirconia (Ce-La-Zr-O); catalyst loading 10% (w/w); CO₂ pressure 75 bar; reaction time 20 h; stirring speed 300 rpm.

6.6.6 Effect of CO₂ pressure

The use of supercritical CO₂ reaction system can cause an increase in mass transfer efficiency of the reactants and lead to a shift in the reaction equilibrium to open up the thermodynamic limitation of this reaction (Baiker, 1999). The effect of CO₂ pressure on SO conversion and SC yield were studied in order to ascertain the optimum CO₂ pressure for the cycloaddition reaction of CO₂ and SO. The experiments were carried out in a high-pressure reactor at 408 K for 20 and 10 % catalyst loading. The pressure range of reaction has been varied from 55 bar to 105 bar as shown in *Figure 6- 14*. All CO₂ pressure used in this study is total pressure, because the experiment has been conducted in a batch-wise process, in which the CO₂ is set at the desired condition. It can be seen in *Figure 6- 14* that an increase in CO₂ pressure from 55 bar to 75 bar increases the SO conversion and the yield of SC. However, beyond 75 bar there were further increase in SO conversion, but the yield of SC dropped progressively. At a CO₂ pressure of 75 bar, SO conversion and SC yield were concluded as 84% and

52%, respectively. The slight drop in SC yield might be attributed to the decomposition of SC to form oligomers (see *Appendix 1-2*). This study shows an improvement in polarity and solubility of styrene conversion at the supercritical condition of CO₂ as the reaction pressure increases. Therefore, it can be concluded that 75 bar is the optimum pressure for the reaction at constant reaction conditions at 408 K, 20 h and 10% catalyst loading. Consequently, reaction pressure has been included within the significant variables for further optimisation using RSM.

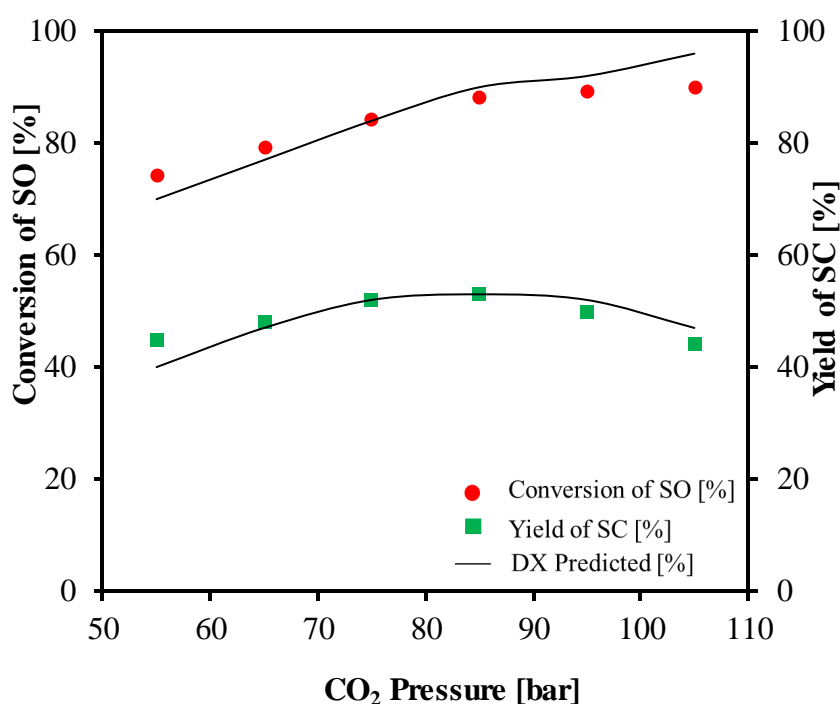


Figure 6- 14. Pressure dependence and prediction by design expert (DX) model on conversion of styrene oxide (SO) against yield of styrene carbonate (SC). Experimental conditions: Catalyst – ceria and lanthana doped zirconia (Ce-La-Zr-O); catalyst loading 10% (w/w); reaction temperature 408 K; reaction time 20 h; stirring speed 300 rpm

6.6.7 Catalyst reusability studies

The catalyst reusability experiments have been conducted to investigate the catalytic activity of the selected catalyst. The reusability study for Ce-La-Zr-O was examined in order to obtain its performance in different runs. The experiments

have been carried out in a high-pressure reactor at reaction conditions of 408 K, 75 bar, fresh 10% (w/w) catalyst loading of Ce-La-Zr-O for 20 h. The result of the first experiment was recorded as run 1 while the used catalyst was recovered by filtration from the reaction mixture, which was washed with acetone and dried in an oven at 343 K for 12 h. The recovered catalyst was reused for run 2 and for subsequent experiments of run 3 - run 5 following the same procedure. It is evident from *Figure 6- 15* that there was no noticeable decrease in the conversion of SO and SC yield after several runs (*Appendix A- 2*). The influence of the dopants increases the performance of the catalyst as compared to Ce-Zr-O and La-Zr-O catalysts. The influence of the dopants also give a stronger peak intensity of Ce-La-Zr-O catalyst and decreases in crystallinity of the zirconia catalyst. Therefore, it can be concluded that Ce-La-Zr-O catalyst can be reused several times maintaining its catalytic activity.

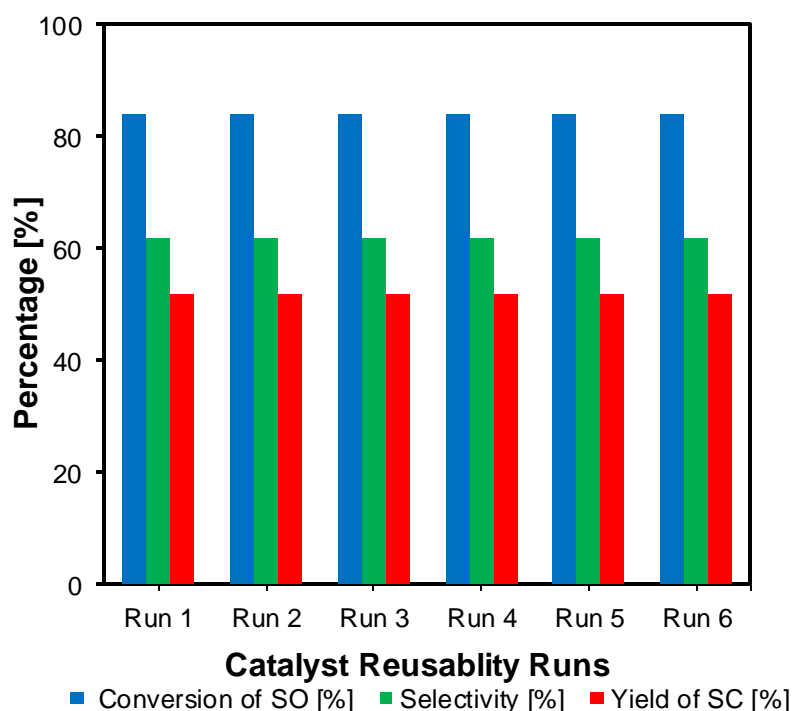


Figure 6- 15. Catalyst reusability studies on conversion of styrene oxide (SO), selectivity and yield of styrene carbonate (SC). Experimental conditions: Catalyst – ceria and lanthana doped zirconia (Ce-La-Zr-O); catalyst loading 10% (w/w); reaction temperature 408 K; CO₂ pressure 75 bar; reaction time 20 h; stirring speed 300 rpm.

6.7 RSM modelling and optimisation

After performing OFAT tests for several potential variables affecting reaction responses, it has been concluded that Ce-La-Zr-O catalyst is the best performing catalyst in comparison with other catalysts examined in this study. In addition, it has been concluded that reaction temperature, pressure, catalyst loading and reaction time are affecting both reaction responses i.e SO conversion and SC yield significantly. Accordingly, these reaction variables have been selected for RSM modeling and optimisation procedures.

6.7.1 Experimental design

RSM was developed to acquire the optimal conditions for SC synthesis by describing the relationship between independent and response variables. The experiments were performed based on the 4 independent variables including reaction temperature (K), pressure (bar), catalyst loading (w/w) and reaction time (h), which has been coded as A, B, C and D, respectively. SO conversion and SC yield were chosen as response variables for the process, which were labelled as Y1 and Y2, respectively. BBD is one of RSM methods, which are used to examine the interaction relationship between reaction variables and responses. BBD was implemented in this study to optimise the reaction conditions using 29-experiments and to conclude the main effects, interaction effects and quadratic effects of reaction variables on each response. The experiments were performed in a randomised order to minimise the effect of unexplained consistency in the responses. Three levels for each independent variable for low, middle and high were coded as -1, 0, 1, respectively as shown in *Table 6- 1*.

Table 6- 1. Experimental design variables and their coded levels

<i>Factor</i>	<i>Code</i>	<i>Levels</i>		
		<i>-1</i>	<i>0</i>	<i>+1</i>
<i>Temperature (K)</i>	<i>A</i>	<i>373</i>	<i>408</i>	<i>443</i>
<i>Pressure (bar)</i>	<i>B</i>	<i>60</i>	<i>75</i>	<i>90</i>
<i>Catalyst Loading (w/w)</i>	<i>C</i>	<i>5</i>	<i>10</i>	<i>15</i>
<i>Time (h)</i>	<i>D</i>	<i>16</i>	<i>20</i>	<i>24</i>

6.7.2 Statistical analysis

The experimental data were fitted to the general quadratic equation as shown in *Equation 6-1* to illustrate each response variable (Y1 and Y2) as a function of the independent variables.

$$Y = b_o + \sum_{i=1}^n b_i x_i + \sum_{i=1}^n b_{ii} x_i^2 + \sum_{i=1}^{j-1} \sum_{j=2}^n b_{ij} x_i x_j + \varepsilon \quad \text{Equation 6-4}$$

Where Y represents each dependent response, b_o represents the coefficient constant of the model, b_i , b_{ii} , b_{ij} , represent the coefficients for intercept of linear, quadratic and interactive terms respectively, while X_i , X_j represent the independent variables ($i \neq j$). The statistical significance test using ANOVA was based on the total error criteria with 95% confidence level ($p < 0.05$). Design Expert software (Version 10, Stat-Ease Inc., Minneapolis, MN, USA) was used for regression analysis, graphical analysis and numerical optimisation. Surface response plots were generated by varying two variables within the specified experimental levels while keeping the other variables at a constant value in their centre points. Numerical optimisation of the reaction conditions was performed using specified variables targets. The optimisation targets were based on maximizing reaction responses (SC yield and SO conversion) at the minimum reaction independent variables.

6.7.3 Model development and adequacy checking

The responses of each randomized experiments in terms of SO conversion and SC yield have been reported in *Table 6-2*. It has been observed from the experimental runs that SO conversion ranges from 39 to 90% while SC yield ranges from 15 to 54%. The variations within the wide range of both responses have shown their significant effect with respect to reaction variables. Multiple regression analysis of the experimental data in *Table 6-2* has been performed using Design Expert software. It has generated two polynomial regression equations for each response variable representing an empirical relationship between reaction variables and each response variable as shown in *Equations 6-1* and *6-2*.

$$Y1 = 84.00 + 9.25 A + 9.92 B + 7.50 C + 7.83 D - 9.00 AB + 8.00 AC + 5.25 AD - 3.75 BC + 3.00 BD + 1.25 CD - 12.58 A^2 - 0.33 B^2 - 8.96 C^2 - 8.21 D^2$$

Equation 6- 5.

$$Y2 = 52.00 + 7.25 A + 4.50 B + 7.92 C + 6.83 D - 10.75 AB + 5.75 AC + 3.25 AD + 3.00 BC + 4.75 BD + 4.50 CD - 10.21 A^2 - 3.58 B^2 - 8.21 C^2 - 9.33 D^2$$

Equation 6- 6.

Where, Y1, Y2 represents response variables including SO conversion and SC yield, respectively. A, B, C, and D represent independent variables including temperature, pressure, catalyst loading and time, respectively.

Table 6- 2. Experimental design matrix with the actual and predicted responses.

Run	A: Temperature	B: Pressure	C: Catalyst Loading	D: Time	Actual Conversion	Y1: Predicted Conversion	Actual Yield	Y2: Predicted Yield
	K	bar	w/w	h	%	%	%	%
1	408	75	10	20	84	84.00	52	52.00
2	443	75	15	20	85	87.21	54	54.50
3	408	75	15	16	67	65.25	32	31.04
4	408	75	5	24	65	65.92	28	28.88
5	408	75	10	20	84	84.00	52	52.00
6	373	75	5	20	52	53.71	23	24.17
7	408	75	10	20	84	84.00	52	52.00
8	373	90	10	20	89	80.75	50	46.21
9	373	75	15	20	54	52.71	30	28.50
10	408	90	10	16	68	74.54	31	32.00
11	373	75	10	16	50	51.37	19	21.62
12	408	75	5	16	50	52.75	24	24.21
13	443	90	10	20	86	81.25	40	39.21
14	408	90	15	20	85	88.38	53	55.63
15	408	60	5	20	60	53.54	35	30.79
16	443	75	10	16	65	59.38	32	29.62
17	443	60	10	20	72	79.42	48	51.71
18	408	75	15	24	87	83.42	54	53.71
19	408	60	15	20	75	76.04	41	40.63
20	443	75	5	20	51	56.21	24	27.17
21	408	90	10	24	89	96.21	53	55.17
22	373	75	10	24	54	56.54	28	28.79
23	408	75	10	20	84	84.00	52	52.00
24	408	60	10	24	73	70.37	36	36.67
25	373	60	10	20	39	42.92	15	15.71
26	408	75	10	20	84	84.00	52	52.00
27	408	60	10	16	64	60.71	33	32.50
28	443	75	10	24	90	85.54	54	49.79
29	408	90	5	20	85	80.88	35	33.79

The predicted RSM models have been examined for adequacy to report the possible problems associated with the normality assumptions. The RSM models have been validated by ANOVA at 95% confidence level. Fisher's F-test and p-value have been used to determine the significance of the corresponding variable.

Equations 6-2 and 6-3 have concluded a good visualisation of the effect of significant variables and their interaction on each response. High values of determination coefficients ($R^2 = 0.947$ and 0.975 for SO conversion and SC yield, respectively) show a good correlation between actual and predicted results. These results indicate that only 0.053 and 0.025 of the total variation have not been well clarified for SO conversion and SC yield, respectively, which indicates very high fitting of the predicted models with the experimental data. The ANOVA for both developed models has been applied to examine the significance of the model for fitting the experimental data. *Table 6-3* summarises the ANOVA results for both SO conversion and SC yield models. The significance of the model is determined at high Fisher's F-value and low probability p-value. Based on the ANOVA results for SO conversion (Y1), F-value and p-value have been reported by 12.85 and <0.0001 , respectively. While for SC yield (Y2), F-value and p-value have been evaluated as 39.24 and <0.0001 , respectively. These results indicate the quadratic developed model is highly statistically significant with 95% confidence level. Moreover, the validity of the models has been confirmed by p-values of lack of fit i.e. 0.123 and 0.325 (more than 0.05) for SO conversion and SC yield, respectively, which indicates that the models have represented most of the experimental data successfully. A plot between predicted versus actual values showed reasonable agreement and high correlation. The efficient estimation of the response values are concluded from the similarity both predicted and actual results of both SO conversion and SC yield as shown in *Figure 6- 16 and 6-19*, respectively. The predicted model's values have been applied to the previously determined OFAT experiments in *Figure 6- 11 to 6-15*. The similarity between predicted and actual experimental values at a wide range of a number of OFAT experiments proved the significance and the adequacy of the predicted regression models.

Table 6- 3. Analysis of variance (ANOVA) for response surface developed a model

Source	Sum of Squares		Mean Squares		F-values		p-values	
	Y ₁	Y ₂	Y ₁	Y ₂	Y ₁	Y ₂	Y ₁	Y ₂
Model	5981.76	4254.55	427.27	303.90	12.85	39.24	< 0.0001	< 0.0001
A- Temperature	1026.75	630.75	1026.75	630.75	30.89	81.45	< 0.0001	< 0.0001
B-Pressure	1180.08	243.00	1180.08	243.00	35.50	31.38	< 0.0001	< 0.0001
C-Catalyst Loading	675.00	752.08	675.00	752.08	20.30	97.12	0.0005	< 0.0001
D-Time	736.33	560.33	736.33	560.33	22.15	72.36	0.0003	< 0.0001
AB	324.00	462.25	324.00	462.25	9.75	59.69	0.0075	< 0.0001
AC	256.00	132.25	256.00	132.25	7.70	17.08	0.0149	0.0010
AD	110.25	42.25	110.25	42.25	3.32	5.46	0.0900	0.0349
BC	56.25	36.00	56.25	36.00	1.69	4.65	0.2143	0.0490
BD	36.00	90.25	36.00	90.25	1.08	11.65	0.3157	0.0042
CD	6.25	81.00	6.25	81.00	0.19	10.46	0.6712	0.0060
A ²	1027.07	675.96	1027.07	675.96	30.89	87.29	< 0.0001	< 0.0001
B ²	0.72	83.29	0.72	83.29	0.022	10.76	0.8850	0.0055
C ²	520.55	437.04	520.55	437.04	15.66	56.44	0.0014	< 0.0001

D^2	437.04	565.05	437.04	565.05	13.15	72.97	0.0028	< 0.0001
Residual	465.42	108.42	33.24	7.74				
Lack of Fit	465.42	108.42	46.54	10.84	2.22	1.12	0.1233	0.3254

Design-Expert® Software
Conversion

Color points by value of
Conversion:

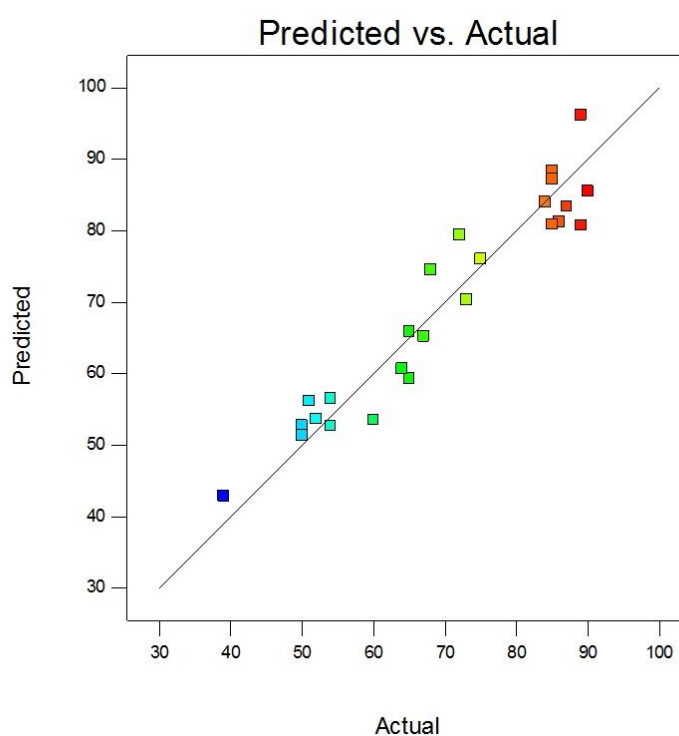


Figure 6- 16. Actual experimental data versus predicted values for SO conversion.

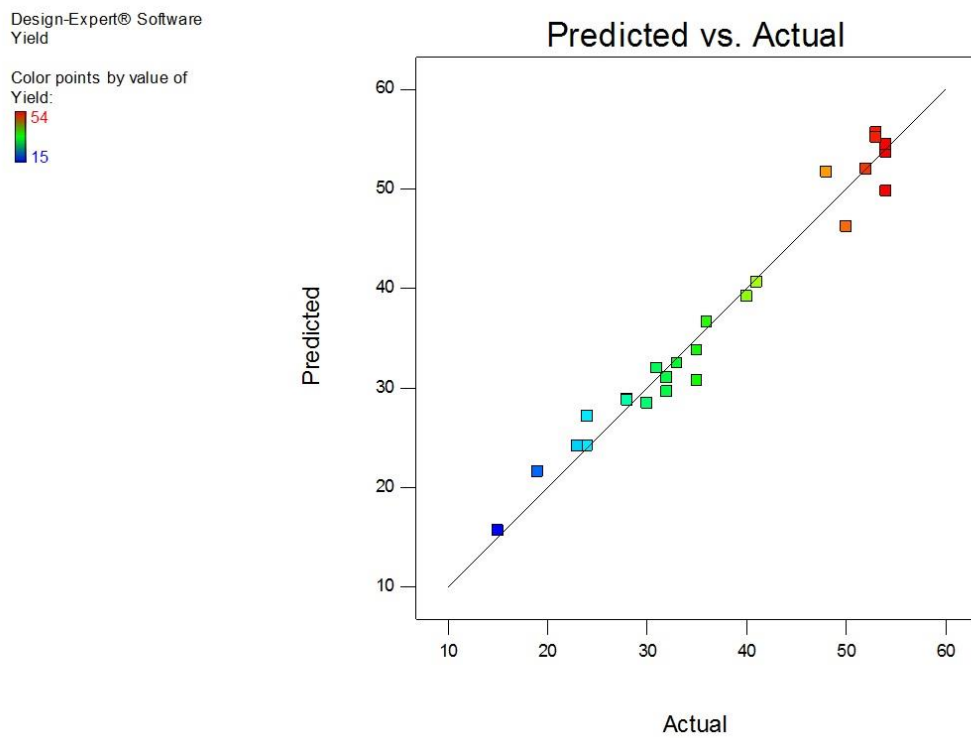


Figure 6- 17. Actual experimental data versus predicted values for SC yield.

6.7.4 Effect of process variables

According to the ANOVA results reported in *Table 3*, it could be concluded that the first order process variables have shown a significant effect on process responses with a p-value lower than 0.05. It could be concluded that reaction pressure (B) is the most significant variable affecting SO conversion recording the highest F-value of 35.50. Similarly, catalyst loading (C) has been concluded as the most significant variable affecting SC yield with F-value of 97.12. These results have been confirmed using analysis of response surface, which provides visualisation of the predicted model with three-dimensional plots. These plots illustrate the effect of process variables on the responses by varying two independent variables and analyse their effect on each response while holding the other variables constant at their centre points.

The effect of reaction temperature and pressure is clearly shown in *Figure 6- 18* and *Figure 6- 19* for SO conversion and SC yield, respectively. It is clearly shown in *Figure 6- 18* and *Figure 6- 19* that both responses increase while increasing reaction temperature at low-pressure levels. However, at increased pressure, the effect of temperature changes and the responses increase the temperature until the specified temperature, which starts to have a negative impact on the responses. These conclusions show the importance of analysing the effect of interaction between variables as it has been concluded from *Figure 6- 13*, that the effect of temperature is directly proportional on both responses, however, this conclusion is only valid at constant pressure values were varying pressure with temperature has shown the different interactive effect on the responses. Similarly, the effect of reaction pressure on both responses is clearly illustrated in *Figure 6- 18* and *6- 19*. At low temperatures, the pressure shows a direct linear relationship with reaction responses, while at higher temperature the responses behaviour changes with increasing reaction pressure. *Figure 6- 20* and *6- 21* show the effect of catalyst loading and reaction time on both SO conversion and SC yield, respectively.

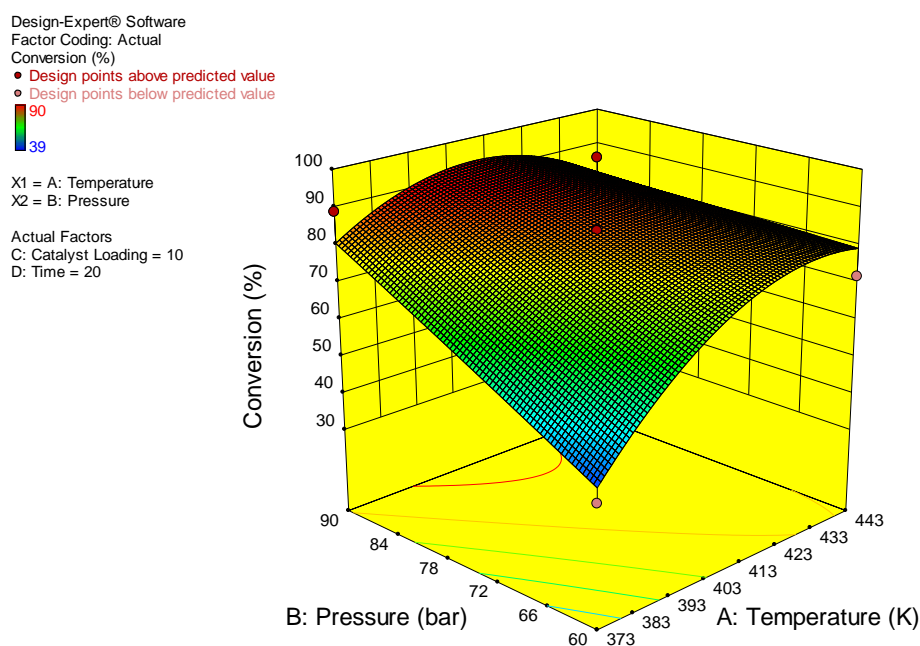


Figure 6- 18. Response surface plot for the effect reaction temperature and pressure on SO conversion.

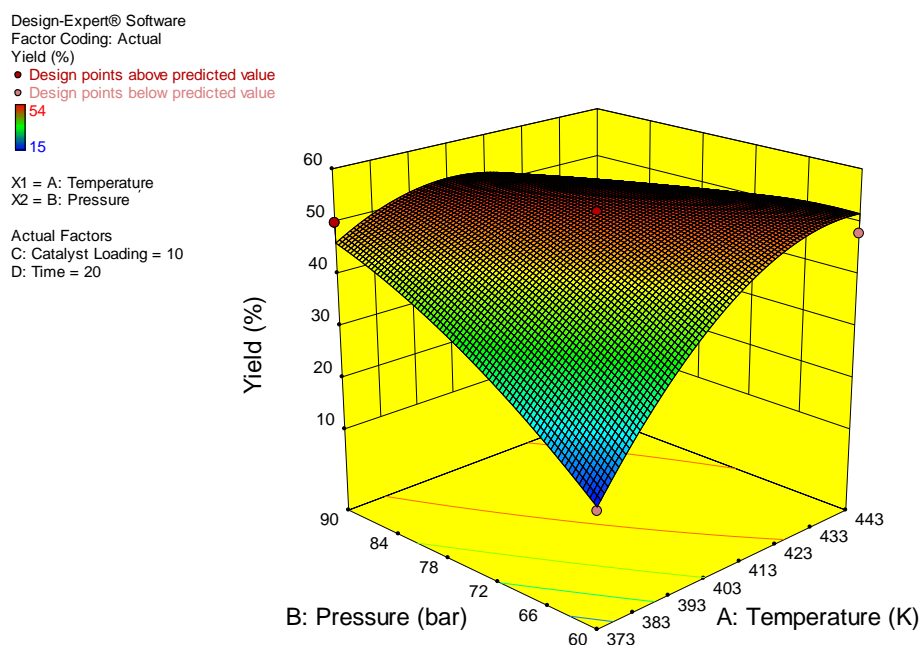


Figure 6- 19. Response surface plot for the effect reaction temperature and pressure on SC yield.

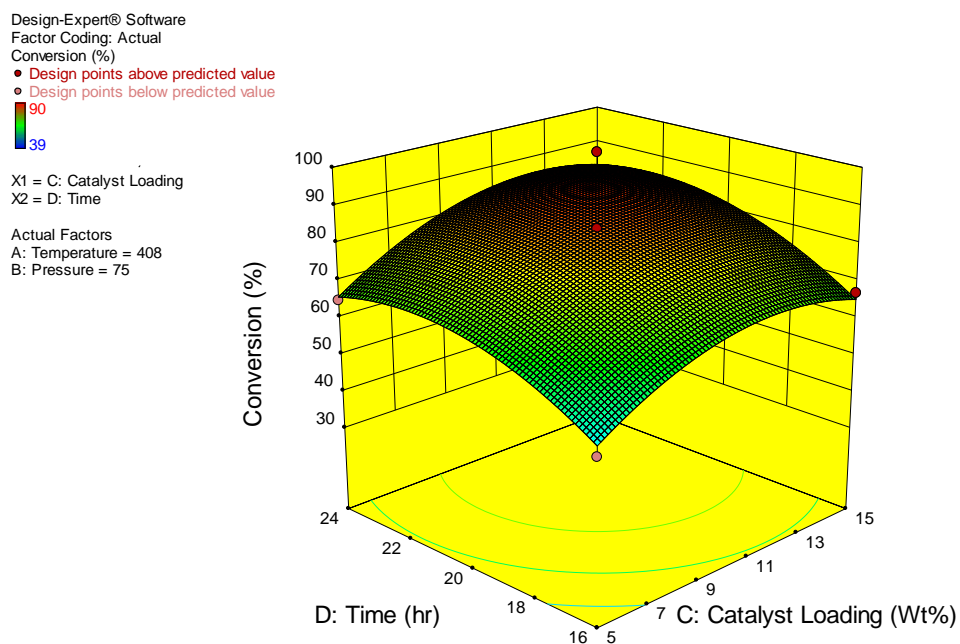


Figure 6- 20. Response surface plot for the effect reaction catalyst loading and reaction time on SO conversion.

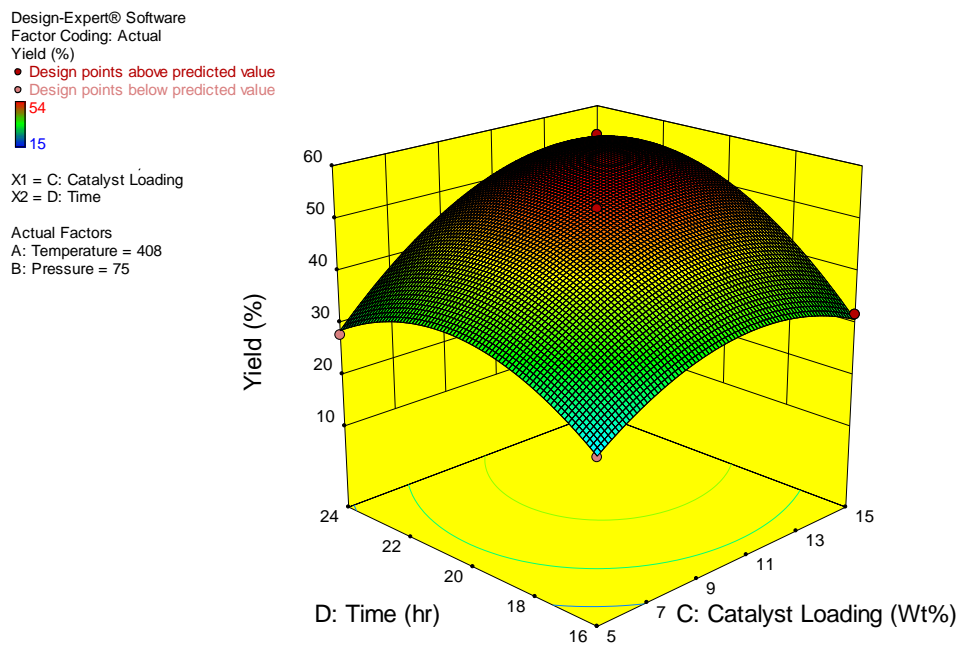


Figure 6- 21. Response surface plot for the effect reaction catalyst loading and reaction time on SC yield.

6.7.4 Multiple responses optimisation

It is relatively simple to determine the optimal conditions for two variables on single response using surface plots, however, this study includes two responses function in four independent variables. The numerical optimisation process of SC synthesis has been performed to conclude the optimal reaction conditions for maximum production of SC. Optimisation step has been carried out using Design-Expert software, which combines the desirability of each process variable into single value then search for optimum values according to the specified responses goals. Accordingly, optimisation goals have been set to maximize both responses while minimising process variables to the lowest acceptable values (Aboelazayem *et al.*, 2018a, 2018b).

The numerical optimisation concluded that 89.5% and 54.7% of SO conversion and SC yield, respectively, could be achieved at optimal reaction conditions of 409 K, 81.2 bar, 10.1% catalyst loading in 20.6 h.

6.7.5 Optimum conditions validation

The predicted optimum conditions have been validated experimentally at 409 K, 81.2 bar, 10.1% catalyst loading and 20.6 h. It has been concluded that SO conversion and SC yield have recorded 89.2% and 54.3%, respectively. These results ensure the validity of the optimisation step with a relative error from the experimental results of 0.335% and 0.731% for SO conversion and SC yield, respectively.

6.8 Conclusions

The synthesis of SC through cycloaddition reaction of CO₂ and SO has been successfully carried out using a high-pressure reactor in the presence of various heterogeneous catalysts without any solvent. Raman spectroscopy, SEM and XRD analysis have been used for catalyst characterization. The effect of various parameters such as the reaction time, reaction temperature, CO₂ pressure, catalyst loading and stirring speed has been studied extensively. Among the used heterogeneous catalysts, the Ce-La-Zr-O catalyst was found to be the best-performed catalyst relative to the other catalysts used in this study. The reaction temperature, pressure, time and catalyst loading have been determined as the

significant variables affecting reaction responses using OFAT method. RSM has been used to develop regression models representing SO conversion and SC yield in the established significant process variables. It has been established that the optimum reaction conditions using OFAT method at 408 K, 75 bar, 10% (w/w) catalyst loading in 20 h reaction time gave a conversion of SO and SC yield of 84% and 52%, respectively. However, using RSM numerical optimisation the optimum conditions have been found to be 409 K, 81.2 bar, 10.1% (w/w) catalyst loading in 20.6 h reaction time and gave SO conversion of 89.5% and SC yield of 54.7%. The predicted optimum conditions have been validated experimentally with 0.335% and 0.731% relative error for both SO conversion and SC yield, respectively. Ce-La-Zr-O catalyst has been recycled easily and reused several times without any reduction in its catalytic performance.

CHAPTER 7

A FACILE AND GREENER SYNTHESIS OF 1,2-BUTYLENE CARBONATE VIA CO₂ UTILISATION USING A NOVEL COPPER–ZIRCONIA OXIDE/GRAPHENE CATALYST

CHAPTER 7: A FACILE AND GREENER SYNTHESIS OF 1,2-BUTYLENE CARBONATE VIA CO₂ UTILISATION USING A NOVEL COPPER–ZIRCONIA OXIDE/GRAPHENE CATALYST

7.1 Introduction

The use of zirconia as one of the mixed metal oxide catalysts offer unique properties such as hardness, good elastic modulus, biocompatibility, high melting temperature, corrosion resistance and high strength. These unique properties make the material useful for advanced ceramics in bio-sensors, abrasives, oxygen sensors, catalyst promoters and supports (Behbahani et al., 2012). Zirconia has a strong ability to interact with active phase, a unique blend of acidic, basic, and redox ability as well as high thermal stability. These qualities favour zirconia to be used as one of the mixed metal oxides. Copper is also an excellent thermal and electrical conductor, which has an invaluable application for industrial manufacturing of electrical products. It has been recognised (Singh *et al.*, 2013) that during the catalysts preparation, surface properties of graphene impacted the interaction between copper, zirconia and graphene leading to higher dispersion of copper, zirconia on tetragonal graphene support (Rahmanto *et al.*, 2002).

Graphene oxide is used as a precursor for synthesising copper, zirconia doped graphene oxide, which is heavily decorated by oxygen-containing groups. These groups not only expand the interlayer distance but also make the atomic-thick layers hydrophilic (Akhavan, 2010). As a result, these oxidised layers can be reduced to graphene-like sheets by removing the oxygen-containing groups through thermal heating. The reduced GO (rGO) sheets are usually considered as one kind of chemically derived graphene. Some other names have also been given to rGO, such as functionalized graphene, chemically modified graphene, thermal vapour chemically converted graphene, or reduced graphene. The exfoliated sheets can be directly named graphene (or chemically derived graphene) rather than GO, which means that the rapid heating process not only exfoliates graphite oxide but also reduces the functionalized graphene sheets by decomposing oxygen-containing groups at elevated temperature (Akhavan, 2010).

It is believed that the thermal reduction of GO was accompanied by the elimination of epoxy and carboxyl groups. In a typical thermogravimetry (TGA) experiment, it is usually found that the GO can be decomposed near 210 °C with a mass loss caused by releasing oxygen from GO (Klinowski et al., 1998). Chua et al. (2008) showed direct evidence of oxygen elimination from GO functionalized with octadecylamine (ODA) by STM studies at 150–200 °C. Wufeng Chen and Lifeng Yan (2010) synthesised graphene from GO by heating its suspension in DMAc/H₂O below 150 °C at atmospheric pressure. Similarly, Zhoa et al. (2016) also showed that graphene oxide start to lose mass upon heating 100 °C, and the major mass loss occurs at below 220 °C. They observed that graphene at ca. 150 °C became fluffy and lost most of oxygen groups during the low-temperature pressure-promoted thermal reduction process, and transformed totally into single and few layered graphene (Shang *et al.*, 2016).

In this work, a new copper, zirconia doped graphene inorganic composite catalysts labelled as Cu-Zr/graphene has been synthesised *via* traditional wet impregnation method. These catalysts have been heat-treated to 573 K (labelled as HTR300), 723 K (labelled as HTR450), and 873 K (labelled as HTR600). The catalytic activities of the HTR450 catalysts have been extensively evaluated using a new facile greener and sustainable process for the synthesis of 1,2-butylene carbonate (BC) in the absence of organic solvent. Various effects of reaction conditions such as catalyst heat-treatment, CO₂ pressure, reaction temperature, catalyst loading and reaction time have been studied thoroughly as well as the reaction conditions optimisation. The catalyst reusability studies have been conducted in order to investigate the long-term stability of the catalyst.

RSM using Box-Behnken Design (BBD) has been used to investigate the effect of process variables and their interactive effect on the response. A quadratic model has been developed representing the interrelationship between process variables and each response. The developed mathematical models have been validated using analysis for variance (ANOVA). The developed optimum conditions have been validated statistically and experimentally.

7.2 Materials

Natural graphite powder (NGP), hydrochloric acid (HCl), sulphuric acid (H₂SO₄), sodium nitrate, potassium hydroxide pellet (KOH), hydrogen peroxide (H₂O₂), acetone (C₃H₆O), octane (C₈H₁₈) and potassium permanganate (KMnO₄) were

purchased from Fisher Scientific UK Ltd. Copper (II) nitrate hydrate ($\text{Cu}(\text{NO}_3)_2 \cdot 2.5\text{H}_2\text{O}$), zirconium (IV) oxynitrate hydrate ($\text{ZrO}(\text{NO}_3)_2 \cdot x\text{H}_2\text{O}$), butylene oxide ($\text{C}_4\text{H}_8\text{O}$), 1,2-butylene carbonate ($\text{C}_5\text{H}_8\text{O}_3$) were purchased from Merck Co. LLC, UK. The liquid CO_2 cylinder (99.9%) equipped with a dip tube was purchased from BOC Ltd., UK. The chemicals were used without any purification or pre-treatment.

7.3. Catalyst preparation and characterisation techniques

An improved Hummer's method has been used to synthesise graphene oxide (GO), which can be found in Chapter 3, section 3.2.1. The prepared GO was used as a precursor for the synthesis of copper, zirconia doped graphene *via* traditional wet impregnation method (see, chapter 3, section 3.2.5.2) and the molar atomic ratio of Cu-Zr: GO used was 1:1. *Figure 7-1* shows the schematic representation of synthesised copper zirconia doped graphene catalyst.

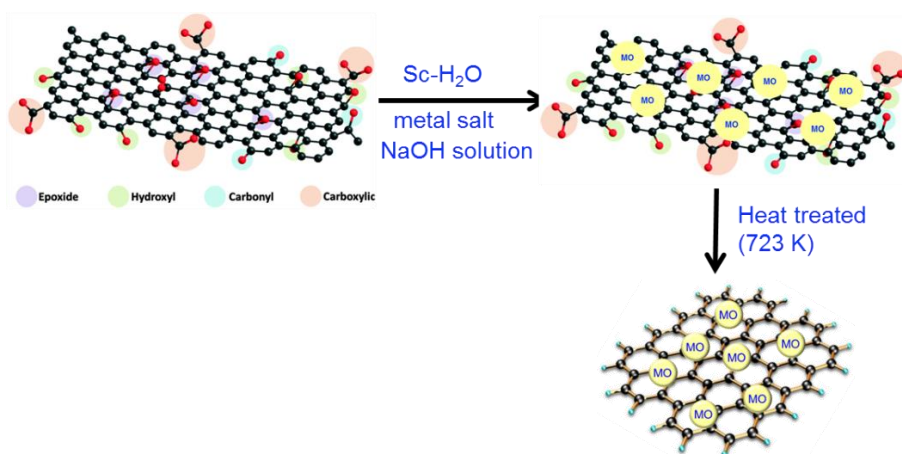


Figure 7- 1. Schematic representation of synthesised copper zirconia doped graphene catalyst (HTR450).

The dried Cu-Zr/GO samples have been heat-treated for 3 h under nitrogen using Carbolite tube furnace at 723 K and 873 K and have been labelled as HTR450 and HTR600, respectively. The photographic image of Cu-Zr/GO, labelled as HTR450 is shown in Chapter 3, *Figure 3- 7*.

7.4 Experimental design

The experimental design has been conducted by using BBD of RSM to design the experiments that have been based on three levels for each process variable. The maximum, minimum and the average range of each variable represent the three levels. Temperature, pressure, catalyst loading and time have been used as the four independent variables for this study and have been coded as A, B, C and D, respectively. Furthermore, this study will show the levels of the independent variables coded as -1, 0 and 1 in *Table 7-1*.

Table 7- 1. Experimental design variables and their coded levels

Factor	Code	Levels		
		-1	0	+1
Temperature (K)	A	373	423	473
Pressure (bar)	B	50	80	110
Catalyst loading (w/w)	C	2.5	7.5	12.5
Time (min)	D	4	12	20

Temperature (A, °C), pressure (B, bar), catalyst loading (C, w/w) and time (D, h) are the analysed variables while the reaction responses include 1,2-butylene carbonate yield (Y_1 , %) and butylene oxide conversion (Y_2 , %). To minimise the effect of inexplicable contradiction in the generated responses twenty-nine runs have been performed in a randomised manner. The experimental results have been described in an improbability matrix shown in *Table 7-2*.

Table 7-2. Experimental design matrix with the actual and predicted responses

Ru n	Temper ature (°C) (B)	Press ure (bar) (C)	Catalyst loading (w/w)	Time (min) (D)	Actual BO Conver sion %	Predicted BO Conversi on %	Actual BC Yield %	Predic ted BC Yield %
2	1	473	50	7.5	12	46	70	2
5	2	423	80	2.5	4	14	55	5
6	3	423	80	12.5	4	20	55	6
9	4	423	80	7.5	12	71	82	9
3	5	373	110	7.5	12	70	90	3
7	6	423	80	2.5	20	45	70	7
10	7	423	80	7.5	12	71	82	10
8	8	423	80	12.5	20	70	87	8
1	9	373	50	7.5	12	41	66	1
4	10	473	110	7.5	12	71	92	4
15	11	423	50	2.5	12	40	68	15
11	12	373	80	7.5	4	19	48	11
18	13	423	110	12.5	12	72	89	18
17	14	423	50	12.5	12	68	84	17
20	15	423	80	7.5	12	71	82	20
14	16	473	80	7.5	20	72	90	14
13	17	373	80	7.5	20	69	85	13
16	18	423	110	2.5	12	52	75	16
19	19	423	80	7.5	12	71	82	19
12	20	473	80	7.5	4	23	60	12
29	21	423	80	7.5	12	71	82	29
28	22	423	110	7.5	20	72	85	28
30	23	423	80	7.5	12	71	82	30
26	24	423	110	7.5	4	22	55	26
25	25	423	50	7.5	4	20	48	25
24	26	473	80	12.5	12	68	90	24
21	27	373	80	2.5	12	43	69	21
27	28	423	50	7.5	20	58	75	27
22	29	473	80	2.5	12	49	74	22
23	30	373	80	12.5	12	64	82	23

Where BO and BC represent butylene oxide and 1,2-butylene carbonate, respectively.

7.5 Statistical analysis

The general quadratic model shown in Equation 7-1 is the mathematical model defined using multiple regression analysis.

$$Y = b_0 + \sum_{i=1}^n b_i x_i + \sum_{i=1}^n b_{ii} x_i^2 + \sum_{i=1}^{n-1} \sum_{j>1}^n b_{ij} x_i x_j + \varepsilon \quad \text{Equation 7- 1}$$

where Y is the predicted response for both BO conversion and BC yield, b_0 model coefficient constant, b_i , b_{ii} , b_{ij} , are coefficients for intercept of linear, quadratic, interactive terms respectively, while x_i , x_j are independent variables ($i \neq j$). A number of independent variables are n and the random error is denoted by ε .

The predicted model adequacy has been checked *via* numerous statistical validations that include the coefficient of correlation (R^2), adjusted coefficient of determination (R^2_{adj}) and the predicted coefficient of determination (R^2_{pred}). The predicted model's statistical significance has been analysed by ANOVA using Fisher's test, of which F-value and p-value, are at 95% confidence interval.

Design Expert 11 software (Stat-Ease Inc., Minneapolis, MN, USA) has been used to execute the initial experimental design, model prediction, statistical analysis and optimisation.

7.6 Results and discussion

7.6.1 Catalyst characterisation

Transmission Electron Microscopy (TEM) images of as-prepared and heat-treated materials are shown in *Figures 7-2 to 7-4* and the TEM mean particle size values are given in *Table 7-3*. TEM image of Cu-Zr/GO synthesised using traditional wet impregnation method (labelled as AP) revealed uniform particles exhibiting a mean particle size of 6.71 ± 1.12 nm (*Figure 7-2*). The TEM images for the corresponding heat-treated sample at 723 K (labelled as HTR450) and heat-treated sample at 873 K (labelled as HTR 600) showed an increase in particle size with a mean size of 6.92 ± 1.32 nm (*Figure 7-3*) and 7.81 ± 1.57 nm (*Figure 7-4*) respectively.

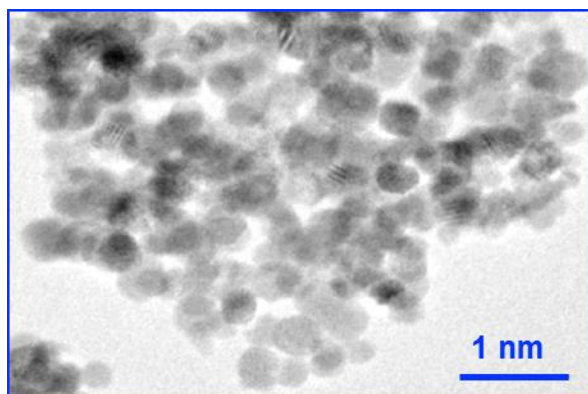


Figure 7- 2. Transmission Electron Microscopy (TEM) image of Cu-Zr/graphene nanocomposite catalyst as-prepared labelled as AP

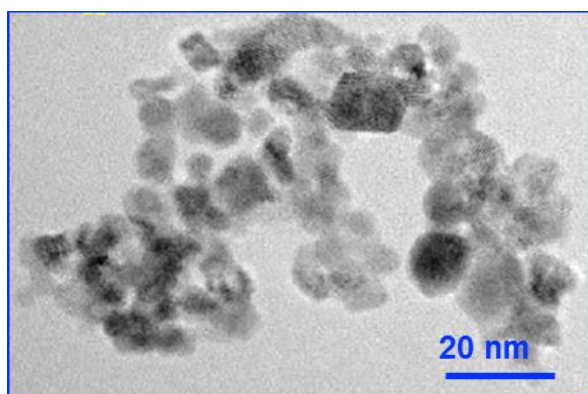


Figure 7- 3. Transmission Electron Microscopy (TEM) image of Cu-Zr/graphene nanocomposite catalyst heat-treated (723 K) sample labelled as HTR450.

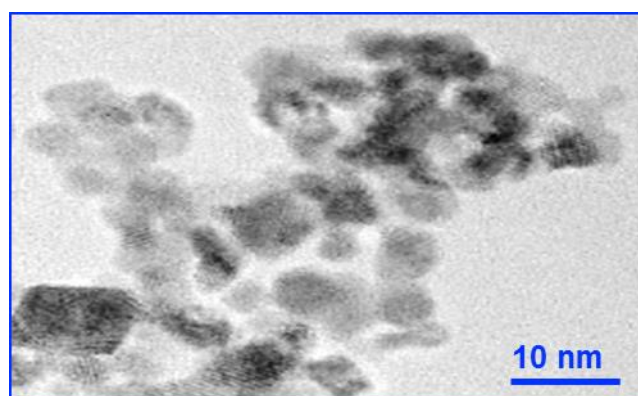


Figure 7- 4. Transmission Electron Microscopy (TEM) image of Cu-Zr/graphene nanocomposite catalyst heat-treated (873 K) sample labelled as HTR600.

The crystallinity of the synthesised and heat treated Cu-Zr/graphene nanocomposite catalysts have been assessed by X-ray powder diffraction (XRD) (see *Figure 7-5*). The XRD pattern for sample synthesised via traditional wet impregnation (HTR450 sample) gave very broad peaks corresponding to the fluorite structure, suggesting the formation of the solid solution. It has been reported that as the zirconium concentration in the solid solutions increases, the positions of the CuO diffraction peaks shift to higher 2θ values, corresponding to a decrease in the lattice parameter. The observed lattice cell shrinkage is caused by the insertion of Zr^{4+} ions into Cu^{2+} lattice (Liang *et al.*, 2008; Valefi *et al.*, 2012). Although, it is too hard to distinguish tetragonal from cubic of as AP and HTR450 because both have almost the same XRD patterns. Although appearance of peaks around 29° , 39° and 58° at upper temperatures can prove these patterns belong to tetragonal phase. As the calcinations temperature increases from 450 to 650 $^\circ\text{C}$, monoclinic phase was also detected and begins to increase. Furthermore, there is a noticeable change in the pattern for the corresponding heat treated sample (HTR600) indicating that at higher temperature beyond 450 $^\circ\text{C}$, we can, therefore, speculate there is a chance of reduced thermal stability and homogeneity of the compound synthesised.

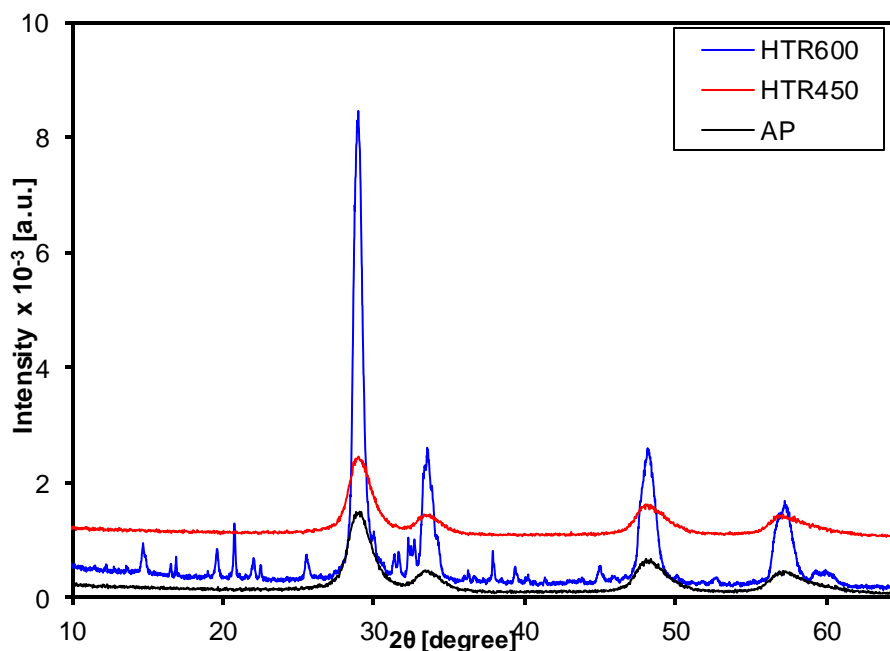


Figure 7- 5. X-ray diffraction (XRD) patterns of copper- zirconia/graphene nanocomposite catalysts (AP, HTR450 and HTR600).

Appendix C- 1 to Appendix C- 3 show the XPS spectra of the catalysts. C 1s of GO is severely changed by the decorative effect of Cu-Zr-O mixed metal oxide as shown in *Appendix C- 1*. The peaks of Cu 2p appear at 912.8 and 932.6 eV. Owing to a minor difference in binding energy between Cu and Cu⁺ and the trace amounts of Cu, resolution between two states is uncertain. Then, they were treated as Cu 2p_{3/2} and Cu 2p_{1/2} originating from Cu⁰ are observed in samples labelled as AP, HTR450 and HTR600 as shown in *Appendix C- 2* (Hiromoto *et al.*, 2000; Kawashima *et al.*, 2011). Zirconium, on heat-treatment forms two states. XPS spectrum of the core level of Zr 3d (*Appendix C- 3*) has a strong spin-orbit doublet due to Zr 3d_{5/2} at 182.2 eV and Zr 3d_{3/2} at 183.7 eV with spin-orbit separation of 2.4 eV, which shows an excellent agreement with the reported literature values (Huang *et al.*, 2010) and characteristic of Zr⁴⁺ ions in full oxidation states. In contrast, the reported value for Zr 3d 5/2 for zirconia is 182.2 eV (Huang *et al.*, 2010).

7.6.2 Model development

The response for randomised experiments in terms of BO conversion and BC yield have been reported as shown in *Table 7-2*. It has been observed from the experimental results that BO conversion ranges from 48 to 92%, while BC yield ranges from 14 to 72%. Multiple regression analysis of the experimental data has been performed using Design Expert software. The software has fitted four models for each response i.e. linear, two factors interactions (2FI), quadratic and cubic polynomials. Amongst the predicted fitted models for each response, the model with highest fitting has been chosen based on several statistical validations. It has been observed that the experimental data of both responses are highly fitting with the quadratic polynomial models. Accordingly, two quadratic models have been developed representing the empirical relationship between process responses (BC yield and BO conversion) and reaction variables as shown in *Equations 7-2 and 7-3*.

It has generated two polynomial regression equations for each response variable representing an empirical relationship between reaction variables and each response variable as shown in *Equations 7-2 and 7-3*.

$$Y1 = 82 + 3A + 6.25B + 6.33C + 14.25D - 0.5AB + 0.75AC - 1.75AD - 0.5BC + 0.75BD + 4.25CD + 0.08A^2 - 2.29B^2 - 2.17C^2 - 12.79D^2 \quad \text{Equation 7-2}$$

$$Y2 = 71 + 1.92A + 7.17B + 9.92C + 22.33D - 1AB - 0.5AC - 0.25AD - 2BC + 3BD + 4.75CD - 5.63A^2 - 6B^2 - 9.38C^2 - 22D^2 \quad \text{Equation 7-3}$$

Where, $Y1$ and $Y2$ represent response variables including BO conversion and BC yield, respectively. While A , B , C , and D represent the independent variables i.e. temperature, pressure, catalyst loading and time, respectively. Further, AB , AC , AD , BC , BD and CD represent the interaction between independent variables. Finally, A^2 , B^2 , C^2 and D^2 represent the excess of each independent variable.

The developed models have demonstrated the effect of each independent variable, variables interactions and excess of each variable on the response. The positive sign of each variable coefficient represents the synergetic effect of the variable on the response, however, the negative sign represents the antagonistic effect on the response.

7.6.3 Models adequacy checking

The models have been examined for adequacy to inspect the fitting accuracy of the predicted results with the experimental results. Different statistical validation techniques have been applied to investigate the accuracy of the predicted models. The significance of the predicted models and the independent variables have been examined using ANOVA at 95% confidence level as shown in *Tables 7-3 and 7-4*. The main test that could examine the significance of the model and the variables is the p-value, where the value smaller than 0.05 of this test indicates the significance of the examined parameter.

Table 7- 3. Analysis of variance of developed model for BO conversion

Source	Sum of Squares	df	Mean Square	F-value	p-value	Significance
Model	4738.72	14	338.48	16.55	< 0.0001	HS
A-Temperature	108.00	1	108.00	5.28	0.0388	HS
B-Pressure	468.75	1	468.75	22.92	0.0004	HS
C-Catalyst loading	481.33	1	481.33	23.53	0.0003	HS
D-Time	2436.75	1	2436.75	119.14	< 0.0001	HS
AB	1.0000	1	1.0000	0.0489	0.0284	S
AC	2.25	1	2.25	0.1100	0.0454	S
AD	12.25	1	12.25	0.5989	0.0528	NS
BC	1.0000	1	1.0000	0.0489	0.8284	NS
BD	2.25	1	2.25	0.1100	0.7454	NS
CD	72.25	1	72.25	3.53	0.0828	NS
A ²	0.0476	1	0.0476	0.0023	0.9622	NS
B ²	36.01	1	36.01	1.76	0.2074	NS
C ²	32.19	1	32.19	1.57	0.2317	NS
D ²	1122.01	1	1122.01	54.86	< 0.0001	HS
Residual	265.88	13	20.45			
Lack of Fit	265.88	10	26.59			
Pure Error	0.0000	3	0.0000			
Cor Total	5027.47	29				

The Model F-value of 16.55 implies the model is significant. There is only a 0.01% chance that an F-value this large could occur due to noise. P-values less than 0.0500 indicate model terms are significant. In this case, A, B, C, D, D² are significant model terms. Values greater than 0.1000 indicate the model terms are not significant. If there are many insignificant model terms (not counting those required to support hierarchy), the model reduction may improve the model.

Table 7- 4. Analysis of variance of developed model for BC yield

Source	Sum Squares	of df	Mean Square	F-value	p-value	Significant
Model	11610.38	14	829.31	31.88	< 0.0001	HS
A-Temperature	44.08	1	44.08	1.69	0.0156	HS
B-Pressure	616.33	1	616.33	23.69	0.0003	HS
C-Catalyst loading	1180.08	1	1180.08	45.36	< 0.0001	HS
D-Time	5985.33	1	5985.33	230.06	< 0.0001	HS
AB	4.00	1	4.00	0.1537	0.0013	HS
AC	1.0000	1	1.0000	0.0384	0.8476	NS
AD	0.2500	1	0.2500	0.0096	0.9234	NS
BC	16.00	1	16.00	0.6150	0.4470	NS
BD	36.00	1	36.00	1.38	0.2606	NS
CD	90.25	1	90.25	3.47	0.0853	NS
A ²	216.96	1	216.96	8.34	0.0127	S
B ²	246.86	1	246.86	9.49	0.0088	HS
C ²	602.68	1	602.68	23.17	0.0003	HS
D ²	3318.86	1	3318.86	127.57	< 0.0001	HS
Residual	338.22	13	26.02			
Lack of Fit	338.22	10	33.82			
Pure Error	0.0000	3	0.0000			
Cor Total	12020.80	29				

Where HS, S and NS represent highly significance, significance and non-significance.

As shown in Tables 7-3 and 7-4, both developed models are highly significant with a p-value of < 0.0001. In addition, the lack of fit analysis, which indicates the failure of the model in fitting the experimental data showed the non-significant result. This illustrates the accuracy of the models in predicting the experimental results. In addition, the values of R², adjusted R², predicted R² have been evaluated for BC yield model as 0.95, 0.89 and 0.57, respectively. The value of adequacy precision, which indicates the ratio between the predicted response and the relative error (signal to noise ratio) has been assessed for both models.

7.6.4 Model validation

The analysis of variance (ANOVA) test results indicates that the model developed is appropriate to define the correlations and interactions of different variables on BO conversion and BC yield. *Figure 7-6* illustrate the experimental vs predicted BO conversion and show that the predicted data are in good agreement with the experimental data elucidating the accuracy and adequacy of the model. Similarly, *Figure 7-7* shows that the BC yield predicted data are also in good agreement with the experimental data of BC yield obtained. Therefore, Response Surface Methodology (RSM) *via* Box-Behnken design (BBD) was used to predict the effect of various reaction parameters on BC synthesis from direct reaction of BO and CO₂ (see *Figures 7-10 to 7-13*).

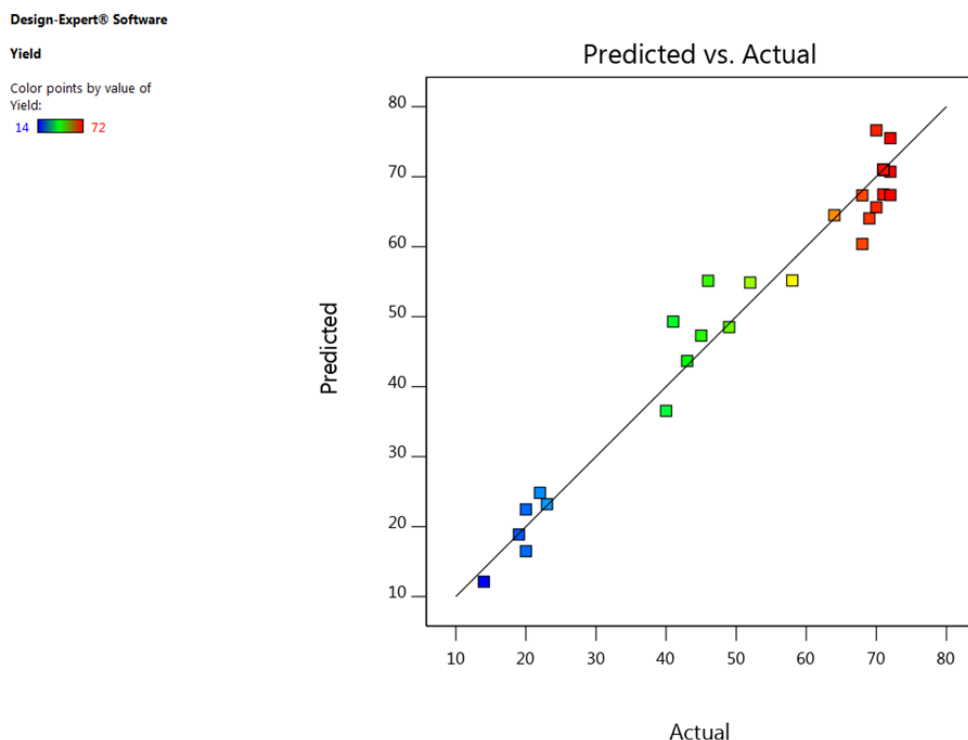


Figure 7- 6. Actual experimental data versus predicted values for BC yield.

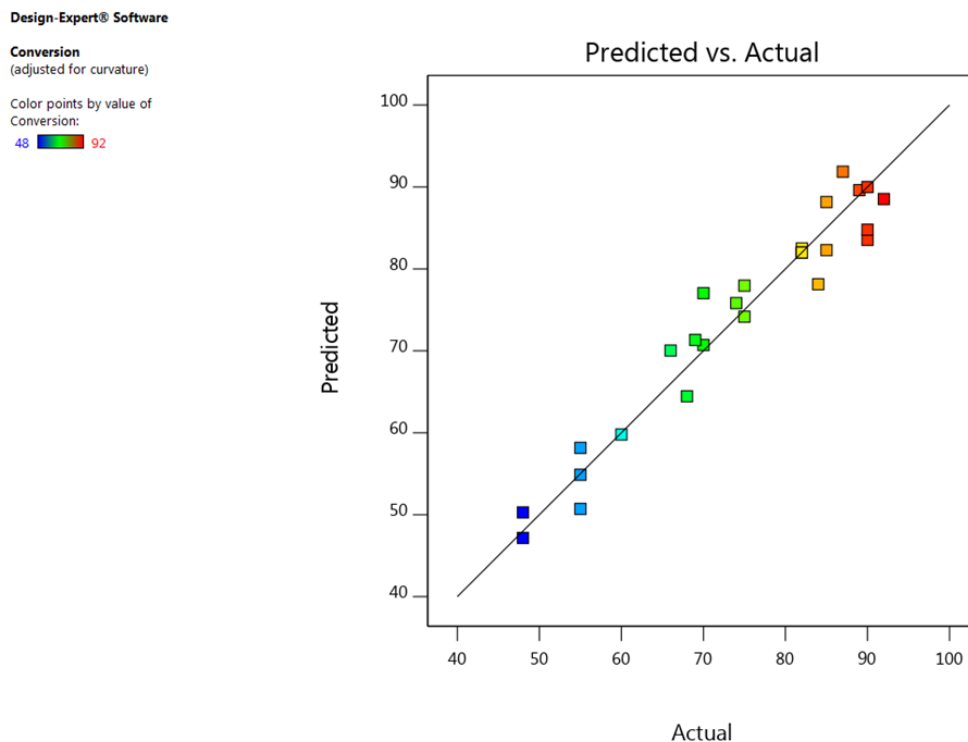


Figure 7-7. Actual experimental data versus predicted values for BO conversion.

7.6.5 Batch experimental results

A facile reaction of BO and CO₂ for the synthesis of BC were carried out at different reaction conditions in a high-pressure reactor in the presence of Cu-Zr/GO inorganic composite catalysts. The effect of mass transfer, catalyst loading, reaction temperature, reaction time, CO₂ pressure on BC yield and BO conversion were carried out using OFAT analysis. Catalyst reusability studies were investigated to examine the long-term stability of Cu-Zr/GO inorganic composite catalyst on the synthesis of BC.

7.6.5.1 Effect of different heterogeneous catalysts

Several heterogeneous catalysts performances were assessed for a greener synthesis of BC from a facile reaction of BO and CO₂ as shown in Figure 7-8. The reaction conditions of 423 K, 80 bar, 7.5% (w/w) catalyst loading in 12 h were set for the experiments using different catalysts. The synthesised catalysts graphene, copper doped zirconia (Cu-ZrO), copper, zirconia doped graphene (Cu-Zr/GO) as prepared and heat treated samples labeled as HTR300, HTR 450 and HTR600 were investigated in order identify the best performing catalyst.

The use of pure mixed metal oxide of Cu-ZrO was used to catalyse a facile reaction of BO and CO₂, and BO conversion and BC yield were 72% and 48.9%, respectively. The use of graphene oxide as a supported catalyst in the formation of Cu-Zr/GO inorganic composite resulted in high catalytic performance of BO conversion of 80.2% and BC yield of 58.1%. The transformation in the catalytic performance between Cu-ZrO and Cu-Zr/GO can be attributed to the phase composition and crystallinity of the catalyst combined with the amazing quality of graphene that improves the acid/basic groups and presence of residual, which can provide supplementary active catalytic sites (Adeleye et al., 2014). The use of heat treatment of catalyst in catalytic industry is to promote catalytic performance, which could be as a result of removing any undesirable impurities resulting from the catalyst after preparation, allowing a uniform dispersion and stable distribution of the metal on the support, improving the morphology of the catalyst, and hence to improve the electrocatalytic activity of the catalysts. Cu-Zr/GO catalyst (AP) was prepared by traditional wet impregnation method and heat treated at a different temperature starting from 573 K– 873 K. Further heat treatment was conducted on AP in order to enhance catalytic activity. It has been established from several studies that graphene oxide becomes graphene at higher temperature above 200 °C (Jeong et al., 2009; Cote et al., 2012; Pei and Cheng, 2012). The heat treated catalysts were assessed at the same reaction condition as AP, HTR300, HTR450 and HTR600 showed a significant increase in both BO conversion and BC yield with error percentage $\pm 3\%$. However, HTR450 and HTR600 showed a similar improvement of BO conversion of 82% and BC yield of 71%. Hence from an energy efficiency point of view, there is no further need to conduct further heat treatment beyond 723 K as an increase in BC yield is not sufficient to carry out the heat treatment. Hence, for this study, HTR450 Cu-Zr/GO was found to be the best performing catalyst for BC synthesis and subsequently used to conduct further studies.

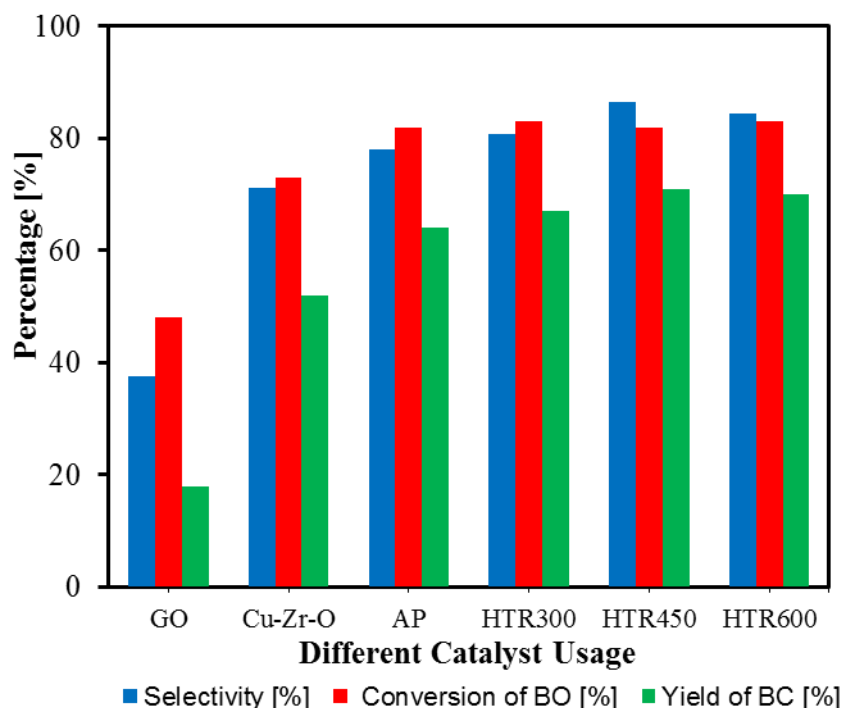


Figure 7- 8. Effect of different heterogeneous catalysts for BC synthesis. Experimental conditions: catalyst loading, 7.5% (w/w); reaction temperature, 423 K; CO₂ pressure, 80 bar; reaction time, 12 h and stirring speed, 200 rpm.

7.6.5.2 Effect of external mass transfer

The study of mass transfer resistance effect on the direct synthesis of BC from the facile reaction of BO and CO₂ is vital in order to establish the factor influencing the rate of chemical reaction toward achieving the desired product. This was investigated in a high-pressure reactor at a different stirring speed of 200 rpm – 600 rpm at reaction conditions of 423 K, 80 bar, 7.5% (w/w) catalyst loading and 12 h. It was observed in *Figure 7-9* there was no significant change in BO conversion and BC yield as the stirring speed was increased from 200 – 600 rpm. This could be attributed to the uniformity of particle size, which is fairly small and porous and that eliminates the internal mass transfer resistance (which is also in agreement with Adeleye et al., 2014). There is no presence of external mass transfer resistance and it could be concluded that 200 rpm is good enough for a homogenous distribution of HTR450 (Cu–Zr/GO inorganic composite catalyst).

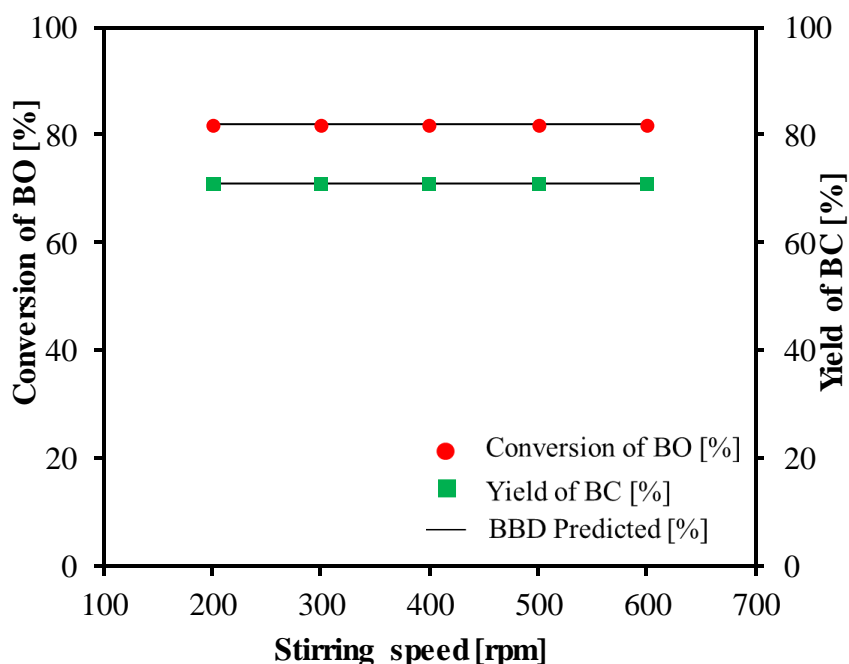


Figure 7- 9. Effect of external mass transfer on BO conversion and BC yield. Experimental conditions: catalyst loading, 7.5% (w/w); reaction temperature, 423 K; CO₂ pressure, 80 bar; and reaction time, 12 h

7.6.5.3 Effect of reaction time

The effect of reaction time was conducted using HTR450 (Cu-Zr/GO) at a different time from 8 - 20 h in order to investigate the effect of time on BC synthesis. This experiment was conducted in a high-pressure reactor at the reaction conditions of stirring speed of 200 rpm, 80 bar of CO₂ pressure, a reaction temperature of 423 K and 7.5% (w/w) catalyst loading. The results are presented in *Figure 7-10* as the reaction proceeds at a low reaction time of 8 h, BO conversion of 68% and BC yield of 48% was achieved. There was a notable change as the reaction time was increased from 8 h to 12 h with the BO conversion of 82% and BC yield of 71% but further increase in reaction time (14 - 20 h) shows no notable change rather a slight drop in the BC yield indicating that equilibrium is achieved at 12 h and beyond the reaction time of 12 h, it would not be beneficial for this reactive system. Hence, based on this study, it can be concluded that optimum reaction time is 12 h and all further investigations were carried out at 12 h reaction time.

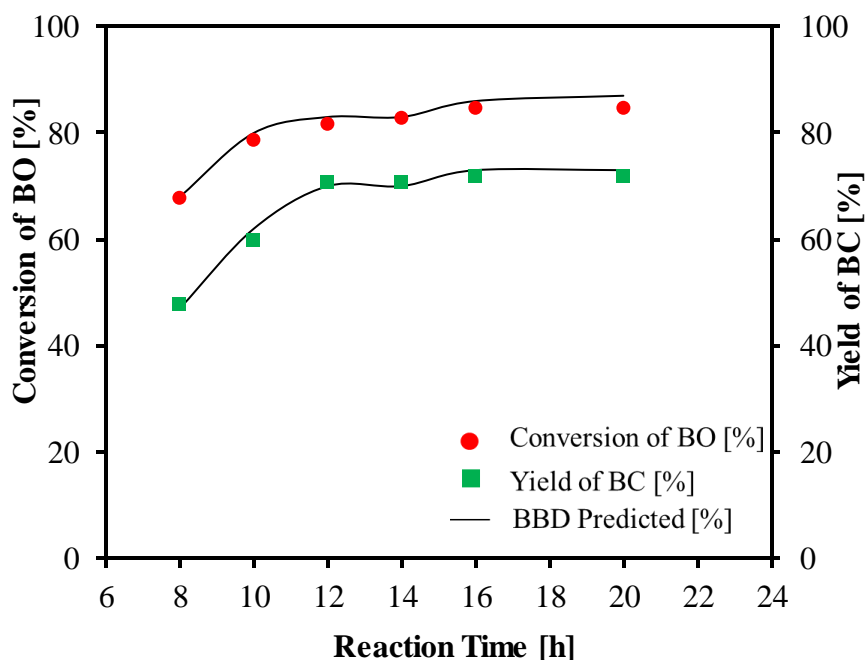


Figure 7- 10. Effect of reaction time on BO conversion and BC yield. Experimental conditions: catalyst loading, 7.5% (w/w); reaction temperature, 423 K; CO₂ pressure, 80 bar; and stirring speed, 200 rpm.

7.6.5.4 Effect of catalyst loading

The catalyst loading is the percentage ratio of the mass of the catalyst to the mass of the limiting reactant (BO). The effect of catalyst loading for the direct synthesis of BC was studied using different amount of HTR450 of Cu-Zr/GO from 2.5% (w/w) to 15% (w/w) at the reaction conditions of stirring speed of 200 rpm, 80 bar of CO₂ pressure, and reaction temperature of 423 K for 12 h. It can be seen in *Figure 7-11* that an increase in the catalyst loading increases the BO conversion and BC yield. For reactions carried out using 2.5% (w/w) catalyst loading, BO conversion and BC yield were 33% and 18%, respectively. Further increase in the conversion of BO of 82% and BC yield of 71% were achieved at 7.5% (w/w) catalyst loading with an experimental error percentage of $\pm 3\%$. Once the catalyst loading was further increased beyond 7.5% (w/w), there was a significant drop of BC yield and the conversion of BO improved. Hence, it appears that the number of active sites for BC synthesis from BO and CO₂ was high enough at 7.5% (w/w) catalyst loading. Therefore, it was not compulsory to increase the catalyst loading above 7.5% (w/w). Based on this study, 7.5% (w/w)

of HTR450 of Cu-Zr/GO was chosen as an optimum, and all subsequent experiments were conducted at a catalyst loading of 7.5%.

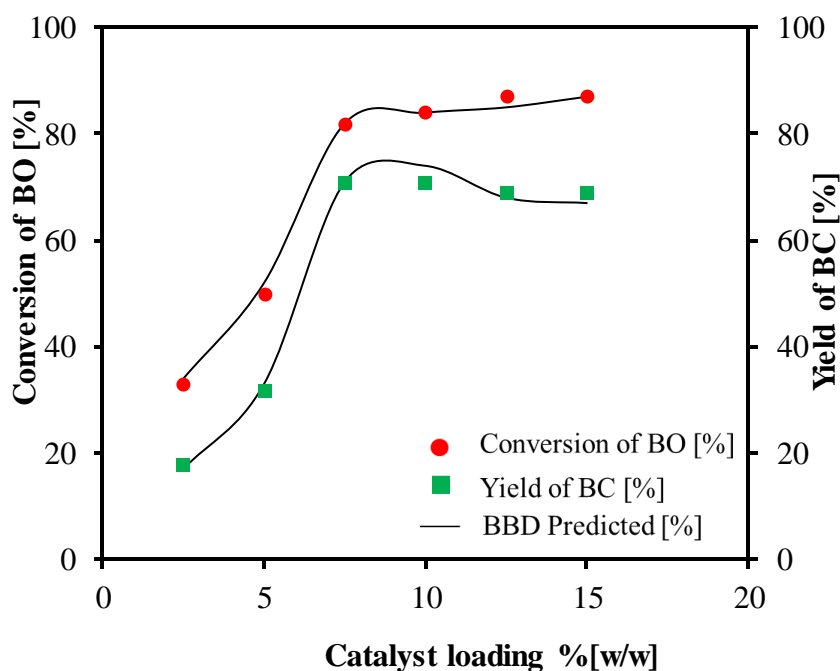


Figure 7- 11. Effect of catalyst loading on BO conversion and BC yield. Experimental conditions: reaction time, 12 h; reaction temperature, 423 K; CO₂ pressure, 80 bar; and stirring speed, 200 rpm.

7.6.5.5 Effect of Reaction Temperature

A series of facile reactions of BO and CO₂ were carried out within a range of 363 K and 483 K to exhaustively examine the effect of reaction temperature on BC synthesis. The experiments conducted were based on the following reaction conditions of 7.5% catalyst loading, 80 bar CO₂ pressure for 12 h. Figure 7-12 shows the effect of the reaction temperature on the BO conversion and BC yield. Figure 7-12 further revealed the pronounced effect of the reaction temperature on the efficiency of the synthesis of BC. It was noticeable that there was a significant increase in BO conversion and BC yield as the reaction temperature was increased from 363 K to 423 K. As the reaction temperature increased from 423 K to 433 K, the BC yield of 71% was constant and beginning to drop to 67%

when the reaction temperature was further increased to 483 K. The drop of BC yield could be attributed to equilibrium nature of the facile reaction, where a higher reaction temperature could shift the equilibrium to the reactant side and leads to a reduction of BC yield (Saada et al., 2018). Similarly, the case was not so for conversion of BO rather from reaction temperature of 423 K to 473K there was a steady increase in BO conversion of 60% to 90%. However, the increase of reaction temperature from 473 K to 483 K showed that BO conversion was constant. This shows that a further increase in reaction temperature will not have an effect on the BO conversion. Therefore, it can be concluded that 423 K is the optimum temperature for the reaction at constant parameters of 7.5 % catalyst loading, 80 bar, and 12 h.

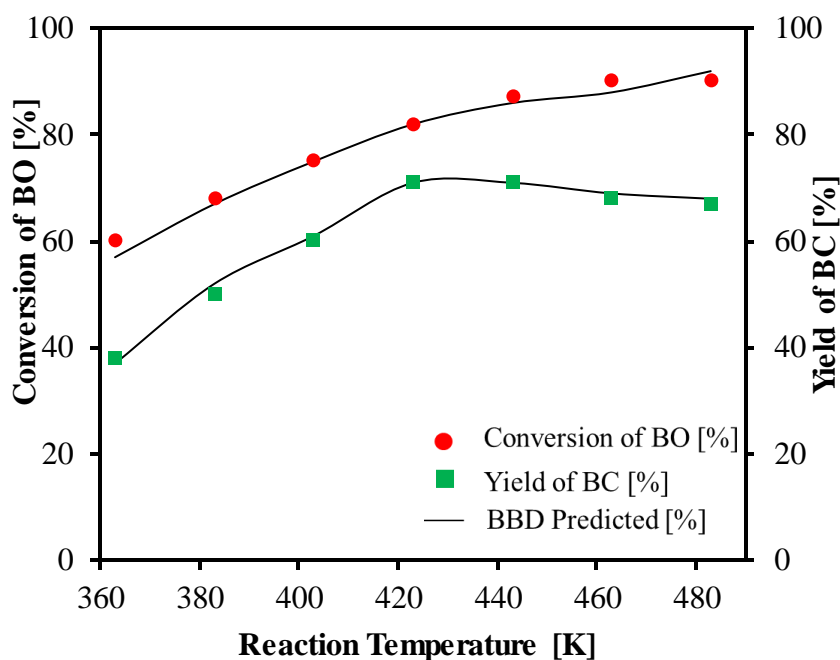


Figure 7- 12. Effect of reaction temperature on BO conversion and BC yield. Experimental conditions: reaction time, 12 h; catalyst loading, 7.5% (w/w); CO₂ pressure, 80 bar; and stirring speed, 200 rpm.

7.6.5.6 Effect of CO₂ pressure

The CO₂ pressure is one of the vital reaction parameters for direct reaction of BO and CO₂ and plays a very significant role. The use of supercritical state CO₂ in a reaction can eliminate the thermodynamic limitation and improve the mass transfer. The effect of CO₂ pressure on BO conversion and BC yield was studied

in order to examine the optimum CO₂ pressure for the facile reaction of BO and CO₂. A high-pressure reactor was used to conduct experiments at 423 K within a different pressure ranging from 60–110 bar for 12 h and results are shown in *Figure 7-13*. As it was expected, in *Figure 7.13* that an increase in CO₂ pressure increases BO conversion and the yield of BC. At a CO₂ pressure of 60 bar, BO conversion and BC yield were 71% and 48%, respectively. CO₂ pressure was further increased to 80 bar, BO conversion and BC yield increased to 71% and 82%, respectively. It can be observed that there was a significant increase in BO conversion but no significant increase in BC yield when CO₂ pressure was beyond 80 bar, but a drop of BC yield as seen in *Figure 7-13*. The reason for such outcomes might be the formation of by-products such as oligomers and isomers (*Appendix 1- 3*), which were out of the detection limit of GC-FID. Thus, it can be concluded that the optimum CO₂ pressure is 80 bar for this study.

This study validates that CO₂ pressure at supercritical conditions increases BO conversion, which was a result of an improvement of the physical properties that include solubility and polarity at supercritical conditions. Cao et al. (2002), highlighted that the use of supercritical CO₂ has a positive effect for CO₂ molecule in catalytic reactions to be activated to a greater extent. Saada et al. (2018), also reported that the use of supercritical CO₂ helps to enhancement of reaction rates and catalyst reusability in heterogeneous catalysis. Furthermore, it assists to limit mass and heat transfer limitation and also avoid catalyst poisoning and coke formation.

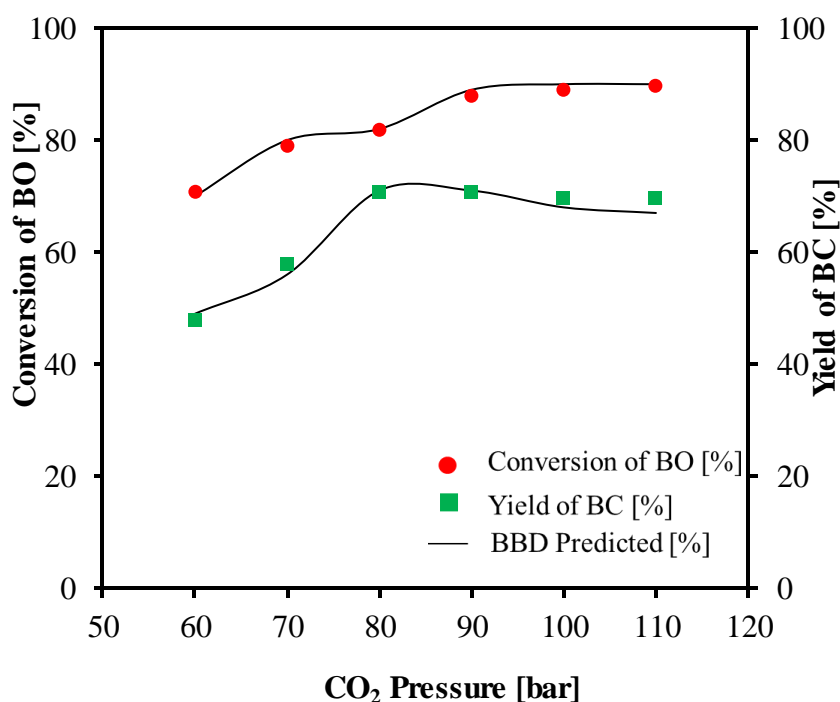


Figure 7- 13. Effect of CO₂ pressure on BO conversion and BC yield. Experimental conditions: reaction time, 12 h; reaction temperature, 423 K; catalyst loading, 7.5% (w/w); and stirring speed, 200 rpm.

7.6.5.7 Catalyst reusability studies

One of the most fundamental properties of an industrial catalyst is the ability to resist attrition, regenerate without deactivation and long-term stability. The catalyst reusability studies were conducted to investigate the long-term stability of HTR450 (Cu-Zr/GO) catalyst for facile synthesis of BC. The experiments were carried out in a high-pressure reactor using a 7.5% (w/w) fresh catalyst, at a reaction temperature of 423 K, CO₂ pressure of 80 bar, stirring speed of 200 rpm and reaction time of 12 h. This was plotted as Run1 (shown in *Figure 7.14*) and the catalyst was separated from the reaction mixture *via* filtration, washed with acetone and dried in an oven at 323 K for 12 h. The dried catalyst was reused for Run 2 with the same procedure used for Run 1, which was also repeated for subsequent runs (Run 3 – Run 6). *Figure 7.14* shows that there was no notable change in BO conversion, BC selectivity and yield after several runs with an experimental error of ($\pm 3\%$) (*Appendix A- 3*). Hence, It can be concluded that copper, zirconia doped graphene (HTR-450) catalyst has exhibited excellent

reusability and stability for BC synthesis. The catalyst can be reused many times without any significant loss in its catalytic performance.

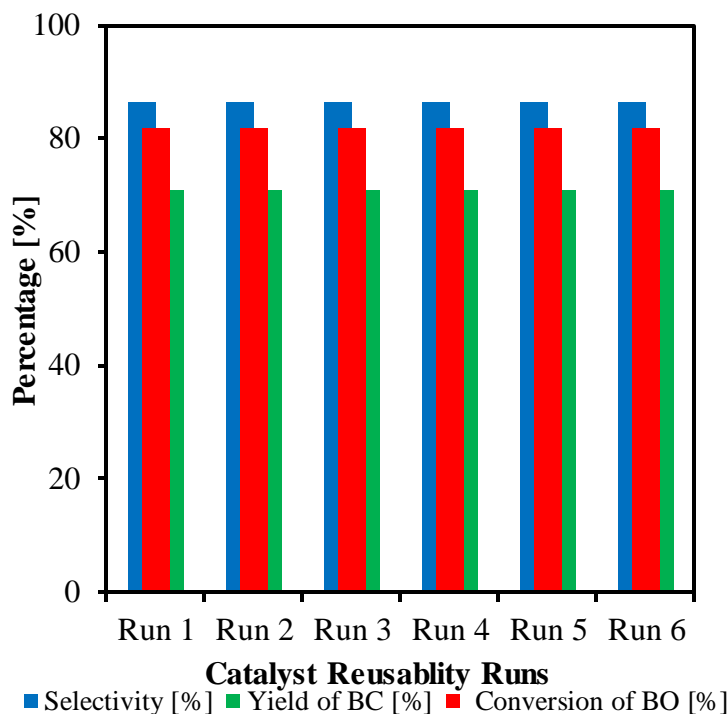


Figure 7- 14. Effect of catalyst reusability studies on BO conversion and BC yield. Experimental conditions: reaction time, 12 h; reaction temperature, 423 K; CO₂ pressure, 80 bar; catalyst loading 7.5% (w/w) and stirring speed, 200 rpm.

7.7 Optimisation of BO conversion, BC yield and Validation.

In this study, the numerical optimisation of BO conversion and BC yield has been concluded using BBD of RSM that involves two responses function in four independent variables in order to achieve the optimum reaction parameters for BC synthesis. The batch studies using OFAT analysis showed that reaction condition of 423 K, 80 bar, 200 rpm and 12 h using 7.5% (w/w) Cu-Zr/GO accomplishes a BO conversion and BC yield of 82% and 71% respectively. The desired target was to maximise the yield of BC and BO conversion with minimising reaction parameters used in the regression model.

The achieved maximum predicted responses of BC yield and BO conversion by BBD model is ~74.6% and ~90.9% respectively at 423 K, 80 bar, 9.8% (w/w) catalyst loading for 14. 2 h. These predicted results were validated experimentally

with the predicted reaction parameters and obtained BC yield of ~74.04% and BO conversion of ~88.9% within an experimental error $\pm 3\%$. RSM *via* BBD used to investigate the interaction between independent variables on the responses that show the effect of factors interaction on the desired response. This is presented in *Figures 7-15 to 7-18*.

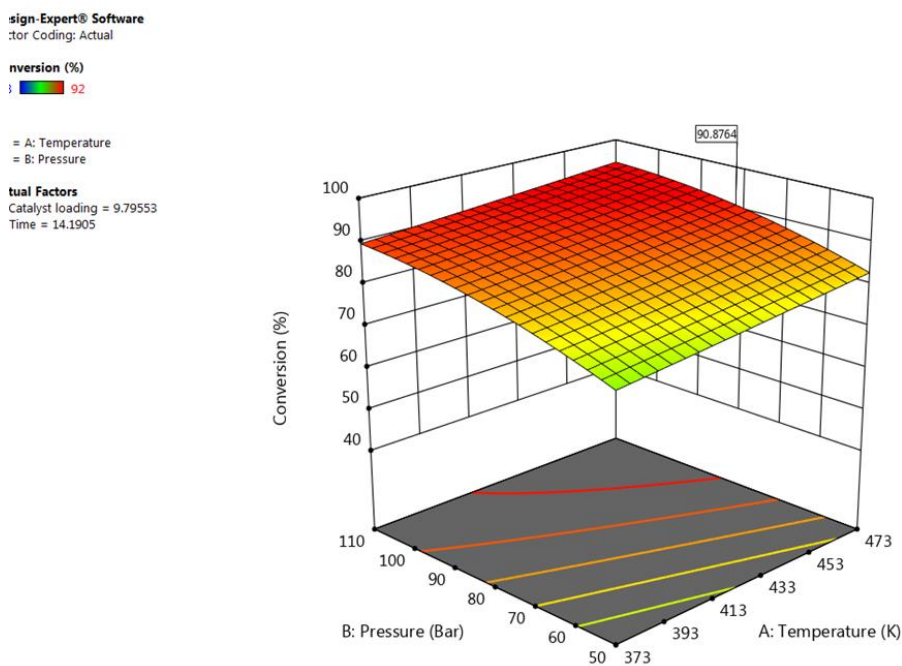


Figure 7- 15. Response surface plot for the effect of CO₂ pressure and reaction temperature on BO conversion after optimisation.

Figure 7- 15 shows the response surface plot for the effect of CO₂ pressure and reaction temperature on BO conversion after optimisation. It can be observed that BO conversion increases as reaction temperature increase with respect to CO₂ pressure. The interaction of reaction temperature and CO₂ pressure on conversion shows that both are significant, which further strengthen the accuracy of the results obtained experimentally. Similarly, the interaction of CO₂ pressure and reaction temperature on BC yield in *Figure 7- 16* show that BC yield increases as both reaction temperature and CO₂ pressure increases but there is a notable observation that CO₂ pressure increased beyond 80 bar there is no or little effect on the yield. This is as a result of the active site of the catalyst not sufficient for the use of more CO₂ pressure, which confirmed the accuracy of the experimental results.

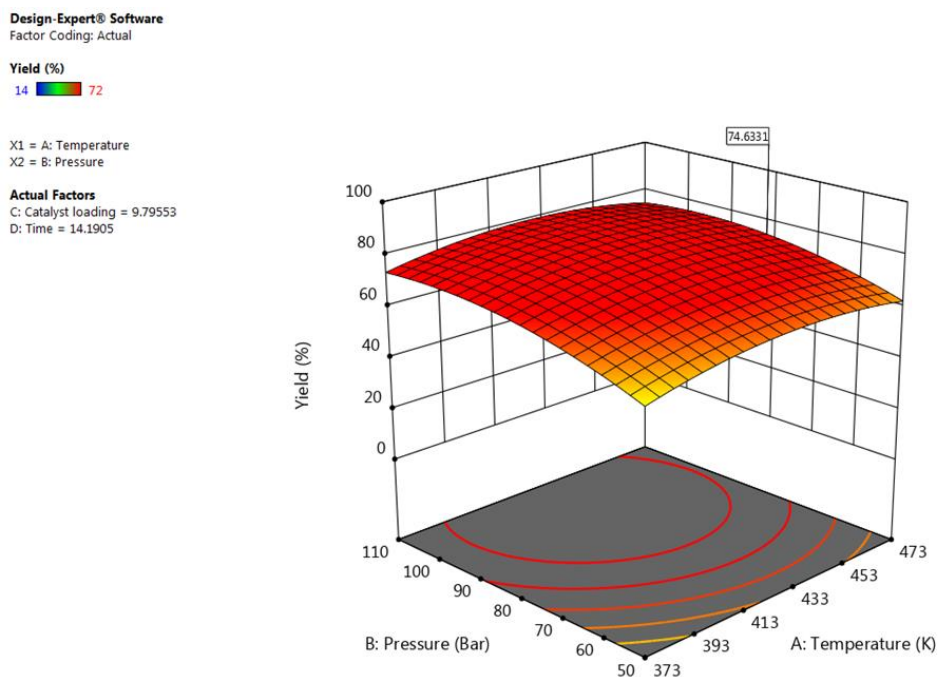


Figure 7- 16. Response surface plot for the effect CO_2 pressure and reaction temperature on BC yield after optimisation.

Figure 7-17 shows the response surface plot for the effect of reaction time and reaction catalyst loading on BO conversion after optimisation at optimum conditions. It can be seen that increasing the reaction time and catalyst loading increases the BO conversion, similarly for BC yield (see Figure 7-18), beyond 10% (w/w) catalyst loading there was a rapid drop in BC yield. However, the reaction time shows a slight change of 1.03% improvement on BC yield as the reaction time is increased to 20 h would not be beneficial for this reactive system.

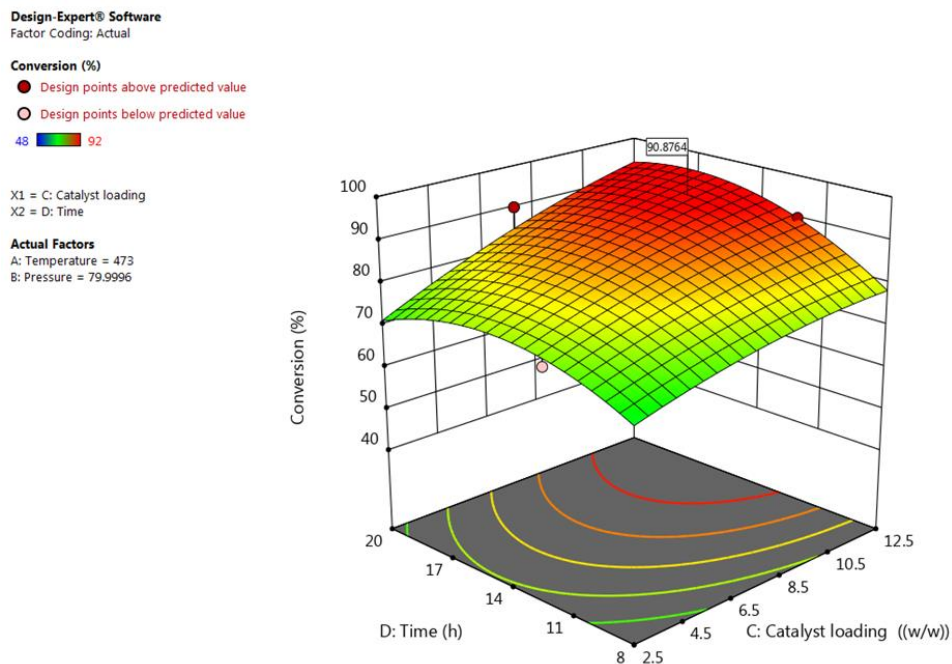


Figure 7- 17. Response surface plot for the effect reaction time and reaction catalyst loading on BO conversion after optimisation.

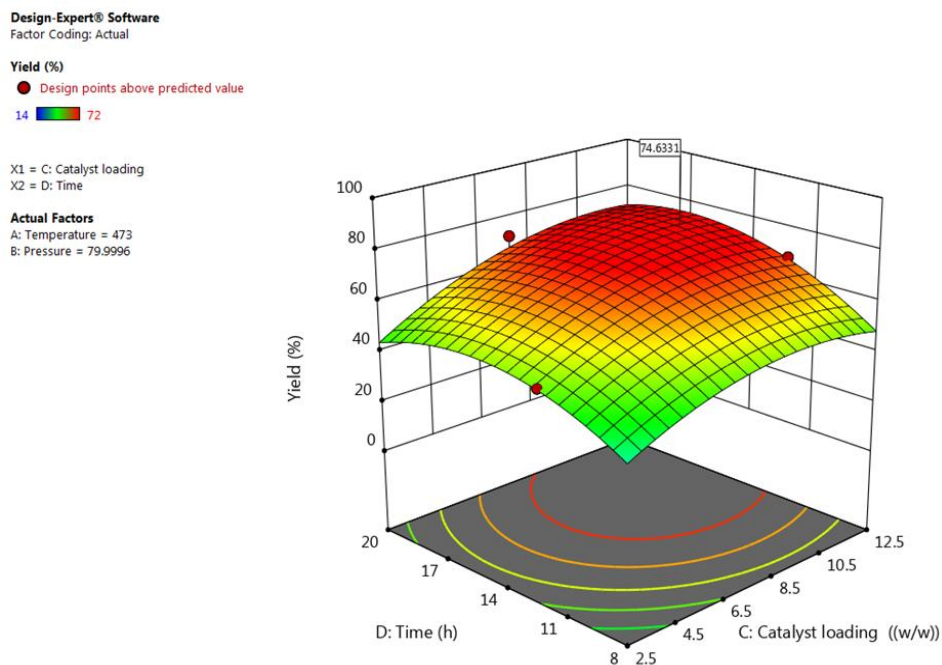


Figure 7- 18. Response surface plot for the effect reaction time and reaction catalyst loading on BC yield after optimisation.

7.8 Conclusions

The synthesised novel Cu–Zr/GO inorganic composite catalyst was successfully prepared *via* traditional wet impregnation method for the synthesis of BC from direct reaction of BO and CO₂ in solvent-free process. Cu-Zr/GO heat-treated at 773 K (HR450) was found to be the best-performed catalyst for the synthesis of BC as compared to other heterogeneous catalysts.

BBD of RSM method was carried out in order to study and optimise the interactive effects of four process variables: catalyst loading, reaction temperature, pressure and reaction time on two responses (BO conversion and BC yield). The use of OFAT method at the optimum reaction conditions at 80 bar, 423 K, 7.5% (w/w) catalyst loading in 12 h reaction time achieved 82% BO conversion and BC yield of 71%.

The application of BBD of RSM numerical optimisation identified the optimum conditions to be 80 bar, 428 K, 9.8% (w/w) catalyst loading in 14.2 h reaction time and with BC yield of 74.6% and BO conversion of 90.9%. The predicted optimum conditions have been validated experimentally with approximate relative errors of $\pm 1.25\%$ for BO conversion and $\pm 0.75\%$ for BC yield. Cu-Zr/GO (HR450) catalyst has been recycled easily and reused several times without any notable reduction in its catalytic performance. This study clearly illustrates a facile and greener route for 1,2-butylene carbonate synthesis using Cu-Zr/GO catalyst *via* CO₂ utilisation.

CHAPTER 8

CONCLUSIONS AND RECOMMENDATIONS FOR FUTURE WORK

CHAPTER 8: CONCLUSIONS AND RECOMMENDATIONS FOR FUTURE WORK

8.1 Conclusions

In this work, direct synthesis of 1,2-butylene carbonate (BC) and styrene carbonate (SC) from cycloaddition reaction of carbon dioxide (CO₂) to respective epoxides (BO and SO) have been investigated in the presence of several heterogeneous catalysts. The batch studies for BC and SC syntheses have been conducted in a high-pressure reactor and the effect of various reaction conditions have been evaluated in which the optimum reaction parameters have been identified. A comprehensive literature review has been presented to provide a wider overview of several existing methods and the catalytic process used for the production of BC and SC.

Several metal oxides, mixed metal oxides and graphene supported heterogeneous catalysts have been studied extensively for the synthesis of cyclic carbonates. The use of graphene oxide (GO) as supported heterogeneous catalysts have been synthesised *via* an improved Hummer's and Offerman method. GO is an advanced class of catalyst material with novel characteristics used as a supported catalyst for heterogeneous catalysis due to its unique chemical, physical and mechanical properties that promote easy surface modifications and very high surface area.

The use of graphene oxide (GO) as supported heterogeneous catalysts improved the yield and selectivity of the BC. Continuous hydrothermal flow synthesis (CHFS) reactor has been used to synthesise ceria, lanthana and zirconia graphene oxide inorganic nanocomposite (Ce-La-Zr/GO) with a pore volume of 0.047 cm³ g⁻¹, particle size 5.78 nm and BET surface area of 115 m² g⁻¹. Ce-La-Zr/GO showed the highest catalytic activity for the synthesis of 1,2-butylene carbonate from the cycloaddition reaction of carbon dioxide (CO₂) to 1,2-butylene oxide. The use of Box-Behnken Design (BBD) of Response Surface Methodology (RSM) for optimisation study. It is also used for study of the interactive effects of four process variables (i.e reaction temperature, pressure, catalyst loading and time) on yield and conversion responses. The optimum conditions have been identified to be 90 bar, 408 K, 15% (w/w) catalyst loading in 20 h reaction time and with BC yield of 66.5% and BO conversion of 91.4%. The predicted optimum

conditions have been validated experimentally with 1.45% and 1.52% relative error for both BO conversion and BC yield, respectively.

Commercially supplied catalysts zirconium oxide (Zr-O), lanthanum oxide (La-O), ceria doped zirconia (Ce-Zr-O), lanthana doped zirconia (La-Zr-O), and ceria and lanthana doped zirconia (Ce-La-Zr-O) have been characterised using scanning electron microscopy (SEM), transmission electron microscopy (TEM), X-ray photoelectron spectroscopy (XPS), X-ray powder diffraction (XRD) and Raman spectroscopy to investigate the morphology, surface area, particle size, catalyst composition and catalytic performance.

The synthesis of styrene carbonate has been successfully in the absence of organic solvents using a high-pressure reactor with several commercially supplied catalysts and ceria, lanthana doped zirconia (Ce-La-Zr-O) has been found to have performed better with a remarkable yield. Ce-La-Zr-O catalyst has been used to assess the synthesis of SC and achieved the optimum reaction conditions of 408 K, 75 bar, 10% (w/w) catalyst loading and 20 h for conversion of SO and SC yield of 84% and 52%, respectively. The use BBD of RSM for process optimisation gave SO conversion of 89.5% and SC yield of 54.7% at the optimum conditions of 409 K, 81.2 bar, 10.1% (w/w) catalyst loading in 20.6 h reaction time. The predicted optimum conditions have been validated experimentally with 0.335% and 0.731% relative error for both SO conversion and SC yield, respectively.

The study the effect of the catalysts particle sizes, morphology, surface area and composition on the catalytic performance of the catalysts (copper, zirconia doped graphene inorganic composite (Cu-Zr/GO) and ceria, lanthana, zirconia doped graphene inorganic composite (Ce-La-Zr/GO)) have been successful using scanning electron microscopy (SEM), transmission electron microscopy (TEM), Brunauer-Emmett-Teller (BET) surface area measurement, x-ray photoelectron spectroscopy (XPS), X-ray powder diffraction (XRD) and micromeritics analyser.

Cu-Zr/GO (AP) inorganic composite catalyst has been synthesised *via* traditional method and heat treated at 723 K (HTR450) exhibited BET surface area of $41 \text{ m}^2\text{g}^{-1}$ with a particle size of $6.92 \pm 1.32 \text{ nm}$. HTR450 showed the highest catalytic activity for the synthesis of 1,2-butylene carbonate from the direct facile reaction of CO_2 and butylene oxide (BO) in a high-pressure reactor. The highest BO

conversion of 82% and BC yield of 71% were achieved at the optimum reaction conditions of 423 K, 7.5% (w/w) 80 bar in 12 h. The use of BBD from RSM has been conducted in order to study and optimise the interactive effect of multiple process variables that includes reaction temperature, catalyst loading, pressure and reaction time on various responses (i.e conversion and yield). A quadratic model equation has been developed and used to analyse the experimental data. The model predicted the yield of BC and BO conversion of ~76% and ~ 85%, respectively at optimum reaction conditions.

The predicted models have been validated statistically and experimentally, where an agreement observed between predicted and experimental results with approximate relative errors of $\pm 1.25\%$ for BO conversion and $\pm 0.75\%$ for BC yield.

8.2 Recommendations for future work

8.2.1 Developing a novel heterogeneous catalyst with higher catalytic performance

The use of heterogeneous catalysts to synthesise organic carbonates have been identified preferably when compared to homogenous catalyst because of several advantages, which are ease of catalyst recovery from the reaction mixture and high stability at high temperature. These advantages are economically viable and therefore, developing a novel heterogeneous catalyst that possesses higher catalytic performance in terms of higher yields of 1,2-butylene carbonate and styrene carbonate syntheses will not only replace the conventional method of synthesis with green process synthesis, but will also contribute to the elimination of climate change and global warming. The performance of the mixed metal oxides heterogeneous catalyst could be further developed by variation of different percentage composition of the mixed metal oxides to identify the appropriate ratio that will be highly efficient and provide a higher yield of 1,2-butylene carbonate and styrene carbonate. Furthermore, calculating the theoretical performance based on physical mixtures and developing a detailed hypothesis of the catalyst performances. The use of other new approaches of advanced materials used as catalyst supports that include activated carbon and 3D graphene could be applied to improve the surface area of the catalyst and could enhance catalytic performances.

8.2.2 Catalyst characterisation

The ability of the heterogeneous catalyst to perform relies on the effect of the acidic and basic sites of the catalysts. The bifunctional action of both acid and basic sites of metal oxides or mixed metal oxides derived from the formation of metal-oxygen bonds, which are highly important for the activation of CO₂ and epoxides (that include butylene oxide and styrene oxide) to produce cyclic carbonates. Hence, the investigation of redox properties of heterogeneous catalyst is very crucial in order to identify appropriate information needed for developing novel catalysts and also improving the existing heterogeneous catalysts. Ammonia temperature programmed desorption (NH₃-TPD) and temperature programmed reduction (TPR) are powerful methods that could be used to determine the surface acidity and redox properties of heterogeneous catalysts. The use of different catalyst supports, different composition metal oxide catalysts on acidic-basic surface properties and redox properties will help to develop catalysts with higher catalytic performance.

8.2.3 Continuous flow syntheses of cyclic carbonates

Ce-La-Zr-O and HT-450 of Cu-Zr/GO catalysts have shown excellent catalytic activities for the cyclic carbonates syntheses such as 1,2-butylene carbonate and styrene carbonate from the cycloaddition reaction of CO₂ to their respective epoxides in a high-pressure reactor. The performances of these catalysts could be examined in a continuous flow process in such a way that the efficiency of producing cyclic carbonates from both processes could be compared.

8.2.4 Synthesis of other valuable organic carbonates

There are other important organic carbonates that are very useful to chemical industries such as propylene carbonate, ethylene carbonate, hexane carbonate, dimethyl carbonate and diphenyl carbonates. These organic carbonates could also be synthesised by using Ce-La-Zr-O and HT-450 of Cu-Zr/GO catalysts.

8.2.5 Valourisation of waste CO₂ for cyclic carbonate synthesis

The waste CO₂ from industries contains different impurities most especial flue gas. The flue gas power station produces CO₂ in larger scale and contains

impurities such as sulphur dioxide, water vapour, and nitrogen dioxide. It would be cost effective if technology is developed to utilise waste CO₂ from source to synthesise cyclic carbonates. This will eliminate the cost associated with carbon capture, storage and CO₂ purification. Therefore, valorisation of waste CO₂ from flue gas using heterogeneous catalyst will not only reduce cost, but also offer technological advancement toward CO₂ emission reduction.

8.2.6 Economic feasibility study of the current process

This research work has been based on practical experiment and technical challenges of CO₂ emission reduction *via* utilisation to produce value-added chemicals such as 1,2-butylene carbonate and styrene carbonate using heterogeneous catalysts in the absence of organic solvents. This work has offered a positive step forward towards CO₂ emissions reduction and greener synthesis of cyclic carbonates. Although no economic feasibility study has been carried out, it requires a comprehensive economic assessment and environmental benefits of these greener routes of syntheses, which will be compared to the existing process of synthesis. The use of life cycle analysis (LCA) as an assessment tool to assess the environmental impact and economic feasibility study of the process, which will reveal more information about the benefits of the greener route for syntheses of 1,2-butylene carbonate and styrene carbonate.

CHAPTER 9

REFERENCES

CHAPTER 9: REFERENCES

Aboelazayem, O., Gadalla, M. and Saha, B. (2018a) Biodiesel production from waste cooking oil via supercritical methanol: Optimisation and reactor simulation, *Renewable Energy*, 124, pp. 144–154. DOI:10.1016/j.renene.2017.06.076.

Aboelazayem, O., Gadalla, M. and Saha, B. (2018b) Valorisation of high acid value waste cooking oil into biodiesel using supercritical methanolysis: Experimental assessment and statistical optimisation on typical Egyptian feedstock, *Energy*, 162, pp. 408–420. DOI:10.1016/j.energy.2018.07.194.

Adeleye, A. I., Kellici, S., Heil, T., Morgan, D., Vickers, M. and Saha, B. (2015) Greener synthesis of propylene carbonate using graphene-inorganic nanocomposite catalysts, *Catalysis Today*, 256 (P2), pp. 347–357. DOI:10.1016/j.cattod.2014.12.032.

Adeleye, A. I., Patel, D., Niyogi, D. and Saha, B. (2014) Efficient and greener synthesis of propylene carbonate from carbon dioxide and propylene oxide, *Industrial and Engineering Chemistry Research*, 53 (49), pp. 18647–18657. DOI:10.1021/ie500345z.

Aghbashlo, M., Hosseinpour, S., Tabatabaei, M. and Dadak, A. (2017) Fuzzy modeling and optimization of the synthesis of biodiesel from waste cooking oil (WCO) by a low power, high frequency piezo-ultrasonic reactor, *Energy*, 132, pp. 65–78. DOI:10.1016/j.energy.2017.05.041.

Akhavan, O. (2010) The effect of heat treatment on formation of graphene thin films from graphene oxide nanosheets, *Carbon*. DOI:10.1016/j.carbon.2009.09.069.

Alvaro, M., Baleizao, C., Carbonell, E., El Ghoul, M., García, H. and Gigante, B. (2005) Polymer-bound aluminium salen complex as reusable catalysts for CO₂ insertion into epoxides, *Tetrahedron*, 61 (51), pp. 12131–12139.

DOI:10.1016/j.tet.2005.07.114.

Anitha, M., Kamarudin, S. K. and Kofli, N. T. (2016) The potential of glycerol as a value-added commodity, *Chemical Engineering Journal*, 295, pp. 119–130. DOI:10.1016/j.cej.2016.03.012.

Appaturi, J. N. and Adam, F. (2013) A facile and efficient synthesis of styrene carbonate via cycloaddition of CO₂ to styrene oxide over ordered mesoporous MCM-41-Ir/Br catalyst, *Applied Catalysis B: Environmental*, 136–137, pp. 150–159. DOI:10.1016/j.apcatb.2013.01.049.

Aresta, M. (2003) Carbon dioxide utilization: Greening both the energy and chemical industry: An overview, *Utilization of Greenhouse Gases*, 852 (2), pp. 2–39. DOI:10.1007/s11027-005-9006-5.

Aresta, M. and Dibenedetto, A. (2002) Carbon dioxide as building block for the synthesis of organic carbonates, *Journal of Molecular Catalysis A: Chemical*, 182–183, pp. 399–409. DOI:10.1016/S1381-1169(01)00514-3.

Aresta, M. and Dibenedetto, A. (2004) The contribution of the utilization option to reducing the CO₂ atmospheric loading: Research needed to overcome existing barriers for a full exploitation of the potential of the CO₂ use, in: *Catalysis Today*, 98, pp. 455–462.

Aresta, M. and Dibenedetto, A. (2007) Utilisation of CO₂ as a chemical feedstock: opportunities and challenges, *Dalton Transactions*, (28), pp. 2975. DOI:10.1039/b700658f.

Aresta, M. and Dibenedetto, A. (2010) Industrial utilization of carbon dioxide (CO₂), in: *Developments and Innovation in Carbon Dioxide (CO₂) Capture and Storage Technology*. Elsevier, 2, pp. 377–410.

Aresta, M., Dibenedetto, A. and Angelini, A. (2013) The changing paradigm in

CO₂ utilization, *Journal of CO₂ Utilization*. DOI:10.1016/j.jcou.2013.08.001.

Aresta, M., Dibenedetto, A. and Quaranta, E. (2015) *Reaction mechanisms in carbon dioxide conversion*, *Reaction Mechanisms in Carbon Dioxide Conversion*. DOI:10.1007/978-3-662-46831-9.

Babad, H. and Zeiler, A. G. (1973) The Chemistry of Phosgene, *Chemical Reviews*, 73 (1), pp. 75–91. DOI:10.1021/cr60281a005.

Baiker, A. (1999) Supercritical Fluids in Heterogeneous Catalysis, *Chemical Reviews*, 99 (2), pp. 453–474. DOI:10.1021/cr970090z.

Barbarini, A., Maggi, R., Mazzacani, A., Mori, G., Sartori, G. and Sartorio, R. (2003) Cycloaddition of CO₂ to epoxides over both homogeneous and silica-supported guanidine catalysts, *Tetrahedron Letters*, 44 (14), pp. 2931–2934. DOI:10.1016/S0040-4039(03)00424-6.

Baş, D. and Boyacı, İ. H. (2007) Modeling and optimization I: Usability of response surface methodology, *Journal of Food Engineering*, 78 (3), pp. 836–845. DOI:10.1016/j.jfoodeng.2005.11.024.

Beckman, E. J. (2004) Supercritical and near-critical CO₂ in green chemical synthesis and processing, *Journal of Supercritical Fluids*. DOI:10.1016/S0896-8446(03)00029-9.

Behr, A., Bahke, P., Klinger, B. and Becker, M. (2007) Application of carbonate solvents in the telomerisation of butadiene with carbon dioxide, *Journal of Molecular Catalysis A: Chemical*, 267 (1–2), pp. 149–156. DOI:10.1016/j.molcata.2006.11.043.

Benaglia, M., Puglisi, A. and Cozzi, F. (2003) Polymer-supported organic catalysts, *Chemical Reviews*, 103 (9), pp. 3401–3429. DOI:10.1021/cr010440o.

Bennett, S. J., Schroeder, D. J. and McCoy, S. T. (2014) Towards a framework for discussing and assessing CO₂ utilisation in a climate context, in: *Energy Procedia*.63, pp. 7976–7992.

Bezerra, M. A., Santelli, R. E., Oliveira, E. P., Villar, L. S. and Escaleira, L. A. (2008) Response surface methodology (RSM) as a tool for optimization in analytical chemistry, *Talanta*. DOI:10.1016/j.talanta.2008.05.019.

Bhanage, B. M., Fujita, S. I., Ikushima, Y. and Arai, M. (2001) Synthesis of dimethyl carbonate and glycols from carbon dioxide, epoxides, and methanol using heterogeneous basic metal oxide catalysts with high activity and selectivity, *Applied Catalysis A: General*, 219 (1–2), pp. 259–266. DOI:10.1016/S0926-860X(01)00698-6.

Bhanage, B. M., Fujita, S. I., Ikushima, Y. and Arai, M. (2003) Transesterification of urea and ethylene glycol to ethylene carbonate as an important step for urea based dimethyl carbonate synthesis, *Green Chemistry*, 5 (4), pp. 429–432. DOI:10.1039/b304182d.

Bo, R., Ma, X., Feng, Y., Zhu, Q., Huang, Y., Liu, Z., *et al.* (2015) Optimization on conditions of Lycium barbarum polysaccharides liposome by RSM and its effects on the peritoneal macrophages function, *Carbohydrate Polymers*, 117, pp. 215–222. DOI:10.1016/j.carbpol.2014.09.060.

Bradshaw, J. and Cook, P. (2001) *Geological Sequestration of Carbon Dioxide Thermodynamics*, *Environmental Geosciences*. Vol. 8. DOI:10.1046/j.1526-0984.2001.008003149.x.

Burton, B., Alexander, D., Klein, H., Garibay-Vasquez, A., Pekank, A. and Henkee, C. (2010) Epoxy formulations using Jeffamine® polyetheramines, *Huntsman Corporation*, pp. 1–100.

Caló, V., Nacci, A., Monopoli, A. and Fanizzi, A. (2002a) Cyclic carbonate

formation from carbon dioxide and oxiranes in tetrabutylammonium halides as solvents and catalysts, *Organic Letters*, 4 (15), pp. 2561–2563. DOI:10.1021/ol026189w.

Caló, V., Nacci, A., Monopoli, A. and Fanizzi, A. (2002b) Cyclic carbonate formation from carbon dioxide and oxiranes in tetrabutylammonium halides as solvents and catalysts, *Organic Letters*, 4 (15), pp. 2561–2563. DOI:10.1021/ol026189w.

Cassetta, A. (2014) X-Ray Diffraction (XRD), in: *Encyclopedia of Membranes*. pp. 1–3.

Cavell, K., Golunski, S. and Miller, D. (2010) 'Handbook of Green Chemistry - Green Catalysis', *Platinum Metals Review*, 54 (4), pp. 233–238. DOI:10.1595/147106710X527928.

Chamú-Muñoz, A., Hernández-Meléndez, O., Hernández-Luna, M., Alcaraz-Cienfuegos, J., Vivaldo-Lima, E. and Bárzana, E. (2015) Ethylene Carbonate used as Reagent and Green Solvent in the Chemical Modification of Corncob, *Macromolecular Materials and Engineering*, 300 (8), pp. 810–822. DOI:10.1002/mame.201500001.

Chi, G., Hu, S., Yang, Y. and Chen, T. (2012) Response surface methodology with prediction uncertainty: A multi-objective optimisation approach, *Chemical Engineering Research and Design*, 90 (9), pp. 1235–1244. DOI:10.1016/j.cherd.2011.12.012.

Choon, S. R., Hwang, J. C., Hong, B. L. and Shim, J. J. (2007) Solvent-free carboxylation of styrene oxide: Enhanced reactivity of quaternary onium salts in ionic liquid-CO₂ system, *Bulletin of the Korean Chemical Society*, 28 (6), pp. 1060–1062. DOI:10.5012/bkcs.2007.28.6.1060.

Clements, J. H. (2003) Reactive Applications of Cyclic Alkylene Carbonates,

Industrial & Engineering Chemistry Research, 42 (4), pp. 663–674.
DOI:10.1021/ie020678i.

Cormos, A. M., Dinca, C., Petrescu, L., Andreea Chisalita, D., Szima, S. and Cormos, C. C. (2018) Carbon capture and utilisation technologies applied to energy conversion systems and other energy-intensive industrial applications, *Fuel*, 211, pp. 883–890. DOI:10.1016/j.fuel.2017.09.104.

Cote, L. J., Cruz-Silva, R., Kim, F., Jang, H. D., Krishnan, D., Luo, J. and Huang, J. (2012) Energetic graphene oxide: Challenges and opportunities, *Nano Today*, 7 (2), pp. 137–152. DOI:10.1016/j.nantod.2012.02.003.

Cui, H., Wang, T., Wang, F., Gu, C., Wang, P. and Dai, Y. (2004) Transesterification of ethylene carbonate with methanol in supercritical carbon dioxide, *Journal of Supercritical Fluids*, 30 (1), pp. 63–69. DOI:10.1016/S0896-8446(03)00164-5.

Curie, M. (2016) *PhD Thesis Novel catalysts for chemical CO₂ utilization*. AGH University of Science and Technology, Faculty of Energy and Fuel.

Dai, W. L., Jin, B., Luo, S. L., Yin, S. F., Luo, X. B. and Au, C. T. (2013) Cross-linked polymer grafted with functionalized ionic liquid as reusable and efficient catalyst for the cycloaddition of carbon dioxide to epoxides, *Journal of CO₂ Utilization*, 3–4, pp. 7–13. DOI:10.1016/j.jcou.2013.08.002.

Dai, W. L., Yin, S. F., Guo, R., Luo, S. L., Du, X. and Au, C. T. (2010) Synthesis of propylene carbonate from carbon dioxide and propylene oxide using Zn-Mg-Al composite oxide as high-efficiency catalyst, *Catalysis Letters*, 136 (1–2), pp. 35–44. DOI:10.1007/s10562-009-0198-2.

Darensbourg, D. J. (2010) Chemistry of carbon dioxide relevant to its utilization: A personal perspective, *Inorganic Chemistry*, 49 (23), pp. 10765–10780. DOI:10.1021/ic101800d.

Darensbourg, D. J., Yoder, J. C., Holtcamp, M. W., Klausmeyer, K. K. and Reibenspies, J. H. (1996) Cyanide-Bridged Heterobimetallic Complexes of the Group 6 Metal Carbonyls and Copper (I). X-ray Structures of $(\text{CO})_5\text{MCNCu}(\text{PPh}_3)_3(\text{M})\text{Cr}, \text{W})$ Derivatives, *Inorganic Chemistry*, 35 (I), pp. 4764–4769.

Deikus, G. and Bechhofer, D. H. (2011) 5' End-independent RNase J1 endonuclease cleavage of *Bacillus subtilis* model RNA, *Journal of Biological Chemistry*, 286 (40), pp. 34932–34940. DOI:10.1074/jbc.M111.287409.

Dincer, I., Colpan, C. O. and Kadioglu, F. (2013) Preface, *Causes, Impacts and Solutions to Global Warming*, pp. v–vi. DOI:10.1007/9781461475880.

Dincer, I., Ozgur Colpan, C., Akif Ezan, M. and Kizilkan, O. (2015) *Progress in Clean Energy, Volume 2, Progress in Clean Energy, Volume 2: Novel Systems and Applications*. DOI:10.1007/978-3-319-17031-2.

Drnovšek, N. (2018) The translation of the seat of metropolitanate of Kiev from Kiev to Moscow, *Bogoslovni Vestnik*. DOI:10.1126/science.1102896.

Du, Y., Kong, D. L., Wang, H. Y., Cai, F., Tian, J. S., Wang, J. Q. and He, L. N. (2005) Sn-catalyzed synthesis of propylene carbonate from propylene glycol and CO_2 under supercritical conditions, *Journal of Molecular Catalysis A: Chemical*, 241 (1–2), pp. 233–237. DOI:10.1016/j.molcata.2005.07.030.

Eckert, H. (2011) Phosgenation reactions with phosgene from triphosgene, *Chimica Oggi*.

EEA (2016) Resource efficiency and the low-carbon economy — European Environment Agency. Available from: <https://www.eea.europa.eu/soer-2015/synthesis/report/4-resourceefficiency> [Accessed 13 May 2018].

Eghbali, N. and Li, C. J. (2007) Conversion of carbon dioxide and olefins into cyclic carbonates in water, *Green Chemistry*, 9 (3), pp. 213–215.

DOI:10.1039/b615612f.

EIA (2017) Today in Energy - U.S. Energy Information Administration (EIA), *US Energy Information Administration*. Available from: <https://www.eia.gov/todayinenergy/index.php?tg=international> [Accessed 13 May 2018].

Feng, T. C., Zheng, W. T., Sun, K. Q. and Xu, B. Q. (2016) CO₂ reforming of methane over coke-resistant Ni-Co/Si₃N₄ catalyst prepared via reactions between silicon nitride and metal halides, *Catalysis Communications*, 73, pp. 54–57. DOI:10.1016/j.catcom.2015.10.009.

Fowler, J. D., Allen, M. J., Tung, V. C., Yang, Y., Kaner, R. B. and Weiller, B. H. (2009) Practical chemical sensors from chemically derived graphene, *ACS Nano*, 3 (2), pp. 301–306. DOI:10.1021/nn800593m.

Fujita, S., Arai, M. and Bhanage, B. M. (2014) *Transformation and Utilization of Carbon Dioxide*, Bhanage, B. M. and Arai, M. (eds.) . Berlin, Heidelberg: Springer Berlin Heidelberg. DOI:10.1007/978-3-642-44988-8.

Fujita, S. I., Nishiura, M. and Arai, M. (2010) Synthesis of styrene carbonate from carbon dioxide and styrene oxide with various zinc halide-based ionic liquids, *Catalysis Letters*, 135 (3–4), pp. 263–268. DOI:10.1007/s10562-010-0286-3.

Fujita, T. and Makio, H. (2007) 11.20 - Polymerization of Alkenes, *Comprehensive Organometallic Chemistry III*, 11, pp. 691–734. DOI:10.1016/B0-08-045047-4/00202-8.

Gabriele, B., Salerno, G. and Costa, M. (2006) Oxidative carbonylations, *Topics in Organometallic Chemistry*. DOI:10.1007/3418_024.

Gerlach, T. (2011) Volcanic versus anthropogenic carbon dioxide, *Eos*, 92 (24), pp. 201–202. DOI:10.1029/2011EO240001.

Gibbins, J. and Chalmers, H. (2008) Carbon capture and storage, *Energy Policy*, 36 (12), pp. 4317–4322. DOI:10.1016/j.enpol.2008.09.058.

Girotra, P., Singh, S. K. and Nagpal, K. (2013) Supercritical fluid technology: A promising approach in pharmaceutical research, *Pharmaceutical Development and Technology*. DOI:10.3109/10837450.2012.726998.

Grunwaldt, J.-D., Caravati, M. and Baiker, A. (2006) In situ extended X-ray absorption fine structure study during selective alcohol oxidation over Pd/Al₂O₃ in supercritical carbon dioxide., *The Journal of Physical Chemistry. B*, 110 (20), pp. 9916–22. DOI:10.1021/jp0605395.

Gupta, R. C. (2015) *Handbook of Toxicology of Chemical Warfare Agents, Handbook of Toxicology of Chemical Warfare Agents: Second Edition*. Elsevier. DOI:10.1016/C2013-0-15402-5.

Gutés, A., Hsia, B., Sussman, A., Mickelson, W., Zettl, A., Carraro, C. and Maboudian, R. (2012) Graphene decoration with metal nanoparticles: Towards easy integration for sensing applications, *Nanoscale*, 4 (2), pp. 438–440. DOI:10.1039/c1nr11537e.

H.Frank, J. S. (1988) *Industrial Aromatic Chemistry: Raw Materials, Processes, Products*. Springer Berlin Heidelberg. DOI:10.1007/978-3-642-73432-8.

Hage, W., Hallbrucker, A. and Mayer, E. (1993) Carbonic Acid: Synthesis by Protonation of Bicarbonate and FTIR Spectroscopic Characterization via a New Cryogenic Technique, *Journal of the American Chemical Society*, 115 (18), pp. 8427–8431. DOI:10.1021/ja00071a061.

Hagen, J., Chorkendorff, I. and Niemantsverdriet, J. W. (2006) *Concepts of Modern Catalysis and Kinetics Catalysis from A to Z Principles and Practice of Heterogeneous Catalysis Catalytic Membranes and Membrane Reactors Spectroscopy in Catalysis, Simulation*.

Han, W., Jiao, H. and Fox, D. (2018) Scanning electron microscopy, in: *Springer Tracts in Modern Physics*.272, pp. 35–68.

He, L.-N., Wang, J.-Q. and Wang, J.-L. (2009) Carbon dioxide chemistry: Examples and challenges in chemical utilization of carbon dioxide, *Pure and Applied Chemistry*, 81 (11), pp. 2069–2080. DOI:10.1351/PAC-CON-08-10-22.

Hewitt, C. N. (1996) Book ReviewCarbon dioxide chemistry: environmental issues., *Journal of Chemical Technology & Biotechnology*, 66 (4), pp. 422–422. DOI:10.1002/(SICI)1097-4660(199608)66:4<422::AID-JCTB3516>3.0.CO;2-U.

Hiroto, S., Tsai, A. P., Sumita, M. and Hanawa, T. (2000) Effect of pH on the polarization behavior of Zr₆₅Al_{7.5}Ni₁₀Cu_{17.5} amorphous alloy in a phosphate-buffered solution, *Corrosion Science*. DOI:10.1016/S0010-938X(00)00056-1.

Hodge, P. (1986) Polymer-supported catalysts and reagents, *Annual Reports on the Progress of Chemistry - Section B*, 83, pp. 283–302. DOI:10.1039/OC9868300283.

Houghton, J. (2005) Global warming, *Reports on Progress in Physics*, 68 (6), pp. 1343–1403. DOI:10.1088/0034-4885/68/6/R02.

Huang, C., Tang, Z. and Zhang, Z. (2010) Differences between Zirconium Hydroxide (Zr(OH)₄·nH₂O) and Hydrous Zirconia (ZrO₂·nH₂O), *Journal of the American Ceramic Society*. DOI:10.1111/j.1151-2916.2001.tb00889.x.

Hummers, W. S. and Offeman, R. E. (1958) Preparation of Graphitic Oxide, *Journal of the American Chemical Society*, 80 (6), pp. 1339–1339. DOI:10.1021/ja01539a017.

Hunt, A. J., Sin, E. H. K., Marriott, R. and Clark, J. H. (2010) Generation, Capture, and Utilization of Industrial Carbon Dioxide, *ChemSusChem*, 3 (3), pp. 306–322. DOI:10.1002/cssc.200900169.

Huntsman Co-operaton (2001) Ethylene Carbonate Propylene Carbonate.

IEA (2015) CO₂ EMISSIONS FROM FUEL COMBUSTION Highlights, *Iea*, S/V (IEA-STATISTICS), pp. 1–139. DOI:10.1787/co2-table-2011-1-en.

Intergovernmental Panel on Climate Change (2007) *Summary for Policymakers. In Climate Change 2007: The Physical Sciences Basis. Working Group I Contribution to the Fourth Assessment Report of the IPCC (eds Solomon, S. et al.)*, Cambridge University Press Cambridge United Kingdom and New York NY USA. Available from: <https://books.google.com.co/books?id=8-m8nXB8GB4C>

Intergovernmental Panel on Climate Change (IPCC) (2005) *IPCC Special Report on Carbon Dioxide Capture and Storage, Working Group III of the Intergovernmental Panel on Climate Change. Vol. 49.* DOI:10.1002/anie.201000431.

J.Tsuji (2005) Palladium Reagents and Catalysts: New Perspectives for the 21st Century, *John Wiley & Sons, Ltd., Chichester*, 9 (2), pp. 670. DOI:10.1595/147106705X46487.

Jadhav, A. H., Thorat, G. M., Lee, K., Lim, A. C., Kang, H. and Seo, J. G. (2016) Effect of anion type of imidazolium based polymer supported ionic liquids on the solvent free synthesis of cycloaddition of CO₂ into epoxide, *Catalysis Today*, 265, pp. 56–67. DOI:10.1016/j.cattod.2015.09.048.

Jaliliannosrati, H., Amin, N. A. S., Talebian-Kiakalaieh, A. and Noshadi, I. (2013) Microwave assisted biodiesel production from *Jatropha curcas* L. seed by two-step in situ process: Optimization using response surface methodology, *Bioresource Technology*, 136, pp. 565–573. DOI:10.1016/j.biortech.2013.02.078.

Jang, B. Z. and Zhamu, A. (2008) Processing of nanographene platelets (NGPs) and NGP nanocomposites: A review, *Journal of Materials Science*, 43 (15), pp. 5092–5101. DOI:10.1007/s10853-008-2755-2.

Ji, X. H., Zhu, N. N., Ma, J. G. and Cheng, P. (2018) Conversion of CO₂ into cyclic carbonates by a Co(II) metal-organic framework and the improvement of catalytic activity: Via nanocrystallization, *Dalton Transactions*, 47 (6), pp. 1768–1771. DOI:10.1039/c7dt04882c.

Jiang, C., Guo, Y., Wang, C., Hu, C., Wu, Y. and Wang, E. (2003) Synthesis of dimethyl carbonate from methanol and carbon dioxide in the presence of polyoxometalates under mild conditions, *Applied Catalysis A: General*, 256 (1–2), pp. 203–212. DOI:10.1016/S0926-860X(03)00400-9.

Jung, J. and Perrut, M. (2001) Particle design using supercritical fluids: Literature and patent survey, *Journal of Supercritical Fluids*. DOI:10.1016/S0896-8446(01)00064-X.

Kafizas, A., Kellici, S., Darr, J. A. and Parkin, I. P. (2009) Titanium dioxide and composite metal/metal oxide titania thin films on glass: A comparative study of photocatalytic activity, *Journal of Photochemistry and Photobiology A: Chemistry*, 204 (2–3), pp. 183–190. DOI:10.1016/j.jphotochem.2009.03.017.

Kawanami, H. and Ikushima, Y. (2000) Chemical fixation of carbon dioxide to styrene carbonate under supercritical conditions with DMF in the absence of any additional catalysts, *Chemical Communications*, (21), pp. 2089–2090. DOI:10.1039/b006682f.

Kawanami, H., Sasaki, A., Matsui, K. and Ikushima, Y. (2003) A rapid and effective synthesis of propylene carbonate using a supercritical CO₂-ionic liquid system, *Chemical Communications*, 3 (7), pp. 896–897. DOI:10.1039/b212823c.

Kawashima, A., Ohmura, K., Yokoyama, Y. and Inoue, A. (2011) The corrosion behaviour of Zr-based bulk metallic glasses in 0.5M NaCl solution, *Corrosion Science*. DOI:10.1016/j.corsci.2011.05.014.

Kellici, S., Gong, K., Lin, T., Brown, S., Clark, R. J. H., Vickers, M., *et al.* (2010)

High-throughput continuous hydrothermal flow synthesis of Zn-Ce oxides: unprecedented solubility of Zn in the nanoparticle fluorite lattice, *Philosophical Transactions of the Royal Society A: Mathematical, Physical and Engineering Sciences*, 368 (1927), pp. 4331–4349. DOI:10.1098/rsta.2010.0135.

Khuri, A. I. and Mukhopadhyay, S. (2010) Response surface methodology, *Wiley Interdisciplinary Reviews: Computational Statistics*. DOI:10.1002/wics.73.

Kim, F., Luo, J., Cruz-Silva, R., Cote, L. J., Sohn, K. and Huang, J. (2010) Self-propagating domino-like reactions in oxidized graphite, *Advanced Functional Materials*, 20 (17), pp. 2867–2873. DOI:10.1002/adfm.201000736.

Kim, M. Il, Choi, S. J., Kim, D. W. and Park, D. W. (2014) Catalytic performance of zinc containing ionic liquids immobilized on silica for the synthesis of cyclic carbonates, *Journal of Industrial and Engineering Chemistry*, 20 (5), pp. 3102–3107. DOI:10.1016/j.jiec.2013.11.051.

Klaewkla, R., Arend, M. and Hoelderich, W. F. (2011) A Review of Mass Transfer Controlling the Reaction Rate in Heterogeneous Catalytic Systems, *Mass Transfer - Advanced Aspects*, (3), pp. 667–684. DOI:10.5772/22962.

Kogure, T. (2013) Electron Microscopy, in: *Developments in Clay Science*.5, pp. 275–317.

Krase, N. W. and Gaddy, V. L. (1922) Synthesis of Urea from Ammonia and Carbon Dioxide, *Industrial and Engineering Chemistry*, 14 (7), pp. 611–615. DOI:10.1021/ie50151a009.

Krizmane, M., Slihte, S. and Borodinecs, A. (2016) Key Criteria Across Existing Sustainable Building Rating Tools, in: *Energy Procedia*.

Krone, C. A. and Klingner, T. D. (2005) Isocyanates, polyurethane and childhood asthma, *Pediatric Allergy and Immunology*. DOI:10.1111/j.1399-

3038.2005.00295.x.

Le Quéré, C., Andres, R. J., Boden, T., Conway, T., Houghton, R. A., House, J. I., *et al.* (2013) The global carbon budget 1959-2011, *Earth System Science Data*, 5 (1), pp. 165–185. DOI:10.5194/essd-5-165-2013.

Le Quéré, C., Moriarty, R., Andrew, R. M., Canadell, J. G., Sitch, S., Korsbakken, J. I., *et al.* (2015) Global Carbon Budget 2015, *Earth System Science Data*, 7 (2), pp. 349–396. DOI:10.5194/essd-7-349-2015.

Le Quéré, C., Peters, G. P., Andres, R. J., Andrew, R. M., Boden, T. A., Ciais, P., *et al.* (2014) Global carbon budget 2013, *Earth System Science Data*, 6 (1), pp. 235–263. DOI:10.5194/essd-6-235-2014.

Lee, E. H., Ahn, J. Y., Dharman, M. M., Park, D. W., Park, S. W. and Kim, I. (2008) Synthesis of cyclic carbonate from vinyl cyclohexene oxide and CO₂ using ionic liquids as catalysts, *Catalysis Today*, 131 (1–4), pp. 130–134. DOI:10.1016/j.cattod.2007.10.012.

Lee, S., Speight, J. G. and Loyalka, S. K. (2015) *Handbook of Alternative Fuel Technologies, Physical chemistry chemical physics : PCCP*. Vol. 9. CRC Press. DOI:10.1039/b702989f.

Leino, E., M??ki-Arvela, P., Eta, V., Kumar, N., Demoisson, F., Samikannu, A., *et al.* (2013) The influence of various synthesis methods on the catalytic activity of cerium oxide in one-pot synthesis of diethyl carbonate starting from CO₂, ethanol and butylene oxide, *Catalysis Today*, 210, pp. 47–54. DOI:10.1016/j.cattod.2013.02.011.

Li, G., Chen, L., Bao, J., Li, T. and Mei, F. (2008) A recoverable catalyst Co(salen) in zeolite Y for the synthesis of methyl N-phenylcarbamate by oxidative carbonylation of aniline, *Applied Catalysis A: General*, 346 (1–2), pp. 134–139. DOI:10.1016/j.apcata.2008.05.014.

Li, Y., Zhang, P., Du, Q., Peng, X., Liu, T., Wang, Z., *et al.* (2011) Adsorption of fluoride from aqueous solution by graphene, *Journal of Colloid and Interface Science*, 363 (1), pp. 348–354. DOI:10.1016/j.jcis.2011.07.032.

Liang, Q., Wu, X., Weng, D. and Lu, Z. (2008) Selective oxidation of soot over Cu doped ceria/ceria-zirconia catalysts, *Catalysis Communications*. DOI:10.1016/j.catcom.2007.06.007.

Liu, J. (2017) Catalysis by Supported Single Metal Atoms, *ACS Catalysis*. DOI:10.1021/acscatal.6b01534.

Liu, M., Lan, J., Liang, L., Sun, J. and Arai, M. (2017) Heterogeneous catalytic conversion of CO₂ and epoxides to cyclic carbonates over multifunctional tri-s-triazine terminal-linked ionic liquids, *Journal of Catalysis*, 347, pp. 138–147. DOI:10.1016/j.jcat.2016.11.038.

Liu, M., Liang, L., Liang, T., Lin, X., Shi, L., Wang, F. and Sun, J. (2015a) Cycloaddition of CO₂ and epoxides catalyzed by dicationic ionic liquids mediated metal halide: Influence of the dication on catalytic activity, *Journal of Molecular Catalysis A: Chemical*, 408, pp. 242–249. DOI:10.1016/j.molcata.2015.07.032.

Liu, Y., Zhao, G., Wang, D. and Li, Y. (2015b) Heterogeneous catalysis for green chemistry based on nanocrystals, *National Science Review*. DOI:10.1093/nsr/nwv014.

Loupy, A. (1999) Solvent-free reactions, in: *Modern Solvents in Organic Synthesis*. pp. 153–207.

Lu, X. B. (2015) *Carbon Dioxide and Organometallics*, *Carbon Dioxide and Organometallics*. DOI:10.1007/978-3-319-22078-9.

Lu, X. B., Xiu, J. H., He, R., Jin, K., Luo, L. M. and Feng, X. J. (2004) Chemical

fixation of CO₂ to ethylene carbonate under supercritical conditions: Continuous and selective, *Applied Catalysis A: General*, 275 (1–2), pp. 73–78. DOI:10.1016/j.apcata.2004.07.022.

MacHin, D. J. (1970) Transition elements, *Nature*, 225 (5228), pp. 203–204. DOI:10.1038/225203b0.

Martens, J. A., Bogaerts, A., De Kimpe, N., Jacobs, P. A., Marin, G. B., Rabaey, K., Saeys, M. and Verhelst, S. (2017) The Chemical Route to a Carbon Dioxide Neutral World, *ChemSusChem*. DOI:10.1002/cssc.201601051.

Marvaniya, H. M., Modi, K. N. and Sen, D. J. (2011) Greener reactions under solvent free conditions, *International Journal of Drug Development and Research*, 3 (2), pp. 34–43.

McConnell, C. (2012) Adding 'Utilization' to Carbon Capture and Storage, *U.S. Energy Department*.

McNeill, A. (2012) Scanning Electron Microscopy and Transmission Electron Microscopy of Mollicutes: Challenges and Opportunities, *Modern Research and Educational Topics in Microscopy*, 13 (9), pp. 1204–1206. DOI:10.2174/138945012802002401.

Meylan, F. D., Moreau, V. and Erkman, S. (2015) CO₂ utilization in the perspective of industrial ecology, an overview, *Journal of CO₂ Utilization*, 12, pp. 101–108. DOI:10.1016/j.jcou.2015.05.003.

Miao, C.-X., Wang, J.-Q. and He, L.-N. (2008) Catalytic Processes for Chemical Conversion of Carbon Dioxide into Cyclic Carbonates and Polycarbonates, *The Open Organic Chemistry Journal*, 2 (1), pp. 68–82. DOI:10.2174/1874095200801020068.

Millero, F. J., Pierrot, D., Lee, K., Wanninkhof, R., Feely, R., Sabine, C. L., Key,

R. M. and Takahashi, T. (2002) Dissociation constants for carbonic acid determined from field measurements, *Deep-Sea Research Part I: Oceanographic Research Papers*, 49 (10), pp. 1705–1723. DOI:10.1016/S0967-0637(02)00093-6.

Montgomery, D. C. (2006) Design and Analysis of Experiments, *Technometrics*, 48 (1), pp. 158–158. DOI:10.1198/tech.2006.s372.

Mori, K., Hara, T., Mizugaki, T., Ebitani, K. and Kaneda, K. (2004) Hydroxyapatite-supported palladium nanoclusters: A highly active heterogeneous catalyst for selective oxidation of alcohols by use of molecular oxygen, *Journal of the American Chemical Society*, 126 (34), pp. 10657–10666. DOI:10.1021/ja0488683.

Motokura, K., Itagaki, S., Iwasawa, Y., Miyaji, A. and Baba, T. (2009) Silica-supported aminopyridinium halides for catalytic transformations of epoxides to cyclic carbonates under atmospheric pressure of carbon dioxide, *Green Chemistry*, 11 (11), pp. 1876–1880. DOI:10.1039/b916764c.

Naderi, M. (2015) Surface Area, in: *Progress in Filtration and Separation*. pp. 585–608.

Nalawade, S. P., Picchioni, F. and Janssen, L. P. B. M. (2006) Supercritical carbon dioxide as a green solvent for processing polymer melts: Processing aspects and applications, *Progress in Polymer Science (Oxford)*, 31 (1), pp. 19–43. DOI:10.1016/j.progpolymsci.2005.08.002.

Nam, J. K., Choi, M. J., Cho, D. H., Suh, J. K. and Kim, S. B. (2013) The influence of support in the synthesis of dimethyl carbonate by Cu-based catalysts, *Journal of Molecular Catalysis A: Chemical*, 370, pp. 7–13. DOI:10.1016/j.molcata.2012.09.032.

National Oceanic and Atmospheric Administration (2011) Carbon Cycle | National

Oceanic and Atmospheric Administration. Available from: <https://www.noaa.gov/resource-collections/carbon-cycle> [Accessed 29 January 2019].

NOAA (2018) ESRL Global Monitoring Division - Global Greenhouse Gas Reference Network, *Journal of Geophysical Research*. DOI:10.1029/95JD03410.

North, M. and Pasquale, R. (2009) Mechanism of Cyclic Carbonate Synthesis from Epoxides and CO₂, *Angewandte Chemie International Edition*, 48 (16), pp. 2946–2948. DOI:10.1002/anie.200805451.

North, M., Pasquale, R. and Young, C. (2010) Synthesis of cyclic carbonates from epoxides and CO₂, *Green Chemistry*, 12 (9), pp. 1514. DOI:10.1039/c0gc00065e.

Öhlmann, G. (1999a) Handbook of Heterogeneous Catalysis, *Zeitschrift Für Physikalische Chemie*, 208 (Part_1_2), pp. 274–278. DOI:10.1524/zpch.1999.208.Part_1_2.274.

Öhlmann, G. (1999b) Handbook of Heterogeneous Catalysis, *Zeitschrift Für Physikalische Chemie*, 208 (Part_1_2), pp. 274–278. DOI:10.1016/0304-405X(84)90012-6.

Olivier, J. G. J., Janssens-Maenhout, G., Peters, J. A. H. W. and Wilson, J. (2011) Long-Term Trend in Global CO₂ Emissions. 2011 report, *The Hague: PBL/JRC*, pp. 42. Available from: http://edgar.jrc.ec.europa.eu/news_docs/C02_Mondiaal_webdef_19sept.pdf [Accessed

Omrani, H., Alizadeh, A. and Emrouznejad, A. (2018) Finding the optimal combination of power plants alternatives: a multi response Taguchi-neural network using TOPSIS and fuzzy best-worst method, *Journal of Cleaner Production*, 203, pp. 210–223. DOI:10.1016/j.jclepro.2018.08.238.

Onyenkeadi, V., Kellici, S. and Saha, B. (2017) Greener Synthesis of 1,2-Butylene Carbonate From CO₂ Using Graphene - Inorganic Nanocomposite Catalysis, (June), pp. 27–30.

Onyenkeadi, V., Kellici, S. and Saha, B. (2018) Greener synthesis of 1,2-butylene carbonate from CO₂ using graphene-inorganic nanocomposite catalyst, *Energy*, 165, pp. 867–876. DOI:10.1016/j.energy.2018.09.135.

Paddock, R. L., Hiyama, Y., McKay, J. M. and Nguyen, S. B. T. (2004) Co(III) porphyrin/DMAP: An efficient catalyst system for the synthesis of cyclic carbonates from CO₂ and epoxides, *Tetrahedron Letters*, 45 (9), pp. 2023–2026. DOI:10.1016/j.tetlet.2003.10.101.

Paddock, R. L. and Nguyen, S. T. (2004) Chiral (salen)Co(III) catalyst for the synthesis of cyclic carbonates Electronic supplementary information (ESI) available: general experimental procedures and analytical data for new compounds. See <http://www.rsc.org/suppdata/cc/b4/b401543f/>, *Chemical Communications*, (14), pp. 1622. DOI:10.1039/b401543f.

Pan, C., Liu, L. and Gai, G. (2017) Recent Progress of Graphene-Containing Polymer Hydrogels: Preparations, Properties, and Applications, *Macromolecular Materials and Engineering*, 302 (10), pp. 1700184. DOI:10.1002/mame.201700184.

Paredes, A. M. (2014) Microscopy: Transmission Electron Microscopy, in: *Encyclopedia of Food Microbiology: Second Edition*. pp. 711–720.

Park, S., Lee, K. S., Bozoklu, G., Cai, W., Nguyen, S. B. T. and Ruoff, R. S. (2008) Graphene oxide papers modified by divalent ions - Enhancing mechanical properties via chemical cross-linking, *ACS Nano*, 2 (3), pp. 572–578. DOI:10.1021/nn700349a.

Park, S. and Ruoff, R. S. (2009a) Chemical methods for the production of

graphenes, *Nature Nanotechnology*, 4 (4), pp. 217–224.
DOI:10.1038/nnano.2009.58.

Park, S. and Ruoff, R. S. (2009b) Chemical methods for the production of graphenes, *Nature Nanotechnology*, 4 (4), pp. 217–224.
DOI:10.1038/nnano.2009.58.

Patel, D. and Saha, B. (2007) Heterogeneous kinetics and residue curve map (RCM) determination for synthesis of n-hexyl acetate using ion-exchange resins as catalysts, *Industrial and Engineering Chemistry Research*, 46 (10), pp. 3157–3169. DOI:10.1021/ie060725x.

Patel, D. and Saha, B. (2012) Esterification of acetic acid with n -hexanol in batch and continuous chromatographic reactors using a gelular ion-exchange resin as a catalyst, *Industrial and Engineering Chemistry Research*, 51 (37), pp. 11965–11974. DOI:10.1021/ie3007424.

Peng, W., Zhao, W., Zhao, N., Li, J., Xiao, F., Wei, W. and Sun, Y. (2008) Direct synthesis of salicylamide from phenol and urea over ZnO catalyst, *Catalysis Communications*, 9 (6), pp. 1219–1223. DOI:10.1016/j.catcom.2007.11.006.

Pérez-Fortes, M., Bocin-Dumitriu, A. and Tzimas, E. (2014) CO₂utilization pathways: Techno-economic assessment and market opportunities, in: *Energy Procedia*.63, pp. 7968–7975.

Perumal, D. (2001) Microencapsulation of ibuprofen and Eudragit® RS 100 by the emulsion solvent diffusion technique, *International Journal of Pharmaceutics*, 218 (1–2), pp. 1–11. DOI:10.1016/S0378-5173(00)00686-4.

Qiao, K., Ono, F., Bao, Q., Tomida, D. and Yokoyama, C. (2009) Efficient synthesis of styrene carbonate from CO₂and styrene oxide using zinc catalysts immobilized on soluble imidazolium-styrene copolymers, *Journal of Molecular Catalysis A: Chemical*, 303 (1–2), pp. 30–34.

DOI:10.1016/j.molcata.2008.12.025.

Quadrelli, E. A., Centi, G., Duplan, J. L. and Perathoner, S. (2011) Carbon dioxide recycling: Emerging large-scale technologies with industrial potential, *ChemSusChem*. DOI:10.1002/cssc.201100473.

Rahmanto, W., Gunawan and Nuryanto, R. (2002) Corrosion Rate of Copper and Iron in Seawater Based on Resistance Measurement, *Journal of Coastal Development*, 5 (2), pp. 1410–5217. Available from: <https://www.omicsonline.com/open-access/corrosion-rate-of-copper-and-iron-in-seawater-based-on-resistance-measurement-1410-5217-5-127.pdf> [Accessed

Ravi, S., Roshan, R., Tharun, J., Kathalikkattil, A. C. and Park, D. W. (2015) Sulfonic acid functionalized mesoporous SBA-15 as catalyst for styrene carbonate synthesis from CO₂ and styrene oxide at moderate reaction conditions, *Journal of CO₂ Utilization*, 10, pp. 88–94. DOI:10.1016/j.jcou.2015.01.003.

Ren, S., Rong, P. and Yu, Q. (2018) Preparations, properties and applications of graphene in functional devices: A concise review, *Ceramics International*. DOI:10.1016/j.ceramint.2018.04.089.

Reverchon, E. and De Marco, I. (2006) Supercritical fluid extraction and fractionation of natural matter, *Journal of Supercritical Fluids*. DOI:10.1016/j.supflu.2006.03.020.

Romano, U., Tesel, R., Mauri, M. M. and Rebora, P. (1980) Synthesis of Dimethyl Carbonate from Methanol, Carbon Monoxide, and Oxygen Catalyzed by Copper Compounds, *Industrial and Engineering Chemistry Product Research and Development*, 19 (3), pp. 396–403. DOI:10.1021/i360075a021.

Ronchin, L., Vavasori, A., Amadio, E., Cavinato, G. and Toniolo, L. (2009) Oxidative carbonylation of phenols catalyzed by homogeneous and

heterogeneous Pd precursors, *Journal of Molecular Catalysis A: Chemical*, 298 (1–2), pp. 23–30. DOI:10.1016/j.molcata.2008.09.028.

Saada, R., AboElazayem, O., Kellici, S., Heil, T., Morgan, D., Lampronti, G. I. and Saha, B. (2018) Greener synthesis of dimethyl carbonate using a novel tin-zirconia/graphene nanocomposite catalyst, *Applied Catalysis B: Environmental*, 226 (December 2017), pp. 451–462. DOI:10.1016/j.apcatb.2017.12.081.

Saada, R., Kellici, S., Heil, T., Morgan, D. and Saha, B. (2015) Greener synthesis of dimethyl carbonate using a novel ceria-zirconia oxide/graphene nanocomposite catalyst, *Applied Catalysis B: Environmental*, 168–169, pp. 353–362. DOI:10.1016/j.apcatb.2014.12.013.

Sakai, T., Tsutsumi, Y. and Ema, T. (2008) Highly active and robust organic–inorganic hybrid catalyst for the synthesis of cyclic carbonates from carbon dioxide and epoxides, *Green Chemistry*, 10 (3), pp. 337–34. DOI:10.1039/b718321f.

Sakakura, T. and Kohno, K. (2009) The synthesis of organic carbonates from carbon dioxide, *Chemical Communications*, (11), pp. 1312. DOI:10.1039/b819997c.

Schäffner, B., Andrushko, V., Bayardon, J., Holz, J. and Börner, A. (2009) Organic carbonates as alternative solvents for asymmetric hydrogenation, in: *Chirality*.21, pp. 857–861.

Schäffner, B., Schäffner, F., Verevkin, S. P. and Börner, A. (2010) Organic carbonates as solvents in synthesis and catalysis, *Chemical Reviews*, 110 (8), pp. 4554–4581. DOI:10.1021/cr900393d.

Schlögl, R. (2015) Heterogeneous catalysis, *Angewandte Chemie - International Edition*. DOI:10.1002/anie.201410738.

Schniepp, H. C., Car, R., Liu, J., Aksay, I. A., Li, J.-L., Abdala, A. A., *et al.* (2007) Single Sheet Functionalized Graphene by Oxidation and Thermal Expansion of Graphite, *Chemistry of Materials*, 19 (18), pp. 4396–4404. DOI:10.1021/cm0630800.

Schniepp, H. C., Li, J. L., McAllister, M. J., Sai, H., Herrera-Alonson, M., Adamson, D. H., *et al.* (2006) Functionalized single graphene sheets derived from splitting graphite oxide, *Journal of Physical Chemistry B*, 110 (17), pp. 8535–8539. DOI:10.1021/jp060936f.

Seibert, E. and Tracy, T. S. (2014) Fundamentals of enzyme kinetics, *Methods in Molecular Biology*, 1113, pp. 9–22. DOI:10.1007/978-1-62703-758-7_2.

Shaikh, A.-A. G. and Sivaram, S. (1996) Organic Carbonates †, *Chemical Reviews*, 96 (3), pp. 951–976. DOI:10.1021/cr950067i.

Shaikh, A. A. G. and Sivaram, S. (1992) Dialkyl and Diaryl Carbonates by Carbonate Interchange Reaction with Dimethyl Carbonate, *Industrial and Engineering Chemistry Research*, 31 (4), pp. 1167–1170. DOI:10.1021/ie00004a028.

Shang, Y., Li, T., Li, H., Dang, A., Zhang, L., Yin, Y., Xiong, C. and Zhao, T. (2016) Preparation and characterization of graphene derived from low-temperature and pressure promoted thermal reduction, *Composites Part B: Engineering*, 99, pp. 106–111. DOI:10.1016/J.COMPOSITESB.2016.06.030.

Shen, Y. M., Duan, W. L. and Shi, M. (2003) Chemical fixation of carbon dioxide catalyzed by binaphthyldiamino Zn, Cu, and Co salen-type complexes, *Journal of Organic Chemistry*, 68 (4), pp. 1559–1562. DOI:10.1021/jo020191j.

Siewniak, A., Jasiak, K. and Baj, S. (2014) An efficient method for the synthesis of cyclic carbonates from CO₂ and epoxides using an effective two-component catalyst system: Polymer-supported quaternary onium salts and aqueous

solutions of metal salts, *Applied Catalysis A: General*, 482, pp. 266–274. DOI:10.1016/j.apcata.2014.05.033.

Sillanpää, M., Ncibi, M. C. and Matilainen, A. (2018) Advanced oxidation processes for the removal of natural organic matter from drinking water sources: A comprehensive review, *Journal of Environmental Management*, 208, pp. 56–76. DOI:10.1016/j.jenvman.2017.12.009.

Singh, B. P., Nayak, S., Nanda, K. K., Jena, B. K., Bhattacharjee, S. and Besra, L. (2013) The production of a corrosion resistant graphene reinforced composite coating on copper by electrophoretic deposition, *Carbon*, 61, pp. 47–56. DOI:10.1016/j.carbon.2013.04.063.

Somorjai, G. A. (1979) Catalysis and surface science, *Surface Science*, 89 (1–3), pp. 496–524. DOI:10.1016/0039-6028(79)90634-4.

Srivastava, R., Srinivas, D. and Ratnasamy, P. (2005) CO₂ activation and synthesis of cyclic carbonates and alkyl/aryl carbamates over adenine-modified Ti-SBA-15 solid catalysts, *Journal of Catalysis*, 233 (1), pp. 1–15. DOI:10.1016/j.jcat.2005.03.023.

Stoller, M. D., Park, S., Yanwu, Z., An, J. and Ruoff, R. S. (2008) Graphene-Based ultracapacitors, *Nano Letters*, 8 (10), pp. 3498–3502. DOI:10.1021/nl802558y.

Styring, P., Jansen, D., de Coninck, H., Reith, H. and Armstrong, K. (2011) *Carbon Capture and Utilisation in the green economy*, Centre for Low Carbon Futures.

Styring, P., Quadrelli, E. A. and Armstrong, K. (2014a) *Carbon Dioxide Utilisation: Closing the Carbon Cycle: First Edition*, Carbon Dioxide Utilisation: Closing the Carbon Cycle: First Edition. DOI:10.1016/C2012-0-02814-1.

Styring, P., Quadrelli, E. and Armstrong, K. (2014b) Carbon dioxide utilisation: closing the carbon cycle, pp. 311. Available from: <https://books.google.co.uk/books?id=ZBV0AwAAQBAJ&printsec=frontcover&dq=co2+utilisation&hl=en&sa=X&ved=0ahUKEwiF6cqC8vDaAhXICsAKHcEPCu0Q6AEIJzAA#v=onepage&q=co2 utilisation&f=false> [Accessed 6 May 2018].

Subramaniam, B., Rajewski, R. A. and Snavely, K. (1997) Pharmaceutical processing with supercritical carbon dioxide, *Journal of Pharmaceutical Sciences*. DOI:10.1021/js9700661.

Sun, J., Fujita, S. I. and Arai, M. (2005a) Development in the green synthesis of cyclic carbonate from carbon dioxide using ionic liquids, *Journal of Organometallic Chemistry*. DOI:10.1016/j.jorganchem.2005.02.011.

Sun, J., Fujita, S. I., Bhanage, B. M. and Arai, M. (2004a) Direct oxidative carboxylation of styrene to styrene carbonate in the presence of ionic liquids, *Catalysis Communications*, 5 2, pp. 83–87. DOI:10.1016/j.catcom.2003.11.016.

Sun, J., Fujita, S. I., Zhao, F. and Arai, M. (2004b) Synthesis of styrene carbonate from styrene oxide and carbon dioxide in the presence of zinc bromide and ionic liquid under mild conditions, *Green Chemistry*, 6 (12), pp. 613–616. DOI:10.1039/b413229g.

Sun, J., Fujita, S. I., Zhao, F. and Arai, M. (2005b) A highly efficient catalyst system of ZnBr₂/n-Bu₄Ni for the synthesis of styrene carbonate from styrene oxide and supercritical carbon dioxide, *Applied Catalysis A: General*, 287 (2), pp. 221–226. DOI:10.1016/j.apcata.2005.03.035.

Sun, J., Wang, Y., Son, J., Xiang, D., Wang, L. and Xiao, F. S. (2009) A facile, direct synthesis of styrene carbonate from styrene and CO₂ catalyzed by Au/Fe(OH)₃-ZnBr₂/Bu₄NBr system, *Catalysis Letters*, 129 (3–4), pp. 437–443. DOI:10.1007/s10562-008-9820-y.

Sundaram, R. S., Gómez-Navarro, C., Balasubramanian, K., Burghard, M. and Kern, K. (2008) Electrochemical modification of grapheme, *Advanced Materials*, 20 (16), pp. 3050–3053. DOI:10.1002/adma.200800198.

Szent-gyorgyi, A. (2006) Diffusion and Reaction, *Elements of Chemical Reaction Engineering*, pp. 813.

Tepzz, T. (2004, July 16) A method of manufacturing an organic carbonates. Japan. Available from: <https://patents.google.com/patent/JP2007505054A/en>

Tomishige, K., Furusawa, Y., Ikeda, Y., Asadullah, M. and Fujimoto, K. (2001) CeO₂-ZrO₂ solid solution catalyst for selective synthesis of dimethyl carbonate from methanol and carbon dioxide, *Catalysis Letters*, 76 (1–2), pp. 71–74. DOI:10.1023/A:1016711722721.

Tomishige, K. and Kunimori, K. (2002) Catalytic and direct synthesis of dimethyl carbonate starting from carbon dioxide using CeO₂-ZrO₂ solid solution heterogeneous catalyst: Effect of H₂O removal from the reaction system, *Applied Catalysis A: General*, 237 (1–2), pp. 103–109. DOI:10.1016/S0926-860X(02)00322-8.

Torrey, M. (2007) The Kyoto Protocol, *INFORM - International News on Fats, Oils and Related Materials*, 18 (8), pp. 527. DOI:10.2968/064001011.

Udayakumar, S., Lee, M. K., Shim, H. L., Park, S. W. and Park, D. W. (2009) Imidazolium derivatives functionalized MCM-41 for catalytic conversion of carbon dioxide to cyclic carbonate, *Catalysis Communications*, 10 (5), pp. 659–664. DOI:10.1016/j.catcom.2008.11.017.

United Nations/Framework Convention on Climate Change (2015) Paris Agreement, *21st Conference of the Parties*. DOI:FCCC/CP/2015/L.9.

Valefi, M., de Rooij, M., Schipper, D. J. and Winnubst, L. (2012) Effect of

temperature on friction and wear behaviour of CuO-zirconia composites, *Journal of the European Ceramic Society*. DOI:10.1016/j.jeurceramsoc.2012.02.006.

Völker, C. (2008) *The Global Carbon Cycle, Cycle*.

Vollmer, J. M., Curtiss, L. A., Vissers, D. R. and Amine, K. (2004) Reduction Mechanisms of Ethylene, Propylene, and Vinylethylene Carbonates, *Journal of The Electrochemical Society*, 151 (1), pp. A178. DOI:10.1149/1.1633765.

Wang, D., Zhang, X., Wei, W. and Sun, Y. (2012) Mg/Al mixed oxides: Heterogeneous basic catalysts for the synthesis of salicylamide from urea and phenol, *Catalysis Communications*, 28, pp. 159–162. DOI:10.1016/j.catcom.2012.09.001.

Wang, J.-L., Wang, J.-Q., He, L.-N., Dou, X.-Y. and Wu, F. (2008) A CO₂/H₂O₂-tunable reaction: direct conversion of styrene into styrene carbonate catalyzed by sodium phosphotungstate/n-Bu₄NBr, *Green Chemistry*, 10 (11), pp. 1218. DOI:10.1039/b807108j.

Wang, J.-Q., Kong, D.-L., Chen, J.-Y., Cai, F. and He, L.-N. (2006) Synthesis of cyclic carbonates from epoxides and carbon dioxide over silica-supported quaternary ammonium salts under supercritical conditions, *Journal of Molecular Catalysis A: Chemical*, 249 (1–2), pp. 143–148. DOI:10.1016/j.molcata.2006.01.008.

Wijte, D., Alblas, M. J., Noort, D., Langenberg, J. P. and van Helden, H. P. M. (2011) Toxic effects following phosgene exposure of human epithelial lung cells in vitro using a CULTEX® system, *Toxicology in Vitro*, 25 (8), pp. 2080–2087. DOI:10.1016/j.tiv.2011.09.003.

Witek-Krowiak, A., Chojnacka, K., Podstawczyk, D., Dawiec, A. and Pokomeda, K. (2014) Application of response surface methodology and artificial neural network methods in modelling and optimization of biosorption process, in:

Bioresource Technology. pp. 11–211.

Xiang, D., Liu, X., Sun, J., Xiao, F. S. and Sun, J. (2009) A novel route for synthesis of styrene carbonate using styrene and CO₂ as substrates over basic resin R201 supported Au catalyst, *Catalysis Today*, 148 (3–4), pp. 383–388. DOI:10.1016/j.cattod.2009.07.068.

Xiaohua, G., Xue, So., Chenghua, S., Peng, Z., Xinkun, L., Xinyuan, S. and Qing, Y. (2014) Electrospinning of poly(butylene-carbonate): Effect of Solvents on the Properties of the Nanofibers Film, *International Journal of Electrochemical Science*, 9, pp. 8045–8056. Available from: <http://www.electrochemsci.org/papers/vol9/91208045.pdf> [Accessed

Xu, J., Wu, F., Jiang, Q., Shang, J. K. and Li, Y. X. (2015) Metal halides supported on mesoporous carbon nitride as efficient heterogeneous catalysts for the cycloaddition of CO₂, *Journal of Molecular Catalysis A: Chemical*, 403, pp. 77–83. DOI:10.1016/j.molcata.2015.03.024.

Yamaguchi, K., Ebitani, K., Yoshida, T., Yoshida, H. and Kaneda, K. (1999) Mg-Al mixed oxides as highly active acid-base catalysts for cycloaddition of carbon dioxide to epoxides, *Journal of the American Chemical Society*, 121 (18), pp. 4526–4527. DOI:10.1021/ja9902165.

Yano, T., Matsui, H., Koike, T., Ishiguro, H., Fujihara, H., Yoshihara, M. and Maeshima, T. (1997) Magnesium oxide-catalysed reaction of carbon dioxide with an epoxide with retention of stereochemistry, *Chemical Communications*, (12), pp. 1129–1130. DOI:10.1039/a608102i.

Yashentech Corporation (2014) - Dimethyl Carbonate Technology from carbon dioxide and methanol. Available from: <http://www.yashentech.com/en/pages/dmc.htm> [Accessed 6 May 2018].

Yasuda, H., He, L. N., Takahashi, T. and Sakakura, T. (2006) Non-halogen

catalysts for propylene carbonate synthesis from CO₂ under supercritical conditions, *Applied Catalysis A: General*, 298 (1–2), pp. 177–180. DOI:10.1016/j.apcata.2005.09.034.

Yin, X., Zhang, J. and Wang, X. (2004) Sequential injection analysis system for the determination of arsenic by hydride generation atomic absorption spectrometry, *Fenxi Huaxue*, 32 (10), pp. 1365–1367. DOI:10.1017/CBO9781107415324.004.

Zhang, J., Davis, T. A., Matthews, M. A., Drews, M. J., LaBerge, M. and An, Y. H. (2006) Sterilization using high-pressure carbon dioxide, *Journal of Supercritical Fluids*, 38 (3), pp. 354–372. DOI:10.1016/j.supflu.2005.05.005.

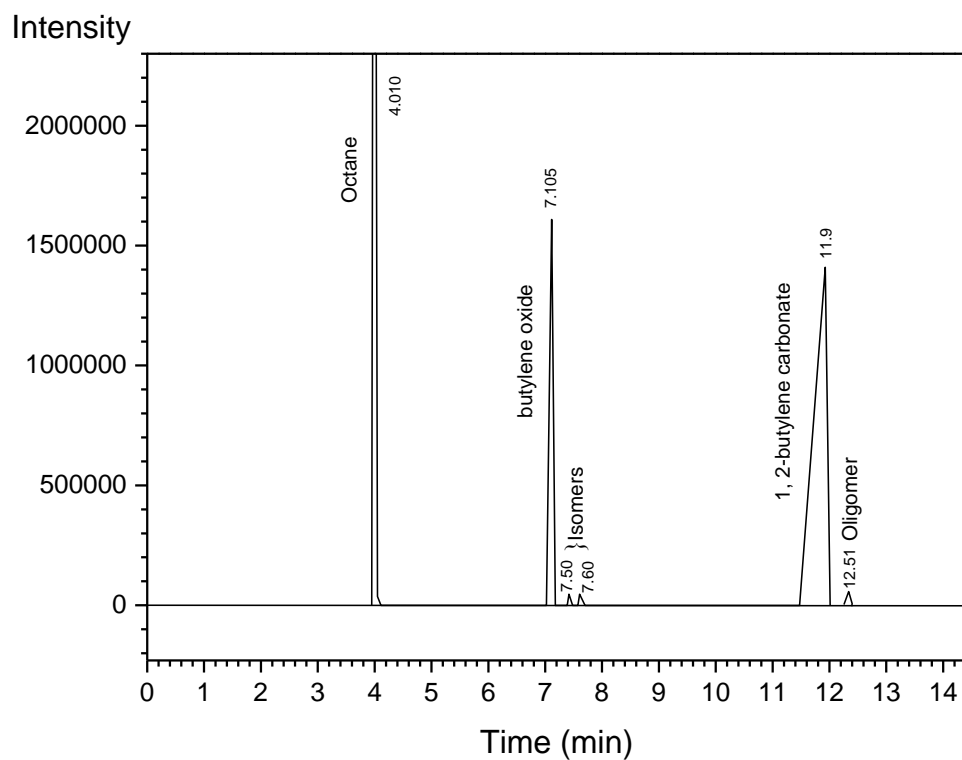
Zhu, M., Srinivas, D., Bhogeswararao, S., Ratnasamy, P. and Carreon, M. A. (2013) Catalytic activity of ZIF-8 in the synthesis of styrene carbonate from CO₂ and styrene oxide, *Catalysis Communications*, 32, pp. 36–40. DOI:10.1016/j.catcom.2012.12.003.

Zhu, Y., James, D. K. and Tour, J. M. (2012) New routes to graphene, graphene oxide and their related applications, *Advanced Materials*. DOI:10.1002/adma.201202321.

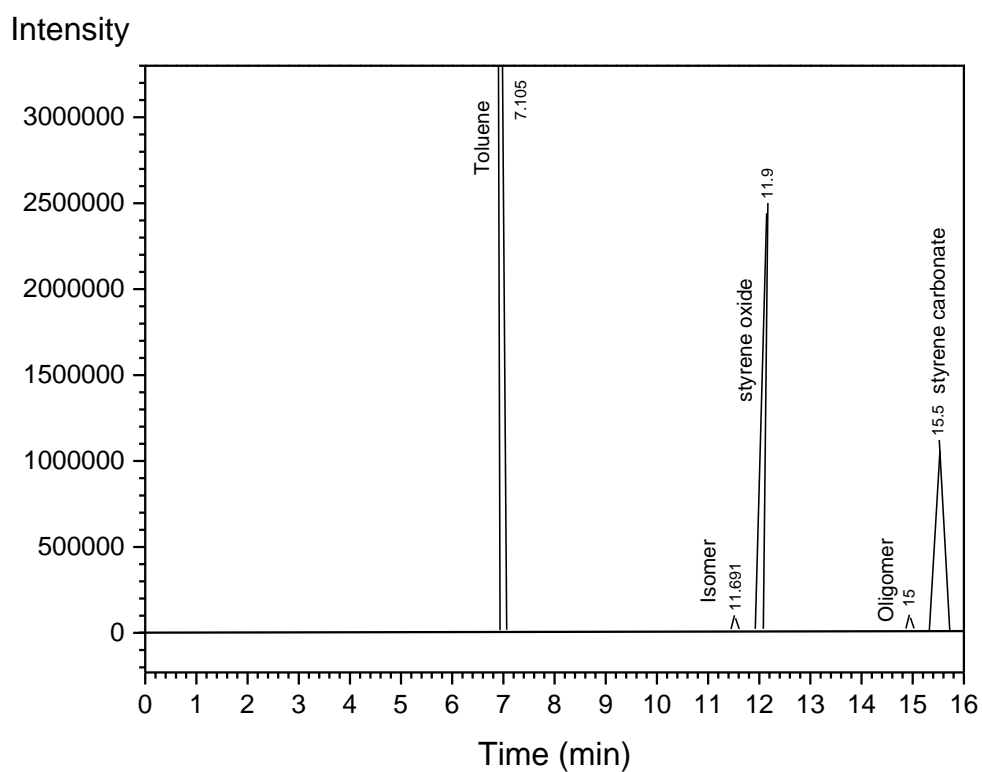
CHAPTER 10
APPENDICES

CHAPTER 10: APPENDICES

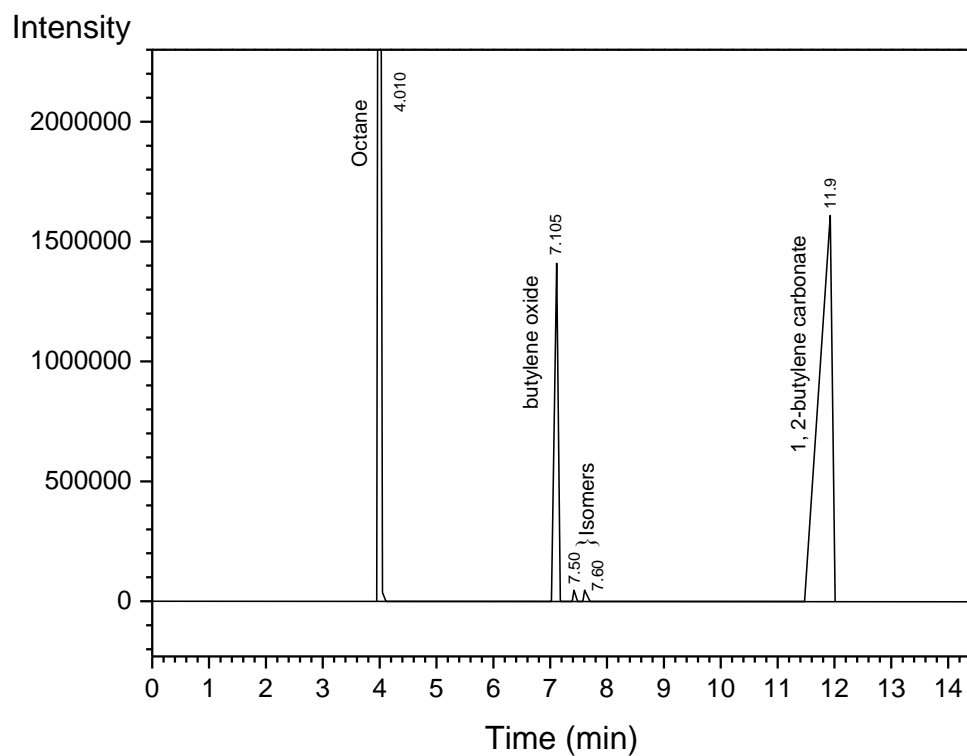
10.1 Appendix 1: Chromatograms



Appendix 1- 1. A typical chromatogram of a reaction mixture analysed by a Shimadzu GC-2014 gas chromatograph showing the speculated isomers and oligomer for 1,2-butylene carbonate synthesis.



Appendix 1- 2. A typical chromatogram of a reaction mixture analysed by a Shimadzu GC-2014 gas chromatograph showing the speculated isomer and oligomer for styrene carbonate synthesis.



Appendix 1- 3. A typical chromatogram of a reaction mixture analysed by a Shimadzu GC-2014 gas chromatograph showing the speculated isomers for 1,2-butylene carbonate synthesis.

10.2 Appendix A: Raw data for catalysts reusability

Appendix A- 1. Raw data for catalysts reusability for greener synthesis of BC via CO₂ using Ce-La-Zr/GO

Catalyst	Reaction time [hr]	Stirring speed (rpm)	Catalyst reusability	Reaction temperature [K]	Catalyst loading [%][w/w]	Conversion of BO [%]	Yield of BC [%]	Selectivity of BC [%]
Ce-La-Zr/GO	20	300	Run 1	408	10	84.42	64.21	76.06
			Run 2			84.13	64.39	76.54
			Run 3			84.21	63.91	75.89
			Run 4			83.91	63.78	76.01
			Run 5			83.78	63.88	76.25
			Run 6			83.87	63.69	75.94

Appendix A- 2. Raw data for catalysts reusability for greener synthesis of SC via CO₂ using Ce-La-Zr-O

Catalyst	Reaction time [hr]	Stirring speed (rpm)	Catalyst reusability	Reaction temperature [K]	Catalyst loading [%][w/w]	Conversion of SO [%]	Yield of SC [%]	Selectivity [%]
Ce-La-Zr-O	20	300	Run 1	408	10	83.78	51.67	61.67
			Run 2			83.55	51.89	62.11
			Run 3			84.01	52.01	61.91
			Run 4			84.33	52.18	61.88
			Run 5			84.41	52.27	61.92
			Run 6			84.02	52.19	62.12

Appendix A- 3. Raw data for catalysts reusability for greener synthesis of BC via CO₂ using Cu-Zr/graphene

Catalyst	Reaction time [hr]	Stirring speed (rpm)	Catalyst reusability	Reaction temperature [K]	Catalyst loading [%][w/w]	Conversion of BO [%]	Yield of BC [%]	Selectivity [%]
Cu-Zr/graphene	12	200	Run 1	423	7.5	82.44	71.31	86.50
			Run 2			82.21	71.11	86.50
			Run 3			82.39	71.21	86.43
			Run 4			81.71	69.91	85.56
			Run 5			81.89	71.15	86.88
			Run 6			81.57	69.88	85.67

10.3 Appendix B: Experimental raw data (samples)

Appendix B- 1. Raw data for effect of reaction temperature for the synthesis of 1,2-butylene carbonate using Ce-La-Zr/GO (At 75 bar, 10% [%] [w/w] catalyst loading, 300 rpm and 20 h)

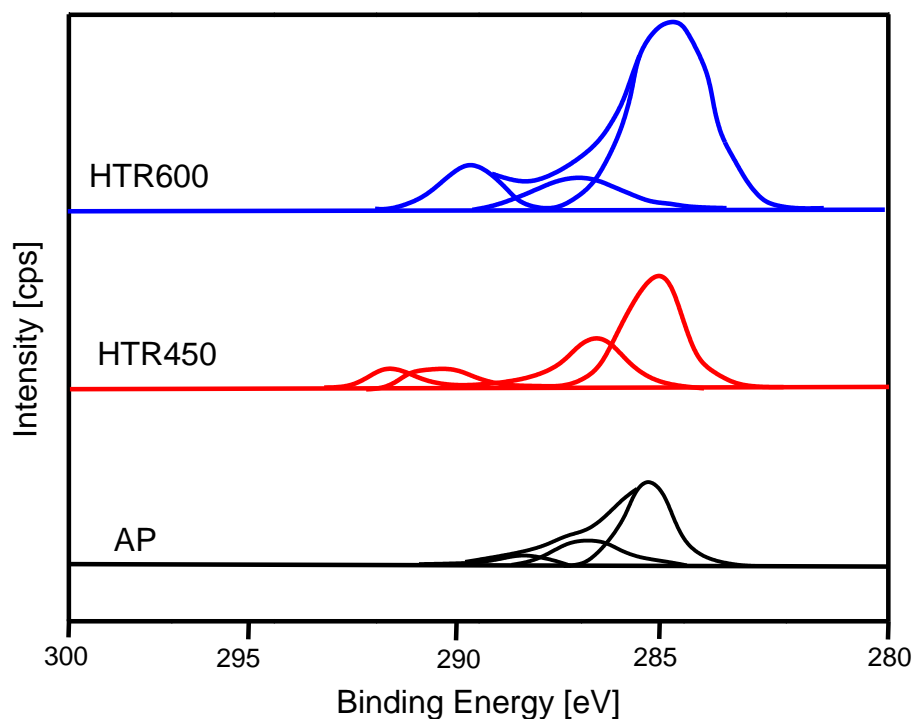
Reaction temperature [K]	1st-Conversion of BO [%]	2nd-Conversion of BO [%]	3rd-Conversion of BO [%]	1st-Yield of BC [%]	2nd-Yield of BC [%]	3rd-Yield of BC [%]	Ave- Conversion of BO [%]	Ave-Yield of BC [%]
363	54	52	51	39	38	37	52	38
383	58	58	59	42	42	43	58	42
403	63	61	59	45	44	43	61	44
423	70	69	73	52	51	53	71	52
443	83	85	84	63	64	64	84	64
463	90	91	90	62	61	60	90	61
483	91	90	91	59	59	59	91	59

Appendix B- 2. Raw data for effect of CO₂ pressure for the synthesis of styrene carbonate using Ce-La-Zr-O (At 408 K, 10% [%] [w/w] catalyst loading, 300 rpm and 20 h)

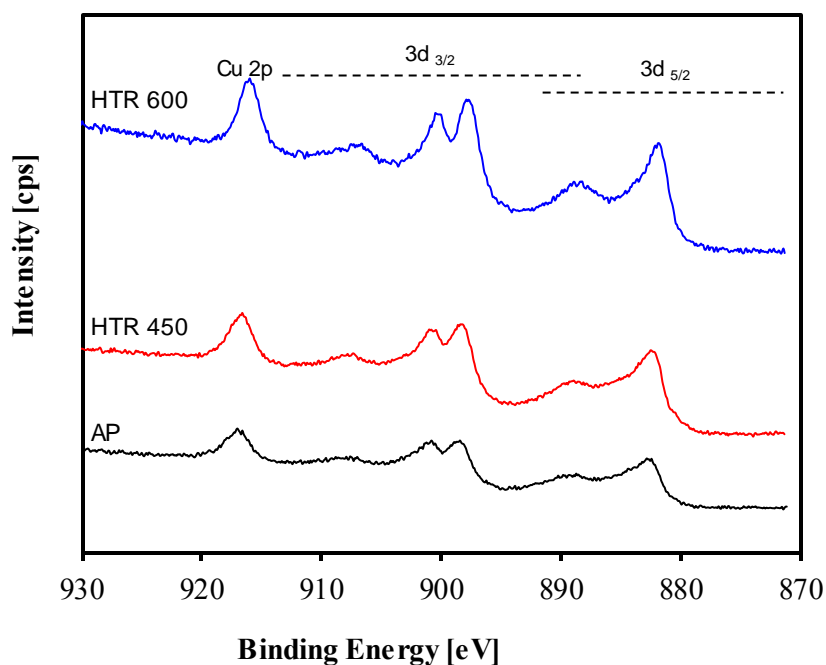
CO ₂ pressure [bar]	1st-Conversion of SO [%]	2nd-Conversion of SO [%]	3rd-Conversion of SO [%]	1st-Yield of SC [%]	2nd-Yield of SC [%]	3rd-Yield of SC [%]	Ave-Conversion of SO [%]	Ave-Yield of SC [%]
55	73	76	74	44	46	45	74	45
65	79	78	79	48	47	48	79	48
75	84	84	84	51	52	52	84	52
85	90	88	87	54	53	52	88	53
95	89	90	88	48	52	50	89	50
105	91	89	89	45	44	44	90	44

Appendix B- 3. Raw data for effect of catalyst loading for the synthesis of 1,2-Butylene carbonate using HTR450 catalyst (At 408 K, 10% [w/w] catalyst loading, 300 rpm and 20 h)

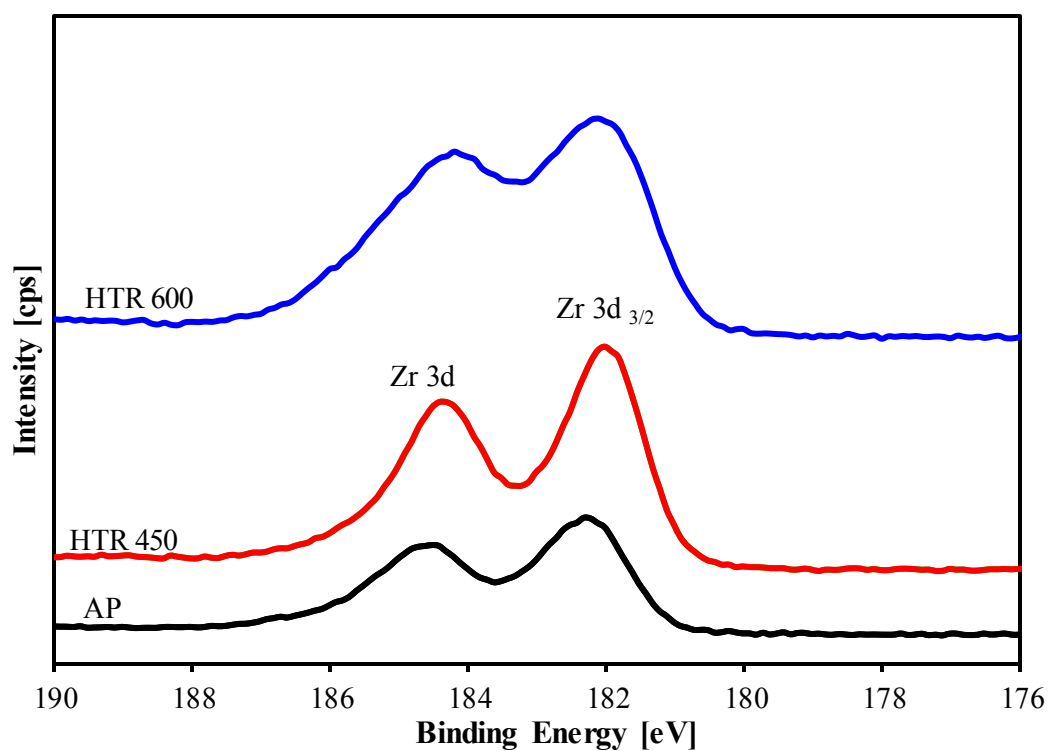
Catalyst loading [%][w/w]	1st-Conversion of BO [%]	2nd-Conversion of BO [%]	3rd-Conversion of BO [%]	1st-Yield of BC [%]	2nd-Yield of BC [%]	3rd-Yield of BC [%]	Ave- Conversion of BO [%]	Ave-Yield of BC [%]
2.5	32	34	33	17	19	18	33	18
5	50	48	52	32	31	33	50	32
7.5	80	82	84	69	71	73	82	71
10	83	85	84	71	72	71	84	71
12.5	86	88	87	68	69	69	87	69
15	86	87	89	69	69	70	87	69



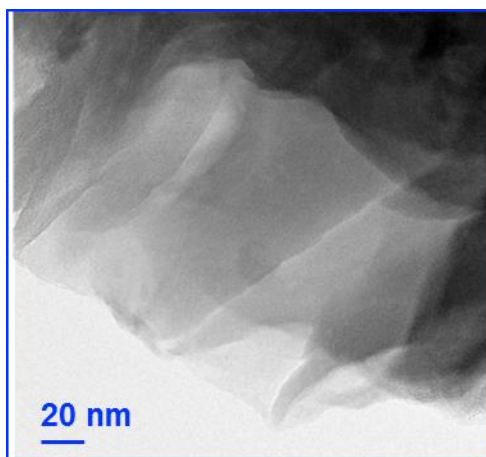
Appendix C- 1. X-ray photoelectron spectroscopy (XPS) spectra showing deconvoluted C 1s region of Cu-Zr/graphene samples synthesised via wet impregnation method.



Appendix C- 2. X-ray photoelectron spectroscopy (XPS) spectra showing Cu 2p region of Cu-Zr/graphene samples synthesised via wet impregnation method.



Appendix C- 3. X-ray photoelectron spectroscopy (XPS) spectra showing the Zr 3d region for Cu-Zr/graphene samples synthesised via wet impregnation method.



Appendix C- 4. Transmission electron microscopy (TEM) image of graphene oxide.

10.4 Research publications

10.4.1 Journal papers

Onyenkeadi, V., Kellici, S. and Saha, B. (2018) Greener synthesis of 1,2-butylene carbonate from CO₂ using graphene-inorganic nanocomposite catalyst, *Energy*, 165, pp. 867–876. DOI:10.1016/j.energy.2018.09.135.

Middelkoop, V., Slater, T., Florea, M., Neațu, F., Danaci, S., **Onyenkeadi, V.**, et al. (2019) Next frontiers in cleaner synthesis: 3D printed graphene-supported CeZrLa mixed-oxide nanocatalyst for CO₂ utilisation and direct propylene carbonate production, *Journal of Cleaner Production*, 214, pp. 606–614. DOI:10.1016/j.jclepro.2018.12.274.

Onyenkeadi, V. N., Aboelazayem, O. and Saha, B. (2019) Systematic multivariate optimisation of butylene carbonate synthesis via CO₂ utilisation using graphene-inorganic nanocomposite catalysts, *Catalysis Today*. DOI:10.1016/j.cattod.2019.03.027.

Onyenkeadi, V and Saha, B A facile and greener synthesis of 1,2-butylene carbonate via CO₂ utilisation using a novel copper–zirconia/graphene catalyst. **Energies (manuscript prepared).**

Onyenkeadi, V and Aboelazayem, O and Adeleye, A and Saha, B Greener synthesis of styrene carbonate from CO₂ using heterogeneous catalyst. **Journal of CO₂ utilisation (manuscript to be submitted).**

Onyenkeadi, V Olaniyan, B and Saha, B A review: “Greener synthesis of organic carbonates via CO₂ utilisation” *Reaction Chemistry & Engineering (manuscript in preparation)*

10.4.2 Conference papers and work presentations

Onyenkeadi, V., Aboelazayem, O., and Saha, B. (2018). A facile and greener synthesis of 1,2-butylene carbonate via CO₂ utilisation using a novel copper–zirconia oxide/graphene catalyst. Paper presented at The 16th International Conference on Carbon Dioxide Utilization (ICCDU XVI), Rio De Janeiro, Brazil, 27 August 2018 - 30 August 2018.

Onyenkeadi, V., Aboelazayem, O., Kellici, S., and Saha, B. (2018). Greener synthesis of 1,2-butylene carbonate via CO₂ utilisation using graphene-inorganic nanocomposite catalysts. Paper presented at GPE 2018 – 6th International Congress on Green Process Engineering, Toulouse, France, 03 June 2018 - 06 June 2018.

Onyenkeadi, V., Kellici, S., and Saha, B. (2017). Greener synthesis of styrene carbonate from CO₂ using graphene-inorganic nanocomposite catalysts. Paper presented at 10th World Congress of Chemical Engineering (WCCE10), Barcelona, Spain, 01 October 2017 - 05 October 2017. London South Bank University

Onyenkeadi, V., Kellici, S., and Saha, B. (2017). Greener synthesis of 1, 2 1,2-butylene carbonate from CO₂ using graphene-inorganic nanocomposite catalysis. Paper presented at SEEP 2017 –10th International Conference on Sustainable Energy & Environmental Protection, Bled, Slovenia, 27 June - 30 June 2017. London South Bank University.

Onyenkeadi, V., and Saha, B. (2017). Greener synthesis of styrene carbonate from CO₂ using heterogeneous catalyst. Paper presented at ChemEngDayUK2017 Better Life, Better World, Birmingham, 27 March 2017 - 28 March 2017. London South Bank University.